Imaging and Treatment of Bronchiectasis

Chest computed tomography to diagnose bronchiectasis and to optimise inhalation treatment

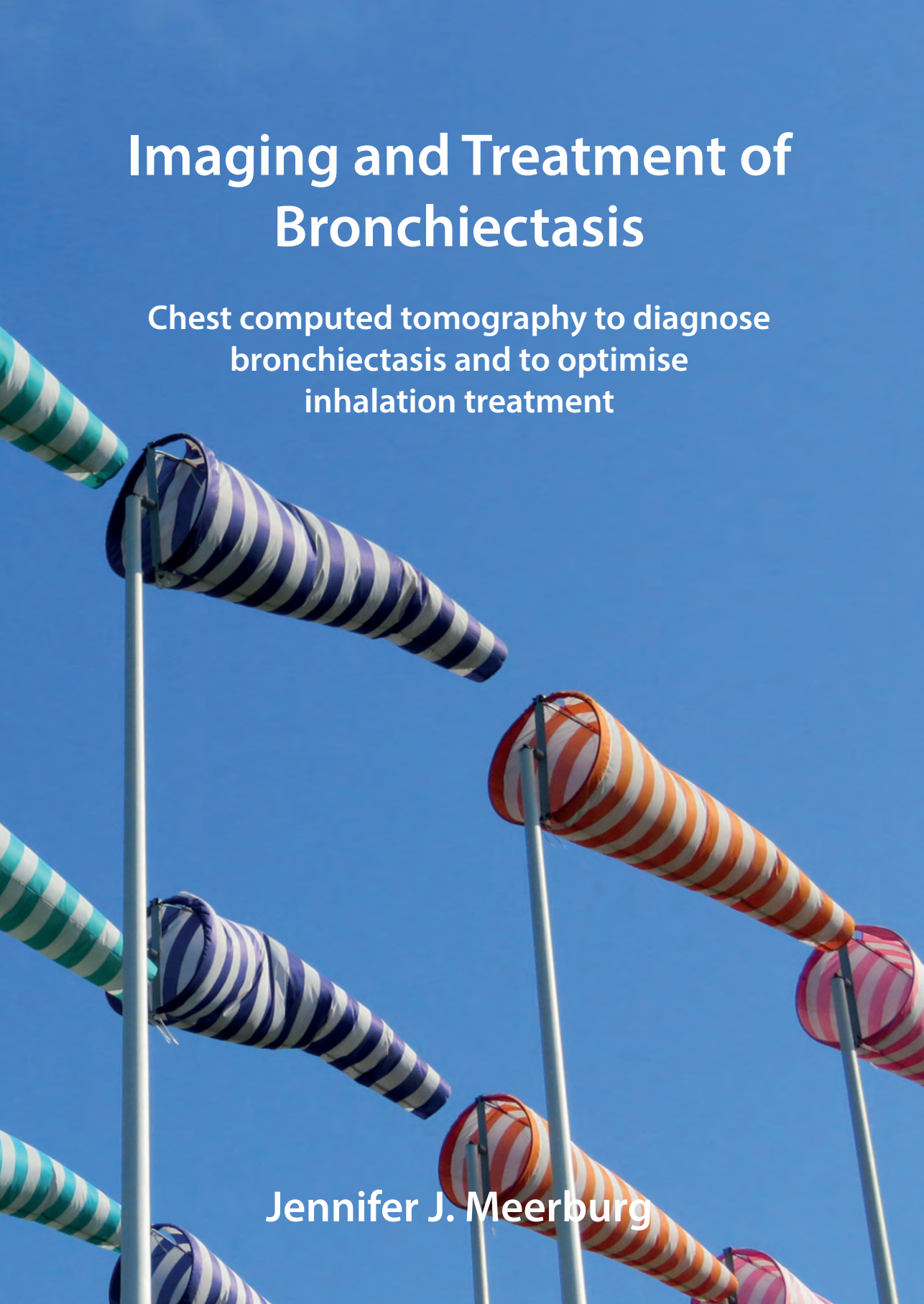

Jennifer J. Meerburg

Imaging and Treatment of Bronchiectasis

Chest computed tomography to diagnose and quantify bronchiectasis, and to optimise inhalation therapy

Jennifer Jane Meerburg

Printed by: Print Service Ede

Cover: "Le vent souffle où il veut", artwork by Daniel Buren, Nieuwpoort, België

Photographer: Jennifer J. Meerburg

The printing of this thesis was financially supported by: Erasmus University Rotterdam, Stichting SBOH, and the department of Radiology and Nuclear Medicines, Erasmus MC

Imaging and Treatment of Bronchiectasis

Chest computed tomography to diagnose and quantify bronchiectasis, and to optimise inhalation therapy

Beeldvorming en behandeling van bronchiectasieën

Computertomografie van de thorax voor het diagnosticeren en kwantificeren van bronchiectasieën, en voor het optimaliseren van inhalatietherapie

Proefschrift

ter verkrijging van de graad van doctor aan de
Erasmus Universiteit Rotterdam
op gezag van de
rector magnificus

Prof.dr. A.L. Bredenoord

en volgens besluit van het College voor Promoties.
De openbare verdediging zal plaatsvinden op

woensdag 10 november 2021 om 15:30 uur

door

Jennifer Jane Meerburg
geboren te Leiden

Erasmus University Rotterdam

Promotiecommissie:

Promotor:	Prof.dr. H.A.W.M. Tiddens
Overige leden:	Prof.dr. A.M.C. van Rossum Prof.dr. J.G.J.V. Aerts Prof.dr. E. Derom
Copromotor:	Dr.ir. M. van Straten

Content thesis

Chapter 1

General introduction

This chapter introduces the two major topics addressed in this thesis. The first topic is the radiological diagnosis and quantification of bronchiectasis (paragraph 1.1 and 1.2). The second topic is the treatment with inhaled antibiotics in bronchiectasis patients with chronic *Pseudomonas aeruginosa (Pa)* infection (paragraph 2.1, 2.2 and 2.3).

Outline general introduction

1. Radiological diagnosis and quantification of bronchiectasis
   - 1.1 Bronchiectasis, pathophysiology and symptoms
   - 1.2 Diagnosis and image analysis of bronchiectasis

2. Inhaled antibiotics in chronic *Pa* infection
   - 2.1 Bronchiectasis and *Pa* infection
   - 2.2 Inhaled antibiotics
   - 2.3 Optimising inhalation therapy

3. Objectives

1. Radiological diagnosis and quantification of bronchiectasis

1.1 Bronchiectasis, pathophysiology and symptoms

Bronchiectasis is defined as an irreversible widening of the airways due to chronic infection and/or inflammation. The gold standard to diagnose bronchiectasis is computed tomography (CT) of the chest. Histological studies of the airways in resected lung specimen of patients diagnosed with bronchiectasis show alterations of the epithelium and elastin layer of the airway wall, and sometimes even of the smooth muscle layer and cartilage [1]. Due to disruption of the epithelium, ciliated cells are lost. Ciliated cells facilitate mucus clearance, which is an important defence mechanism against pathogens. As such, bronchiectatic airways are more vulnerable for pathogens compared to healthy airways. The vicious cycle of infection, inflammation and airway destruction in bronchiectasis was first described by Cole et al. [2], and an updated version is shown in Figure 1 [3].

Bronchiectasis can be a feature of many different lung diseases. An important example of such a disease is cystic fibrosis (CF). CF is a severe congenital genetic disease characterised by chronic lung inflammation and infection starting in infancy. In most

CF patients, bronchiectasis develops below the age of five years [4]. Examples of other lung diseases characterised by bronchiectasis are chronic obstructive pulmonary disease, primary ciliary dyskinesia, connective tissue diseases and immunodeficiency diseases. Furthermore, bronchiectasis can develop as complication of a pulmonary infection without an underlying disease. In cases without an associated disease or a history of infection, we refer to idiopathic bronchiectasis. Patients with radiologically confirmed bronchiectasis who also suffer from symptoms such as chronic cough, increased sputum production and exacerbations are defined as *bronchiectasis disease*. As bronchiectasis disease can have many different associated diseases, patient populations are very heterogeneous in their composition (Figure 2). Because CF is a well-defined distinct disease it is not included in the *bronchiectasis disease* category.

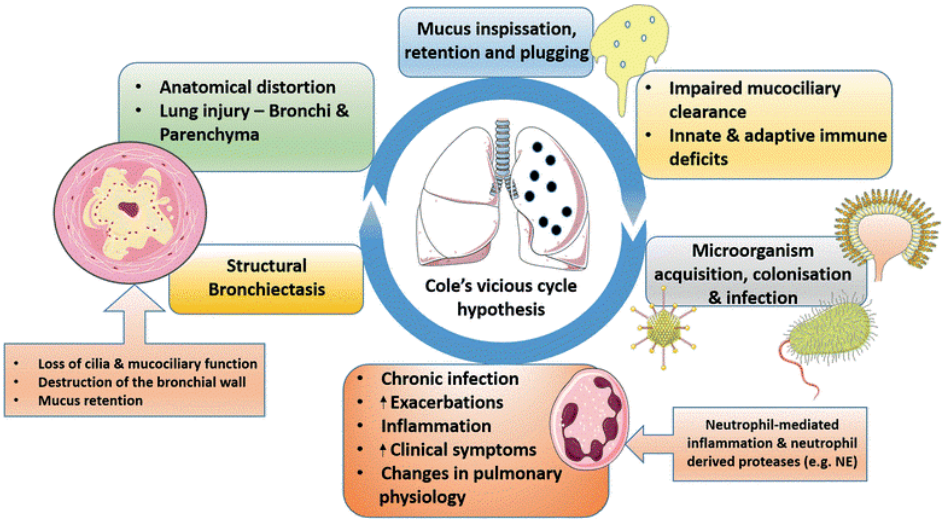

Figure 1. Pathophysiology of bronchiectasis.

This figure shows the vicious cycle hypothesis of infection, inflammation and structural damage of the airways in bronchiectasis patients. NE = Neutrophil elastase. Image from Chandrasekaran et al., republished with permission [3].

In 2017, the European Respiratory Society published its first guidelines for the clinical management of adult bronchiectasis [5]. However, to date there are no licenced therapies for bronchiectasis patients [6]. Many clinical drug trials have been performed, but failed to meet their primary endpoint, and thus did not result in a licensed therapeutic product for bronchiectasis patients [7]. Such trials are complicated by the heterogeneous character of this patient group. Consequently, bronchiectasis patients are often treated with off-label medications like inhaled

antibiotics that are registered for the treatment of other diseases, such as CF. Meanwhile, there is a search for relevant and sensitive outcomes that can be used in clinical studies. Outcome measures such exacerbation rates or changes in forced expiratory volume in one second are clinically relevant but are not very sensitive to be used as primary outcomes. As bronchiectasis is a radiological diagnosis, it makes sense to use imaging-related outcome measures. In this thesis we developed image analysis techniques for chest CT to generate outcome measures that can serve as endpoints in clinical studies. Such outcomes could also be used to monitor patients in daily care.

1.2 Diagnosis and image analysis of bronchiectasis

There are no universally accepted objective criteria to define bronchiectasis. Clear diagnostic criteria for bronchiectasis are of key importance to define inclusion criteria for clinical studies. Another hurdle in the assessment of bronchiectasis is that the analysis of CT images is mostly based on expert opinion. Radiologists report chest CT images in a qualitative way, resulting in an essay-like report. It is not possible to extract quantitative data from these reports to capture the pattern or extent of bronchiectasis and other structural lung abnormalities.

To use CT scan related outcome measures in clinical studies in bronchiectasis patients, sensitive quantitative image analysis systems are needed. In studies with CF patients, well defined CT scoring methods have already been used [8, 9]. Currently, relatively insensitive radiological scoring methods are used to quantify bronchiectasis disease. For example, in the Bronchiectasis Severity Index (BSI), a four-point radiological scale is combined with clinical scores to classify disease severity. The BSI is not suitable to serve as outcome measure in a clinical study, as it is a composite score and due to its simplicity, the BSI has a poor sensitivity to detect any effect of the study drug on structural lung disease.

In chapter 2 and 3 of this thesis we studied the diagnostic criteria and analysis systems that were used in studies with bronchiectasis patients. In chapter 4 and 5 we developed a sensitive, reproducible, and quantitative image analysis system for bronchiectasis patients, to phenotype structural abnormalities and to generate relevant outcome measures for clinical studies.

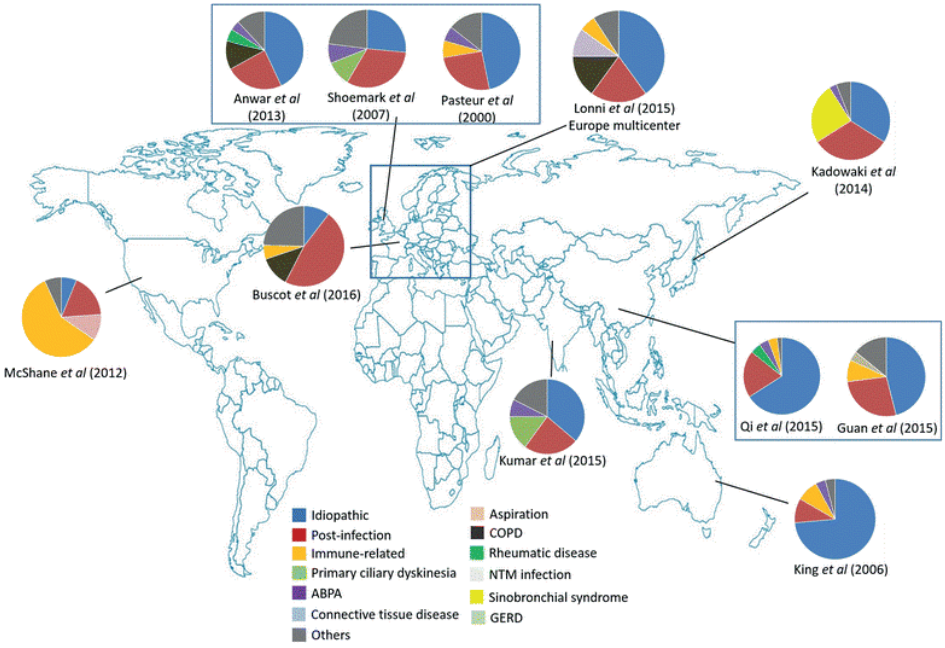

Figure 2. Predominant associated diseases in bronchiectasis populations in different regions in the world.

This figure shows the predominant associated diseases in bronchiectasis patient populations per region. ABPA = Allergic broncho-pulmonary aspergillosis. COPD = Chronic obstructive pulmonary disorder. GERD = Gastro-oesophageal reflux disease. NTM = Non-tuberculosis mycobacteria. Image from Chandrasekaran et al., republished with permission [3].

2. Inhaled antibiotics in chronic *Pa* infection

2.1 Bronchiectasis and *Pa* infection

Bronchiectasis is associated with an increased risk for the acquisition of *Pa*, which is an aerobic gram-negative rod-shaped bacterium. Chronic *Pa* infection occurs in 30% of the European CF patients older than 30 years [10]. *Pa* is also considered a key pathogen in patients with bronchiectasis disease, as 20% of these patients are chronically infected with *Pa*. In both CF and bronchiectasis disease, the presence of *Pa* infection is associated with a shortened life span, loss of lung function [11], increased number of exacerbations [12], and a decreased quality of life [13].

2.2 Inhaled antibiotics

Most CF patients with chronic *Pa* infection are treated with inhaled antibiotics [10]. Tobramycin is the most often prescribed antibiotic inhalation treatment and available as dry powder and as solution for nebulisation. However, there is no registered therapy for *Pa* infection for patients with bronchiectasis disease. In some countries, including the Netherlands, inhaled antibiotics (mostly tobramycin) are being prescribed off-label to bronchiectasis patients. Inhalation is the preferred route for the treatment of chronic *Pa* infections with antibiotics, because high local doses can be reached while systemic doses remain low, thereby minimising systemic side effects. However, this administration route has shortcomings: First, adherence to prescribed inhalation therapy is low. Importantly, inhalation therapy is time consuming, and contains multiple steps including medicine preparation, administration of the drug and cleaning and disinfection of the device after its use. Furthermore, negative side effects, such as cough immediately after inhalation, could discourage patients to continue treatment. Second, the inhalation skills of patients can fall short, which can reduce the efficacy of the treatment. Training at first prescription, and repeating the training whenever a patient visits the outpatient clinic, is important to check the inhalation technique and correct mistakes if necessary. Chapter 6 contains a study in which patients were video-recorded during inhalations with tobramycin inhalation powder; to analyse peak inspiratory flow, the relation of flow with cough, and inhalation technique.

2.3 Optimising inhalation therapy

For success of inhaled antibiotics, it is of key importance to deliver the medication to the affected area of the lungs. This is challenging as a large fraction of the inhaled antibiotics will be deposited in the upper airways and thus will not contribute to effective treatment of *Pa* in the lower airways. In CF, small airways are the major target, however the total surface of small airways is large [14]. Therefore, drug concentrations in the upper and large airways are substantially higher than the concentrations in the small airways [15]. In silico analysis using computational fluid dynamics were developed to assess deposition of aerosols [16]. With this method, aerosol deposition can be assessed for each airway using accurate and realistic three-dimensional models of the lungs. These lung models are developed from chest CT scans of patients. Aerosol deposition studies can be executed in silico using patient specific data, for example by using patient-specific inhalation flows. In CF patients, we learned from studies by Bos et al. that for aztreonam, concentrations can be too low in especially the smaller airways [17]. In chapter 7, we show how much tobramycin inhalation powder is deposited in the large and small airways, the effect of inspiratory flow on its deposition, and how its deposition differs from that of tobramycin inhalation solution.

Objectives

In this thesis, studies were performed with the following objectives:

Section I

- To identify the most common used diagnostic criteria for bronchiectasis.
- To evaluate how the severity and extent of bronchiectasis have been quantified in previous clinical studies.
- To assess the radiologic features on CT scans of the patients with granulomatous lymphocytic interstitial lung disease using two scoring methods.
- To develop a sensitive CT scoring method to phenotype and quantify structural lung disease in bronchiectasis patients.

Section II

- To record inhalations with tobramycin inhalation powder by CF patients on video in the home setting, to study the association between inspiratory flow and cough.
- To study inhalation technique of CF patients using tobramycin inhalation powder.
- To assess deposition patterns of tobramycin inhalation powder and solution with computational fluid dynamics.

References

[1] Boaventura R SA, Chalmers JD. Pathophysiology. In: Chalmers JD, Polverino E, Aliberti S, eds. Bronchiectasis (ERS Monograph). Sheffield, European Respiratory Society, 2018; pp. 8-28.

[2] Cole PJ. Inflammation: a two-edged sword--the model of bronchiectasis. Eur J Respir Dis Suppl. 1986;147:6-15.

[3] Chandrasekaran R, Mac Aogain M, Chalmers JD, Elborn SJ, Chotirmall SH. Geographic variation in the aetiology, epidemiology and microbiology of bronchiectasis. BMC Pulm Med. 2018;18:83.

[4] Mott LS, Park J, Murray CP, Gangell CL, de Klerk NH, Robinson PJ, et al. Progression of early structural lung disease in young children with cystic fibrosis assessed using CT. Thorax. 2012;67:509-16.

[5] Polverino E, Goeminne PC, McDonnell MJ, Aliberti S, Marshall SE, Loebinger MR, et al. European Respiratory Society guidelines for the management of adult bronchiectasis. Eur Respir J. 2017;50.

[6] Chalmers JD, Chotirmall SH. Bronchiectasis: new therapies and new perspectives. Lancet Respir Med. 2018;6:715-26.

[7] Metersky M, Chalmers J. Bronchiectasis insanity: Doing the same thing over and over again and expecting different results? F1000Res. 2019;8.

[8] Rosenow T, Oudraad MC, Murray CP, Turkovic L, Kuo W, de Bruijne M, et al. PRAGMA-CF. A Quantitative Structural Lung Disease Computed Tomography Outcome in Young Children with Cystic Fibrosis. American journal of respiratory and critical care medicine. 2015;191:1158-65.

[9] Wainwright CE, Vidmar S, Armstrong DS, Byrnes CA, Carlin JB, Cheney J, et al. Effect of bronchoalveolar lavage-directed therapy on Pseudomonas aeruginosa infection and structural lung injury in children with cystic fibrosis: a randomized trial. Jama. 2011;306:163-71.

[10] Zolin A OA, Naehrlich L, Jung A, van Rens J et al. ECFSPR Annual Report 2018. 2020.

[11] Martínez-García MA, Soler-Cataluña JJ, Perpiñá-Tordera M, Román-Sánchez P, Soriano J. Factors associated with lung function decline in adult patients with stable non-cystic fibrosis bronchiectasis. Chest. 2007;132:1565-72.

[12] Chalmers JD, Aliberti S, Filonenko A, Shteinberg M, Goeminne PC, Hill AT, et al. Characterization of the "Frequent Exacerbator Phenotype" in Bronchiectasis. American journal of respiratory and critical care medicine. 2018;197:1410-20.

[13] Wilson CB, Jones PW, O'Leary CJ, Hansell DM, Cole PJ, Wilson R. Effect of sputum bacteriology on the quality of life of patients with bronchiectasis. Eur Respir J. 1997;10:1754-60.

[14] Phalen RF OM, Kleinman MT, Crocker TT. Tracheobronchial deposition predictions for infants, childern and adolescents. Ann occup Hyg. 1988;32:11-21.

[15] Bos AC, van Holsbeke C, de Backer JW, van Westreenen M, Janssens HM, Vos WG, et al. Patient-specific modeling of regional antibiotic concentration levels in airways of patients with cystic fibrosis: are we dosing high enough? PLoS One. 2015;10:e0118454.

[16] De Backer JW, Vos WG, Gorle CD, Germonpre P, Partoens B, Wuyts FL, et al. Flow analyses in the lower airways: patient-specific model and boundary conditions. Med Eng Phys. 2008;30:872-9.

[17] Galeva I, Konstan MW, Higgins M, Angyalosi G, Brockhaus F, Piggott S, et al. Tobramycin inhalation powder manufactured by improved process in cystic fibrosis: the randomized EDIT trial. Curr Med Res Opin. 2013;29:947-56.

SECTION I

Chapter 2

Diagnosis and quantification of bronchiectasis using computed tomography or magnetic resonance imaging: a systematic review

Respiratory Medicine 2020; 170:105954

Jennifer J. Meerburg, G.D. Marijn Veerman, Stefano Aliberti, Harm A.W.M. Tiddens

Abstract

Background Bronchiectasis is an irreversible dilatation of the airways caused by inflammation and infection. To diagnose bronchiectasis in clinical care and to use bronchiectasis as outcome parameter in clinical trials, a radiological definition with exact cut-off values along with image analysis methods to assess its severity are needed. The aim of this study was to review diagnostic criteria and quantification methods for bronchiectasis.

Methods A systematic literature search was performed using Embase, Medline Ovid, Web of Science, Cochrane and Google Scholar. English written, clinical studies that included bronchiectasis as outcome measure and used image quantification methods were selected. Criteria for bronchiectasis, quantification methods, patient demographics, and data on image acquisition were extracted.

Results We screened 4182 abstracts, selected 972 full texts, and included 122 studies. The most often used criterion for bronchiectasis was an inner airway-artery ratio ≥ 1.0 (42%), however no validation studies for this cut-off value were found. Importantly, studies showed that airway-artery ratios are influenced by age. To quantify bronchiectasis, 42 different scoring methods were described.

Conclusion Different diagnostic criteria for bronchiectasis are being used, but no validation studies were found to support these criteria. To use bronchiectasis as outcome in future studies, validated and age-specific cut-off values are needed.

Introduction

Bronchiectasis is defined as an abnormal and permanent dilatation of the airways, usually sustained by local inflammation and chronic infection [1]. Bronchiectasis is associated with different genetic or acquired conditions including cystic fibrosis (CF), primary or secondary immune deficiencies, and ciliopathies, or can develop as a result of low respiratory tract infections [2, 3]. However, in the majority of the patients, bronchiectasis is present without a clear underlying disease [3].

Chest computed tomography (CT) is considered the gold standard for the radiological diagnosis. To determine whether airways are dilated, airway diameters are usually compared with diameters of their adjacent arteries. To date, no exact radiological criteria of bronchiectasis exist. A widely accepted definition of bronchiectasis is described by the Fleischner society in the glossary of terms for thoracic imaging [4]. In this guideline bronchiectasis is defined as a "bronchial dilatation with respect to the adjacent pulmonary artery (signet ring sign), lack of tapering of bronchi, and identification of bronchi within 1 cm of the pleural surface" [4]. However, several challenges with this diagnosis might be identified. First, the threshold width for bronchiectasis of the airway compared to that of the artery is not specified. Second, it is unclear whether inner [luminal] or outer airway diameters should be measured. To use bronchiectasis as outcome measure in both daily care and clinical trials, precise criteria with clear cut-off values for bronchiectasis are needed.

In light of the absence of exact radiological criteria of bronchiectasis and the heterogeneity of definitions reported in literature, we decided to conduct a systematic review with the following objectives:

1) To identify the most common diagnostic criteria for bronchiectasis used in clinical trials.
2) To evaluate how the severity and extent of bronchiectasis have been quantified.

Methods

Search

We conducted the initial literature search at December 9th, 2016, and an additional search was performed on July 11th, 2018. Literature search was conducted with help of a biomedical information specialist (dr. WM Bramer) using the following search terms: bronchiectasis, radiology, diagnostic imaging, magnetic resonance imaging (MRI), CT, X-ray, Röntgen. The search was restricted by papers written in English. The

following databases were searched: Embase, Medline Ovid, Web of Science, Cochrane, and Google Scholar. Search queries are presented in Table S1 (Supplementary material).

Review registration

This review was registered at PROSPERO, registration number: CRD42017055001.

Review process

The systematic search was performed in two phases. First, title and abstract screening was done independently by two authors (JM and GV), and a consensus on selected papers was reached after face-to-face meetings. Second, a full text screening was done independently by the same authors, which was also followed by face-to-face meetings to reach a consensus on the selected papers.

A full list of inclusion and exclusion criteria is reported in Table 1. In short, we searched for clinical studies in which: 1) criteria to diagnose bronchiectasis were described; 2) bronchiectasis was used as an outcome measure; and 3) severity of bronchiectasis was measured.

Missing papers

We searched for full texts in journals that were included in the licenses of the library of Erasmus Medical Center. For journals not included in the licenses, we requested a copy of the paper by approaching the corresponding author by e-mail and/or ResearchGate. Papers that could not be found were excluded from the analysis.

Data extraction

The following data were extracted from the selected studies: criteria for bronchiectasis diagnosis; imaging modality; standardisation of lung volume; patient groups and characteristics (age, gender, race); scoring methods for bronchiectasis; and reproducibility measures.

Referring to multiple publications

Due to the large number of studies selected by this systematic review, references in relation to a specific topic that include more than ten studies are tabulated in Table 2.

Table 1. Inclusion and exclusion criteria

Title abstract screening	
Inclusion criteria	Bronchiectasis
	Radiological assessment of bronchiectasis
	Clinical study
Exclusion criteria	Reviews
	Case reports n < 10
Full text screening	
Inclusion criteria	Clear criteria of bronchiectasis that are used in the study are presented
	Bronchiectasis is used as outcome measure
	Bronchiectasis outcomes are statistically validated against other clinical parameters or against a control group
	Underlying mechanism of the development of bronchiectasis is inflammation/infection of the bronchial wall (for example studies about traction bronchiectasis in case of fibrosis or widened airways due to collagen or cartilage disorder were not included)
	Imaging (X-ray, computed tomography, bronchography or magnetic resonance imaging)
	Humans
	Original study
	English written
	If published more than once, the most recent study is selected
	Severity and/or extent of bronchiectasis is evaluated
Exclusion criteria	Reviews
	Case reports n < 10
	Papers of which the full text could not be found
	Papers that we did not have access to (Erasmus MC university database and no response or e-mail authors)

Table 2. Reference legend for topics that include more than ten studies

Topic	Studies
Studies in which the inner diameter of the airway was used to assess the airway-artery ratio	[5-63]
Studies in which it was not stated whether the inner or outer diameter of the airway was used for the airway-artery ratio	[64-108]
Lack of tapering included in definition of bronchiectasis	[5, 6, 8, 11, 12, 14, 15, 17-20, 25, 30, 31, 37, 40, 41, 47, 48, 51, 53, 54, 56, 57, 59, 60, 62, 67, 69, 75, 77, 78, 89, 90, 97, 107, 109]
Definition visibility of airway 1 cm from pleura	[5, 6, 8, 12, 14, 19, 20, 25, 30, 56, 62, 67, 69, 75, 107]
Studies that referred to Naidich et al. for a description of bronchiectasis [110]	[39, 56, 57, 62, 111-121]
The in- or expiratory level of the lungs during scanning was discussed	[5-7, 9-15, 18-21, 26, 28, 32, 33, 35, 38, 39, 41, 42, 44, 46, 47, 49, 53-59, 61-63, 65, 66, 68-70, 73-75, 79-81, 83-89, 91, 94, 97-101, 103-108, 112-115, 117, 118, 122-127]
CT scanning was performed during inspiratory breath hold without further specification	[6, 7, 9-15, 18-21, 26-28, 32, 33, 35, 39, 41, 42, 44, 45, 49, 50, 53, 54, 56, 57, 59, 61, 65, 66, 68-70, 73, 75, 79-81, 86, 87, 89, 94, 97, 98, 103, 104, 106, 107, 113-115, 117, 118, 122, 123]
Volume standardisation during CT scanning was pressured controlled under general anaesthesia	[15, 38, 58, 62, 74, 84, 99, 105, 108, 126, 127]
Studies that did not mention the level of inspiration	[8, 16, 17, 22-25, 29-31, 34, 36, 37, 40, 43, 48, 51, 52, 60, 64, 67, 71, 72, 76-78, 82, 83, 90, 92, 93, 95, 96, 102, 109, 111, 116, 119-121]
Lungs were also scanned after maximal expiration	[5, 8-10, 14, 15, 18, 21, 33, 41, 46, 48, 56, 63, 65, 69, 70, 74, 79, 81, 84-86, 89, 91, 93, 94, 99-101, 103, 105-107, 112, 125-127]
Only adults in study	[6, 8, 9, 11-13, 16, 19-26, 29-32, 34-37, 39-43, 49, 52-57, 59-62, 64, 66, 71, 73, 75, 77, 78, 80, 82, 87, 91, 93, 96, 97, 104, 107, 111-117, 119-121]
Only children in study	[15, 17, 18, 38, 68-70, 74, 76, 84, 86, 88, 89, 99, 101, 103, 105, 106, 108, 118, 122-127]
Both adults and children in study	[7, 10, 14, 27, 28, 33, 44-46, 50, 63, 65, 67, 72, 79, 81, 83, 85, 90, 92, 94, 95, 98, 100, 102, 109]
Patients with bronchiectasis that was either post-infective, idiopathic or not further specified were included	[5, 11, 15, 17, 23-26, 29-32, 35-37, 39, 40, 44, 45, 47, 48, 51, 53, 57, 58, 60, 61, 65, 75, 76, 78, 80, 82, 89, 91, 93, 97, 104, 107, 111, 113-121]
Patients with cystic fibrosis were included	[7, 8, 10, 14, 18, 27, 28, 33, 38, 39, 43, 46, 50, 63, 68-70, 72, 74, 79, 81, 84-86, 88, 89, 92, 94, 96, 98-103, 105-109, 115, 122-127]
Patients with primary ciliary dyskinesia were included	[11, 17, 30, 36, 37, 39, 44, 45, 47, 51, 52, 67, 75, 76, 83, 89, 90, 95, 97, 115, 117, 118, 120]
Patients with immune deficiencies were included	[11, 15, 17, 21-25, 37, 44, 45, 47, 51, 71, 75, 76, 88, 93, 97, 115, 117, 120]
Patients with chronic obstructive pulmonary disease were included	[9, 19, 20, 23-26, 49, 56, 62, 65, 66, 73, 75, 77, 107, 115]
Patients with asthma were included	[23-26, 51, 54, 59, 64, 65, 76, 107]

Table 2. Continued

Patients with allergic bronchopulmonary aspergillosis were included	[11, 36, 37, 64, 75, 93, 111, 114, 117, 120]
Actual measurements of airways	[8, 12, 13, 34, 38, 42, 63, 84, 88, 106-108, 123-125]
Airway-artery ratios were measured	[12, 13, 34, 38, 42, 84, 88, 107, 108, 123-125]
Used Brody or CF-CT scoring method	[8, 18, 67-70, 72, 79, 81, 83-86, 88, 92-95, 98, 100-103, 106, 122-124]
Used Bhalla scoring method	[7, 10, 14, 17, 27, 28, 30, 31, 33, 35-37, 44, 45, 50, 53, 56-58, 62, 80, 82, 85, 90, 122]
Bronchiectasis scores validated against spirometry	[5, 6, 7, 9, 10, 12, 13, 15, 17, 18, 20-23, 25-31, 35, 39-41, 43, 44, 46, 48, 52-57, 61, 63-69, 71, 72, 76, 77, 79, 81-83, 85-87, 89-98, 101, 103, 106, 107, 109, 112, 114, 118, 121-123]
Bronchiectasis scores validated against clinical symptoms	[13, 20, 27, 40, 41, 48, 56-59, 62, 73, 76, 77, 79, 80, 87, 101, 102, 109, 111, 114, 117]
Bronchiectasis scores validated against bacterial infections	[18-20, 35, 40, 49, 52, 56, 57, 59, 60, 68, 77, 90, 95, 99, 101, 105, 117, 120]
Bronchiectasis scores validated against inflammatory markers	[10, 16, 22, 28, 32, 49, 56, 61, 64, 74, 76, 77, 92, 99, 106, 126]
Bronchiectasis scores validated against pulmonary exacerbations	[48, 49, 56, 57, 68, 77, 78, 81, 98, 100, 101, 111]
Bronchiectasis scores validated against mortality or survival	[11, 20, 28, 37, 47, 51, 58, 75, 104, 111, 115, 119]
Longitudinal studies with bronchiectasis as outcome measure	[22, 71, 72, 83, 85, 98, 103, 104, 108, 122, 123]
Scoring was performed by 1 observer	[6, 8, 10, 12, 13, 15-17, 25, 32, 36, 42, 48, 52, 67, 74, 76, 81, 86, 88, 90, 99-105, 108, 115, 120, 122-126]
Scoring was performed by 2 observers	[5, 9, 11, 14, 19-22, 26-29, 31, 33-35, 37-41, 43-45, 47, 49, 53-57, 59, 61, 62, 64-66, 68, 69, 71-73, 75, 77, 80, 83, 84, 87, 89, 92, 93, 96-98, 106, 107, 112-114, 117-119, 121]
The final score was decided upon consensus	[9, 11, 14, 19-21, 26-28, 33-35, 39-41, 44-46, 49, 50, 53, 55-57, 61, 62, 64, 69, 71, 77, 85, 97, 107, 119, 121]
The mean score of the observers was used	[31, 37, 43, 65, 66, 68, 72, 80, 82, 87, 89, 91, 109, 112, 117]
Reported inter-observer agreement for bronchiectasis score	[15, 21, 31, 53, 54, 57, 68, 69, 72, 83, 86, 88, 89, 91-93, 95, 97-99, 112-114, 117]
Reported intra- and inter-observer agreement for bronchiectasis score	[12, 13, 18, 38, 48, 67, 70, 81, 84, 100, 123, 125, 126]

This table presents references in relation to a specific topic that included more than ten studies, sorted in order of appearance.

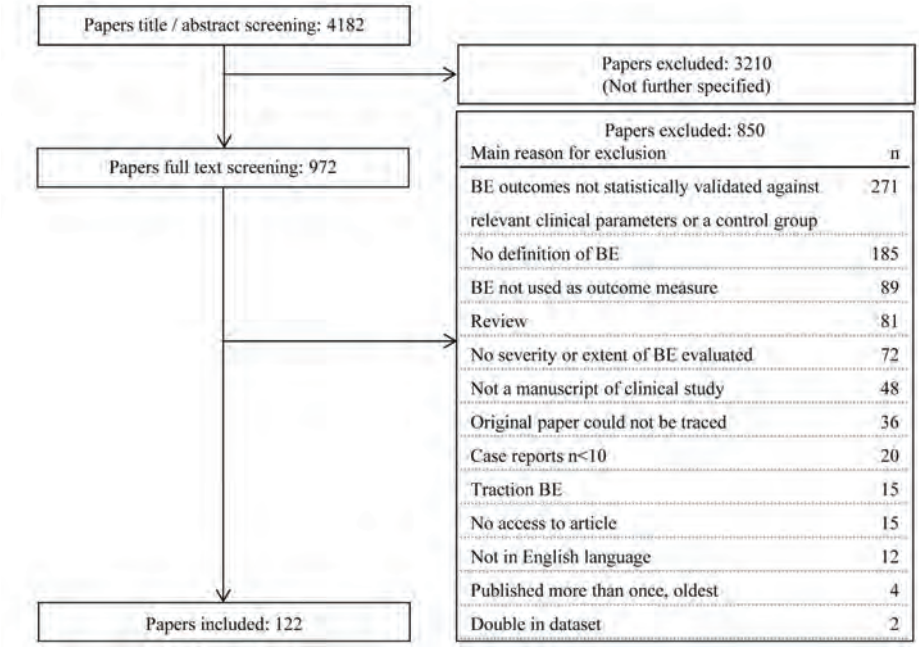

Main reason for exclusion	n
BE outcomes not statistically validated against relevant clinical parameters or a control group	271
No definition of BE	185
BE not used as outcome measure	89
Review	81
No severity or extent of BE evaluated	72
Not a manuscript of clinical study	48
Original paper could not be traced	36
Case reports n<10	20
Traction BE	15
No access to article	15
Not in English language	12
Published more than once, oldest	4
Double in dataset	2

Figure 1. Flowchart of inclusions and exclusions

Two reasons for exclusion require extra explanation. Firstly, 48 selected papers were "not a manuscript of clinical study" meaning that these papers were not full manuscripts of clinical studies, but poster-presentations or meeting abstracts. Secondly, we had "no access to paper" in 15 cases, neither via the journal license of the Erasmus Medical Center university library, nor after sending request for a copy of the paper to the corresponding author by e-mail or ResearchGate. BE = Bronchiectasis.

Results

Search

A flowchart of the included and excluded papers along with the main reasons for exclusion of full texts is presented in Figure 1. A total of 4182 papers were identified. After screening all titles and abstracts, 972 papers were selected for full text evaluation, and 122 were included in the analysis [5-38, 40-86, 88-109, 111-129].

Radiological criteria to define bronchiectasis

Criteria for radiological diagnosis of bronchiectasis across 122 studies are reported in Table 3. The most used criterion, reported in 108 (89%) studies, was an increased ratio of the cross-sectional diameter of an airway and its adjacent artery [airway-artery

ratio] with cut-off values ranging from 1.0 to 1.5. In 59 (48%) studies inner airway diameters were used to assess this ratio, and four studies (3%) used outer airway diameters [124-127].

Table 3. Criteria for bronchiectasis

Criterion	n studies (%)
Airway-artery ratio	108 (89%)
≥ 1.0	
inner airway diameter	52 (43%)
outer airway diameter	4 (3%)
not specified	42 (34%)
≥ 1.1	
inner airway diameter	7 (6%)
outer airway diameter	0 (0%)
not specified	1 (1%)
≥ 1.5	
inner airway diameter	1 (1%)
outer airway diameter	0 (0%)
not specified	2 (2%)
Lack of tapering	37 (30%)
Visibility of airways in periphery	25 (20%)

The most frequent used criteria to diagnose bronchiectasis are presented. Airway-artery ratios are calculated by dividing the cross-sectional diameter of an airway by that of its adjacent artery.

Exact measurements of airway-artery ratios were presented in eight (7%) studies. Four (3%) studies presented mean inner airway-artery ratios in healthy adults, being 0.68 (n = 85), 0.70 (n = 33), 0.71 (n = 42), and 0.79 (n = 106) [12, 13, 34, 115]. Four other studies (3%) studied airway-artery ratios of children with CF or common variable immunodeficiency disorders [38, 88, 108, 125]. Long et al. reported significantly different inner airway-artery ratios in CF patients (n = 23) and controls (n = 20), of 0.77 and 0.55 respectively [38]. Perez et al. reported that outer airway-artery ratios of diseased and control subjects were significantly different (1.17 versus 1.02 respectively); while inner airway-artery ratios were not [88]. Kuo et al. also reported

that outer airway-artery ratios were more precise than inner airway-artery ratios, and presented cut-off values for outer airway-artery ratios of 1.06 for children younger than six years [108], and 1.11 for children above six years of age [125].

The second most used criterion to define bronchiectasis was the lack of tapering of the airways, which was mentioned in 37 (30%) studies.

The third most used criterion was the visibility of airways in the periphery of the lung, reported in 25 (20%) studies. The following cut-off values for a pathognomonic distance of visible airways with respect to the pleura were described: 1.0 cm (n = 15, 12%); 2.0 cm (n = 1, 1%) [54]; 3.0 cm (n = 3, 2%) [37, 47, 97]; and the peripheral 1/3 of the lung (n = 3, 2%) [48, 89, 90].

Imaging modality

All evaluated studies used chest CT to diagnose bronchiectasis. No chest X-ray or bronchography studies were found. In four (3%) studies, bronchiectasis outcomes of MRI scans were compared with those of CT scans [44, 45, 50, 101]. Puderbach et al. concluded that MRI overall performed well, but that subtle morphologic changes such as peripheral bronchiectasis were missed [50]. Montella et al. showed good to excellent agreement between MRI and CT bronchiectasis scores [44, 45]. Tepper et al. reported an overestimation of bronchiectasis scores when comparing MRI with CT [101]. All studies emphasised that longitudinal trials are needed to further validate the use of MRI.

Standardisation of lung volume

Lung volume, i.e. the level of inspiration during scanning was discussed in 82 (67%) studies. In 59 (48%) studies CT scanning was performed during inspiratory breath hold without further specification. In 11 (9%) paediatric studies lung volume was pressure controlled, using a manometer to assess transpulmonary pressure while the patient was under general anaesthesia. In ten (8%) studies breath hold practise sessions were held before CT scanning [5, 46, 47, 55, 63, 85, 100, 101, 112]. Four (3%) studies used a spirometer to establish lung volume [88, 124, 125, 127]. Expiratory CT scans were made in 38 (31%) studies, mostly to detect trapped air. However, two (2%) studies also used expiratory scans to assess bronchiectasis. Both Mott et al. and Do Amaral et al. concluded, in a paediatric and adult study respectively, that expiratory scans were inferior to inspiratory scans to assess bronchiectasis since fewer airways were detected [84, 107].

Patient groups and age characteristics

A total of 11,581 subjects were described in 122 evaluated studies, of which 51% were female, 44% were male, and in 5% gender was not specified. Only nine (7%) studies reported the race of the subjects; in these studies the majority of patients was Caucasian [12, 13, 47, 86, 98, 118, 129-131]. Median size of study population was 60 [IQR range 30-102]. Enrolled populations contained only adults in 65 studies (53%), only children in 26 studies (21%), and both in 26 studies (21%). As the remaining studies reported mean ages around 50 years, it is likely that only adults were included [5, 47, 51, 58, 132].

Bronchiectasis aetiology of enrolled subjects (reported in ten or more studies) was post-infective or idiopathic/not further specified bronchiectasis (49 studies, 40%), CF (47 studies, 38%), primary ciliary dyskinesia (23 studies, 19%), immune deficiencies (22 studies, 18%), chronic obstructive pulmonary disease (17 studies, 14%), asthma (11 studies, 8%), and ten (8%) studies included patients with allergic bronchopulmonary aspergillosis.

Scoring methods for bronchiectasis

To quantify bronchiectasis 42 different scoring methods have been reported across the 122 included studies. Two approaches to quantify bronchiectasis were identified: exact measurements and semi-quantified scoring methods.

Fifteen (12%) studies assessed the amount of bronchiectasis with exact measurements:

1) Airway-artery ratios were calculated in 12 (10%) studies. Measurements were done manually in all studies, and both manually and automatically in one study [133].
2) Airway dimensions were measured in three (2%) studies and expressed in cumulative airway diameters [134], total airway surfaces of bronchiectic airways [107], or mean airway diameters [63].
3) The total number of airways visible on CT was counted in three (2%) studies [63, 108, 124].

In semi-quantified scoring methods, amount of extent or severity of structural abnormalities are rated by an observer. An overview from 42 scoring methods, divided in extent and severity of dilatation, is presented in Table S2a and S2b (Supplementary material). The two most frequently reported scoring methods were both developed for CF lung disease. Twenty-seven (22%) studies used a method published in 2004 by Brody et al. [69], or an upgraded version, the CF-CT method [135]. Twenty-five (20%) studies used the Bhalla method [7].

Reproducibility of scoring

Measures to determine inter- and intra-observer agreement of bronchiectasis scores were reported in 36 (30%) studies: five (4%) studies reported only intra-observer agreement [74, 101, 105, 108, 124], 24 (20%) studies only inter-observer agreement, and 13 (11%) studies reported both. Intra-class correlation coefficients for bronchiectasis ranged between 0.73 and 0.95 and Cohen's kappa values ranged between 0.47 and 0.88. Roughly, both methods can be interpreted as follows: < 0.4 = poor; 0.4-0.6 = fair; 0.6-0.8 = good; > 0.8 = excellent.

Discussion

We assessed radiological criteria and quantification methods for bronchiectasis in 122 clinical studies. The main findings of the present review are: a) there are no validated criteria to diagnose bronchiectasis; b) cut-off values to diagnose bronchiectasis should be age-specific; c) many different scoring methods are being used to quantify bronchiectasis; d) image acquisition and analysis are often not standardised.

Validation studies containing normal values of criteria for bronchiectasis, i.e. means and standard deviations of airway-artery ratios or tapering of the healthy population, were not found. Cut-off values for airway-artery ratios that can be used to label airways as bronchiectasis are essential. Reported studies on bronchiectasis mainly included relatively small populations of patients with airways disease and even fewer smaller studies reported data airway-artery ratios on healthy volunteers. Clearly such studies are valuable as starting point but their generalisability is doubtful. For other clinical parameters used in respiratory medicine such as spirometry data, reference values have been extensively studied and means and standard deviations are published per age, sex and race. Ideally, similar studies are needed to generate reference values for airway-artery ratios and tapering. However, due to radiation risk, population-based studies using CT scanning have not being conducted to date. As radiation dose needed for chest CT scans have come down considerably in the last decade such studies might become feasible. Similar for MRI reference values have to be generated. Also for MRI being a radiation free alternative no proper reference data for bronchiectasis are available. Until proper validation studies have been performed, it is important to take this limitation into consideration when interpreting data on bronchiectasis patients.

The most used criterion for a radiological diagnosis of bronchiectasis is an airway-artery ratio of more than 1.0, although no study validated the use of this specific cut-off value.

Reported cut-off for airway-artery ratios values varied between 1.0 and 1.5, and no consensus exists on whether inner or outer airway diameters should be used to compute this ratio. The use of inner diameters probably originates from the time that bronchography was used to diagnose bronchiectasis, as the acquired images only revealed inner diameters [136]. However, in diseased lungs airway walls are often thickened, reducing inner diameters as seen on CT. This may lead to false-negative diagnoses of bronchiectasis. Until larger comparison studies have been performed, we suggest to take both the inner and the outer diameter of the airways into account.

Furthermore, optimal cut-off values to detect bronchiectasis seem to be age-dependent [42, 108, 124]. In older age the ratio seem to increase [137], which is thought to be the result of loss of elastic recoil of the ageing airways [138]. A population based cohort study would be suitable to assess this phenomenon.

While using airway-artery ratios, we assume that artery diameters are unaffected by the underlying disease. Importantly, this assumption has been challenged, as Diaz et al. showed that airway-artery ratios can be altered from the perspective of the arteries in case of smoking, due to local hypoxia [12].

A large number of scoring methods for bronchiectasis have been described. For scientific purposes, scoring methods need to be well validated. Actual measurements are likely more accurate to assess bronchiectasis than semi-quantitative scoring methods. Unfortunately, manual measurements are time consuming. Furthermore, also for these measurements diagnostic criteria and cut-off values should be defined.

Semi-quantitative scoring methods are often not suitable for automated analysis. However, the PRAGMA-CF method, used in three studies [124, 126, 127], provides scaled outcomes. Eventually, automated systems will replace labour-intensive manual scoring systems, as they are more reproducible, faster, and probably cheaper.

Although chest CT is the current gold standard to detect bronchiectasis, a major disadvantage is the radiation risk. The potential damage of ionising radiation is cumulative, and younger patients are more vulnerable to this effect. This issue is especially important for chronic diseases such as CF as many patients will have multiple CT scans during lifetime often starting from a young age. Even though the lifelong radiation risk for monitoring CF lung disease using biennial chest CT is considered to be low it restricts its use [139]. For this reason MRI being a radiation free imaging modality is an interesting but still technical challenging alternative for chest CT for the sensitive diagnosis of bronchiectasis. In this review, against 122 CT based studies, we identified only four that additionally collected MRI scans, of which the

authors' preferences pointed towards CT due to its high sensitivity [44, 45, 50, 101]. More sensitive chest MRI protocols are in development. Importantly, validation of these protocols is needed before MRI can be used as imaging modality for diagnosis of bronchiectasis.

Standardisation of lung volume is not routinely pursued in clinical trials, even though airway-artery ratios, and consequently the detection of bronchiectasis, are dependent on lung volume. It is highly likely that in such studies CT scans were acquired with suboptimal lung volumes. In one study of 20 subjects with CF it was shown that when patients were asked to inhale maximally without any further training and monitoring, CT scans were acquired on average at volume levels of 77% total lung capacity [140], which is a strong argument to introduce standardisation of lung volume for chest CT.

Data of reproducibility of used scoring methods were reported in only 44% of the studies. Providing data on intra- or inter-observer agreement belong to transparent data sharing and strengthens the credibility of the research reports [141]. Published intra- and inter-agreement scores showed overall good results.

Many aetiologies of bronchiectasis were described. Nowadays bronchiectasis is acknowledged as disease entity by itself. The large amount of recent publications between our initial search in December 2016 and our final search July 2018 indicates a growing interest in bronchiectasis. The development of the European patient registry for bronchiectasis patients (www.bronchiectasis.eu) will contribute importantly to improve our knowledge and facilitate new clinical trials in bronchiectasis patients [142].

Limitations of this systematic review were the following. First of all, some studies seemed to have used overlapping data. Only if exactly the same studies were published twice, we excluded older versions. However, the literature is reported in a descriptive manner and no statistical analyses were performed.

The lack of a meta-analysis of outcomes is another limitation. Due to the use of many different scoring methods and incomplete description of image acquisition and analyses, we felt that we were unable to perform such analyses. Therefore, we made five hypotheses along with research implications on how to diagnose and quantify bronchiectasis (Table 4).

Table 4. Research implications and hypotheses on how to diagnose and quantify bronchiectasis

Topic	Hypotheses	Research implications
Airway-artery ratio	Airway-artery ratios are age specific	Studies including a large number of diseased and healthy subjects from infancy into adulthood in which airway-artery ratios are measured and receiver operating characteristic curves are plotted
	The use of inner airway-artery ratios results in different outcomes than the use of outer airway-artery ratios	
Tapering	Lack of tapering is difficult to detect by eye, but is suitable for automated analysis	Studies using objective automated methods to quantify tapering
Imaging modality	Standardised, volume controlled MRI is suitable to diagnose bronchiectasis	Longitudinal studies with standardised MRI protocols that compare MRI outcomes with other clinical parameters
Scoring methods	Bronchiectasis scoring methods can serve as sensitive outcome measure in clinical studies	Longitudinal studies in which bronchiectasis is scored with standardised methods, of which both sensitivity to monitor changes in disease as well as reproducibility are being assessed

To conclude, different radiological criteria for bronchiectasis are being used but we found no validation studies supporting these criteria. Longitudinal studies including various bronchiectasis patient populations are needed to further validate bronchiectasis criteria and quantification methods. To set up validated criteria for the radiological diagnosis of bronchiectasis, an international taskforce of experts including both pulmonologists and radiologists would be needed.

Acknowledgments

We would like to acknowledge Wichor Bramer, biomedical information specialist of the medical library of Erasmus Medical Center for his help with the literature search.

References

[1] Polverino E, Goeminne PC, McDonnell MJ, Aliberti S, Marshall SE, Loebinger MR, et al. European Respiratory Society guidelines for the management of adult bronchiectasis. Eur Respir J. 2017;50.

[2] Brower KS, Del Vecchio MT, Aronoff SC. The etiologies of non-CF bronchiectasis in childhood: A systematic review of 989 subjects. BMC Pediatr. 2014;14.

[3] Chandrasekaran R, Mac Aogain M, Chalmers JD, Elborn SJ, Chotirmall SH. Geographic variation in the aetiology, epidemiology and microbiology of bronchiectasis. BMC Pulm Med. 2018;18:83.

[4] Hansell DM, Bankier AA, MacMahon H, McLoud TC, Muller NL, Remy J. Fleischner Society: glossary of terms for thoracic imaging. Radiology. 2008;246:697-722.

[5] Alzeer A. HRCT score in bronchiectasis: Correlation with pulmonary function tests and pulmonary artery pressure. Ann Thorac Med. 2008;3:82-6.

[6] Andonopoulos AP, Yarmenitis S, Georgiou P, Bounas A, Vlahanastasi C. Bronchiectasis in systemic sclerosis. A study using high resolution computed tomography. Clin Exp Rheumatol. 2001;19:187-90.

[7] Bhalla M, Turcios N, Aponte V, Jenkins M, Leitman BS, McCauley DI, et al. Cystic fibrosis: scoring system with thin-section CT. Radiology. 1991;179:783-8.

[8] Boon M, Verleden SE, Bosch B, Lammertyn EJ, McDonough JE, Mai C, et al. Morphometric Analysis of Explant Lungs in Cystic Fibrosis. American journal of respiratory and critical care medicine. 2016;193:516-26.

[9] da Silva SMD, Paschoal IA, de Capitani EM, Moreira MM, Palhares LC, Pereira MC. COPD phenotypes on computed tomography and its correlation with selected lung function variables in severe patients. Int J COPD. 2016;11:503-13.

[10] Dakin CJ, Pereira JK, Henry RL, Wang H, Morton JR. Relationship between sputum inflammatory markers, lung function, and lung pathology on high-resolution computed tomography in children with cystic fibrosis. Pediatr Pulmonol. 2002;33:475-82.

[11] Devaraj A, Wells AU, Meister MG, Loebinger MR, Wilson R, Hansell DM. Pulmonary hypertension in patients with bronchiectasis: Prognostic significance of CT signs. Am J Roentgenol. 2011;196:1300-4.

[12] Diaz AA, Young TP, Maselli DJ, Martinez CH, Maclean ES, Yen A, et al. Bronchoarterial ratio in never-smokers adults: Implications for bronchial dilation definition. Respirology. 2016.

[13] Diaz AA, Young TP, Maselli DJ, Martinez CH, Gill R, Nardelli P, et al. Quantitative CT Measures of Bronchiectasis in Smokers. Chest. 2017;151:1255-62.

[14] Dodd JD, Barry SC, Barry RBM, Gallagher CG, Skehan SJ, Masterson JB. Thin-section CT in patients with cystic fibrosis: Correlation with peak exercise capacity and body mass index. Radiology. 2006;240:236-45.

[15] Edwards EA, Metcalfe R, Milne DG, Thompson J, Byrnes CA. Retrospective review of children presenting with non cystic fibrosis bronchiectasis: HRCT features and clinical relationships. Pediatr Pulmonol. 2003;36:87-93.

[16] Emad A, Emad Y. CD4/CD8 ratio and cytokine levels of the BAL fluid in patients with bronchiectasis caused by sulfur mustard gas inhalation. J Inflamm. 2007;4.

[17] Erdem E, Ersu R, Karadag B, Karakoc F, Gokdemir Y, Ay P, et al. Effect of night symptoms and disease severity on subjective sleep quality in children with non-cystic-fibrosis bronchiectasis. Pediatr Pulmonol. 2011;46:919-26.

[18] Farrell PM, Collins J, Broderick LS, Rock MJ, Li Z, Kosorok MR, et al. Association between mucoid Pseudomonas infection and bronchiectasis in children with cystic fibrosis. Radiology. 2009;252:534-43.

[19] Gallego M, Pomares X, Espasa M, Castañer E, Solé M, Suárez D, et al. Pseudomonas aeruginosa isolates in severe chronic obstructive pulmonary disease: Characterization and risk factors. BMC Pulm Med. 2014;14.

[20] Gatheral T, Kumar N, Sansom B, Lai D, Nair A, Vlahos I, et al. COPD-related bronchiectasis; independent impact on disease course and outcomes. COPD J Chronic Obstructive Pulm Dis. 2014;11:605-14.

[21] Gregersen S, Aalokken TM, Mynarek G, Kongerud J, Aukrust P, Froland SS, et al. High resolution computed tomography and pulmonary function in common variable immunodeficiency. Respiratory medicine. 2009;103:873-80.

[22] Gregersen S, Aalokken TM, Mynarek G, Fevang B, Holm AM, Ueland T, et al. Development of pulmonary abnormalities in patients with common variable immunodeficiency: associations with clinical and immunologic factors. Ann Allergy Asthma Immunol. 2010;104:503-10.

[23] Guan WJ, Gao YH, Xu G, Lin ZY, Tang Y, Li HM, et al. Characterization of lung function impairment in adults with bronchiectasis. PLoS ONE. 2014;9.

[24] Guan WJ, Gao YH, Xu G, Lin ZY, Tang Y, Li HM, et al. Six-minute walk test in Chinese adults with clinically stable bronchiectasis: Association with clinical indices and determinants. Curr Med Res Opin. 2015;31:843-52.

[25] Guan WJ, Yuan JJ, Gao YH, Li HM, Zheng JP, Chen RC, et al. Maximal mid-expiratory flow is a surrogate marker of lung clearance index for assessment of adults with bronchiectasis. Sci rep. 2016;6:28467.

[26] Habesoglu MA, Tercan F, Ozkan U, Eyuboglu FO. Effect of radiological extent and severity of bronchiectasis on pulmonary function. Multidiscip Resp Med. 2011;6:284-90.

[27] Helbich TH, Heinz-Peer G, Fleischmann D, Wojnarowski C, Wunderbaldinger P, Huber S, et al. Evolution of CT findings in patients with cystic fibrosis. AJR Am J Roentgenol. 1999;173:81-8.

[28] Helbich TH, Heinz-Peer G, Eichler I, Wunderbaldinger P, Götz M, Wojnarowski C, et al. Cystic fibrosis: CT assessment of lung involvement in children and adults. Radiology. 1999;213:537-44.

[29] Hung TC, Lin HC, Lin KJ, Kuo HP. 133Xenon ventilation scan as a functional assessment in bronchiectasis. Chang Gung Med J. 1998;21:403-8.

[30] Ibrahim RM, Elnekeidy A, Rizk A, Yossef A, Abdelrahman S. Correlation between a proposed MDCT severity score of bronchiectasis and pulmonary function tests. Egypt J Radiol Nucl Med. 2016;47:413-20.

[31] Jong WS, Koh WJ, Kyung SL, Ji YL, Myung JC, Tae SK, et al. High-resolution CT findings of Mycobacterium avium-intracellulare complex pulmonary disease: Correlation with pulmonary function test results. Am J Roentgenol. 2008;191:W160-W6.

[32] Kharitonov SA, Wells AU, O'Connor BJ, Cole PJ, Hansell DM, Logan- Sinclair RB, et al. Elevated levels of exhaled nitric oxide in bronchiectasis. American journal of respiratory and critical care medicine. 1995;151:1889-93.

[33] Kilcoyne A, Lavelle LP, McCarthy CJ, McEvoy SH, Fleming H, Gallagher A, et al. Chest CT abnormalities and quality of life: Relationship in adult cystic fibrosis. Ann Transl Med. 2016;4.

[34] Kim JS, Muller NL, Park CS, Lynch DA, Newman LS, Grenier P, et al. Bronchoarterial ratio on thin section CT: Comparison between high altitude and sea level. J Comput Assist Tomogr. 1997;21:306-11.

[35] Lee JH, Kim YK, Kwag HJ, Chang JH. Relationships between High-Resolution Computed Tomography, Lung Function and Bacteriology in Stable Bronchiectasis. J Korean Med Sci. 2004;19:62-8.

[36] Lee AL, Button BM, Ellis S, Stirling R, Wilson JW, Holland AE, et al. Clinical determinants of the 6-Minute Walk Test in bronchiectasis. Respiratory medicine. 2009;103:780-5.

[37] Loebinger MR, Wells AU, Hansell DM, Chinyanganya N, Devaraj A, Meister M, et al. Mortality in bronchiectasis: A long-term study assessing the factors influencing survival. Eur Respir J. 2009;34:843-9.

[38] Long FR, Williams RS, Castile RG. Structural airway abnormalities in infants and young children with cystic fibrosis. J Pediatr. 2004;144:154-61.

[39] Lopes AJ, Camilo GB, de Menezes SL, Guimaraes FS. Impact of different etiologies of bronchiectasis on the pulmonary function tests. Clin Med Res. 2015;13:12-9.

[40] Lynch DA, Newell J, Hale V, Dyer D, Corkery K, Fox NL, et al. Correlation of CT findings with clinical evaluations in 261 patients with symptomatic bronchiectasis. Am J Roentgenol. 1999;173:53-8.

[41] Mahadeva R, Walsh G, Flower CDR, Shneerson JM. Clinical and radiological characteristics of lung disease in inflammatory bowel disease. Eur Respir J. 2000;15:41-8.

[42] Matsuoka S, Uchiyama K, Shima H, Ueno N, Oish S, Nojiri Y. Bronchoarterial ratio and bronchial wall thickness on high-resolution CT in asymptomatic subjects: Correlation with age and smoking. Am J Roentgenol. 2003;180:513-8.

[43] McMahon CJ, Dodd JD, Hill C, Woodhouse N, Wild JM, Fichele S, et al. Hyperpolarized 3helium magnetic resonance ventilation imaging of the lung in cystic fibrosis: Comparison with high resolution CT and spirometry. Eur Radiol. 2006;16:2483-90.

[44] Montella S, Santamaria F, Salvatore M, Pignata C, Maglione M, Iacotucci P, et al. Assessment of chest high-field magnetic resonance imaging in children and young adults with noncystic fibrosis chronic lung disease: comparison to high-resolution computed tomography and correlation with pulmonary function. Invest Radiol. 2009;44:532-8.

[45] Montella S, Maglione M, Bruzzese D, Mollica C, Pignata C, Aloj G, et al. Magnetic resonance imaging is an accurate and reliable method to evaluate non-cystic fibrosis paediatric lung disease. Respirology. 2012;17:87-91.

[46] Oikonomou A, Manavis J, Karagianni P, Tsanakas J, Wells AU, Hansell DM, et al. Loss of FEV1 in cystic fibrosis: Correlation with HRCT features. Eur Radiol. 2002;12:2229-35.

[47] Onen ZP, Eris Gulbay B, Sen E, Akkoca Yildiz O, Saryal S, Acican T, et al. Analysis of the factors related to mortality in patients with bronchiectasis. Respiratory medicine. 2007;101:1390-7.

[48] Ooi GC, Khong PL, Chan-Yeung M, Ho JC, Chan PK, Lee JC, et al. High-resolution CT quantification of bronchiectasis: clinical and functional correlation. Radiology. 2002;225:663-72.

[49] Patel IS, Vlahos I, Wilkinson TMA, Lloyd-Owen SJ, Donaldson GC, Wilks M, et al. Bronchiectasis, exacerbation indices, and inflammation in chronic obstructive pulmonary disease. American journal of respiratory and critical care medicine. 2004;170:400-7.

[50] Puderbach M, Eichinger M, Gahr J, Ley S, Tuengerthal S, Schmahl A, et al. Proton MRI appearance of cystic fibrosis: comparison to CT. Eur Radiol. 2007;17:716-24.

[51] Qi Q, Li T, Li JC, Li Y. Association of body mass index with disease severity and prognosis in patients with non-cystic fibrosis bronchiectasis. Braz J Med Biol Res. 2015;48:715-24.

[52] Shah A, Shoemark A, MacNeill SJ, Bhaludin B, Rogers A, Bilton D, et al. A longitudinal study characterising a large adult primary ciliary dyskinesia population. Eur Respir J. 2016;48:441-50.

[53] Song JW, Koh WJ, Lee KS, Lee JY, Chung MJ, Kim TS, et al. High-resolution CT findings of Mycobacterium avium-intracellulare complex pulmonary disease: correlation with pulmonary function test results. AJR Am J Roentgenol. 2008;191:1070.

[54] Wang D, Luo J, Du W, Zhang LL, He LX, Liu CT. A morphologic study of the airway structure abnormalities in patients with asthma by high-resolution computed tomography. J Thorac Dis. 2016;8:2697-708.

[55] Yang CF, Wu MT, Chiang AA, Lai RS, Chen C, Tiao WM, et al. Correlation of high-resolution CT and pulmonary function in bronchiolitis obliterans: A study based on 24 patients associated with consumption of Sauropus androgynus. AM J ROENTGENOL. 1997;168:1045-50.

[56] Bak SH, Kim S, Hong Y, Heo J, Lim MN, Kim WJ. Quantitative computed tomography features and clinical manifestations associated with the extent of bronchiectasis in patients with moderate-to-severe COPD. Int J COPD. 2018;13:1421-31.

[57] Bedi P, Chalmers JD, Goeminne PC, Mai C, Saravanamuthu P, Velu PP, et al. The BRICS (Bronchiectasis Radiologically Indexed CT Score): A Multicenter Study Score for Use in Idiopathic and Postinfective Bronchiectasis. Chest. 2018;153:1177-86.

[58] Çiftci F, Şen E, Saryal SB, Önen ZP, Gülbay B, Yildiz Ö, et al. The factors affecting survival in patients with bronchiectasis. Turk J Med Sci. 2016;46:1838-45.

[59] Dimakou K, Gousiou A, Toumbis M, Kaponi M, Chrysikos S, Thanos L, et al. Investigation of bronchiectasis in severe uncontrolled asthma. Clin Respir J. 2018;12:1212-8.

[60] Gao YH, Guan WJ, Zhu YN, Chen RC, Zhang GJ. Antibiotic-resistant Pseudomonas aeruginosa infection in patients with bronchiectasis: Prevalence, risk factors and prognostic implications. Int J COPD. 2018;13:237-46.

[61] Tsikrika S, Dimakou K, Papaioannou AI, Hillas G, Thanos L, Kostikas K, et al. The role of non-invasive modalities for assessing inflammation in patients with non-cystic fibrosis bronchiectasis. Cytokine. 2017;99:281-6.

[62] Yang X, Xu Y, Jin J, Li R, Liu X, Sun Y. Chronic rhinosinusitis is associated with higher prevalence and severity of bronchiectasis in patients with COPD. Int J COPD. 2017;12:655-62.

[63] Wielputz MO, Eichinger M, Weinheimer O, Ley S, Mall MA, Wiebel M, et al. Automatic airway analysis on multidetector computed tomography in cystic fibrosis: correlation with pulmonary function testing. J Thorac Imaging. 2013;28:104-13.

[64] Angus RM, Davies ML, Cowan MD, McSharry C, Thomson NC. Computed tomographic scanning of the lung in patients with allergic bronchopulmonary aspergillosis and in asthmatic patients with a positive skin test to Aspergillus fumigatus. THORAX. 1994;49:586-9.

[65] Arakawa H, Fujimoto K, Fukushima Y, Kaji Y. Thin-section CT imaging that correlates with pulmonary function tests in obstructive airway disease. Eur J Radiol. 2011;80:e157-e63.

[66] Aziz ZA, Wells AU, Desai SR, Ellis SM, Walker AE, MacDonald S, et al. Functional impairment in emphysema: Contribution of airway abnormalities and distribution of parenchymal disease. Am J Roentgenol. 2005;185:1509-15.

[67] Boon M, Vermeulen FL, Gysemans W, Proesmans M, Jorissen M, De Boeck K. Lung structure-function correlation in patients with primary ciliary dyskinesia. Thorax. 2015;70:339-45.

[68] Bortoluzzi CF, Volpi S, D'Orazio C, Tiddens HAWM, Loeve M, Tridello G, et al. Bronchiectases at early chest computed tomography in children with cystic fibrosis are associated with increased risk of subsequent pulmonary exacerbations and chronic pseudomonas infection. J Cyst Fibrosis. 2014;13:564-71.

[69] Brody AS, Klein JS, Molina PL, Quan J, Bean JA, Wilmott RW. High-resolution computed tomography in young patients with cystic fibrosis: distribution of abnormalities and correlation with pulmonary function tests. J Pediatr. 2004;145:32-8.

[70] Brody AS, Kosorok MR, Li Z, Broderick LS, Foster JL, Laxova A, et al. Reproducibility of a scoring system for computed tomography scanning in cystic fibrosis. J Thorac Imaging. 2006;21:14-21.

[71] de Gracia J, Vendrell M, Alvarez A, Pallisa E, Rodrigo MJ, de la Rosa D, et al. Immunoglobulin therapy to control lung damage in patients with common variable immunodeficiency. International Immunopharmacology. 2004;4:745-53.

[72] De Jong PA, Lindblad A, Rubin L, Hop WCJ, De Jongste JC, Brink M, et al. Progression of lung disease on computed tomography and pulmonary function tests in children and adults with cystic fibrosis. Thorax. 2006;61:80-5.

[73] Ekici A, Bulcun E, Karakoc T, Senturk E, Ekici M. Factors associated with quality of life in subjects with stable COPD. Respir Care. 2015;60:1585-91.

[74] Garratt LW, Sutanto EN, Ling KM, Looi K, Iosifidis T, Martinovich KM, et al. Matrix metalloproteinase activation by free neutrophil elastase contributes to bronchiectasis progression in early cystic fibrosis. Eur Respir J. 2015;46:384-94.

[75] Goeminne PC, Nawrot TS, Ruttens D, Seys S, Dupont LJ. Mortality in non-cystic fibrosis bronchiectasis: A prospective cohort analysis. Respiratory medicine. 2014;108:287-96.

[76] Guran T, Ersu R, Karadag B, Akpinar IN, Demirel GY, Hekim N, et al. Association between inflammatory markers in induced sputum and clinical characteristics in children with non-cystic fibrosis bronchiectasis. Pediatr Pulmonol. 2007;42:362-9.

[77] Jin J, Yu W, Li S, Lu L, Liu X, Sun Y. Factors associated with bronchiectasis in patients with moderate-severe chronic obstructive pulmonary disease. Medicine. 2016;95.

[78] Kadowaki T, Yano S, Wakabayashi K, Kobayashi K, Ishikawa S, Kimura M, et al. An analysis of etiology, causal pathogens, imaging patterns, and treatment of Japanese patients with bronchiectasis. Respir Invest. 2015;53:37-44.

[79] Khalilzadeh S, Kahkouee S, Hassanzad M, Parsanejad N, Baghaie N, Bloorsaz MR. The correlation of brody high resolution computed tomography scoring system with clinical status and pulmonary function test in patients with cystic fibrosis. Iran J Med Sci. 2011;36:18-23.

[80] Kosar M, Kurt A, Keskin S, Keskin Z, Arslan H. Evaluation of effects of bronchiectasis on bronchial artery diameter with multidetector computed tomography. Acta Radiol. 2014;55:171-8.

[81] Loeve M, Gerbrands K, Hop WC, Rosenfeld M, Hartmann IC, Tiddens HA. Bronchiectasis and pulmonary exacerbations in children and young adults with cystic fibrosis. Chest. 2011;140:178-85.

[82] Maekawa K, Ito Y, Oga T, Hirai T, Kubo T, Fujita K, et al. High-resolution computed tomography and health-related quality of life in Mycobacterium avium complex disease. International Journal of Tuberculosis and Lung Disease. 2013;17:829-35.

[83] Maglione M, Bush A, Montella S, Mollica C, Manna A, Esposito A, et al. Progression of lung disease in primary ciliary dyskinesia: is spirometry less accurate than CT? Pediatr Pulmonol. 2012;47:498-504.

[84] Mott LS, Graniel KG, Park J, De Klerk NH, Sly PD, Murray CP, et al. Assessment of early bronchiectasis in young children with cystic fibrosis is dependent on lung volume. Chest. 2013;144:1193-8.

[85] Oikonomou A, Tsanakas J, Hatziagorou E, Kirvassilis F, Efremidis S, Prassopoulos P. High resolution computed tomography of the chest in cystic fibrosis (CF): Is simplification of scoring systems feasible? Eur Radiol. 2008;18:538-47.

[86] Owens CM, Aurora P, Stanojevic S, Bush A, Wade A, Oliver C, et al. Lung clearance index and HRCT are complementary markers of lung abnormalities in young children with CF. Thorax. 2011;66:481-8.

[87] Parr DG, Guest PG, Reynolds JH, Dowson LJ, Stockley RA. Prevalence and impact of bronchiectasis in alpha1-antitrypsin deficiency. American journal of respiratory and critical care medicine. 2007;176:1215-21.

[88] Perez-Rovira A, Kuo W, Petersen J, Tiddens HA, de Bruijne M. Automatic airway-artery analysis on lung CT to quantify airway wall thickening and bronchiectasis. Med Phys. 2016;43:5736.

[89] Pifferi M, Caramella D, Bulleri A, Baldi S, Peroni D, Pietrobelli A, et al. Pediatric bronchiectasis: Correlation of HRCT, ventilation and perfusion scintigraphy, and pulmonary function testing. Pediatr Pulmonol. 2004;38:298-303.

[90] Pifferi M, Bush A, Pioggia G, Caramella D, Tartarisco G, Di Cicco M, et al. Evaluation of pulmonary disease using static lung volumes in primary ciliary dyskinesia. Thorax. 2012;67:993-9.

[91] Roberts HR, Wells AU, Milne DG, Rubens MB, Kolbe J, Cole PJ, et al. Airflow obstruction in bronchiectasis: Correlation between computed tomography features and pulmonary function tests. Thorax. 2000;55:198-204.

[92] Robroeks CMHHT, Roozeboom MH, De Jong PA, Tiddens HAWM, Jöbsis Q, Hendriks HJ, et al. Structural lung changes, lung function, and non-invasive inflammatory markers in cystic fibrosis. Pediatric allergy and immunology : official publication of the European Society of Pediatric Allergy and Immunology. 2010;21:493-500.

[93] Rowan SA, Bradley JM, Bradbury I, Lawson J, Lynch T, Gustafsson P, et al. Lung clearance index is a repeatable and sensitive indicator of radiological changes in bronchiectasis. American journal of respiratory and critical care medicine. 2014;189:586-92.

[94] Sanders DB, Li ZH, Brody AS, Farrell PM. Chest Computed Tomography Scores of Severity Are Associated with Future Lung Disease Progression in Children with Cystic Fibrosis. Am J Respir Crit Care Med. 2011;184:816-21.

[95] Santamaria F, Montella S, Tiddens HAWM, Guidi G, Casotti V, Maglione M, et al. Structural and functional lung disease in primary ciliary dyskinesia. Chest. 2008;134:351-7.

[96] Shah R, Sexauer W, Ostrum BJ, Fiel S, Friedman AC. High-resolution CT in the acute exacerbation of cystic fibrosis: Evaluation of acute findings, reversibility of those findings, and clinical correlation. AM J ROENTGENOL. 1997;169:375-80.

[97] Sheehan RE, Wells AU, Copley SJ, Desai SR, Howling SJ, Cole PJ, et al. A comparison of serial computed tomography and functional change in bronchiectasis. Eur Respir J. 2002;20:581-7.

[98] Sheikh SI, Long FR, McCoy KS, Johnson T, Ryan-Wenger NA, Hayes D. Computed tomography correlates with improvement with ivacaftor in cystic fibrosis patients with G551D mutation. J Cyst Fibrosis. 2015;14:84-9.

[99] Stick SM, Brennan S, Murray C, Douglas T, von Ungern-Sternberg BS, Garratt LW, et al. Bronchiectasis in Infants and Preschool Children Diagnosed with Cystic Fibrosis after Newborn Screening. J Pediatr. 2009;155:623-8.e1.

[100] Tepper LA, Utens EM, Caudri D, Bos AC, Gonzalez-Graniel K, Duivenvoorden HJ, et al. Impact of bronchiectasis and trapped air on quality of life and exacerbations in cystic fibrosis. Eur Respir J. 2013;42:371-9.

[101] Tepper LA, Ciet P, Caudri D, Quittner AL, Utens EM, Tiddens HA. Validating chest MRI to detect and monitor cystic fibrosis lung disease in a pediatric cohort. Pediatr Pulmonol. 2016;51:34-41.

[102] Van Der Giessen L, Loeve M, De Jongste J, Hop W, Tiddens H. Nocturnal cough in children with stable cystic fibrosis. Pediatr Pulmonol. 2009;44:859-65.

[103] Widger J, Ranganathan S, Robinson PJ. Progression of structural lung disease on CT scans in children with cystic fibrosis related diabetes. Journal of Cystic Fibrosis. 2013;12:216-21.

[104] Zoumot Z, Boutou AK, Gill SS, Van Zeller M, Hansell DM, Wells AU, et al. Mycobacterium avium complex infection in non-cystic fibrosis bronchiectasis. Respirology. 2014;19:714-22.

[105] Caudri D, Turkovic L, Ng J, de Klerk NH, Rosenow T, Hall GL, et al. The association between Staphylococcus aureus and subsequent bronchiectasis in children with cystic fibrosis. J Cyst Fibrosis. 2018;17:462-9.

[106] DeBoer EM, Kroehl ME, Wagner BD, Accurso FJ, Harris JK, Lynch DA, et al. Proteomic profiling identifies novel circulating markers associated with bronchiectasis in cystic fibrosis. Proteomics Clin Appl. 2017;11.

[107] do Amaral RH, Nin CS, de Souza VVS, Alves GRT, Marchiori E, Irion K, et al. Computed Tomography Findings of Bronchiectasis in Different Respiratory Phases Correlate with Pulmonary Function Test Data in Adults. Lung. 2017;195:347-51.

[108] Kuo W, Soffers T, Andrinopoulou ER, Rosenow T, Ranganathan S, Turkovic L, et al. Quantitative assessment of airway dimensions in young children with cystic fibrosis lung disease using chest computed tomography. Pediatr Pulmonol. 2017;52:1414-23.

[109] Nathanson I, Conboy K, Murphy S, Afshani E, Kuhn JP. Ultrafast computerized tomography of the chest in cystic fibrosis: a new scoring system. Pediatr Pulmonol. 1991;11:81-6.

[110] Naidich DP, McCauley DI, Khouri NF. Computed tomography of bronchiectasis. J COMPUT ASSISTED TOMOGR. 1982;6:437-44.

[111] Chalmers JD, Goeminne P, Aliberti S, McDonnell MJ, Lonni S, Davidson J, et al. The bronchiectasis severity index an international derivation and validation study. American journal of respiratory and critical care medicine. 2014;189:576-85.

[112] Hansell DM, Rubens MB, Padley SPG, Wells AU. Obliterative bronchiolitis: Individual CT signs of small airways disease and functional correlation. Radiology. 1997;203:721-6.

[113] Martinez-Garcia MA, Perpina-Tordera M, Roman-Sanchez P, Soler-Cataluna JJ. Quality-of-life determinants in patients with clinically stable bronchiectasis. Chest. 2005;128:739-45.

[114] Martínez-García MA, Perpiñá-Tordera M, Soler-Cataluña JJ, Román-Sánchez P, Lloris-Bayo A, González-Molina A. Dissociation of lung function, dyspnea ratings and pulmonary extension in bronchiectasis. Respiratory medicine. 2007;101:2248-53.

[115] Martínez-García MA, De Gracia J, Relat MV, Girón RM, Carro LM, De La Rosa Carrillo D, et al. Multidimensional approach to non-cystic fibrosis bronchiectasis: The FACED score. Eur Respir J. 2014;43:1357-67.

[116] McDonnell MJ, Aliberti S, Goeminne PC, Restrepo MI, Finch S, Pesci A, et al. Comorbidities and the risk of mortality in patients with bronchiectasis: an international multicentre cohort study. Lancet Respir Med. 2016;4:969-79.

[117] Miszkiel KA, Wells AU, Rubens MB, Cole PJ, Hansell DM. Effects of airway infection by Pseudomonas aeruginosa: A computed tomographic study. THORAX. 1997;52:260-4.

[118] Santamaria F, Montella S, Camera L, Palumbo C, Greco L, Boner AL. Lung structure abnormalities, but normal lung function in pediatric bronchiectasis. Chest. 2006;130:480-6.

[119] Tang X, Bi J, Yang D, Chen S, Li Z, Chen C, et al. Emphysema is an independent risk factor for 5-year mortality in patients with bronchiectasis. Clin Respir J. 2016.

[120] Wilson CB, Jones PW, O'Leary CJ, Hansell DM, Cole PJ, Wilson R. Effect of sputum bacteriology on the quality of life of patients with bronchiectasis. EUR RESPIR J. 1997;10:1754-60.

[121] Wong-You-Cheong JJ, Leahy BC, Taylor PM, Church SE. Airways obstruction and bronchiectasis: Correlation with duration of symptoms and extent of bronchiectasis on computed tomography. CLIN RADIOL. 1992;45:256-9.

[122] de Jong PA, Nakano Y, Lequin MH, Mayo JR, Woods R, Pare PD, et al. Progressive damage on high resolution computed tomography despite stable lung function in cystic fibrosis. Eur Respir J. 2004;23:93-7.

[123] De Jong PA, Nakano Y, Hop WC, Long FR, Coxson HO, Paré PD, et al. Changes in airway dimensions on computed tomography scans of children with cystic fibrosis. American journal of respiratory and critical care medicine. 2005;172:218-24.

[124] Kuo W, Andrinopoulou ER, Perez-Rovira A, Ozturk H, de Bruijne M, Tiddens HAWM. Objective airway artery dimensions compared to CT scoring methods assessing structural cystic fibrosis lung disease. J Cyst Fibrosis. 2017;16:116-23.

[125] Kuo W, de Bruijne M, Petersen J, Nasserinejad K, Ozturk H, Chen Y, et al. Diagnosis of bronchiectasis and airway wall thickening in children with cystic fibrosis: Objective airway-artery quantification. Eur Radiol. 2017;27:4680-9.

[126] Rosenow T, Oudraad MC, Murray CP, Turkovic L, Kuo W, de Bruijne M, et al. PRAGMA-CF. A Quantitative Structural Lung Disease Computed Tomography Outcome in Young Children with Cystic Fibrosis. American journal of respiratory and critical care medicine. 2015;191:1158-65.

[127] Ramsey KA, Rosenow T, Turkovic L, Skoric B, Banton G, Adams AM, et al. Lung clearance index and structural lung disease on computed tomography in early cystic fibrosis. American journal of respiratory and critical care medicine. 2016;193:60-7.

[128] Lopes AJ, Camilo GB, de Menezes SLS, Guimarães FS. Impact of different etiologies of bronchiectasis on the pulmonary function tests. Clin Med Res. 2015;13:12-9.

[129] Parr DG, Guest PG, Reynolds JH, Dowson LJ, Stockley RA. Prevalence and impact of bronchiectasis in α1-antitrypsin deficiency. American journal of respiratory and critical care medicine. 2007;176:1215-21.

[130] Gregersen S, Aaløkken TM, Mynarek G, Kongerud J, Aukrust P, Frøland SS, et al. High resolution computed tomography and pulmonary function in common variable immunodeficiency. Respiratory medicine. 2009;103:873-80.

[131] Gregersen S, Aaløkken TM, Mynarek G, Fevang B, Holm AM, Ueland T, et al. Development of pulmonary abnormalities in patients with common variable immunodeficiency: associations with clinical and immunologic factors. Ann Allergy Asthma Immunol. 2010;104:503-10.

[132] Ooi GC, Khong PL, Chan-Yeung M, Ho JCM. High-Resolution CT Quantification of Bronchiectasis: Clinical and Functional Correlation 1. Radiology. 2002.

[133] Perez-Rovira A, Kuo W, Petersen J, Tiddens HAWM, De Bruijne M. Automatic airway-artery analysis on lung CT to quantify airway wall thickening and bronchiectasis. Med Phys. 2016;43:5736-44.

[134] Boon M, Verleden SE, Bosch B, Lammertyn EJ, McDonough JE, Mai C, et al. Morphometric Analysis of Explant Lungs in Cystic Fibrosis. Am J Respir Crit Care Med. 2016;193:516-26.

[135] Wainwright CE, Vidmar S, Armstrong DS, Byrnes CA, Carlin JB, Cheney J, et al. Effect of bronchoalveolar lavage-directed therapy on Pseudomonas aeruginosa infection and structural lung injury in children with cystic fibrosis: a randomized trial. Jama. 2011;306:163-71.

[136] Joress MMH RS. The diagnosis of bronchiectasis: Clinical and roentgenological observations. Chest. 1944;10:489-508.

[137] Copley SJ, Wells AU, Hawtin KE, Gibson DJ, Hodson JM, Jacques AE, et al. Lung morphology in the elderly: comparative CT study of subjects over 75 years old versus those under 55 years old. Radiology. 2009;251:566-73.

[138] Janssens JP, Pache JC, Nicod LP. Physiological changes in respiratory function associated with ageing. Eur Respir J. 1999;13:197-205.

[139] Kuo W, Ciet P, Tiddens HA, Zhang W, Guillerman RP, van Straten M. Monitoring cystic fibrosis lung disease by computed tomography. Radiation risk in perspective. American journal of respiratory and critical care medicine. 2014;189:1328-36.

[140] Loeve M, Lequin MH, De Bruijne M, Hartmann IJC, Gerbrands K, Van Straten M, et al. Cystic fibrosis: Are volumetric ultra-low-dose expiratory CT scans sufficient for monitoring related lung disease? Radiology. 2009;253:223-9.

[141] Szczesniak R, Turkovic L, Andrinopoulou ER, Tiddens H. Chest imaging in cystic fibrosis studies: What counts, and can be counted? J Cyst Fibros. 2017;16:175-85.

[142] Chotirmall SH, Chalmers JD. Bronchiectasis: an emerging global epidemic. BMC Pulm Med. 2018;18:76.

Supplementary Materials

Table S1. Search query per database

Database	Search query
Embase.com	('bronchiectasis'/exp/mj OR (bronchiectas*):ab,ti) AND ('diagnostic imaging'/exp OR 'computer assisted tomography'/exp OR 'nuclear magnetic resonance imaging'/exp OR 'X ray'/de OR 'radiodiagnosis'/de OR 'radiography'/de OR 'computer assisted diagnosis'/de OR 'diagnostic imaging equipment'/exp OR 'radiology'/de OR ((diagnos* NEAR/3 (imag*)) OR (compute* NEAR/3 tomogra*) OR ((ct OR cat) NEAR/3 (scan OR imag*)) OR hrct OR (magnetic* NEAR/3 resonan*) OR mri OR 'X ray' OR rontgen OR roentgen OR radiodiagnos* OR radiogra* OR radiolog* OR (compute* NEAR/3 assist* NEAR/3 diagnos*)):ab,ti) NOT ({Conference Abstract}/lim OR {Pappalettera, #1118}/lim OR {Note}/lim OR {Editorial}/lim) AND {english}/lim NOT ({animals}/lim NOT {humans}/lim)
Medline Ovid	("Bronchiectasis"/ OR (bronchiectas*).ab,ti.) AND ("Diagnostic Imaging"/ OR exp "Tomography"/ OR "X-Rays"/ OR exp "Radiography"/ OR exp "Image Interpretation, Computer-Assisted"/ OR "radiology"/ OR ((diagnos* ADJ3 (imag*)) OR (compute* ADJ3 tomogra*) OR ((ct OR cat) ADJ3 (scan OR imag*)) OR hrct OR (magnetic* ADJ3 resonan*) OR mri OR "X ray" OR rontgen OR roentgen OR radiodiagnos* OR radiogra* OR radiolog* OR (compute* ADJ3 assist* ADJ3 diagnos*)).ab,ti.) NOT (letter OR news OR comment OR editorial OR congresses OR abstracts).pt. AND english.la. NOT (exp animals/ NOT humans/) Cochrane ((bronchiectas*):ab,ti) AND (((diagnos* NEAR/3 (imag*)) OR (compute* NEAR/3 tomogra*) OR ((ct OR cat) NEAR/3 (scan OR imag*)) OR hrct OR (magnetic* NEAR/3 resonan*) OR mri OR 'X ray' OR rontgen OR roentgen OR radiodiagnos* OR radiogra* OR radiolog* OR (compute* NEAR/3 assist* NEAR/3 diagnos*)):ab,ti)
Web of Science	TS=(((bronchiectas*)) AND (((diagnos* NEAR/2 (imag*)) OR (compute* NEAR/2 tomogra*) OR ((ct OR cat) NEAR/2 (scan OR imag*)) OR hrct OR (magnetic* NEAR/2 resonan*) OR mri OR "X ray" OR rontgen OR roentgen OR radiodiagnos* OR radiogra* OR radiolog* OR (compute* NEAR/2 assist* NEAR/2 diagnos*))))
Google Scholar	bronchiectasis "diagnostic imaging"|"computed tomography"|"computer*tomography"|"ct|cat scan"|"magnetic resonance"|mri|"X ray"|rontgen|roentgen|radiodiagnosis|radiography|radiology|"computer assisted diagnosis"

Table S2. Scoring items of the semi-quantified methods

Table S2a. Scoring items of the semi-quantified methods to assess the extent of bronchiectasis

Items for extent of bronchiectasis	n studies (%)
1) 0-33% of the lobe 2) 33-66% of the lobe 3) 66-100% of the lobe	27 (22%)*
1) 1-5 of the segments 2) 6-9 of the segments 3) > 9 of the segments	27 (22%)#
1) 1 segment 2) ≥ 2 segments 3) Generalised cystic bronchiectasis	18 (15%)
1) > 25% of the bronchi 2) 25-49% of the bronchi 3) 50-74% of the bronchi 4) ≥ 75% of the bronchi	9 (7%)
Number of lobes	4 (3%)
1) Up to the central part of lung 2) Up to the middle part of lung 3) Up to the peripheral part of lung	4 (3%)
1) ≤ 50% of the airways 2) > 50% of the airways	3 (2%)
1) ≤ 50% of the lobe 2) > 50% of the lobe	2 (2%)
1) 1 segment 2) ≥ 2 segments	2 (2%)
1) < 25% of the bronchi 2) 25-49% of the bronchi 3) 50-100% of the bronchi	2 (2%)
Number of segments	1 (1%)
1) < 50% of the segment 2) ≥ 50% of the segment 3) Cystic bronchiectasis in the segment	1 (1%)
1) < 20% of the lobe 2) 20-50% of the lobe 3) > 50% of the lobe	1 (1%)

*Scores used in the scoring method described by Brody et al. and by the CF-CT method [70, 135]. # Extent scores used in the method described by Bhalla et al. [7].

Table S2b. Scoring items of the semi-quantified methods to assess the severity of dilatation.

Items for severity of dilatation	n studies (%)
1) Airway-artery ratio = 1-2 2) Airway-artery ratio = 2-3 3) Airway-artery ratio > 3	65 (53%)*
1) Cylindrical 2) Varicose 3) Cystic	12(10%)
1) Airway-artery ratio = 1-2 2) Airway-artery ratio > 2	6 (5%)
1) Airway-artery ratio = 1.5-2 2) Airway-artery ratio = 2-3 3) Airway-artery ratio > 3	3 (2%)
1) Airway-artery ratio = 1.1-1.5 2) Airway-artery ratio > 1.5	2 (2%)
1) Airway-artery ratio > 1 2) Obvious dilatation 3) Cystic dilatation	1 (1%)
1) Mild and rare dilatation 2) Severe and diffuse dilatation	1 (1%)
1) Maximal airway diameter < 10 mm 2) Maximal airway diameter = 10-15 mm 3) Maximal airway diameter > 15 mm	1 (1%)
1) Cylindrical, airway-artery ratio = 1.5-3 2) Cylindrical, airway-artery ratio > 3 3) Varicose 4) Cystic	1 (1%)
1) Slightly dilated and non-tapering airways in <4 segments 2) Focal dilated airways slightly enlarged in 4-6 segments 3) Multiple foci of mildly dilated airways or a few foci of moderately dilated airways 4) Diffuse moderate to severe dilatation in most lobes, with other features such as cystic or varicose bronchiectasis	1 (1%)
1) Cylindrical - minimal 2) Cylindrical - extensive 3) Saccular - minimal 4) Saccular - extensive 5) Cystic	1 (1%)

*The most often reported methods, used for the Bhalla, Brody, and CF-CT scoring system to assess the severity of dilatation [7, 70, 135].

Chapter 3

The radiological diagnosis of bronchiectasis: What's in a name?

European Respiratory Review 2020; 29: 190120

Harm A.W.M. Tiddens, Jennifer J. Meerburg, Menno M. van der Eerden and Pierluigi Ciet

Abstract

Diagnosis of bronchiectasis is usually made using chest computed tomography (CT) scan, the current gold standard method. A bronchiectatic airway can show abnormal widening and thickening of its airway wall. In addition, it can show an irregular wall and lack of tapering, and/or can be visible in the periphery of the lung. Its diagnosis is still largely expert based. More recently, it has become clear that airway dimensions on CT and therefore the diagnosis of bronchiectasis are highly dependent on lung volume. Hence, control of lung volume is required during CT acquisition to standardise the evaluation of airways. Automated image analysis systems are in development for the objective analysis of airway dimensions and for the diagnosis of bronchiectasis. To use these systems, clear and objective definitions for the diagnosis of bronchiectasis are needed. Furthermore, the use of these systems requires standardisation of CT protocols and of lung volume during chest CT acquisition. In addition, sex- and age-specific reference values are needed for image analysis outcome parameters. This review focusses on today's issues relating to the radiological diagnosis of bronchiectasis using state-of-the-art CT imaging techniques.

Introduction

Bronchiectasis is derived from the Greek words bronckos meaning airway and ectasis meaning widening. However, depending on which specialist you are speaking to in the medical arena, bronchiectasis will have a different meaning and definition. A pathologist will associate bronchiectasis with the typical histological features, which include an abnormally widened airway with loss of the ciliary epithelial layer, a damaged epithelium and destruction of the elastin layer [1]. A radiologist will associate bronchiectasis with the typical chest computed tomography (CT) scan features, consisting of an abnormally widened and thickened airway with an irregular wall, lack of tapering and/or visibility of the airway in the periphery of the lung [2]. A (paediatric) pulmonologist will mostly diagnose bronchiectasis in a patient experiencing specific symptoms, such as dyspnoea, productive cough, loss of appetite and weight loss, recurrent airway infections and localised persistent rhonchi, with or without the radiological evidence of bronchiectasis [3, 4]. In general, bronchiectasis is a man-made "diagnosis" that does not have the clear boundaries of diagnosis of conditions such as asthma or chronic obstructive pulmonary disease. There are many causes of bronchiectasis, such as immune deficiencies, smoking-related airways disease, foreign body aspiration, recurrent gastric acid aspiration, cystic fibrosis (CF), autoimmune diseases, pneumonia and primary ciliary dyskinesia (PCD). However, in a large group of patients, no underlying disease was identified [5].

The diagnosis of bronchiectasis has varied over time. Before imaging, a diagnosis of bronchiectasis was primarily made post mortem through pathology findings. Imaging then allowed us to observe highly abnormally widened airways on chest radiographs, and later with more precision using bronchography techniques [6]. Since the mid-1990s, thanks to the development of high-resolution CT algorithms, chest CT became the gold standard for the diagnosis of bronchiectasis, as it was a more precise and less invasive technique than bronchography [2, 7]. More recently, it was shown that it is possible to use magnetic resonance imaging (MRI) to diagnose bronchiectasis [8]. These more advanced diagnostic imaging techniques have allowed identification of the underlying pathophysiology of bronchiectasis in more patients. Hence, when reading literature on bronchiectasis, the timeframe should be taken into consideration. For this review, we will primarily focus on today's issues relating to the radiological diagnosis of bronchiectasis using state-of-the-art CT imaging techniques.

Radiological definition of bronchiectasis

In today's medical practice, the radiological diagnosis of bronchiectasis is mostly made using chest CT, as this technique is more sensitive than chest radiographs. However, the criteria for bronchiectasis are in general not well defined. When asking

a radiologist about the definition of bronchiectasis, the answer will mostly include: "when the diameter of the airway is larger than the adjacent artery", "when an airway is clearly visible in the periphery of the lung", "when an airway has an irregular wall" and when "lack of tapering" can be observed. Interestingly, for these definitions, proper age- and sex-related reference values are lacking. These definitions probably work quite well in daily clinical practice for highly abnormally widened airways and/or in those who show a lack of tapering over multiple generations. For such advanced bronchiectasis airways, there will be fair to good inter- or intra-observer reproducibility of the diagnosis [9]. However, for the detection of early or mild stages of bronchiectasis disease, the radiological diagnosis becomes more critical and there will be more variability between observers. Precise and well-standardised diagnostic criteria are needed for the correct diagnosis of subtler airway changes.

When comparing the airway to artery (AA) ratio to diagnose bronchiectasis, a number of questions are unresolved. To begin with, should the inner or outer airway diameter be used for comparison with the adjacent artery? Currently, the inner airway diameter is generally used. However, this definition does not take into account the fact that the inner airway diameter of a widened airway can be reduced due to mucus attached to the airway wall and folding of the mucosa [10]. This results in a reduction of the internal diameter (Figure 1) and also of the AA ratio. As a result, when using the internal diameter for comparison with the artery, such an airway might no longer meet the bronchiectasis criteria. In addition, in comparison with outer diameter, the inner diameter is more dependent on the lung volume level during CT acquisition [11].

At lung volumes below total lung capacity (TLC), the AA ratio will reduce more quickly when the inner airway diameter is used relative to the outer airway diameter [11, 12]. Hence, when the CT is performed at lung volumes below TLC, bronchiectasis may be missed when the inner airway diameter is used. Another issue with using the AA ratio for the diagnosis of bronchiectasis is the assumption that the arterial diameters remain unchanged in relation to lung disease. It is likely that there are conditions that can affect arterial diameters. The pulmonary artery system reduces blood flow to diseased areas of the lung thanks to the so-called hypoxic pulmonary vasoconstriction response. When this response includes a large region of the lung and when it persists for longer periods of time, it is possible that this will affect arterial diameters in such a region. Hence, the hypoxic pulmonary vasoconstriction response in diseased areas of the lung can result in an increase of the AA ratio. Other conditions that can reduce the dimensions of the pulmonary arteries are smoking and high altitude [13, 14]. In chronic lung diseases, such as interstitial lung disease, the volume of pulmonary vessels tends to increase with the severity of disease [15].

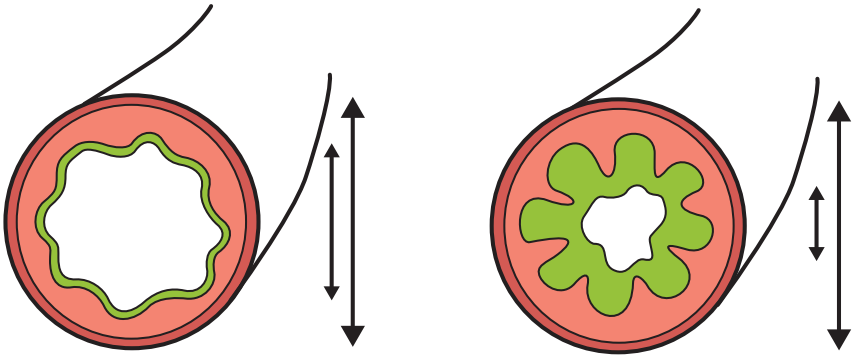

Figure 1. Consequences of using the inner or outer airway diameter for the diagnosis of bronchiectasis

On the left a healthy airway and on the right an inflamed airway with a thickened wall at full inspiration. On inspiration, the mucosa of the healthy airway is only slightly folded. The inflamed airway has larger folds compared with the normal airway. Mucus fills up the gaps between the mucosal folds. On chest CT, the folds and mucus will be interpreted as a thickened airway wall. This figure also illustrates why the outer diameter is a more robust parameter for diagnosing and quantifying bronchiectasis because in contrast to the inner diameter, it is not influenced by the presence of mucus in the lumen. Image provided by, and reproduced and modified with the kind permission of, Marloes Meerburg (Amsterdam, the Netherlands).

Clearly, there is a need for age- and sex-related reference values for both airway and arterial dimensions. Such reference values should include children, because it is as yet unclear whether the same cut-off values for the AA ratio can be used as for adults and for children [11, 16-18]. To obtain such data is challenging as it will expose a healthy population to ionising radiation. Fortunately, the radiation doses needed for chest CTs have come down substantially, which has opened up the feasibility of using chest CTs in a healthy population. In addition, software is in development that allows the automatic and thus objective and reproducible measurements of AA dimensions of all visible AA pairs throughout the bronchial tree [19].

The presence of thickened and widened airways in the periphery of the lung is an important feature of bronchiectasis [20]. In the periphery of the lung, airways are small and are therefore mostly not visible, as their diameter is beyond the resolution of the CT scanner. It has been shown that in children with CF, the number of airways visible on a chest CT scan was doubled in relation to control subjects [20]. This is largely due to small airways that have become visible thanks to thickening of the airway wall. On routine examination, these airways can easily be overlooked as being abnormal because their walls are thin.

For "lack of tapering", the other definition of bronchiectasis, objective and sensitive criteria are also lacking, similar to the AA ratio. Currently, lack of tapering is visually determined by the radiologist. Automated systems to assess inter- and intra-airway branch tapering are in development and could be a sensitive approach to detecting airways disease [21]. A major advantage of using tapering as a parameter of bronchiectasis, is that it does not require comparison to the pulmonary arteries, which makes it an important additional feature to the AA ratio. A challenge when analysing tapering is the automated system's recognition of airways that are occluded by mucus. Artificial intelligence techniques can be of help to reconstruct the complete bronchial tree to overcome this problem.

Therefore, for the objective and sensitive diagnosis of bronchiectasis on CT, objective quantitative criteria are needed to define widening, thickening and lack of tapering of the airways. To do so, age- and sex-dependent reference values for normal airway dimensions need to be developed.

Standardisation of lung volume

The importance of volume control during chest CT imaging has been understood since the late 1990s. Airway and arterial dimensions, parenchymal density and orientation of anatomical structures are all highly dependent on the respiratory phase and lung volume at which the chest CT is acquired (Figure 2). Standardisation of the lung volume at TLC for the inspiratory CT scan and residual volume for an expiratory CT scan facilitates the objective and reproducible evaluation of AA dimensions, and reduces the risk of misinterpretation. Hence, volume standardisation for the acquisition of a chest CT fits the "as low as reasonably achievable" paradigm as the best diagnostic result will be obtained for the radiation given to the subject. Furthermore, standardising lung volume facilitates the longitudinal comparison between CT scans, as it allows slice by slice comparison.

Implementation of volume standardisation in cooperative patients is relatively easy to organise and has been extensively described [22, 23]. Clinical implementation of this is not rocket science. In short, a spirometry training session with the lung function scientist is scheduled on the day of the CT, generally half an hour prior to the CT scan. Lung function scientists are highly experienced in obtaining maximal respiratory effort from patients; they are practised in training patients and are able to coach patients to execute the correct breathing manoeuvres during CT scanning. The training session serves to: train the patient to execute the appropriate breathing manoeuvres; obtain the targeted lung volumes; collect spirometry values to be used during scanning; and alleviate anxiety by familiarising the patient with the scanner, the technique and instructions. Half an hour is generally sufficient for nearly all

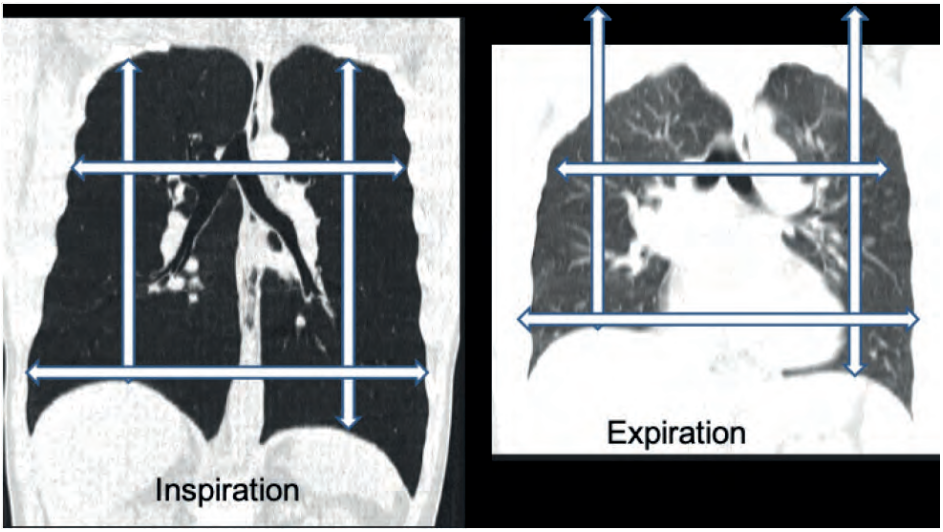

Figure 2. Lung volume on computed tomography at total lung capacity and after full expiration

A spirometer-controlled chest computed tomography scan of a healthy adult showing the lung in the coronal plane at a) total lung capacity (TLC) and b) after full expiration at residual volume level. a) Arrows indicate the maximal height and width of the lung at TLC. b) The same dimensions projected over the lung in expiration. Note that the largest displacement is in the cranial caudal direction. Also note the differences in lung density and the altered orientation of the left and right main stem bronchi between inspiration and expiration. Finally, at full inspiration, the pleura parietalis is bulging out between the ribs, while on expiration the pleura parietalis is bulging in.

patients ≥ 5 years of age to achieve the training goals. In our centre the session is scheduled just prior to the scan in the lung function department, or in a preparation room close to the scanner. During the scan, the lung function scientist coaches the patient and collaborates closely with the radiographer, who can focus on operating the scanner. Importantly, the spirometer-controlled procedure does not take up more time in the scanner for the patient; therefore, there is no reduction in CT productivity.

Spirometer-guided chest imaging is a viable method that can be implemented in cooperative patients. It was introduced in our centre for school-aged children as part of our clinical routine in 2007, and it has been successful in 90% of scans [22]. The technical equipment needed and the logistics required to implement spirometer-guided chest imaging are feasible for most centres. Where it is not feasible for a patient to use a spirometer, a good volume result can also be obtained when breathing manoeuvres are given by the lung function technician during the CT scan.

Therefore, volume standardisation of chest CTs can and should be implemented in clinical routine as a shared responsibility of pulmonologists and radiologists.

Standardisation of CT protocols

As for standardisation of the lung volume of chest CTs, a higher level of standardisation of CT scan settings and image reconstruction is required for the sensitive evaluation of airway dimensions. In today's radiology practice, chest CT protocols still vary widely between and even within hospitals, and often depend on local preferences by radiologists [24]. The following CT settings need to be standardised.

Volumetric techniques should be used. It is also important that a CT protocol is used that allows the reconstruction of ≤ 1 mm slices. Such a protocol is often referred to as a high-resolution CT. For evaluation, the images should be reconstructed with a slice thickness of ≤ 1 mm in the axial, sagittal and coronal plane, meaning airways can easily be followed through the bronchial tree, thereby making it possible to differentiate bronchiectasis from other abnormalities, such as cysts, abscesses and bulla. This CT protocol also allows a slice by slice comparison between two chest CT scans to evaluate disease progression. In addition, slice thickness is an important determinant of airway wall thickness. The wall of an airway cut in cross-section appears thicker on a 3- or 5-mm reconstructed slice compared with a 1 mm slice.

Reconstruction kernels should be standardised, as they impact upon the appearance of the lung tissue. For the comparison of two consecutive CTs, reconstruction filters should be similar. To allow the use of automated analysis methods, it is recommended that a series that uses filtered back projection is included where available [19, 25]. If using iterative reconstruction techniques, it is recommended that a kernel specifically designed for quantitative analysis is included.

Finally, a low-dose CT protocol can be used as it been shown that low-dose thin-section CTs are sufficiently sensitive for the detection of bronchiectasis in paediatric and adult patients [26, 27].

To achieve uniformity in CT protocols within and between centres, task forces involving respiratory societies, radiology societies and image analysis companies are required. These standardisation efforts are a prerequisite for the inclusion of chest CT-related bronchiectasis outcome measures that use automated image analysis tools in registries and clinical trials [24].

Image analysis

Today's radiology reports of chest images for routine care are still largely expert based, mostly unstandardised and generally do not contain quantitative outcome data. In other clinical specialities like cardiology, quantitative post-processing methods to acquire objective measures of coronary artery stenosis and of pulmonary artery and aorta dimensions are available and well-implemented [28, 29].

For bronchiectasis patients, there are currently three multidimensional scores that include radiological assessment: the Bronchiectasis Severity Index (BSI) [30]; the FACED (forced expiratory volume in 1 s (FEV_1), age, chronic colonisation, extension and dyspnoea) score [31]; and the E-FACED (FACED plus exacerbations) score [32]. In the BSI, 1 point is assigned where the number of affected lobes is three or higher, or where cystic bronchiectasis is present (maximum BSI score: 26). Other parameters are age, body mass index, FEV_1 % predicted, hospital admissions, exacerbations, dyspnoea score, *Pseudomonas aeruginosa (Pa)* colonisation and colonisation with other organisms. In the FACED score, 1 point is assigned where more than two lobes are affected (max score: 7 points). Other parameters are chronic *Pa* colonisation, dyspnoea score, FEV_1 % predicted and age. For the E-FACED score, the number of exacerbations in the year before the CT scan is included to predict future yearly exacerbations.

The Bronchiectasis Radiologically Indexed CT Score (BRICS) is a very quick and simple radiological score that was developed for use in bronchiectasis patients [33]. It contains the amount of bronchial dilatation and the number of bronchopulmonary segments with emphysema, resulting in an outcome between 0 and 5. Due to their multi-dimensional character and simplicity, these scores are unlikely to pick up subtle changes on chest CTs to monitor disease progression and to be used as outcome measure in clinical trials.

More detailed semi-quantitative scoring systems have been developed to quantify bronchiectasis and other key characteristics related to CF [34-37]. Initially, these systems were developed for research purposes but increasingly they find their way into routine clinical care. More recently, a quantitative grid-based method (the Perth-Rotterdam Annotated Grid Morphometric Analysis for CF (PRAGMA-CF)) was developed based on morphometric principles [37]. It was shown to be sensitive for quantifying and monitoring airway changes, including bronchiectasis [38]. Bronchiectasis-related semi-quantitative and PRAGMA-CF scores have been shown to correlate well with more objective assessments of AA dimensions [38]. Quantitative grid-based methods are now also being developed and applied for PCD and for bronchiectasis studies. An advantage of grid-based scoring systems is that it can be automated using machine learning techniques.

Another promising method for the detection of airways disease is the objective measurement of airway [25] or AA dimensions [11]. On a chest CT scan, hundreds of airways and AA pairs can be measured. Manual measurement of AA dimensions in CF has shown early and diffuse widening of the airways and airway wall thickening throughout the bronchial tree, with higher mean AA ratios and more severe thickening in the smaller airways [38]. An important observation was that in children with normal chest CTs, the mean outer AA ratio was 1.1 and was independent of segmental generation. However, outer AA ratios of > 1.1 could also be detected on the chest CTs of control subjects without lung disease. There are reasons to believe that this ratio might also change in relation to age [17]. On the chest CTs of young subjects without lung disease, the bronchial tree can be followed up to the seventh segmental generation, depending on age and size of the subject. For diseases such as CF where the small airways are heavily involved, the bronchial tree can become visible all the way up to the 12th segmental generation [11]. In healthy adults, automated analyses can detect 10-14 segmental generations [39, 40]. Unfortunately, manual measurements of all AA pairs on a chest CT is hugely time consuming, and therefore not suitable for routine clinical care. Fortunately, image analysis techniques that allow automated analysis of all visible AA pairs are in development [19]. As previously discussed, age- and sex-specific reference values need to be developed that allow the comparison of single patient outcomes with reference values. As radiation doses have come down considerably for chest CT scans, collection of such data might become feasible. Clinicians can use these chest CT outcome measures for the objective assessment and monitoring of bronchiectasis patients, in a similar way to spirometry outcomes.

These automated systems will be of great value to registries such as the European Multicentre Bronchiectasis Audit and Research Collaboration (EMBARC) [41] and the European Cystic Fibrosis Society Patient Registry. Adequate phenotyping and quantification of structural lung abnormalities on chest CT using automated image analysis systems will improve our understanding of the pathophysiology of bronchiectasis and will be important to the improvement of patient care.

Reversibility of bronchiectasis

Bronchiectasis is generally defined as an irreversible widening of the airway. The reversibility of radiological bronchiectasis has been discussed in a number of case reports [42, 43], and in a few small retrospective studies including both adult and paediatric patients [44-47]. A few critical notes are needed. In some of these papers [43], the methodology of both image acquisition and analysis are not well defined. This is highly relevant, as a volumetric CT protocol is required to allow a slice by slice comparison at identical anatomical levels between the baseline scan and the

follow-up scan. When sequential CT protocols are used, this is not usually possible and smaller bronchiectasis visible on the baseline scan can therefore be easily missed on the follow-up scan. This is especially relevant for older studies reporting reversibility of bronchiectasis when sequential protocols were more likely to be used [45, 47]. Differences in slice thickness and/or image reconstruction kernels between the baseline CT scan and follow-up scan can also result in "disappearance" of a bronchiectasis airway. Furthermore, reduction of bronchial wall thickening in the follow-up scan of smaller more peripheral airways after a therapeutic intervention can reduce visibility or make it disappear due to limitations in resolution. Sometimes airways with a normal diameter are misdiagnosed as bronchiectasis because of a thickened airway wall. Such thickening can be reversed in response to effective therapy. Differences in lung volume between baseline and follow-up CT can also result in the "disappearance" of bronchiectasis.

In general, advanced bronchiectasis is an irreversible condition. For critical follow-up of subtle bronchiectasis, the same standardised sensitive CT protocol needs to be used for both the baseline and follow-up scan.

Differentiation between diffuse and local disease

For the management of bronchiectasis, it is important to understand whether the condition developed as the result of an underlying chronic disease or whether it developed in relation to a single event, such as pneumonia of foreign body aspiration. In CF lung disease, bronchiectasis is the result of chronic and diffuse airway inflammation and infection. Measurements of all AA pairs visible on chest CT have shown that subtle but diffuse and progressive airway widening and thickening can be detected in patients as young as 2-4 years old [18]. With increasing age, more AA pairs show abnormal thickening and widening. For CF, it has therefore become clear that bronchiectasis is the "tip of the iceberg" and an end-stage local condition of progressive and diffuse airway disease. These and other related observations have led to a paradigm shift in the treatment of CF, namely that airway disease is diffuse and starts in infancy, and that it should be treated at an early stage to prevent the development of bronchiectasis [12]. Whether this phenomenon of mild diffuse airway disease preceding the development of bronchiectasis also occurs in other diseases, such as PCD, or immune deficiencies, needs to be further investigated. Clearly, when mild diffuse airway disease leads to bronchiectasis, early detection and treatment are also relevant for these diseases to prevent development into bronchiectasis.

In bronchiectasis patients without diffuse airway disease, the pathophysiology of bronchiectasis is more likely to be the result of a local event, such as pneumonia or whooping cough. Hence, we feel that distinguishing between diffuse or local airways

disease can be important for the differential diagnosis of the underlying disease causing bronchiectasis, and for the management of such a disease. We speculate that a sensitive read-out of all visible AA ratios throughout the bronchial tree can be helpful for differentiating between diffuse or local disease.

MRI and bronchiectasis

Obtaining detailed and reproducible morphological images of the lung with MRI in a clinical routine that is comparable to that of CT is still a major challenge. However, lung imaging using MRI has made substantial progress over the last two decades [48]. As for CT, consensus on the classification of bronchiectasis is lacking. Furthermore, standardisation across centres and vendors for lung MRI is in its early days [49-51]. However, there have been important developments that may significantly contribute to the future of bronchiectasis research, as follows.

First, new sequences are in development that allow high-resolution lung images to be obtained [52, 53].

Secondly, MRI allows more detailed tissue characterisation in comparison with CT. Hence, when using MRI, the contribution of mucus to airway wall thickening can be investigated [54, 55]. Such techniques can be of great importance when studying, for example, physiotherapy techniques in bronchiectasis patients to improve mucocilliary clearance [56].

Thirdly, MRI techniques like diffusion weighted imaging are in development to identify inflammatory hotspots that can potentially be used to monitor treatment efficacy [57].

Fourthly, using functional MRI, the relation between perfusion and ventilation can be studied. A concept has been put forward to develop a set of sequences to obtain information on ventilation inflammation perfusion and structure (VIPS-MRI) in one session in CF patients [58]. The challenge is that the set of sequences: can be completed in ~30 min; does not require a contrast agent; and runs on all major MRI platforms. Clearly, the VIPS-MRI platform could be of interest for all lung diseases that include severe bronchiectasis.

MRI is therefore likely to play a more important role in the near future for bronchiectasis-related research. However, for larger scale use in the day-to-day clinical practice of bronchiectasis, important issues such as standardisation, spatial resolution, accessibility and validation of outcome measures need to be addressed.

Summary

The gold standard for bronchiectasis diagnosis in vivo over the last two decades has been chest CT. Bronchiectasis is diagnosed when an abnormally wide and mostly thickened airway can be observed, which often also shows a lack of tapering. Bronchiectasis can be the result of a clearly defined underlying disease, but in many patients, the underlying disorder that led to bronchiectasis cannot be identified. Standardisation of lung volume during chest CT acquisition and of the scanner protocol is needed to allow a more robust diagnosis of bronchiectasis. In addition, this standardisation is needed to allow automated sensitive image analysis for the objective diagnosis of bronchiectasis. It is important that outcome measures derived from automated image analysis methods of chest CTs are used in clinical care and registries. Chest MRI can play an important role in bronchiectasis research, allowing the study of both lung structure and functional aspects.

References

[1] Boaventura R SA, Chalmers JD. Pathophysiology. Chalmers JD, Polverino E, Aliberti S, eds Bronchiectasis (ERS Monograph)2018. p. 8-28.

[2] Hansell DM, Bankier AA, MacMahon H, McLoud TC, Muller NL, Remy J. Fleischner Society: glossary of terms for thoracic imaging. Radiology. 2008;246:697-722.

[3] Polverino E, Goeminne PC, McDonnell MJ, Aliberti S, Marshall SE, Loebinger MR, et al. European Respiratory Society guidelines for the management of adult bronchiectasis. Eur Respir J. 2017;50.

[4] McDonnell MJ, Aliberti S, Goeminne PC, Restrepo MI, Finch S, Pesci A, et al. Comorbidities and the risk of mortality in patients with bronchiectasis: an international multicentre cohort study. Lancet Respir Med. 2016;4:969-79.

[5] Chandrasekaran R, Mac Aogain M, Chalmers JD, Elborn SJ, Chotirmall SH. Geographic variation in the aetiology, epidemiology and microbiology of bronchiectasis. BMC Pulm Med. 2018;18:83.

[6] Hedblom CA. The diagnosis and treatment of bronchiectasis. Jama. 1927;89:1384-90.

[7] McGuinness G, Naidich DP. CT of airways disease and bronchiectasis. Radiol Clin North Am. 2002;40:1-19.

[8] Dournes G, Menut F, Macey J, Fayon M, Chateil JF, Salel M, et al. Lung morphology assessment of cystic fibrosis using MRI with ultra-short echo time at submillimeter spatial resolution. Eur Radiol. 2016;26:3811-20.

[9] de Brito MC, Ota MK, Leitao Filho FS, Meirelles GS. Radiologist agreement on the quantification of bronchiectasis by high-resolution computed tomography. Radiol Bras. 2017;50:26-31.

[10] Lambert RK, Codd SL, Alley MR, Pack RJ. Physical determinants of bronchial mucosal folding. J Appl Physiol (1985). 1994;77:1206-16.

[11] Kuo W, de Bruijne M, Petersen J, Nasserinejad K, Ozturk H, Chen Y, et al. Diagnosis of bronchiectasis and airway wall thickening in children with cystic fibrosis: Objective airway-artery quantification. Eur Radiol. 2017;27:4680-9.

[12] Mott LS, Graniel KG, Park J, De Klerk NH, Sly PD, Murray CP, et al. Assessment of early bronchiectasis in young children with cystic fibrosis is dependent on lung volume. Chest. 2013;144:1193-8.

[13] Diaz AA, Young TP, Maselli DJ, Martinez CH, Gill R, Nardelli P, et al. Quantitative CT Measures of Bronchiectasis in Smokers. Chest. 2017;151:1255-62.

[14] Kim JS, Muller NL, Park CS, Lynch DA, Newman LS, Grenier P, et al. Bronchoarterial ratio on thin section CT: Comparison between high altitude and sea level. J Comput Assist Tomogr. 1997;21:306-11.

[15] Jacob J, Bartholmai BJ, Rajagopalan S, Kokosi M, Nair A, Karwoski R, et al. Mortality prediction in idiopathic pulmonary fibrosis: evaluation of computer-based CT analysis with conventional severity measures. Eur Respir J. 2017;49.

[16] Matsuoka S, Uchiyama K, Shima H, Ueno N, Oish S, Nojiri Y. Bronchoarterial ratio and bronchial wall thickness on high-resolution CT in asymptomatic subjects: Correlation with age and smoking. Am J Roentgenol. 2003;180:513-8.

[17] Copley SJ, Wells AU, Hawtin KE, Gibson DJ, Hodson JM, Jacques AE, et al. Lung morphology in the elderly: comparative CT study of subjects over 75 years old versus those under 55 years old. Radiology. 2009;251:566-73.

[18] Kuo W, Soffers T, Andrinopoulou ER, Rosenow T, Ranganathan S, Turkovic L, et al. Quantitative assessment of airway dimensions in young children with cystic fibrosis lung disease using chest computed tomography. Pediatr Pulmonol. 2017;52:1414-23.

[19] Perez-Rovira A, Kuo W, Petersen J, Tiddens HA, de Bruijne M. Automatic airway-artery analysis on lung CT to quantify airway wall thickening and bronchiectasis. Med Phys. 2016;43:5736.

[20] Naidich DP, McCauley DI, Khouri NF. Computed tomography of bronchiectasis. J COMPUT ASSISTED TOMOGR. 1982;6:437-44.

[21] Kuo W, Perez-Rovira A, Tiddens H, de Bruijne M, Normal Chest CTsg. Airway tapering: an objective image biomarker for bronchiectasis. Eur Radiol. 2020;30:2703-11.

[22] Salamon E, Lever S, Kuo W, Ciet P, Tiddens HA. Spirometer guided chest imaging in children: It is worth the effort! Pediatr Pulmonol. 2017;52:48-56.

[23] Kongstad T, Buchvald FF, Green K, Lindblad A, Robinson TE, Nielsen KG. Improved air trapping evaluation in chest computed tomography in children with cystic fibrosis using real-time spirometric monitoring and biofeedback. J Cyst Fibros. 2013;12:559-66.

[24] Kuo W, Kemner-van de Corput MP, Perez-Rovira A, de Bruijne M, Fajac I, Tiddens HA, et al. Multicentre chest computed tomography standardisation in children and adolescents with cystic fibrosis: the way forward. Eur Respir J. 2016;47:1706-17.

[25] Wielputz MO, Eichinger M, Weinheimer O, Ley S, Mall MA, Wiebel M, et al. Automatic airway analysis on multidetector computed tomography in cystic fibrosis: correlation with pulmonary function testing. J Thorac Imaging. 2013;28:104-13.

[26] Kubo T, Ohno Y, Nishino M, Lin PJ, Gautam S, Kauczor HU, et al. Low dose chest CT protocol (50 mAs) as a routine protocol for comprehensive assessment of intrathoracic abnormality. Eur J Radiol Open. 2016;3:86-94.

[27] O'Connor OJ, Vandeleur M, McGarrigle AM, Moore N, McWilliams SR, McSweeney SE, et al. Development of low-dose protocols for thin-section CT assessment of cystic fibrosis in pediatric patients. Radiology. 2010;257:820-9.

[28] Johnson PT, Fishman EK. Postprocessing techniques for cardiac computed tomographic angiography. Radiol Clin North Am. 2010;48:687-700.

[29] Schulz-Menger J, Bluemke DA, Bremerich J, Flamm SD, Fogel MA, Friedrich MG, et al. Standardized image interpretation and post-processing in cardiovascular magnetic resonance - 2020 update : Society for Cardiovascular Magnetic Resonance (SCMR): Board of Trustees Task Force on Standardized Post-Processing. J Cardiovasc Magn Reson. 2020;22:19.

[30] Chalmers JD, Goeminne P, Aliberti S, McDonnell MJ, Lonni S, Davidson J, et al. The bronchiectasis severity index an international derivation and validation study. American journal of respiratory and critical care medicine. 2014;189:576-85.

[31] Martínez-García MA, De Gracia J, Relat MV, Girón RM, Carro LM, De La Rosa Carrillo D, et al. Multidimensional approach to non-cystic fibrosis bronchiectasis: The FACED score. Eur Respir J. 2014;43:1357-67.

[32] Martinez-Garcia MA, Athanazio RA, Giron R, Maiz-Carro L, de la Rosa D, Olveira C, et al. Predicting high risk of exacerbations in bronchiectasis: the E-FACED score. Int J Chron Obstruct Pulmon Dis. 2017;12:275-84.

[33] Bedi P, Chalmers JD, Goeminne PC, Mai C, Saravanamuthu P, Velu PP, et al. The BRICS (Bronchiectasis Radiologically Indexed CT Score): A Multicenter Study Score for Use in Idiopathic and Postinfective Bronchiectasis. Chest. 2018;153:1177-86.

[34] Bhalla M, Turcios N, Aponte V, Jenkins M, Leitman BS, McCauley DI, et al. Cystic fibrosis: scoring system with thin-section CT. Radiology. 1991;179:783-8.

[35] Brody AS, Klein JS, Molina PL, Quan J, Bean JA, Wilmott RW. High-resolution computed tomography in young patients with cystic fibrosis: distribution of abnormalities and correlation with pulmonary function tests. J Pediatr. 2004;145:32-8.

[36] Wainwright CE, Vidmar S, Armstrong DS, Byrnes CA, Carlin JB, Cheney J, et al. Effect of bronchoalveolar lavage-directed therapy on Pseudomonas aeruginosa infection and structural lung injury in children with cystic fibrosis: a randomized trial. Jama. 2011;306:163-71.

[37] Rosenow T, Oudraad MC, Murray CP, Turkovic L, Kuo W, de Bruijne M, et al. PRAGMA-CF. A Quantitative Structural Lung Disease Computed Tomography Outcome in Young Children with Cystic Fibrosis. American journal of respiratory and critical care medicine. 2015;191:1158-65.

[38] Kuo W, Andrinopoulou ER, Perez-Rovira A, Ozturk H, de Bruijne M, Tiddens HAWM. Objective airway artery dimensions compared to CT scoring methods assessing structural cystic fibrosis lung disease. J Cyst Fibrosis. 2017;16:116-23.

[39] Montaudon M, Desbarats P, Berger P, de Dietrich G, Marthan R, Laurent F. Assessment of bronchial wall thickness and lumen diameter in human adults using multi-detector computed tomography: comparison with theoretical models. J Anat. 2007;211:579-88.

[40] Kirby M, Tanabe N, Tan WC, Zhou G, Obeidat M, Hague CJ, et al. Total Airway Count on Computed Tomography and the Risk of Chronic Obstructive Pulmonary Disease Progression. Findings from a Population-based Study. American journal of respiratory and critical care medicine. 2018;197:56-65.

[41] Chalmers JD, Aliberti S, Polverino E, Vendrell M, Crichton M, Loebinger M, et al. The EMBARC European bronchiectasis registry: Protocol for an international observational study. ERS Monogr. 2016;2.

[42] Hayes D, Long FR, McCoy KS, Sheikh SI. Improvement in Bronchiectasis on CT Imaging in a Pediatric Patient with Cystic Fibrosis on Ivacaftor Therapy. Respiration. 2014.

[43] Yap VL, Metersky ML. Reversible bronchiectasis in an adult: a case report. J Bronchology Interv Pulmonol. 2012;19:336-7.

[44] Eastham KM, Fall AJ, Mitchell L, Spencer DA. The need to redefine non-cystic fibrosis bronchiectasis in childhood. Thorax. 2004;59:324-7.

[45] Cukier A, Stelmach R, Kavakama JI, Terra Filho M, Vargas F. Persistent asthma in adults: comparison of high resolution computed tomography of the lungs after one year of follow-up. Rev Hosp Clin Fac Med Sao Paulo. 2001;56:63-8.

[46] Piccione JC, McPhail GL, Fenchel MC, Brody AS, Boesch RP. Bronchiectasis in chronic pulmonary aspiration: Risk factors and clinical implications. Pediatr Pulmonol. 2012;47:447-52.

[47] Gaillard EA, Carty H, Heaf D, Smyth RL. Reversible bronchial dilatation in children: Comparison of serial high-resolution computer tomography scans of the lungs. Eur J Radiol. 2003;47:215-20.

[48] Liszewski MC, Ciet P, Lee EY. MR Imaging of Lungs and Airways in Children:: Past and Present. Magn Reson Imaging Clin N Am. 2019;27:201-25.

[49] Triphan SMF, Biederer J, Burmester K, Fellhauer I, Vogelmeier CF, Jörres RA, et al. Design and application of an MR reference phantom for multicentre lung imaging trials. PLoS One. 2018;13:e0199148.

[50] Wielpütz MO, von Stackelberg O, Stahl M, Jobst BJ, Eichinger M, Puderbach MU, et al. Multicentre standardisation of chest MRI as radiation-free outcome measure of lung disease in young children with cystic fibrosis. J Cyst Fibros. 2018;17:518-27.

[51] Nguyen AH, Perez-Rovira A, Wielopolski PA, Hernandez Tamames JA, Duijts L, de Bruijne M, et al. Technical challenges of quantitative chest MRI data analysis in a large cohort pediatric study. Eur Radiol. 2019;29:2770-82.

[52] Dournes G, Grodzki D, Macey J, Girodet PO, Fayon M, Chateil JF, et al. Quiet Submillimeter MR Imaging of the Lung Is Feasible with a PETRA Sequence at 1.5 T. Radiology. 2016;279:328.

[53] Gibiino F, Sacolick L, Menini A, Landini L, Wiesinger F. Free-breathing, zero-TE MR lung imaging. Magma. 2015;28:207-15.

[54] Ciet P, Tiddens HA, Wielopolski PA, Wild JM, Lee EY, Morana G, et al. Magnetic resonance imaging in children: common problems and possible solutions for lung and airways imaging. Pediatr Radiol. 2015;45:1901-15.

[55] Scholz O, Denecke T, Böttcher J, Schwarz C, Mentzel HJ, Streitparth F, et al. MRI of cystic fibrosis lung manifestations: sequence evaluation and clinical outcome analysis. Clin Radiol. 2017;72:754-63.

[56] Woodhouse N, Wild JM, van Beek EJ, Hoggard N, Barker N, Taylor CJ. Assessment of hyperpolarized 3He lung MRI for regional evaluation of interventional therapy: a pilot study in pediatric cystic fibrosis. J Magn Reson Imaging. 2009;30:981-8.

[57] Ciet P, Bertolo S, Ros M, Andrinopoulou ER, Tavano V, Lucca F, et al. Detection and monitoring of lung inflammation in cystic fibrosis during respiratory tract exacerbation using diffusion-weighted magnetic resonance imaging. Eur Respir J. 2017;50.

[58] Tiddens HA, Stick SM, Wild JM, Ciet P, Parker GJ, Koch A, et al. Respiratory tract exacerbations revisited: ventilation, inflammation, perfusion, and structure (VIPS) monitoring to redefine treatment. Pediatr Pulmonol. 2015;50 Suppl 40:S57-65.

Chapter 4

Analysis of granulomatous lymphocytic interstitial lung disease using two scoring systems for computed tomography scans - a retrospective cohort study

Frontiers of Immunology 2020;11:589148

Jennifer J. Meerburg, Ieneke J.C. Hartmann, Sigune Goldacker, Ulrich Baumann, Annette Uhlmann, Eleni-Rosalina Andrinopoulou, Mariette P.C. Kemner v/d Corput, Klaus Warnatz and Harm A.W.M. Tiddens, on behalf of the STILPAD study group

Abstract

Background Granulomatous lymphocytic interstitial lung disease (GLILD) is present in about 20% of patients with common variable immunodeficiency disorders (CVID). GLILD is characterized by nodules, reticulation, and ground-glass opacities on CT scans. To date, large cohort studies that include sensitive CT outcome measures are lacking, and severity of structural lung disease remains unknown. The aim of this study was to introduce and compare two scoring methods to phenotype CT scans of GLILD patients.

Methods Patients were enrolled in the "Study of Interstitial Lung Disease in Primary Antibody Deficiency" (STILPAD) international cohort. Inclusion criteria were diagnosis of both CVID and GLILD, as defined by the treating immunologist and radiologist. Retrospectively collected CT scans were scored systematically with the Baumann and Hartmann methods.

Results In total, 356 CT scans from 138 patients were included. Cross-sectionally, 95% of patients met a radiological definition of GLILD using both methods. Bronchiectasis was present in 82% of patients. Inter-observer reproducibility (intra-class correlation coefficients) of GLILD and airway disease were 0.84 and 0.69 for the Hartmann method and 0.74 and 0.42 for the Baumann method.

Conclusions In both the Hartmann and Baumann scoring method, the composite score GLILD was reproducible and therefore might be a valuable outcome measure in future studies. Overall, the reproducibility of the Hartmann method appears to be slightly better than that of the Baumann method. With a systematic analysis, we showed that GLILD patients suffer from extensive lung disease, including airway disease. Further validation of these scoring methods should be performed in a prospective cohort study involving routine collection of standardized CT scans.

Introduction

Common variable immunodeficiency disorders (CVID) are a heterogeneous group of primary antibody deficiency syndromes [1]. Clinical diagnosis is based on a decreased level of IgG, IgA, and/or IgM, an impaired immune response to vaccines, and the absence of defined causes for hypogammaglobinaemia [2]. CVID result in a broad spectrum of clinical presentations [3]. In the early stages of disease, patients often present with recurrent upper and lower respiratory tract infections. Although the use of immunoglobulin replacement therapy can significantly reduce the risk of lower respiratory tract infection in these patients [4], a substantial proportion of patients develop progressive airway disease [5, 6].

In addition, 30%-50% of CVID patients develop noninfectious autoimmune disease, organ inflammation or malignancies. Since adequate immunoglobulin replacement therapy has been introduced, these comorbidities have a larger impact on patient prognosis than the recurrent infections [3, 7]. Granulomatous lymphocytic interstitial lung disease (GLILD) belongs to these comorbidities and affects 8%-20% of CVID patients [8, 9]. GLILD patients show signs of lymphoproliferative pulmonary disease, including lymphocytic interstitial pneumoniae, follicular bronchiolitis, or lymphoid hyperplasia in combination with granulomas. The diagnosis is made by performing both radiological and histopathological examinations of the lungs [6, 9]. Although the pathogenesis of GLILD is not well understood, autoimmune and inflammatory dysregulation and their association with other autoimmune disorders are thought to play a role [5]. It was shown that CVID patients with GLILD (n = 13) have a markedly reduced survival rate of 50% compared to patients without GLILD (n = 56) and this finding led to a heightened clinical interest in the GLILD patient group [9]. Importantly, this interstitial lung disease can lead to clinical complaints such as reduced exercise tolerance and dyspnoea. Furthermore, GLILD patients have a more complex clinical course, as they tend to have a higher frequency of B-cell lymphoma and autoimmune diseases compared to non-GLILD patients [9, 10]. Currently, the gold standard to assess GLILD-related structural lung changes is chest computed tomography (CT). Frequently observed lung abnormalities in GLILD include: ground-glass opacities (GGO), diffuse nodules, lymphadenopathy, diffuse patchy consolidations, and reticulation [9, 11, 12]. This is distinct from signs of airway disease, like bronchiectasis, airway wall thickening and trapped air [11, 13-16]. Two typical CT images of GLILD patients are shown in Figure 1.

Most studies on GLILD-related CT structural lung abnormalities involve retrospectively extracted data from radiologic reports [9, 12, 17-19]. However, these reports are generally not well standardized nor quantitative, making it difficult to compare findings.

A more systematic and reproducible approach to quantify these abnormalities is to use standardized CT scoring methods. Outcome measures derived from scoring methods can be used both for research purposes and in clinical follow-up [20]. Furthermore, they can be used to phenotype patients for personalized clinical care. Few studies have employed scoring methods to systematically assess chest CT scans of GLILD patients. Van de Ven et al. used a scoring system for pediatric CVID or CVID-like patients (n = 54), which was subsequently applied to adults with CVID (n = 47) [15, 21]. Similarly, Gregersen et al. used a simplified scoring method to assess CVID in adults (n = 65) [22]. Chase et al. evaluated the efficacy of chemotherapy in seven GLILD patients by assessing CT scans performed before and after treatment [23]. A major limitation of these studies is that only a small number of patients with GLILD were included. This warrants the need for larger cohort studies to better understand the radiologic characteristics of GLILD and to optimize methods to quantify disease severity in these patients [6, 9, 24].

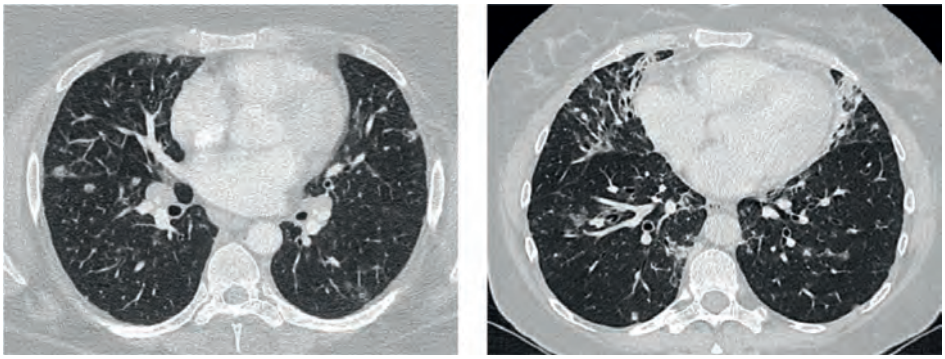

Figure 1. Features of granulomatous lymphocytic interstitial lung disease (GLILD)
Images of two study patients. Left: diffuse nodules and lymphadenopathy. Right: combination of diffuse nodules, reticulation and ground-glass opacities. Apart from GLILD features, also signs of airway disease are visible.

From 2012 to 2014, a large international observational study, The STudy of Interstitial Lung Disease in Primary Antibody Deficiency (STILPAD), was initiated by the Centre of Chronic Immunodeficiency at the University Medical Centre Freiburg in Freiberg, Germany. The purpose of STILPAD was to describe the natural course and different treatment responses of GLILD. Fourteen medical centers across three countries retrospectively collected clinical data of 146 GLILD patients, from which all available chest CT scans were analyzed to phenotype pulmonary abnormalities in these patients. The aim of this present study was to assess the radiologic features on retrospectively collected chest CT scans of the STILPAD subjects using and comparing two independent scoring methods developed for CVID patients.

Methods and materials

Study population

Patients with the clinical diagnosis of GLILD enrolled in STILPAD between 2012 and 2014 were included in this study. Inclusion criteria were as follows: 1) CVID defined by criteria approved by the European Society for Immunodeficiencies and the Pan-American Group for Immunodeficiency [2], 2) age of 18 years and above, and 3) a radiological diagnosis of interstitial lung disease or granuloma on chest CT scan, characterized by the presence of nodules, reticulation, or GGO. This evaluation was performed by the radiologist at each participating medical center.

Given the unresolved discussion whether a histological proof of GLILD is required, a histopathological diagnosis of GLILD was made only in few patients based on the policy of each center, and this was not an inclusion criterion.

Collection of CT scans

All available digital CT scans of the STILPAD cohort were collected retrospectively between December 2013 and April 2015. Exclusion criteria for image analysis were as follows: incomplete display of the lung, substantial motion artefacts, pneumothorax, or the absence of a reconstruction series required for lung image analysis. To evaluate the presence and severity of pulmonary abnormalities in GLILD patients, the most recent CT scan of each patient was analyzed. For the assessment of change in disease over time, patients with at least two CT scans were included.

CT scan characteristics

Information on CT parameters, including slice thickness, lung volume during acquisition, volumetric or sequential acquisition, and the reconstruction kernels were noted for each scan.

CT scan analysis

CT scans were scored using two methods developed for scoring CVID CT scans: the Baumann method and the Hartmann method. Key features of these methods are outlined in Table 1. Both scoring methods evaluate not only CT changes associated with interstitial lung disease but also airway disease as outlined below.

Baumann scoring method

The Baumann scoring method, shown in Table S1 (Supplementary material), was developed by an international interdisciplinary group known as the Chest CT Antibody Deficiency Group. One of its objectives is to standardize the reporting of chest CT findings of patients with antibody deficiencies in a reproducible and clinically

applicable manner. The group recently published a report on the distribution of bronchial pathologies in CVID patients in a large international cohort [25]. The Baumann method evaluates the presence of 13 different abnormalities without assessing their distribution within specific lobes of the lung. These include: bronchial wall thickening, bronchiectasis (excluding traction bronchiectasis), mucus plugging, atelectasis, nodules, reticulation ("lines"), consolidation, GGO, cysts, emphysema or bullae, linear scars and bands, trapped air, and lymphadenopathy. Briefly, the extent of each abnormality is evaluated by counting the number of affected lung lobes; the lingula being considered as a separate lobe. Furthermore, a score between 0 and 3 denotes the severity of bronchial wall thickening and bronchiectasis. Nodules are divided into three size-based categories and in cases of lymphadenopathy; the size of the largest lymph node is measured. This results in 22 scoring items per CT scan.

Table 1. Differences between the Baumann and Hartmann scoring methods for common variable immunodeficiency disorders

	Baumann	**Hartmann**
Abnormalities scored per	Whole lung	Lobe
Number of values	22	157
Time needed per CT (minutes)	15	30
Origin	Newly designed for CVID as a scoring system for clinical use	Based on the cystic fibrosis-CT scoring method, and designed as a sensitive scoring system for CVID patients for research purposes
Emphysema	Scored together with bullae	Scored as separate entity
Reticulation	The presence and subtype of reticulation (inflammatory, fibrotic or mixed) are noted	Differentiation between reticulation with or without distortion
Lymphadenopathy	Size of the largest lymph node is measured in mm	Only the presence is scored defined by a short axis diameter ≥ 10 mm
Ground-glass opacities (GGO)	Both the presence and subtype of GGO (inflammatory or fibrotic) are noted	No subtypes of GGO are noted

This table presents the key differences between the Baumann and Hartmann scoring method for computed tomography (CT) scans of patients with common variable immunodeficiency disorders (CVID).

Hartmann scoring method

The Hartmann scoring method, shown in Table S2 (Supplementary material), is derived from the validated cystic fibrosis - CT scoring method, with additional items describing abnormalities typical of immunodeficiency syndromes [26]. The Hartmann

method evaluates abnormalities in more detail than the Baumann method to detect more subtle changes over time. This method was designed for research purposes and is less suitable for clinical practice due to its extensiveness. In summary, the following abnormalities are assessed: bronchial wall thickening, bronchiectasis (excluding traction bronchiectasis), mucus plugging, atelectasis, nodules, reticulation, consolidation, GGO, bullae and cysts, emphysema, distortion, trapped air, and lymphadenopathy. Unlike the Baumann method, each lobe is scored separately, with the lingula being considered as a separate lobe. The extent and severity of specific abnormalities are scored on a scale of 0 to 3. A total of 26 items are scored per lobe, and lymphadenopathy is only scored once. This results in 157 scoring items per CT scan.

Component and composite scores

In both methods, individual component scores for bronchiectasis, bronchial wall thickening, mucus plugging, nodules, reticulation and GGO are expressed as a percentage of the maximum score.

Component scores of bronchiectasis and bronchial wall thickening were calculated by multiplying the extent of disease by a factor (multiplier), such that the higher the severity of disease, the higher the multiplier [27, 28]. Bronchiectasis severity scores of 1.0, 1.5, 2.0, 2.5, and 3.0 had multipliers of 1.00, 1.25, 1.50, 1.75, and 2.00, respectively. Likewise, bronchial wall thickening scores of 1.0, 2.0, and 3.0 had respective multipliers of 1.00, 1.25, and 1.50.

Besides the component scores for single abnormalities, three composite scores were calculated and expressed as a percentage of the maximum score. The GLILD composite score comprised the combined score of GGO, nodules, and reticulation. The composite score for airway disease consisted of bronchial wall thickening, bronchiectasis and mucus plugging combined. In addition, the total disease composite score was derived from the sum of all scored abnormalities.

In case no signs of GLILD were found with both the Baumann and Hartmann scores, the CT scans were analyzed by a thoracic radiologist (P. Ciet).

Observers

The CT scans were scored by two extensively trained observers (a medical doctor and a final year medical student). Observers were trained and certified using standardized chest CT training modules that were developed by a chest radiologist (IH) and the LungAnalysis Core Laboratory. These modules consist of studying a defined list of literature [29], followed by PowerPoint presentations to train used definitions and reference images to be used for scoring. Finally, the observers had to score training

batches of CT scans. Furthermore, each observer received one to- one training sessions with the chest radiologist (IH). For logistical reasons, the scans were divided into two batches (n = 251 and n = 105), based on order of arrival. Each batch was scored by a single observer. To assess inter- and intra-observer reliability each observer re-scored a randomly selected and randomized batch of 25 and 30 CT scans, respectively.

Statistical analysis

Patient demographics are reported as mean (standard deviation) and scoring outcome parameters are presented as the median (interquartile range, total ranges).

Agreement within and between observers was determined using the intra-class correlation coefficients (ICCs) of both scoring methods (two-way mixed-effects model, single measurements, studied relationship consistency) [30]. ICC ranges are defined as follows: 0-0.39 poor, 0.40-0.59 fair, 0.60- 0.74 good, and > 0.75 excellent [31].

To investigate changes in disease over time, mixed-effects models (generalized estimating equations) were used for the following CT outcomes of both scoring methods: the component score bronchiectasis and composite scores GLILD, and airway disease and total disease scores. Models were adjusted for multiple visits, with p-values < 0.05 considered significant.

Square root-transformed Hartmann component scores of bronchiectasis were used, as the assumption of homoscedasticity (constant variance) was not satisfied in the original scale. Likelihood-ratio tests were used to assess whether a nonlinear assumption would better represent the evolution of disease over time.

Statistical analyses were performed using SPSS version 21.0 (SPSS Inc., Chicago, IL) and R version 3.3.1 (https://cran.rproject. org/).

Ethics approval

Approval for this study was obtained from the local ethics committee of the University of Freiburg in Freiburg, Germany (IRB: 189/12), and the national ethical review boards of all participating centers. Written informed consent was obtained from all participants prior to inclusion in this study.

Results

Study population

For this CT analysis eight patients from the STILPAD cohort (n = 146) were excluded, because they had no digital CT scans available (n = 7) or the available CT scans did not meet the inclusion criteria (n = 1). Hence, 138 patients were included in this retrospective CT study, of which 88 (64%) females. The mean age at time of inclusion was 45 (± 15) years, and mean age of diagnosis was 41 (± 15) years.

Collection of CT scans

A total of 462 CT scans were collected. A flowchart of the CT scan selection process is shown in Figure 2. We excluded 105 CT scans as they failed to meet the inclusion criteria and one CT because it was unintentionally scored using only the Hartmann method. Ultimately, the final cohort compromised 356 CT scans from 138 patients.

For the longitudinal analysis, 299 scans were collected from 81 patients. Figure 3 shows the number of CT scans that were analyzed per patient. Median interval (interquartile range, total range) between the CT scans was 12 months (5-24, 0-114).

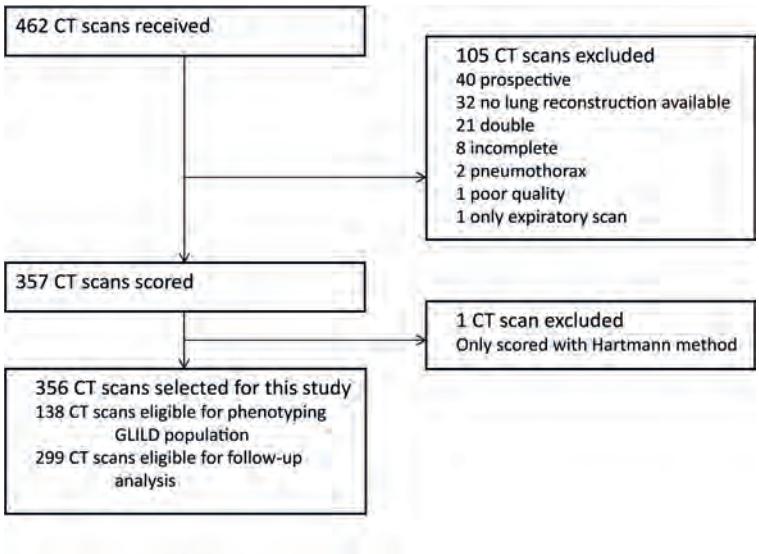

Figure 2. Flowchart CT selection

Flowchart of the in- and exclusion of CT scans. For phenotyping the granulomatous lymphocytic interstitial lung disease (GLILD) population 138 most recent CT scans were used. A total of 356 CT scans from 138 STILPAD subjects were analyzed and selected for this study. The most recent scan of each patient was used to phenotype the GLILD population. For follow-up analysis, 299 CT scans from 81 patients were analyzed.

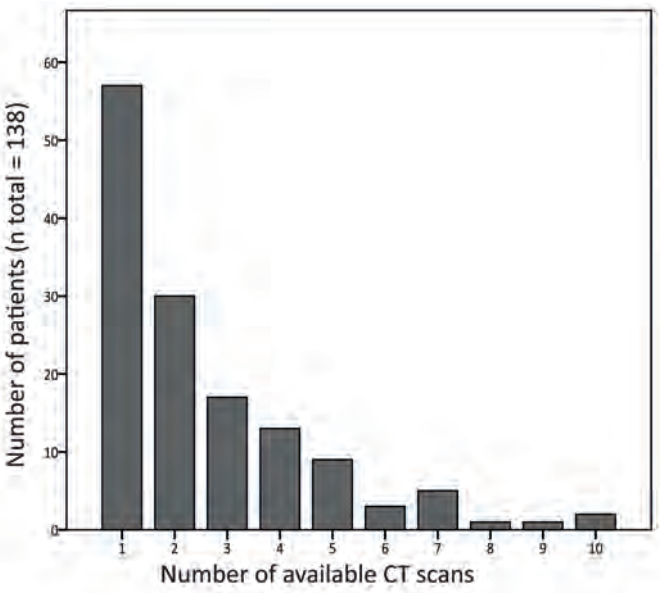

Figure 3. Number of computed tomography (CT) scans available per patient

The number of CT scans that was analysed per patient is shown in this graph. Of 81 patients, two or more CT scans were collected, and these scans were used for follow-up analysis.

CT Scan characteristics

An overview of the scan characteristics is provided in Table S3 (Supplementary material). In short: The majority of CT scans (n = 274, 77%) were volumetric. Slice thickness ranged between 0.6 and 8.0 mm, with 267 (75%) of scans having a slice thickness below 3.0 mm. Because only two expiratory CT scans could be collected, trapped air had to be excluded from the analysis.

CT scan analysis of the most recent CT

Presence of abnormalities

Figures 4A and 4B display the prevalence of component and composite scores of GLILD and airway disease on the most recent CT scan using the Baumann and Hartmann scoring methods. Bronchiectasis was the most common abnormality, with a prevalence of 113 (82%) in all patients for both scoring methods. Other common findings include: bronchial wall thickening, GGO, reticulation and nodules. Signs of GLILD, as calculated by combining the scores of GGO, nodules and/or reticulation, were found on the most recent CT in 131 (95%) of patients for both methods. Figure 5 demonstrates the relationships between GLILD features. In 56% and 60% of these patients, all features of GLILD were detected with the Baumann and Hartmann method respectively. Signs of GLILD were not detected on the most recent CT scan

Figure 4a. Scoring items Baumann method

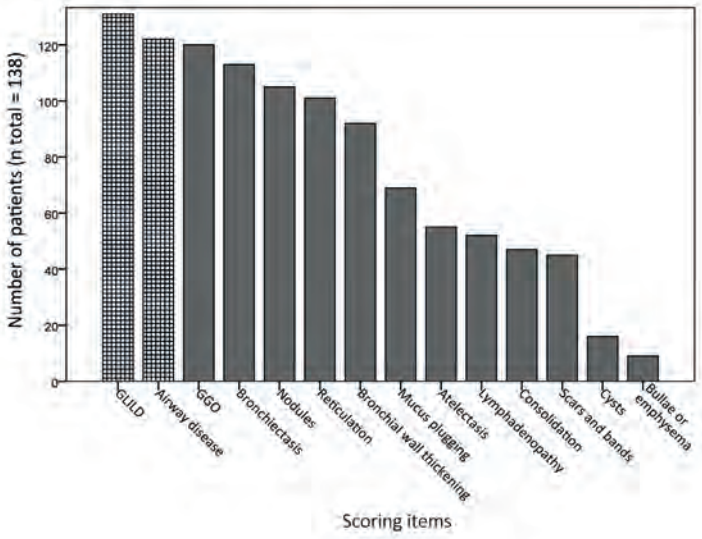

Figure 4b. Scoring items Hartmann method

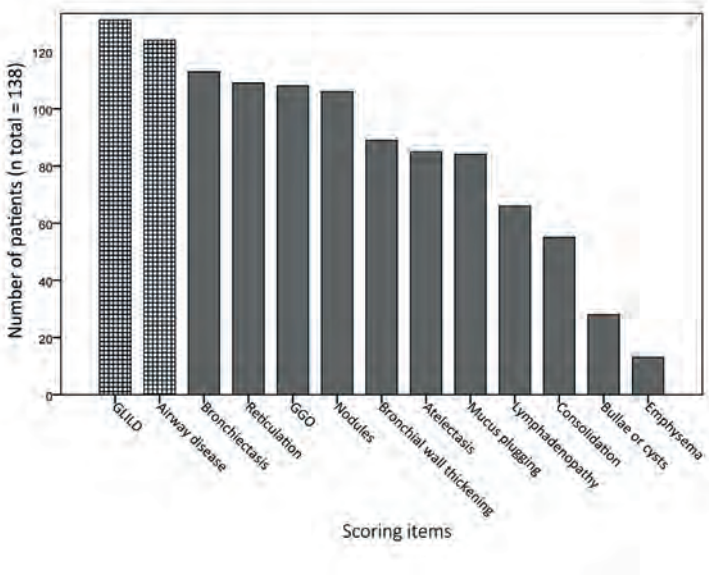

Figure 4. Prevalence of abnormalities on computed tomography (CT) scan

Component and composite scores are sorted based on the number of patients that have a positive score. Granulomatous lymphocytic interstitial lung disease (GLILD) and airway disease are composite scores; GLILD is a combination of subscores for ground-glass opacities (GGO), nodules and reticulation, airway disease is the sum of bronchial wall thickening, bronchiectasis and mucus plugging subscores.

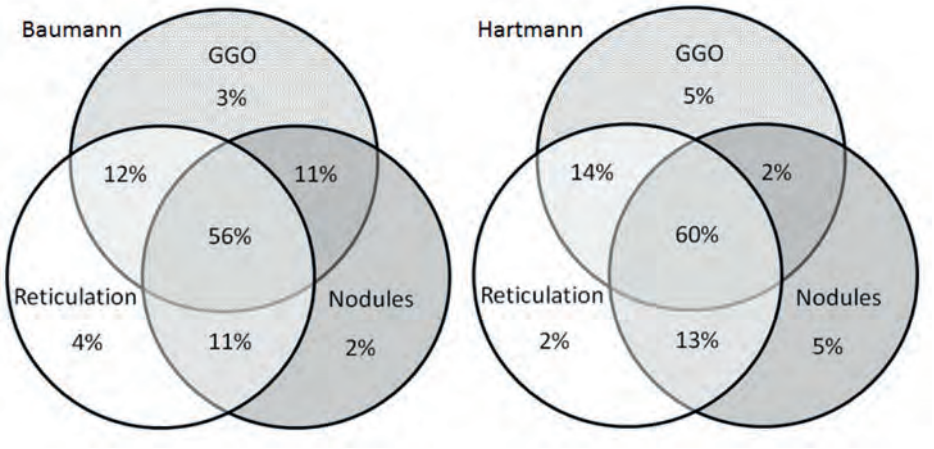

Figure 5. Venn diagrams of features of granulomatous lymphocytic interstitial lung disease (GLILD)

Venn diagrams showing the presence of the in the patients method with signs of GLILD on their most recent chest CT scan for both the Baumann (left) and Hartmann (right) (n total = 131). In 56% (Baumann) and 60% (Hartmann) of the 131 patients all features of GLILD were detected. GGO = Ground-glass opacities.

of five (4%) STILPAD patients in any of the two scoring methods. Of these patients, one patient (1%) had positive GLILD scores on previous scans. The CT scans of the four patients without positive GLILD composite scores on any of their CT scans were re-evaluated by a thoracic radiologist, and signs of GLILD were detected in two of the four patients. Airway disease, defined as bronchiectasis and/or bronchial wall thickening and/or mucus plugging, was present in 122 (88%) (Baumann) and 124 (90%) (Hartmann) of patients. Enlarged lymph nodes were found in 52 (38%) (Baumann) and 70 (51%) (Hartmann) of patients.

Severity of abnormalities

The maximal severity scores for bronchiectasis, bronchial wall thickening and nodules are presented in Table 2. Mild bronchiectasis and mild bronchial wall thickening were most frequently observed. In addition, the maximum severity score for bronchial wall thickening was never reached. If nodules were present, the diameter of the largest nodule exceeded the size of 5 mm in 89 (85%) (Baumann) and 87 (83%) (Hartmann) of patients.

Table 2. Severity of component scores bronchiectasis, bronchial wall thickening and nodules

Severity of abnormalities	Baumann n (%)	Hartmann n (%)
Bronchiectasis (total)	113 (100)	113 (100)
Highest score of CT scan		
Airway > 1 - < 2x vessel	93 (82)	73 (65)
Airway > 2 - < 3x vessel	14 (12)	26 (23)
Airway > 3x vessel	6 (5)	14 (12)
Bronchial wall thickening (total)	92 (100)	89 (100)
Highest score of CT scan		
BW > 0.33 - < 0.5x vessel	85 (92)	75 (84)
BW > 0.5 - < 1x vessel	7 (8)	14 (16)
BW > 1x vessel	0 (0)	0 (0)
Nodules (total)	105 (100)	106 (100)
Highest score of CT scan		
Largest nodule < 5 mm	16 (15)	19 (18)
Largest nodule > 5 - < 10 mm	46 (44)	43 (41)
Largest nodule > 10 mm	43 (41)	44 (42)

Maximal severity scores for the component scores bronchiectasis, bronchial wall thickening and nodules are presented for both methods. Numbers and percentages represent their distribution within the group on the most recent CT scan of patients (n = 138). CT = Computed tomography. BW = Bronchial wall.

Component and composite scores

Component scores (bronchiectasis, bronchial wall thickening, mucus plugging, nodules, reticulation, and GGO) and composite scores for airway disease, GLILD, and total disease (comprising all parameters) are shown in Table 3. The range between minimum and maximum scores using the Baumann method was wide, particularly for the component scores of bronchiectasis, nodules, GGO, reticulation, and the composite score GLILD which ranged between 0% and 100%. Differences in scores assessed with the Hartmann method were in a lower range compare to the Baumann method, and only the component score for nodules reached a maximum of 100%.

Longitudinal analysis

Longitudinal analysis of all follow up scans (n = 299) using generalized estimating equation models showed that the squared root-transformed Hartmann bronchiectasis component score increased significantly over time (p = 0.0097). We found no statistically significant longitudinal change in the Baumann bronchiectasis component score and the Baumann and Hartmann composite scores for GLILD, airway disease, and total disease. Prediction plots of bronchiectasis component scores are presented in Figure 6. Complete statistical results of the analysis and prediction plots are displayed in Figure S1 (supplementary material).

Table 3. Subscores and composite scores as a percentage of the maximum Baumann and Hartmann score

Subscore or composite score	Median (%)		Interquartile range (%)		Minimum - maximum (%)	
	Baumann	Hartmann	Baumann	Hartmann	Baumann	Hartmann
Bronchiectasis	25	6	8 - 42	1 - 11	0 - 100	0 - 68
Bronchial wall thickening	22	4	0 - 44	0 - 7	0 - 83	0 - 49
Mucus plugging	4	6	0 - 33	0 - 11	0 - 67	0 - 50
Nodules	22	28	6 - 56	6 - 53	0 - 100	0 - 100
Reticulation	50	11	0 - 83	3 - 17	0 - 100	0 - 42
GGO	67	17	33 - 100	6 - 33	0 - 100	0 - 78
Airway disease	17	6	8 - 30	2 - 9	0 - 65	0 - 44
GLILD	40	20	20 - 40	11 - 31	0 - 100	0 - 63
Total disease	21	9	14 - 28	6 - 13	0 - 56	0 - 32

Subscores of most common abnormalities and the composite scores of airway disease (sum of bronchiectasis, airway wall thickening and mucus plugging), granulomatous lymphocytic interstitial lung disease (GLILD) (sum of nodules, reticulation and ground-glass opacities (GGO)) and total disease (sum of all component scores) for both Baumann and Hartmann scoring methods are presented as the median, interquartile range and total range.

Inter- and intra-observer agreement

ICCs of the most common abnormalities are presented in Table 4. Both inter- as intra-observer agreement for the Hartmann method was for most items slightly higher than for the Baumann method. Between observers, the Hartmann component scores of reticulation and GGO only had poor inter-observer agreement, while within observers, the agreement for these items varied from poor to excellent. Of the component scores, nodules showed the highest agreement, while bronchial wall thickening and mucus plugging showed only poor to fair agreement. Subtypes of GGO (inflammatory or fibrotic) and reticulation (inflammatory, fibrotic, or mixed), which are exclusive to the Baumann method, showed a poor inter-observer agreement.

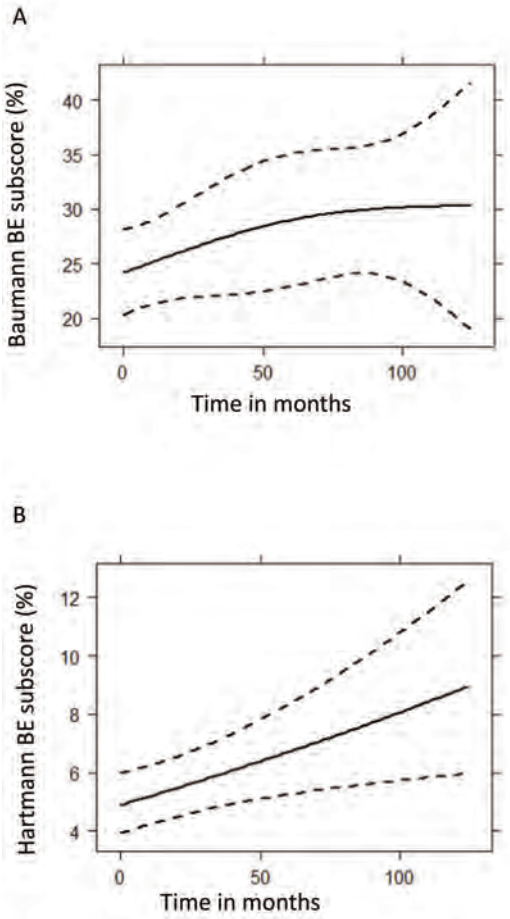

Figure 6. Prediction plots of bronchiectasis (BE) subscores from mixed-effects model analysis

These graphs show the predicted progression in computed tomography BE subscores (%) over time (months) for the Baumann (Figure 6A) and Hartmann (Figure 6B) scoring method, using mixed model analysis. A total of 299 CT scans were used for this follow up analysis. The Baumann BE subscore showed no significant change over time ($p = 0.1248$), while the squared root of Hartmann BE subscore increased significantly ($p = 0.0097$).

Table 4. Intra-class correlation coefficients for intra- and inter- observer agreement

Subscores and composite scores	Intra-observer 1		Intra-observer 2		Inter-observer	
	Baumann	Hartmann	Baumann	Hartmann	Baumann	Hartmann
GLILD (GGO + NOD + RET)	0.88	0.90	0.85	0.85	0.74	0.84
AD (BE + BWT + MP)	0.48	0.78	0.72	0.76	0.42	0.69
Nodules	0.93	0.90	0.86	0.79	0.78	0.85
Bronchiectasis	0.42	0.63	0.78	0.82	0.53	0.66
Reticulation	0.57	0.66	0.61	0.83	0.47	0.38
Bronchial wall thickening	0.55	0.72	0.45	0.47	0.34	0.49
GGO	0.60	0.38	0.86	0.83	0.44	0.35
Consolidation	0.89	0.33	0.73	0.77	0.55	0.72
Mucus plugging	0.48	0.42	0.52	0.57	0.05	0.38

Intra- and inter-observer agreement expressed as the intra-class coefficient values are presented in this table. Intra-class correlation coefficients were defined as follows: 0-0.39 poor; 0.4-0.59 fair, 0.6-0.74 good and > 0.75 excellent [31]. GLILD = Granulomatous lymphocytic interstitial lung disease. GGO = Ground-glass opacities. NOD = Nodules. RET = Reticulation. AD = Airway disease. BE = Bronchiectasis. BWT = Bronchial wall thickening. MP = Mucus plugging.

Discussion

In this retrospective study, chest CT features of CVID patients with a radiological diagnosis of GLILD were described. A total of 356 CT scans of 138 patients were included and scored using two dedicated CVID scoring systems. A limitation of our study is that histopathological proof of GLILD was rarely available. However it seems that GLILD is not often misdiagnosed in clinical practice: Maglione et al. showed that in 15 of 61 patients in which biopsies were available, diagnosis did not change [16]; and Mannina et al. demonstrated that there was no detectable difference between the patients biopsied and not biopsied in regard to the CT morphology or prognosis of the lung function [32]. Furthermore, CT patterns compatible with the diagnosis of GLILD were confirmed by the evaluation of the independent readers in this study for all except four participants. Therefore, we consider the effect of lacking biopsy proven GLILD in regard to the goal of this study as minor.

Phenotyping GLILD patients

The current pathogenic concept of GLILD comprises mixed T- and B-lymphocytic infiltration of the interstitium of the lungs, partly forming tertiary lymphoid structures next to granulomatous inflammation, follicular bronchiolitis, and reactive lymphoid hyperplasia [6, 33]. Typical features of GLILD on CT are patchy GGO, both sharp and

unsharp nodules, and reticular lesions varying from fine-lined to course [34]. Of the full cohort of 138 included patients, these features were present on their most recent CT scan in 95% of patients, and when also older CT scans were included this was 97% of patients. The two patients, without detectable features of GLILD even after re-evaluation by a thoracic radiologist (P. Ciet), were likely to be misdiagnosed by the radiologists of the participating centers. Overall, this is quite a good result, since reported inter-observer agreement between thoracic radiologists for the diagnosis of general interstitial pneumonia, which has similarities with GLILD, was only 0.52. That of non-thoracic radiologists was even less, namely, 0.48 [35]. In the patients with signs of GLILD on their most recent CT, only a small majority exhibited all key features of GLILD. In general, substantial heterogeneity of radiological features was observed in these patients. Enlarged lymph nodes were detected in only 38% of the patients for the Baumann score and in 51% for the Hartmann score. This low prevalence might be explained by the fact that intravenous contrast for better evaluation of lymph nodes was used in only half of the patients. There is no consensus whether contrast medium should be administered in these patients [36]. The lower percentage of CTs with lymph nodes for the Baumann score relative to the Hartmann score is probably related to the fact that for this method the exact size in mm of lymph nodes has to be measured which is challenging in the absence of contrast. Other studies report different results: Bates et al. described enlarged lymph nodes in only one out of thirteen GLILD patients [9], while Torigian et al. described enlarged lymph nodes in all five included patients [11].

Although bronchiectasis is not a feature of GLILD, it was the most common CT abnormality, present in 82% of GLILD patients. This result substantially exceeds previously published findings by Torigian et al. (20%), Hartono et al. (35%), Bates et al. (46%), Bouvry et al. (65%), and Mannina et al. (41% diffuse bronchiectasis, 59% focal) [9, 11, 12, 32, 37]. Importantly, the patients in some of these studies were younger [9, 11, 32], and in some studies, the interval between time of diagnosis and the CT scan acquisition was shorter [12, 37]. Furthermore, the studies by Hartono and Bates did not use scoring methods to analyze the CT scans systematically, which may have led to the underdiagnosis of bronchiectasis. Based on these findings, CVID patients with GLILD have a higher risk of airway disease compared to the risk previously reported for the general CVID cohort [13-16, 25, 38, 39].

Longitudinal analysis

Longitudinal follow-up analysis of 299 CT scans from 81 patients showed that only the Hartmann bronchiectasis component scores increased significantly over time. No increase was observed for the composite scores of GLILD, airway disease or total disease. When interpreting the longitudinal data, it is important to consider that we

did not correct for any treatment that was given to the patient, and that it is likely that treatment affects the amount of structural lung disease. In a longitudinal study of 54 CVID patients, scores for bronchiectasis and linear and/or irregular opacities were found to significantly decrease while nodules and GGO did not change [14]. Conversely, in another study 14 out of 20 CVID patients exhibited worsening of parenchymal changes on their follow up CT scan [13]. However, it should be noted that CT scoring was less standardized and statistical analyses were not performed in this study. Maglione et al. presented CVID cases with waxing and- waning CT features of ILD over time [5].

To study the natural course of disease progression of GLILD, a cohort study involving the routine acquisition of CT scans is required. Importantly, the risk benefit ratio of such a monitoring strategy is warranted as the radiation exposure needed for chest CT is low and taking into account the considerable morbidity and mortality in GLILD patients. Lung volume, CT protocols, and reconstruction kernels should be standardized, in order to improve the diagnostic yield of each CT scan and allow more sensitive monitoring of disease progression [40-42].

Comparison of scoring methods

In this study, two independent CT scoring methods were used to assess GLILD. Baumann scores (Table 3) were generally higher, related to the methodology how abnormalities are scored. For example, to compute bronchiectasis component scores for the Baumann method only the most bronchiectatic airways are included. Conversely, to compute bronchiectasis component scores for the Hartmann method also the mean severity of bronchiectasis is included. Consequently, the Baumann method results in higher scores whereas the Hartmann score are in a lower range. Hence, it is not possible to compare the component scores of both methods one-to-one. Longitudinally, the Hartmann method seemed to be more sensitive in assessing bronchiectasis progression over time compared to the Baumann method. The Hartmann method is performed in a lobe-specific manner. Because the Hartmann method provides more precise information about the extent and distribution of lung abnormalities than the Baumann method, this method is more suitable for clinical studies. However, in daily clinical care where time is a limiting factor, the Baumann method might be more feasible to implement.

The Hartmann method also had a slightly higher rate of reproducibility than the Baumann method. The observer agreement for the component score GGO was relatively low for both methods, which might reflect the severe nature of lung disease in GLILD patients: in cases of severe lung disease, the presence and extent of GGO might be harder to assess. Due to the retrospective nature of our study, it is likely

that the variable quality of CT scans and reconstruction protocols had a negative impact on the ICCs. Especially the component score reticulation produced low ICCs, which indicates that not all component scores are suitable to monitor GLILD lung disease. Two scoring items exclusive of the Baumann method performed very poor in our study: the subtype of GGO (inflammatory or fibrotic) and subtype of reticulation (inflammatory, fibrotic, or mixed). Thus, these items failed to provide reliable information and to our opinion their relevance is debatable.

However, the component score nodules showed excellent ICCs, and furthermore, the GLILD composite score produced good (Baumann) and excellent (Hartmann) ICCs. A suggestion is to proceed with such scores as main outcomes, while further investigating and improving scoring items with lower reproducibility. Once the relevant changes are agreed upon it will be of interest to transfer the analysis to computer based image analysis in order to render such a scoring method also feasible in regard to time. For this purpose this collection of CT scans will be an excellent resource [43].

Conclusions

As CT morphology is the one of the major parameters for evaluation during the follow up of GLILD in CVID patients, reliable scoring methods for the longitudinal comparison of interstitial lung changes are required. In this study, we established and evaluated two scoring methods with CT scans of 138 GLILD patients. The composite score for GLILD showed high reproducibility especially according to the Hartmann score, and may become a valuable tool for monitoring disease in longitudinal studies. Once the clinical value of such a score has been demonstrated, automated image analysis systems are needed to optimize the assessment of GLILD and render it suitable for routine diagnostics.

Acknowledgments

We would like to acknowledge the following members of the STILPAD study group: Helen Baxendale, Claire Bethune, Audrey Gorse, Sofia Grigoriadou, Aarnoud Huissoon, Anne-Sophie Korganow, Hilary Longhurst, Marion Malphettes, Joanne Miller, Carla Neumann, Eric Oksenhendler, Jean- Louis Pasquali, Smita Patel, Hendrik Schulze-Koops, Eva C. Schwaneck, Borggia Seemampillai, Suranjith Seneviratne, Hans-Peter Tony, Jean-Francois Viallard, Torsten Witte and Gabriel Wong.

References

[1] Bonilla FA, Barlan I, Chapel H, Costa-Carvalho BT, Cunningham-Rundles C, de la Morena MT, et al. International Consensus Document (ICON): Common Variable Immunodeficiency Disorders. The journal of allergy and clinical immunology In practice. 2016;4:38-59.

[2] Conley ME, Notarangelo LD, Etzioni A. Diagnostic criteria for primary immunodeficiencies. Representing PAGID (Pan-American Group for Immunodeficiency) and ESID (European Society for Immunodeficiencies). Clinical immunology (Orlando, Fla). 1999;93:190-7.

[3] Gathmann B, Mahlaoui N, Gerard L, Oksenhendler E, Warnatz K, Schulze I, et al. Clinical picture and treatment of 2212 patients with common variable immunodeficiency. The Journal of allergy and clinical immunology. 2014;134:116-26.

[4] Orange JS, Grossman WJ, Navickis RJ, Wilkes MM. Impact of trough IgG on pneumonia incidence in primary immunodeficiency: A meta-analysis of clinical studies. Clinical immunology (Orlando, Fla). 2010;137:21-30.

[5] Maglione PJ, Overbey JR, Cunningham-Rundles C. Progression of Common Variable Immunodeficiency Interstitial Lung Disease Accompanies Distinct Pulmonary and Laboratory Findings. The journal of allergy and clinical immunology In practice. 2015;3:941-50.

[6] Park JH, Levinson AI. Granulomatous-lymphocytic interstitial lung disease (GLILD) in common variable immunodeficiency (CVID). Clinical immunology (Orlando, Fla). 2010;134:97-103.

[7] Resnick ES, Moshier EL, Godbold JH, Cunningham-Rundles C. Morbidity and mortality in common variable immune deficiency over 4 decades. Blood. 2012;119:1650-7.

[8] Cunningham-Rundles C, Bodian C. Common variable immunodeficiency: clinical and immunological features of 248 patients. Clinical immunology (Orlando, Fla). 1999;92:34-48.

[9] Bates CA, Ellison MC, Lynch DA, Cool CD, Brown KK, Routes JM. Granulomatous-lymphocytic lung disease shortens survival in common variable immunodeficiency. The Journal of allergy and clinical immunology. 2004;114:415-21.

[10] Chapel H, Lucas M, Lee M, Bjorkander J, Webster D, Grimbacher B, et al. Common variable immunodeficiency disorders: division into distinct clinical phenotypes. Blood. 2008;112:277-86.

[11] Torigian DA, LaRosa DF, Levinson AI, Litzky LA, Miller WT, Jr. Granulomatous-lymphocytic interstitial lung disease associated with common variable immunodeficiency: CT findings. J Thorac Imaging. 2008;23:162-9.

[12] Hartono S, Motosue MS, Khan S, Rodriguez V, Iyer VN, Divekar R, et al. Predictors of granulomatous lymphocytic interstitial lung disease in common variable immunodeficiency. Ann Allergy Asthma Immunol. 2017;118:614-20.

[13] Bondioni MP, Soresina A, Lougaris V, Gatta D, Plebani A, Maroldi R. Common variable immunodeficiency: computed tomography evaluation of bronchopulmonary changes including nodular lesions in 40 patients. Correlation with clinical and immunological data. Journal of computer assisted tomography. 2010;34:395-401.

[14] Gregersen S, Aalokken TM, Mynarek G, Fevang B, Holm AM, Ueland T, et al. Development of pulmonary abnormalities in patients with common variable immunodeficiency: associations with clinical and immunologic factors. Ann Allergy Asthma Immunol. 2010;104:503-10.

[15] Maarschalk-Ellerbroek LJ, de Jong PA, van Montfrans JM, Lammers JW, Bloem AC, Hoepelman AI, et al. CT screening for pulmonary pathology in common variable immunodeficiency disorders and the correlation with clinical and immunological parameters. Journal of clinical immunology. 2014;34:642-54.

[16] Maglione PJ, Overbey JR, Radigan L, Bagiella E, Cunningham-Rundles C. Pulmonary radiologic findings in common variable immunodeficiency: clinical and immunological correlations. Ann Allergy Asthma Immunol. 2014;113:452-9.

[17] Thickett KM, Kumararatne DS, Banerjee AK, Dudley R, Stableforth DE. Common variable immune deficiency: respiratory manifestations, pulmonary function and high-resolution CT scan findings. QJM : monthly journal of the Association of Physicians. 2002;95:655-62.

[18] Ardeniz O, Basoglu OK, Gunsar F, Unsel M, Bayraktaroglu S, Mete N, et al. Clinical and immunological analysis of 23 adult patients with common variable immunodeficiency. Journal of investigational allergology & clinical immunology. 2010;20:222-36.

[19] Costa-Carvalho BT, Wandalsen GF, Pulici G, Aranda CS, Sole D. Pulmonary complications in patients with antibody deficiency. Allergol Immunopathol. 2011;39:128-32.

[20] Szczesniak R, Turkovic L, Andrinopoulou ER, Tiddens H. Chest imaging in cystic fibrosis studies: What counts, and can be counted? J Cyst Fibros. 2017;16:175-85.

[21] van de Ven AA, van Montfrans JM, Terheggen-Lagro SW, Beek FJ, Hoytema van Konijnenburg DP, Kessels OA, et al. A CT scan score for the assessment of lung disease in children with common variable immunodeficiency disorders. Chest. 2010;138:371-9.

[22] Gregersen S, Aalokken TM, Mynarek G, Kongerud J, Aukrust P, Froland SS, et al. High resolution computed tomography and pulmonary function in common variable immunodeficiency. Respiratory medicine. 2009;103:873-80.

[23] Chase NM, Verbsky JW, Hintermeyer MK, Waukau JK, Tomita-Mitchell A, Casper JT, et al. Use of combination chemotherapy for treatment of granulomatous and lymphocytic interstitial lung disease (GLILD) in patients with common variable immunodeficiency (CVID). Journal of clinical immunology. 2013;33:30-9.

[24] Chapel H, Lucas M, Patel S, Lee M, Cunningham-Rundles C, Resnick E, et al. Confirmation and improvement of criteria for clinical phenotyping in common variable immunodeficiency disorders in replicate cohorts. The Journal of allergy and clinical immunology. 2012;130:1197-8 e9.

[25] Schutz K, Alecsandru D, Grimbacher B, Haddock J, Bruining A, Driessen G, et al. Imaging of Bronchial Pathology in Antibody Deficiency: Data from the European Chest CT Group. Journal of clinical immunology. 2019;39:45-54.

[26] Wainwright CE, Vidmar S, Armstrong DS, Byrnes CA, Carlin JB, Cheney J, et al. Effect of bronchoalveolar lavage-directed therapy on Pseudomonas aeruginosa infection and structural lung injury in children with cystic fibrosis: a randomized trial. Jama. 2011;306:163-71.

[27] Brody AS, Klein JS, Molina PL, Quan J, Bean JA, Wilmott RW. High-resolution computed tomography in young patients with cystic fibrosis: distribution of abnormalities and correlation with pulmonary function tests. J Pediatr. 2004;145:32-8.

[28] Rosenow T, Oudraad MC, Murray CP, Turkovic L, Kuo W, de Bruijne M, et al. PRAGMA-CF. A Quantitative Structural Lung Disease Computed Tomography Outcome in Young Children with Cystic Fibrosis. American journal of respiratory and critical care medicine. 2015;191:1158-65.

[29] Hansell DM, Bankier AA, MacMahon H, McLoud TC, Muller NL, Remy J. Fleischner Society: glossary of terms for thoracic imaging. Radiology. 2008;246:697-722.

[30] Koo TK, Li MY. A Guideline of Selecting and Reporting Intraclass Correlation Coefficients for Reliability Research. J Chiropr Med. 2016;15:155-63.

[31] Cicchettie DV. Guidelines, criteria, and rules of thumb for evaluating normed and standardized assessment instruments in psychology. Psychological Assessment. 1994;6:284-90.

[32] Mannina A, Chung JH, Swigris JJ, Solomon JJ, Huie TJ, Yunt ZX, et al. Clinical Predictors of a Diagnosis of Common Variable Immunodeficiency-related Granulomatous-Lymphocytic Interstitial Lung Disease. Ann Am Thorac Soc. 2016;13:1042-9.

[33] Maglione PJ, Gyimesi G, Cols M, Radigan L, Ko HM, Weinberger T, et al. BAFF-driven B cell hyperplasia underlies lung disease in common variable immunodeficiency. JCI Insight. 2019;4.

[34] Prasse A, Kayser G, Warnatz K. Common variable immunodeficiency-associated granulomatous and interstitial lung disease. Current opinion in pulmonary medicine. 2013;19:503-9.

[35] Walsh SL, Calandriello L, Sverzellati N, Wells AU, Hansell DM, Consort UIPO. Interobserver agreement for the ATS/ERS/JRS/ALAT criteria for a UIP pattern on CT. Thorax. 2016;71:45-51.

[36] Hurst JR, Verma N, Lowe D, Baxendale HE, Jolles S, Kelleher P, et al. British Lung Foundation/United Kingdom Primary Immunodeficiency Network Consensus Statement on the Definition, Diagnosis, and Management of Granulomatous-Lymphocytic Interstitial Lung Disease in Common Variable Immunodeficiency Disorders. The journal of allergy and clinical immunology In practice. 2017;5:938-45.

[37] Bouvry D, Mouthon L, Brillet PY, Kambouchner M, Ducroix JP, Cottin V, et al. Granulomatosis-associated common variable immunodeficiency disorder: a case-control study versus sarcoidosis. Eur Respir J. 2013;41:115-22.

[38] Touw CM, van de Ven AA, de Jong PA, Terheggen-Lagro S, Beek E, Sanders EA, et al. Detection of pulmonary complications in common variable immunodeficiency. Pediatric allergy and immunology : official publication of the European Society of Pediatric Allergy and Immunology. 2010;21:793-805.

[39] Tanaka N, Kim JS, Bates CA, Brown KK, Cool CD, Newell JD, et al. Lung diseases in patients with common variable immunodeficiency: chest radiographic, and computed tomographic findings. Journal of computer assisted tomography. 2006;30:828-38.

[40] Kuo W, Kemner-van de Corput MP, Perez-Rovira A, de Bruijne M, Fajac I, Tiddens HA, et al. Multicentre chest computed tomography standardisation in children and adolescents with cystic fibrosis: the way forward. Eur Respir J. 2016;47:1706-17.

[41] Salamon E, Lever S, Kuo W, Ciet P, Tiddens HA. Spirometer guided chest imaging in children: It is worth the effort! Pediatr Pulmonol. 2017;52:48-56.

[42] do Amaral RH, Nin CS, de Souza VVS, Alves GRT, Marchiori E, Irion K, et al. Computed Tomography Findings of Bronchiectasis in Different Respiratory Phases Correlate with Pulmonary Function Test Data in Adults. Lung. 2017;195:347-51.

[43] Bartholmai BJ, Raghunath S, Karwoski RA, Moua T, Rajagopalan S, Maldonado F, et al. Quantitative computed tomography imaging of interstitial lung diseases. J Thorac Imaging. 2013;28:298-307.

Supplementary material

Table S1. Scoring items Baumann method

Scoring item	Scoring type	Meaning score	Score range
Bronchial wall thickening Bronchiectasis Mucus large airways Mucus small airways Atelectasis Nodules <5 mm Nodules >5 - <10 mm Nodules >10 mm Lines Consolidation Linear scars and bands Ground-glass opacities Cysts Emphysema or bullae	Extent	Number of lobes	0-6
Thickest bronchial wall thickening	Severity	0 = None 1 = BW < 0.5 x V 2 = 0.5 x V < BW < V 3 = BW > V	0-3
Largest bronchiectasis	Severity	0 = None 1 = B < 2 x V 2 = 2 x V < B < 3 x V 3 = B > 3 x V	0-3
Predominant type lines	Pathologic mechanism	0 = Inflammation 1 = Fibrosis 2 = Mixed type	0-2
Cause ground-glass opacities	Pathologic mechanism	0 = Fibrosis 1 = Inflammation	0-1
Trapped air inspiratory scan Trapped air expiratory scan Lymphadenopathy hilar mediastinal	Presence	0 = No 1 = Yes	0-1
Lymphadenopathy hilar mediastinal	Size	Size (shortest axis) of largest lymph node in mm	…

This table presents all scorings items of the Baumann scoring method for computed tomography scans. BW = Bronchial wall. V = Accompanying vessel. B = Bronchial lumen.

Table S2. Scoring items of Hartmann method

Scorings item per lobe	Scoring type	Meaning score	Score range
Bronchiectasis large airways Bronchiectasis small airways Bronchial wall thickening large airways Bronchial wall thickening small airways Mucus large airways Mucus small airways Bullae cysts Ground-glass opacities Reticulation without distortion Reticulation with distortion Distortion alone Consolidation Atelectasis Emphysema Trapped air	Extent	0 = None 1 = > 0 - 33% 2 = 33-66% 3 = > 66%	0-3
Bronchiectasis large airways Bronchiectasis small airways Bronchial wall thickening large airways Bronchial wall thickening small airways	Extent	Number of segments	0-5
Largest bronchiectasis Average bronchiectasis	Severity	0 = None 1 = B < 2 x V 2 = 2 x V < B < 3 x V 3 = B > 3 x V	0-3
Bronchial wall thickening	Severity	0 = None 1 = BW < 0.5 x V 2 = 0.5 x V < BW < V 3 = BW > V	0-3
Number of nodules	Amount	None 1 = < 5 nodules 2 = 5-10 nodules 3 = >10 nodules	0-3
Contour nodules	Contour	0 = None 1 = Unsharp 2 = Sharp	0-2
Largest nodules	Size	None 1 = < 0,5 cm 2 = 0.5 – 1.0 cm 3 = > 1 cm	0-3
Pattern trapped air	Pattern	0 = None 1 = Subsegmental 2 = Segmental	0-2
Lymphadenopathy hilar mediastinal	Presence	0 = No 1 = Yes	0-1

This table presents all scorings items of the Hartmann scoring method for computed tomography scans. B = Bronchial lumen. V = Accompanying vessel. BW = Bronchial wall.

Table S3. Computed tomography scan characteristics

CT scan details	n (%)
Volumetric	275 (77)
Sequential	81 (23)
Slice thickness in mm	
0.6-1	150 (42)
> 1-3	117 (33)
> 3-5	83 (24)
> 5-8	6 (2)
Lung window	356 (100)
Mediastinal window	335 (94)
Contrast given	175 (49)
Expiratory	2 (0)

This table presents the computed tomography (CT) scan characteristics of all included scans (n total = 356). Data are presented as absolute numbers (n) and percentages.

Figure S1. Prediction plots of composite scores of granulomatous lymphocytic interstitial lung disease (GLILD), airway disease (AD) and total disease from mixed-effects model analysis

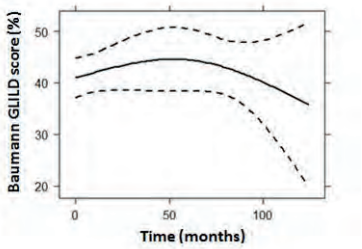

a. Baumann GLILD prediction plot

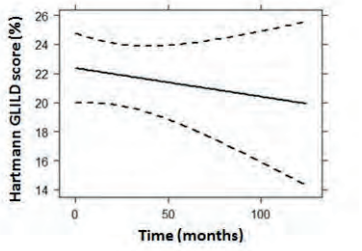

b. Hartmann GLILD prediction plot

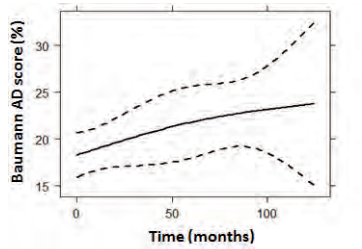

c. Baumann AD prediction plot

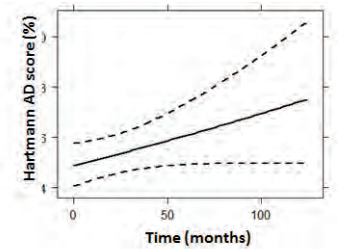

d. Hartmann AD prediction plot

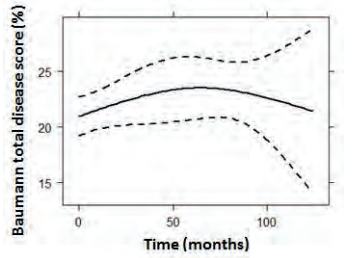

e. Baumann total disease prediction plot

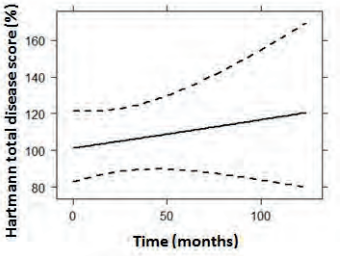

f. Hartmann total disease prediction plot

These graphs show the predicted progression in computed tomography scores (%) over time (months). The composite score GLILD is a combined score of ground-glass opacities, reticulation, and nodules. The composite score airway disease is the sum of bronchiectasis, bronchial wall thickening and mucus plugging scores. The composite score total disease score is derived from the sum of all scored abnormalities. Figure a and b: Baumann and Hartmann GLILD score ($p = 0.512$ and 0.453 respectively). Figure c and d: Baumann and Hartmann AD score ($p = 0.061$ and $p = 0.073$ respectively). Figure e and f: Baumann and Hartmann total disease score ($p = 0.539$ and $p = 0.171$ respectively).

Chapter 5

Quantitative chest computed tomography scoring technique for bronchiectasis (BEST-CT)

Submitted

Jennifer J. Meerburg, Antonio Garcia-Uceda, Olivier Dragt, Eleni-Rosalina Andrinopoulou, Mariette P.C. Kemner van de Corput , Pierluigi Ciet, Gerhild Angyalosi, J. Stuart Elborn, James D. Chalmers, Michael Tunney, Marleen de Bruijne, Harm A.W.M. Tiddens, on behalf of the iABC study group

Abstract

Aim To develop a sensitive computed tomography (CT) scoring system to phenotype and quantify structural lung disease in bronchiectasis (BE) patients.

Methods Recent CT scans of BE patients with chronic *Pseudomonas aeruginosa* infection enrolled in the iBEST study were collected and analysed with the BE scoring technique for CT (BEST-CT). Inclusion criteria: volumetric CT scans and slice thickness ≤ 3 mm. BEST-CT scores are expressed as % of total lung volume. Scoring items in hierarchical order are: consolidation/ atelectasis, BE with mucus plugging (BEMP), BE without mucus plugging (BEwMP), airway wall thickening (AWT), MP, ground-glass opacities, emphysema/ bullae, healthy airways (HA), and healthy parenchyma (HP). Furthermore, composite scores total bronchiectasis (%TBE = %BEMP + %BEwMP), airway disease (%AD = %TBE + %MP + %AWT) and total disease (%DIS = all but %HA and %HP) were calculated. Intra-class correlation coefficients (ICC) were calculated within and between observers. BEST-CT scores were compared with the Hartmann CT scoring method, intra-branch tapering, FEV_1, bronchiectasis severity index (BSI), quality of life (QOL), and exacerbations. Median [interquartile range] values are reported.

Results 84 Inspiratory CT scans were included. BEST-CT composite scores: %TBE 3.0 [1.4-5.1], %AD 6.5 [3.4-11.8], and %DIS 9.4 [6.0-17.7]. ICC values for %TBE, %AD and %DIS were good to excellent. Significant correlations were found between %TBE and Hartmann BE scores ($r = 0.69$, $p < 0.001$), FEV_1 ($r = -0.24$, $p = 0.027$), and intra-branch tapering ($r = -0.34$, $p = 0.002$). No significant correlations were found between BEST-CT scores and BSI, QOL, or exacerbations.

Conclusion BEST-CT is a reproducible CT scoring system to quantify and phenotype BE patients. Considerable heterogeneity of structural changes was observed.

Introduction

Bronchiectasis (BE) is defined as abnormal airway widening, lack of tapering, and visibility of small airways in the periphery of the lung [1]. This is now usually determined by chest computed tomography (CT) [2]. The term BE primarily refers to the anatomical change, but also is used to describe the disease constellation associated with these structural changes {Aliberti, in press Lancet Respiratory}. BE can be caused by and associated with a wide range of diseases, resulting in a heterogeneous patient population [3]. Chronic bacterial lower airway infection plays an important role in BE disease. *Pseudomonas aeruginosa* (*Pa*) is present in 12-31% of the European BE population [4]. Chronic infection with *Pa* is associated with a reduced quality of life and shortened life expectancy [5].

To date, no approved therapies are registered for BE patients. However, inhaled antibiotics for anti-*Pa* treatment are included in BE guidelines as a treatment option and prescribed off-label in many BE patients [6]. In randomised controlled trials in BE patients, outcomes such as forced expiratory volume in 1 second (FEV_1), exacerbation rate, and hospitalisation failed to show any decisive effect of inhaled antibiotic agents [6]. Surprisingly, chest CT related outcome measures have been poorly investigated for BE disease. As BE is a radiological diagnosis, chest CT scans contain data that could potentially be used as outcome measures for clinical trials and for clinical care.

The first step to use chest CT scans for these purposes is to develop a sensitive and well-standardised image analysis method that can quantify all relevant structural abnormalities. Two CT scoring methods previously used for other lung diseases could potentially work for the BE population. The first method is the Hartmann chest CT scoring method, which was initially developed for common variable immunodeficiency disease (CVID) patients and includes structural abnormalities that can also be present in BE patients [7]. A disadvantage of this method is the semi-quantitative approach where the extent of disease is determined by eye-balling. The second method is PRAGMA-CF which is a grid-based quantitative scoring method developed to quantify structural changes in cystic fibrosis (CF) lung disease [8]. An advantage is that annotated images can be used as ground truth for the development of an automated system. A disadvantage of PRAGMA-CF is that it only captures abnormalities that are common in CF patients, making it less suitable for the BE population. A combination of the two methods might result in a sensitive and robust analysis method for bronchiectasis. Once a sensitive image analysis method is developed, the second step is to validate this new method with other CT outcome measures and with clinical outcome measures that indicate BE disease.

Besides the Hartmann method, another CT outcome measure that could be used for validation is the amount of intra-branch tapering of the airways [9]. Tapering refers to the progressive reduction of airway diameter along the branch, and a reduced tapering is an important hallmark of BE. Kuo et al. showed that reduced tapering could reliably be detected across central and peripheral airways [9].

The aim of this study was to develop a sensitive image analysis method for chest CT scans to phenotype and quantify structural lung disease in BE patients. We first developed the grid based BronchiEctasis Scoring Technique for CT (BEST-CT). Next, we validated BEST-CT scores against the Hartmann method and to intra-branch tapering measurements. Furthermore, BEST-CT scores were correlated to FEV1, quality of life scores, *Pa* sputum density, and the bronchiectasis severity index (BSI) to determine face validity [10].

Methods

Study population

The iBEST study was a randomised placebo controlled trial designed to evaluate the efficacy, safety and tolerability of tobramycin inhalation powder in BE patients with a chronic *Pa* infection [11, 12]. As part of this trial, the BEST-CT substudy was performed. Duration of iBEST study was from February 2017 until March 2019. Main inclusion criteria for the iBEST study were: age ≥ 18 years, a proven diagnosis of BE confirmed on CT scan by the local radiologist, and *Pa* infection. Main exclusion criteria were a diagnosis of CF, asthma, or chronic obstructive pulmonary disease with a smoking history of at least 20 pack years. A complete list of in- and exclusion criteria can be found in Supplement 1 (Supplementary material) [12]. For the BEST-CT study we collected CT scans of patients enrolled in the iBEST study.

CT collection

We aimed to collect from all patients the most recent chest CT scan relative to the time of enrolment in the iBEST study. The participating centres de-identified the CT scans prior to transfer to the Erasmus MC LungAnalysis core laboratory (Rotterdam, the Netherlands). Inclusion criteria for the CT scans collected for the BEST-CT substudy were: digital format, volumetric protocol, and slice thickness ≤ 3 mm. CT scans with severe motion artefacts or incomplete display of the lungs were excluded from further analysis.

Clinical parameters

For all patients included in the BEST-CT substudy the following clinical data were collected at the first iBEST study visit: FEV_1% predicted using the Global Lung Initiative prediction equations [13], Quality of Life Questionnaire for Bronchiectasis (QOL-B) [14], BSI [10], and *Pa* sputum density in log colony forming units (CFU) per gram. Over the six month study period, the number of exacerbations were recorded. More details on the QOL-B, BSI, microbiology and the definition of exacerbation can be found in Supplement 2 [12].

CT scan analysis

De-identified CT scans were analysed in random order by three certified and experienced independent observers (a medical doctor, a MSc LungAnalysis technician and medical master student). Certification was obtained by completion of standardised training modules (CF-CT [15], PRAGMA-CF [8]). All CT scans were analysed with the newly developed BEST-CT and the Hartmann method. One observer scored all CT scans using the BEST-CT, another observer scored all CT scans with the Hartmann method. Both observers scored 20 randomly selected CT scans for intra-observer agreement analysis, and the third observer scored 20 CT scans with both the BEST-CT and the Hartmann method to assess inter-observer agreement analysis.

BEST-CT

The BEST-CT is a grid based scoring system using an in house developed software program (Saldsegvol, Erasmus MC, Rotterdam) that was previously used for the development of grid based scoring systems for CF [8], bronchopulmonary dysplasia [16], and congenital lung abnormalities [17]. In short: a grid is placed on top of the axial CT slice. The content of each grid cell that falls for at least 50% within the lung is annotated according a list of possible components in a hierarchical order (see paragraph component scores BEST-CT). After all selected slices have been annotated component scores are automatically computed and expressed as % of the total lung volume. The steps that were taken to develop the BEST-CT method are shown in the flowchart (Figure 1). A more detailed description of the development of the BEST-CT is presented in Supplement 3.

Components BEST-CT

For the inspiratory scans, the following nine components are annotated, in hierarchical order (Figure 2):

1. Atelectasis and/or consolidation (ATCON);
2. BE with mucus plugging (BEMP)
3. BE without mucus plugging (BEwMP)
4. Airway wall thickening (AWT)
5. Mucus plugging without BE (MP)
6. Ground-glass opacities (GGO)
7. Emphysema and/or bullae (EMPBUL)
8. Healthy airways (HA)
9. Healthy parenchyma (HP)

If a grid cell contains more than one of these components, it is assigned the component with the highest rank. The following composite scores are calculated from the component scores: total bronchiectasis (%TBE) = %BEMP + %BEwMP; total mucus plugging (%TMP) = %BEMP + %MP; airway disease (%AD) = %TBE + %AWT + %TMP; total disease (%DIS) = %ATCON + %TBE + %AWT + %MP + %GGO + %EMPBUL.

For expiratory CT scans, the following two component scores are assessed:

1. Low attenuation regions (LAR)
2. Normal or high attenuation regions (NOR)

LAR are regions where the lung parenchyma is darker than it should be on expiration. LAR can be caused by hypo-perfusion, trapped air, emphysema or a combination of these components. Normal or high attenuation regions are regions that appear lighter (grey) on expiratory CT scans.

Hartmann method

The Hartmann method is a semi-quantitative CT scoring method developed for CVID patients (Chapter 4, Table S2, Supplementary material) [7]. The extent of the structural abnormalities is scored by eye-balling for each lobe including the lingula. The total Hartmann score for bronchiectasis (HM-BE), total score for mucus plugging (HM-MP), total airway disease score (HM-AD) and the total disease score (HM-DIS) are used for correlation analyses.

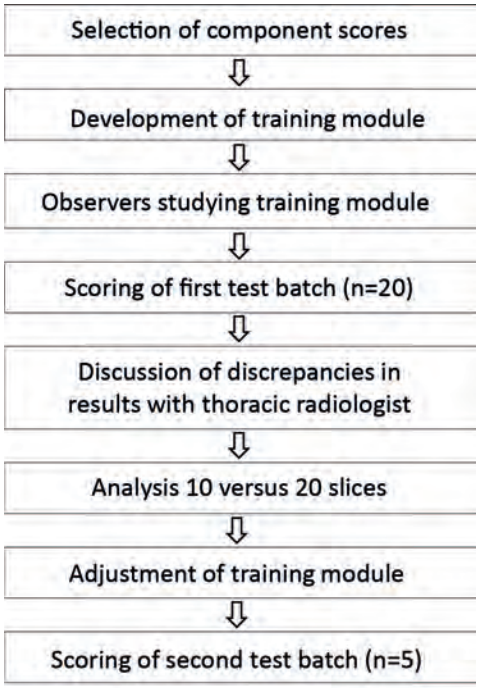

Figure 1. Flowchart of BEST-CT development

This flowchart shows the steps taken in the development of the BronchiEctasis Scoring Technique for Computed Tomography (BEST-CT).

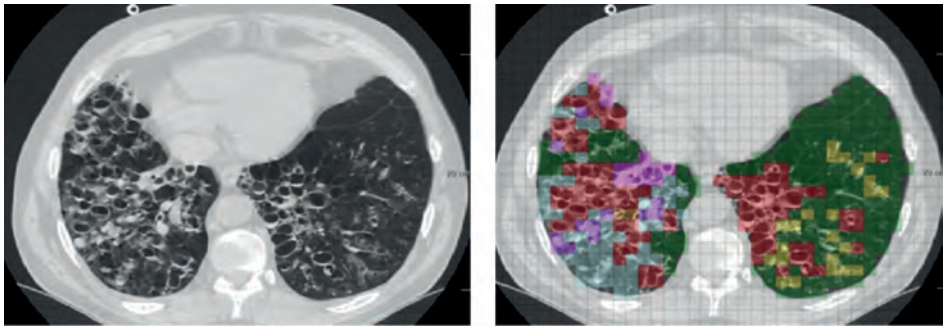

Figure 2. CT slice scored with the BEST-CT

The image on the left is an axial chest CT slice of a bronchiectasis patient. The image on the right is the annotated image. Each grid cell with >50% lung tissue is annotated, scoring items are assessed in hierarchical order: atelectasis and/or consolidation (pink), bronchiectasis with mucus (purple), bronchiectasis without mucus plugging (red), airway wall thickening (not present in example), mucus plugging (yellow), ground-glass opacities (light blue), emphysema and/or bullae (not present in example), healthy airways (bright green), and healthy parenchyma (dark green).

Intra-branch tapering

Reduced airway tapering is considered a feature of BE. Intra-branch tapering is defined as the average percentage reduction of the airway lumen diameter per mm along the centreline within one branch (Supplement 4) [9]. The median intra-branch tapering over all measured branches in a scan was used for correlation analyses.

Ethics

The iBEST study was approved by the Institutional Review Board of participating centres or independent ethics committees. Written informed consent was obtained from all study subjects.

Statistics

Descriptive data are presented as median [interquartile range] or percentage.

Pearson correlation coefficients were calculated to study the association between BEST-CT component and composite scores and Hartmann scores and FEV_1 % predicted, *Pa* sputum density, QOL-B scores, and tapering measurements. Mann-Whitney U tests were used to compare outcomes of the BEST-CT and Hartmann scores between BSI groups. A p-value of < 0.05 was considered significant, we did not correct for multiple testing.

The relation between %TBE and %AD and exacerbations during the iBEST study was assessed with logistic regression models, taking into account the FEV1 and the treatment regimen (tobramycin inhalation powder or placebo) [12].To study intra- and inter-observer agreement of CT scoring methods, intra-class correlation coefficients (ICC) were calculated with two-way mixed-effects models, assessing consistency of single measures. ICC values < 0.50 were considered poor, 0.50-0.75 moderate, 0.75-0.90 good, and > 0.90 excellent [18].

For statistical analyses, SPSS version 27.0 (SPSS Inc., Chicago, IL) and statistical software package R, version 3.6.1 (free download from www.rproject.org) were used.

Results

CT collection

In total, 99 inspiratory CT scans were collected from 17 participating centres. Fifteen CT scans were excluded (Figure 3). Hence, 84 inspiratory scans were analysed using the BEST-CT, Hartmann method, and intra-branch tapering method. The median [interquartile range (IQR)] time between CT scan and first iBEST study visit was 15 [6-29] months.

Sixteen expiratory CT scans were collected, of which only 4 scans met the inclusion criteria. Therefore, we did not further investigate correlations between %LAR and other parameters.

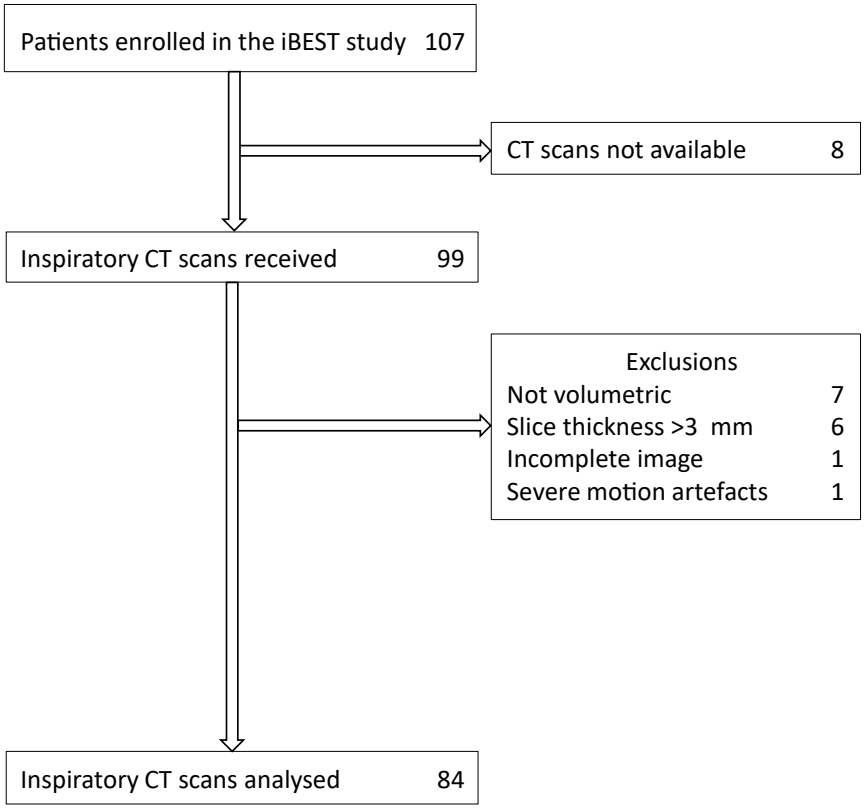

Figure 3. Flow chart CT selection

This flow-chart shows the selection of computed tomography (CT) scans. The most recent scan was collected from each study patient, and ultimately a total of 84 inspiratory CT scans were included for image analysis.

Study population

A total of 84 patients with appropriate CT scans for analysis were recruited. Demographical data are presented in Table 1.

Table 1. Patient demographics at iBEST study initiation visit

Demographics	Value
Female sex (n (%))	54 (64)
Age in years (median [IQR])	66 [58-74]
BMI (median [IQR])	24 [22-27]
Country (n (%))*	
Spain	22 (26)
United Kingdom	20 (24)
France	16 (19)
Italy	13 (16)
Germany	7 (8)
Belgium	6 (7)
Ethnicity (n (%))	
Caucasian	74 (88)
Asian	1 (1)
Pacific Islander	1 (1)
Other	8 (10)
Spirometry (median [IQR])	
FEV_1 % predicted	59 [46-70]
FVC % predicted	72 [64-88]
FEF_{25-75} % predicted	30 [23-47]
Bronchiectasis severity index (median [IQR])	10 [7-13]
Pulmonary exacerbations 12 months before start of the iBEST study (median [IQR])	2 [2-3]

IQR = Interquartile range. BMI = Body mass index. FEV_1= Forced expiratory volume in 1 second. FVC = Forced vital capacity. FEF_{25-75} = Forced expiratory flow from 25% until 75% of FVC. *The sum of the percentages adds up to 99% due to rounding.

CT scan analysis

BEST-CT

BEST-CT outcomes of the inspiratory scans per study patient are shown in a stacked-bar graph (Figure 4). Table 2 presents the median [IQR] of each component score, and the composite scores %TBE, %TMP, %AD and %DIS. BE, MP and GGO were present in almost all patients. %DIS varied from between 0.96-44.38%. Of the four expiratory scans, two scans showed LAR (%LAR = 12.85 and 29.88), and in the other two scans LAR were absent.

Table 2. Component and composite scores BEST-CT and corresponding Hartmann scores

	BEST-CT			Hartmann		
	Median	**IQR**	**Prevalence (%)**	**Median**	**IQR**	**Prevalence (%)**
Component scores						
%ATCON	1.46	0.60 - 3.19	99	13.89	11.11 - 16.67	100
%BEMP	0.10	0.00 - 0.47	58	-	-	-
%BEwMP	2.69	1.29 - 4.78	99	-	-	-
%AWT	0.07	0.00 - 0.21	64	7.41	3.70 - 12.96	93
%MP	2.57	1.06 - 5.76	98	-	-	-
%GGO	0.34	0.06 - 1.05	80	5.56	1.39 - 16.67	75
%EMPBUL	0.00*	0.00 - 0.00	16	0.00	0.00 - 0.00	20
%HA	3.78	2.71 - 4.48	100	-	-	-
%HP	86.48	78.64 - 89.65	100	-	-	-
Composite scores						
%TBE	2.99	1.43 - 5.10	99	21.18	13.89 - 29.17	100
%TMP	2.77	1.48 - 6.19	98	15.28	6.25 - 27.08	94
%AD	6.48	3.42 - 11.80	100	16.67	9.57 -22.22	100
%DIS	9.44	5.96 - 17.65	100	11.11	7.38 - 14.84	100

This table presents the median, interquartile ranges [IQR] and prevalence of BronchiEctasis Scoring Technique for Computed Tomography (BEST-CT) component and composite scores, and if applicable corresponding Hartmann scores. The order in the table is according to the hierarchical order by which the components are scored. ATCON = Atelectasis and/or consolidation. BEMP = Bronchiectasis with mucus plugging. BEwMP = Bronchiectasis without mucus plugging. AWT = Airway wall thickening. MP = Mucus plugging. GGO = ground-glass opacities. EMPBUL = emphysema and/or bullae. HA = healthy airways. HP = healthy parenchyma. TBE = Total bronchiectasis. TMP = Total mucus plugging. AD = Airway disease. DIS = Total disease. All BEST-CT subscores are expressed in % of total lung volume, and Hartmann subscores are expressed as % of the maximum score. *As EMPBUL were present in relatively few CT scans (n = 13), the median and IQR are 0.00.

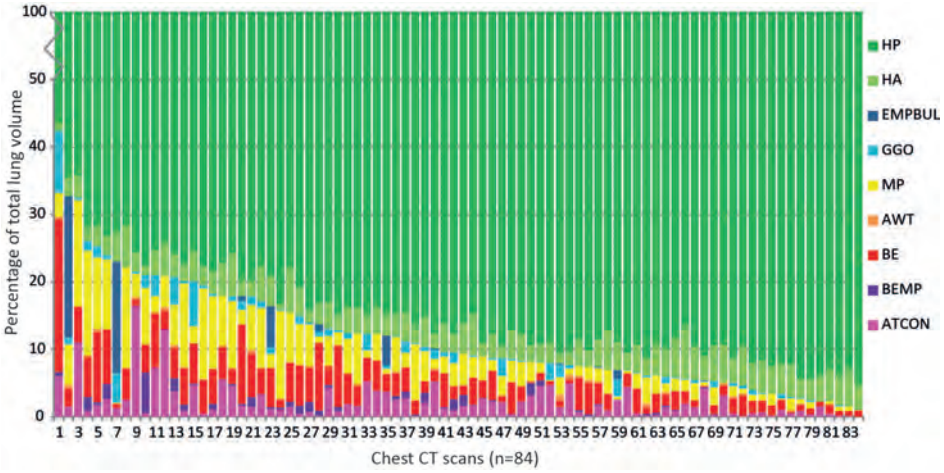

Figure 4. Stacked bar chart BEST-CT component scores of inspiratory scans.

This stacked bar chart shows the BronchiEctasis Scoring Technique for Computed Tomography (BEST-CT) component scores of the inspiratory chest computed tomography (CT) scans (n = 84). Each bar represents one CT scan. The outcomes are sorted based on the total amount of disease. Component scores are expressed as percentage lung volume and add up to 100%. Note that the scale on the Y-axis is adjusted after 50% to improve visibility. HP = Healthy parenchyma. HA = Healthy airways. EMPBUL = Emphysema and/or bullae. GGO = Ground-glass opacities. MP = Mucus plugging. AWT = Airway wall thickening. BE = Bronchiectasis. BEMP= Bronchiectasis with mucus plugging. ATCON = Atelectasis and/or consolidation.

Table 3. Correlation BEST-CT and Hartmann scores

Subscores	r	p-value
%TBE vs HM-BE	0.69	< 0.001
%TMP vs HM-MP	0.41	< 0.001
%AD vs HM-AD	0.66	< 0.001
%DIS vs HM-DIS	0.71	< 0.001
%ATCON vs HM-ATCON	0.32	0.003
%GGO vs HM-GGO	0.40	< 0.001

This table presents the Pearson correlation coefficients (r) of BronchiEctasis Scoring Technique for computed tomography (BEST-CT) scores with the corresponding Hartmann (HM) scores. TBE = Total bronchiectasis. BE = Bronchiectasis. TMP = Total mucus plugging. MP = Mucus plugging. AD = Airway disease. DIS = Total disease. ATCON = Atelectasis and/or consolidation. GGO = Ground-glass opacities.

Correlation of BEST-CT with Hartmann method

The Pearson correlation coefficients between the BEST-CT sub- and composite scores %TBE, %TMP, %AD, %DIS, %ATCON and %GGO and the corresponding Hartmann scores are shown in Table 3. Figure 5 shows the scatter dot plots of %TBE, %TMP, %AD and %DIS and the corresponding Hartmann scores. All parameters showed a significant correlation, p-values were 0.003 or lower.

BEST-CT versus tapering

For tapering analyses, a total of 22,533 airways were measured. The median number of airways that were measured was 262 [178-326] per patient. The correlations between luminal intra-branch tapering and %TBE, HM-BE and FEV_1 were assessed. A reduced tapering was correlated with a higher %TBE score (r = -0.34, p = 0.002) (Figure 6), with a higher HM-BE score (r = -0.29, p = 0.009) and with a lower FEV1 (r = -0.36, p = 0.001).

BEST-CT versus clinical parameters

The correlation between BEST-CT composite scores %TBE, %TMP, %AD and %DIS, the equivalent Hartmann scores (HM-BE, HM-MP, HM-AD and HM-DIS) and FEV_1 and *Pa* sputum density are presented in Table 4.

Spirometry (FEV_1)

Baseline spirometry data were available for all but one patient. Correlation between %TBE, %TMP, %AD and %DIS and the corresponding scores of HM and FEV_1 are presented in Table 4. BEST-CT scores were negatively correlated with the FEV_1 values. These correlations were significant (r =-0.24, -0.33, -0.35 and -0.42; and p = 0.027, 0.002, 0.001 and < 0.001 respectively). HM-MP, HM-AD and HM-DIS were also significantly correlated (r = -0.34, -0.32 and -0.32; and p = 0.002, 0.004, and 0.004), while HM-BE was not. Scatter dot plots of %BE and %DIS and FEV_1 are shown in Figure 7.

Bronchiectasis severity index (BSI)

Baseline BSI was available for all patients, and the patients were divided in mild (n = 2), moderate (n = 28) or severe disease (n = 54). When comparing median scores per group (Mann-Whitney U test), no significant correlations were found between BSI and %TBE, %TMP, %AD and %DIS, or between BSI and HM-BE, HM-MP, HM-AD and HM-DIS.

Table 4. Correlations between BEST-CT and Hartmann and clinical parameters

Clinical parameter	BEST-CT			Hartmann		
	Score	r	p-value	Score	r	p-value
FEV_1 (n=83)	%TBE	-0.24	0.027*	HM-BE	-0.20	0.069
	%TMP	-0.33	0.002*	HM-MP	-0.34	0.002*
	%AD	-0.35	0.001*	HM-AD	-0.32	0.004*
	%DIS	-0.42	< 0.001*	HM-DIS	-0.32	0.004*
Pa sputum density (n=79)	%TBE	0.132	0.246	HM-BE	0.25	0.027*
	%TMP	0.172	0.129	HM-MP	0.16	0.170
	%AD	0.163	0.151	HM-AD	0.24	0.031*
	%DIS	0.070	0.538	HM-DIS	0.19	0.094

This table shows Pearson correlation coefficients (r) for BronchiEctasis Scoring Technique (BEST-CT) and Hartmann, and clinical parameters of bronchiectasis patients. * Correlation is statistically significant. FEV_1 = forced expiratory volume in 1 second % predicted. *Pa* = *Pseudomonas aeruginosa*. TBE = Total bronchiectasis. TMP = Total mucus plugging.
AD = Airway disease. DIS = Total disease. BE = Bronchiectasis. MP = Mucus plugging.

Pa sputum density (CFU/G sputum)

Baseline *Pa* sputum density (CFU/G sputum) data was available for 79 out of the 84 study patients. No correlation was found between *Pa* sputum density and %TBE, %TMP, %AD and %DIS. For the Hartmann composite scores, we found weak but significant positive correlations between HM-TBE ($r = 0.25$, $p = 0.03$) and HM-AD ($r = 0.24$, $p = 0.03$).

Quality of life (QOL-B)

QOL-B data was available of 55 out of the 84 study patients. Correlation between %TBE, %TMP, %AD and %DIS and the corresponding HM scores and of all eight scales of the QOL-B were explored at baseline. No significant correlations between BEST-CT and HM scores and any of the QOL-B outcomes (emotional functioning, health perceptive, physical functioning, respiratory symptoms, role functioning, social functioning, treatment burden and vitality) were found. Data are presented in Supplement 5.

Exacerbations during iBEST study period

Exacerbation number was available for all patients. A total of 31 patients in the study experienced at least one exacerbation. Logistic regression models, corrected for FEV_1 and the treatment group (placebo yes or no), showed no correlation between %TBE and %AD and the event exacerbation.

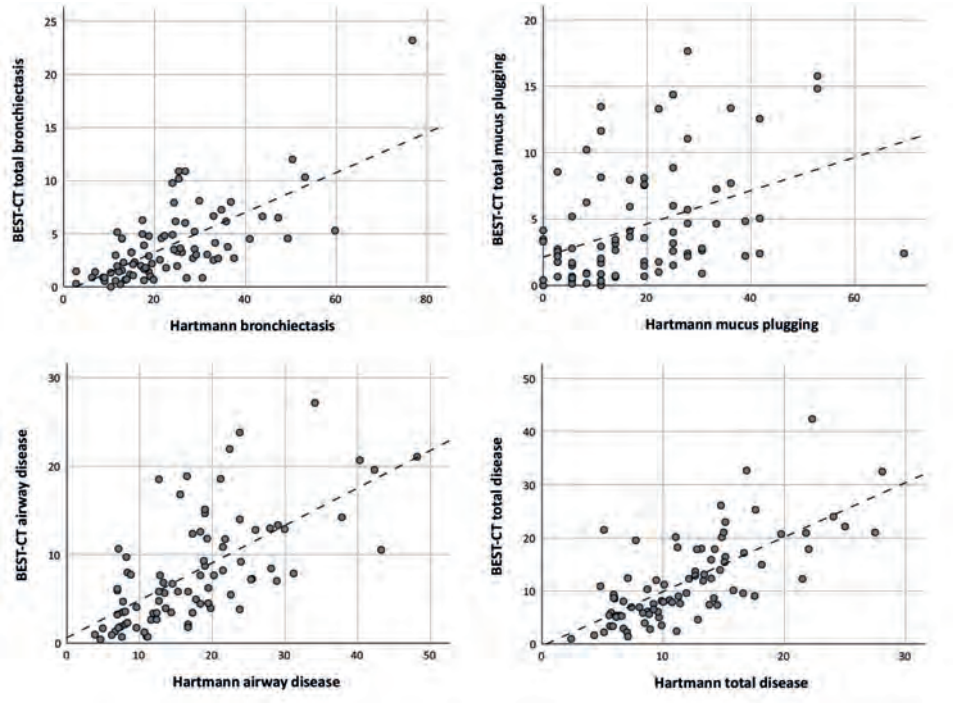

Figure 5. Scatter dot plots of %TBE, %TMP, %AD and %DIS and corresponding Hartmann scores

These figures show the correlation between BronchiEctasis Scoring Technique for Computed Tomography (BEST-CT) scores with the equivalent Hartmann (HM) scores. The dotted line is a regression line. All correlations were statistically significant. TBE = Total bronchiectasis. TMP = Total mucus plugging. AD = Airway disease. DIS = Total disease. BE = Bronchiectasis. MP = Mucus plugging.

Reproducibility

Intra-class correlation coefficients of the BEST-CT and Hartmann method are presented in Supplement 6. For the BEST-CT method, ICC scores within the main observer were good to excellent for all parameters except for %BEMP which was moderate, and %AWT which was poor. Between the observers, ICC scores were good to excellent for %BE, %MP, %GGO, %HP, %TBE, %TMP, %AD and %DIS, moderate for %BEMP and %AWT, and poor for %EMPBUL and %HA.

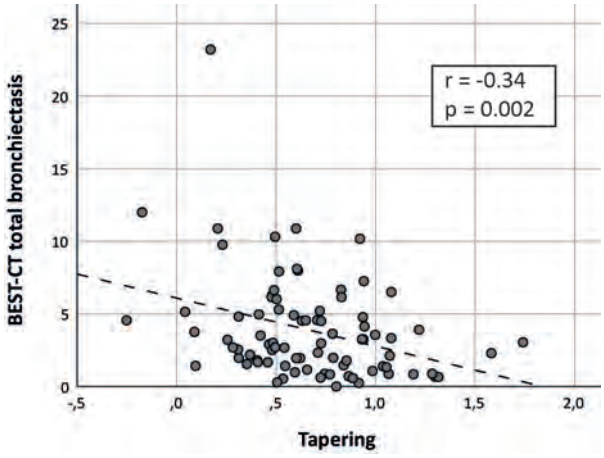

Figure 6. Tapering versus %TBE

This figure presents the Pearson correlation between luminal intra-branch tapering and the percentage of lung volume with bronchiectasis according to the BEST-CT (%TBE) for each patient. The dotted line is a regression line. Reduced tapering reflects bronchiectasis.

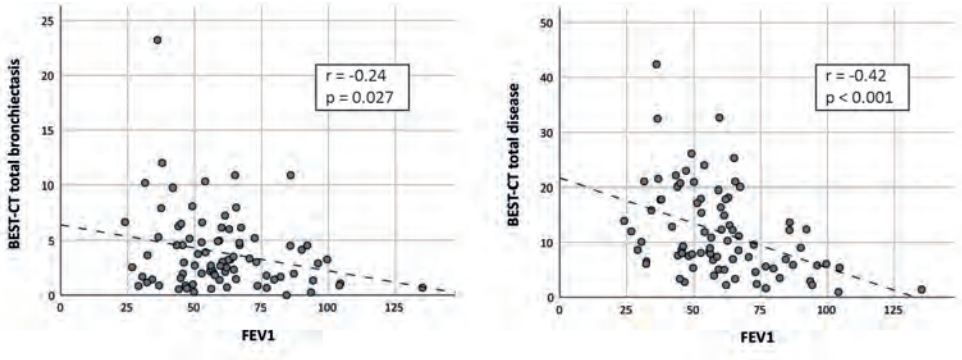

Figure 7. Scatter dot plots of FEV_1 and %TBE and %DIS

These figures show the Pearson correlations between forced expiratory volume in 1 second % predicted (FEV_1) and % of total bronchiectasis (%TBE) (left) and % of total disease (%DIS) (right). The dotted line is a regression line. The correlations are statistically significant ($p = 0.027$ and $p < 0.001$), meaning a higher FEV_1 is correlated with a lower amount of %TBE and a lower %DIS on computed tomography scan.

Discussion

The BEST-CT showed substantial heterogeneity of structural lung diseases components and in the extent of these components. Structural abnormalities related to the airways (%TBE) was the largest contributor to lung disease, with a median of 3% of the total lung volume. In almost all patients atelectasis or consolidation, mucus plugging and ground-glass opacities were present. The extent of abnormal lung tissue (%DIS) varied widely between 1%-42%. The median volume of lung tissue that showed any abnormality was 9%, which is considerable. For the interpretation of these numbers it is relevant to keep in mind that all patients were selected from the iBEST study, which included BE patients who were all *Pa* positive and had a history of at least two exacerbations in the previous year. In general, *Pa* positive BE patients have more severe symptoms relative to BE patients without *Pa* [5]. This was reflected by the fact that the BSI of our studied population was nine or higher in 64% of the cases, indicating severe disease [19]. We conclude that structural lung disease in BE patients with *Pa* is heterogeneous and extensive.

Importantly, the quantitative BEST-CT scores correlated well with equivalent semi-quantitative scores of the Hartmann method. In particular %TBE, %AD and %DIS scores showed strong and significant correlations. Furthermore, we found significant correlations between %TBE and intra-branch tapering. Intra-branch tapering is a promising quantitative marker of BE as its evaluation does not rely on the dimension of the adjacent artery for comparison. The diameter of the artery can be reduced due to hypoxic pulmonary vasoconstriction which therefore can result in the false diagnosis of BE [2].

The significant correlation in the cross-sectional analysis between %TBE and FEV_1 are supportive of using %TBE as outcome parameter. However, BEST-CT subscores did not correlate to quality of life scores assessed by QOL-B. This might well be explained by the retrospective nature of the CT collection. CT scans were made on average 15 months before the QOL-B assessment. Furthermore, BEST-CT scores were not predictive for the number of exacerbations recorded during the iBEST study. In CF multiple studies showed that BE scores were predictive for the number of exacerbations in the years following the CT. It is well possible that we did not observe a correlation because of the retrospective nature of the CT collection but also because of the relative short observation of 24 weeks, and the small sample size. Similarly, we were limited in our ability to show differences between mild, moderate and severe bronchiectasis using the BSI scoring system as this study enrolled a severe population infected with *Pa*. The correlation between BEST-CT scores and exacerbations and disease severity deserves further study on a larger population as included in the EMBARC registry or in a prospective study with at least one year follow up [20].

The BEST-CT proved to be a reproducible tool to analyse lung disease. The good to excellent reproducibility of especially the composite scores %TBE, %TMP, %AD and %DIS is of key importance, as these scores are most relevant to be used in clinical studies and follow up. The ICCs of the BEST-CT method outspanned those of the Hartmann scoring method. This might be explained by the grid system used in the BEST-CT, for which less eyeballing is needed.

An important advantage of the BEST-CT scoring system is that it, due to its localised annotations, can be automated more easily than lobe-based visual assessment scores such as the Hartmann score, as is already shown for PRAGMA-CF [21]. This is an important advantage because it allows processing of a large number chest CT scans, for registries and for clinical studies. Including the BEST-CT scores into the EMBARC registry allows to include CT outcomes capturing the heterogeneity of structural changes to identify subcategories of patients. To investigate the utility of chest CT outcomes in the EMBARC registry, a pilot study has started within the iABC consortium to analyse the CT scans of a 1000 BE patients using the BEST-CT. The annotated CT scans will be used as ground truth for the development of an automated algorithm using artificial intelligence strategies.

In addition to the limitations already noted, our study suffers from several other limitations. Most important, the CT scans were collected retrospectively. Consequently, the acquisition and image reconstructions of the chest CT scans in this study were not standardised, nor was the lung volume during scanning. Especially lung volume is an important confounder for the diagnosis of BE as airway diameters are dependent on lung volume [22].

A further limitation is the median time interval of 15 months between the CT scan and the first iBEST study visit, when clinical parameters were collected. As discussed this may have affected our correlations between CT subscores and clinical data collected at the first study visit.

Finally, we compared the scores with those of the Hartmann method, which was designed for patients with CVID, and with airway tapering measurements. Although BEST-CT scores were significantly correlated with those of the Hartmann method, the latter scoring method is not validated for BE patients. We did not compare the BEST-CT with other BE methods such as the Reiff score [23], the BRICS score [24] and the FACED score [25]. The Reiff score is a radiological score that shows similarities with the Hartmann method but less abnormalities are included, and as multiple abnormalities are assessed in the BEST-CT, the Hartmann is more suitable for comparison. The BRICS score is a validated BE score that only accounts for the amount of bronchial

dilatation and the number of segments with emphysema [24]. Both items are also included in the Hartmann score. The FACED score is a combination of clinical scores and radiology, and includes FEV1, age, *Pa* infection, dyspnoea scale and radiological extension [25]. Instead, we choose to compare the results with the BSI, as this score was incorporated in the iBEST study.

To conclude, the BEST-CT is a reproducible quantitative scoring system that is able to capture the heterogeneity of structural lung changes in BE patients. BEST-CT scores correlated well with two other systems to assess structural lung disease in BE. Once automated, BEST-CT can play an important role in BE registries to phenotype the structural changes of BE patients. To investigate whether BEST-CT outcomes can serve as a sensitive outcome measure, prospective clinical trials are needed that include well standardised CT scans acquired at baseline and at the end of treatment.

Acknowledgments

We would like to acknowledge Merlijn Bonte, LungAnalysis laboratory Erasmus MC, Rotterdam, for CT analysis, and collaborators from the iBEST study: Sinead Cahill, Queen's University Belfast, project manager iABC project; Krishna Duvvuri, Associate Global Trial Director, Novartis Healthcare Pvt. Ltd, India, trial manager; and the members of the iBEST trial steering committee: Dr. Katherine O'Neill, Queen's University Belfast; Dr. Charles Haworth, Royal Papworth Hospital NHS Foundation Trust; Prof. dr. Adam Hill, University of Edinburgh; Prof. dr. Michael Loebinger, Royal Brompton & Harefield NHS Foundation Trust; Dr. Eva Polverino, Hospital Vall d'Hebron Barcelona; Prof. dr. Francesco Blasi, Università degli Studi di Milano.

References

[1] Hansell DM, Bankier AA, MacMahon H, McLoud TC, Muller NL, Remy J. Fleischner Society: glossary of terms for thoracic imaging. Radiology. 2008;246:697-722.

[2] Meerburg JJ, Veerman GDM, Aliberti S, Tiddens H. Diagnosis and quantification of bronchiectasis using computed tomography or magnetic resonance imaging: A systematic review. Respiratory medicine. 2020;170:105954.

[3] Lonni S, Chalmers JD, Goeminne PC, McDonnell MJ, Dimakou K, De Soyza A, et al. Etiology of Non-Cystic Fibrosis Bronchiectasis in Adults and Its Correlation to Disease Severity. Ann Am Thorac Soc. 2015;12:1764-70.

[4] Chandrasekaran R, Mac Aogain M, Chalmers JD, Elborn SJ, Chotirmall SH. Geographic variation in the aetiology, epidemiology and microbiology of bronchiectasis. BMC Pulm Med. 2018;18:83.

[5] Araújo D, Shteinberg M, Aliberti S, Goeminne PC, Hill AT, Fardon TC, et al. The independent contribution of Pseudomonas aeruginosa infection to long-term clinical outcomes in bronchiectasis. Eur Respir J. 2018;51.

[6] Polverino E, Goeminne PC, McDonnell MJ, Aliberti S, Marshall SE, Loebinger MR, et al. European Respiratory Society guidelines for the management of adult bronchiectasis. Eur Respir J. 2017;50.

[7] Meerburg JJ, Hartmann IJC, Goldacker S, Baumann U, Uhlmann A, Andrinopoulou ER, et al. Analysis of Granulomatous Lymphocytic Interstitial Lung Disease Using Two Scoring Systems for Computed Tomography Scans-A Retrospective Cohort Study. Frontiers in immunology. 2020;11:589148.

[8] Rosenow T, Oudraad MC, Murray CP, Turkovic L, Kuo W, de Bruijne M, et al. PRAGMA-CF. A Quantitative Structural Lung Disease Computed Tomography Outcome in Young Children with Cystic Fibrosis. American journal of respiratory and critical care medicine. 2015;191:1158-65.

[9] Kuo W, Perez-Rovira A, Tiddens H, de Bruijne M, Normal Chest CTsg. Airway tapering: an objective image biomarker for bronchiectasis. Eur Radiol. 2020;30:2703-11.

[10] Chalmers JD, McHugh BJ, Doherty C, Smith MP, Govan JR, Kilpatrick DC, et al. Mannose-binding lectin deficiency and disease severity in non-cystic fibrosis bronchiectasis: A prospective study. Lancet Respir Med. 2013;1:224-32.

[11] Loebinger MR, Polverino E, Chalmers JD, Tiddens HAWM, Goossens H, Tunney M, et al. Efficacy and safety of TOBI Podhaler® in Pseudomonas aeruginosa-infected bronchiectasis patients: iBEST study. European Respiratory Journal. 2020:2001451.

[12] Loebinger MR, Polverino E, Blasi F, Elborn SJ, Chalmers JD, Tiddens HA, et al. Efficacy and safety of tobramycin inhalation powder in bronchiectasis patients with P. aeruginosa infection: Design of a dose-finding study (iBEST-1). Pulm Pharmacol Ther. 2019;58:101834.

[13] Quanjer PH, Stanojevic S, Cole TJ, Baur X, Hall GL, Culver BH, et al. Multi-ethnic reference values for spirometry for the 3-95-yr age range: the global lung function 2012 equations. Eur Respir J. 2012;40:1324-43.

[14] Quittner AL, Marciel KK, Salathe MA, O'Donnell AE, Gotfried MH, Ilowite JS, et al. A preliminary quality of life questionnaire-bronchiectasis: a patient-reported outcome measure for bronchiectasis. Chest. 2014;146:437-48.

[15] Wainwright CE, Vidmar S, Armstrong DS, Byrnes CA, Carlin JB, Cheney J, et al. Effect of bronchoalveolar lavage-directed therapy on Pseudomonas aeruginosa infection and structural lung injury in children with cystic fibrosis: a randomized trial. Jama. 2011;306:163-71.

[16] van Mastrigt E, Kakar E, Ciet P, den Dekker HT, Joosten KF, Kalkman P, et al. Structural and functional ventilatory impairment in infants with severe bronchopulmonary dysplasia. Pediatr Pulmonol. 2017;52:1029-37.

[17] Hermelijn SM, Dragt OV, Bosch JJ, Hijkoop A, Riera L, Ciet P, et al. Congenital lung abnormality quantification by computed tomography: The CLAQ method. Pediatr Pulmonol. 2020;55:3152-61.

[18] Koo TK, Li MY. A Guideline of Selecting and Reporting Intraclass Correlation Coefficients for Reliability Research. J Chiropr Med. 2016;15:155-63.

[19] Chalmers JD, Goeminne P, Aliberti S, McDonnell MJ, Lonni S, Davidson J, et al. The bronchiectasis severity index an international derivation and validation study. American journal of respiratory and critical care medicine. 2014;189:576-85.

[20] Chalmers JD, Aliberti S, Polverino E, Vendrell M, Crichton M, Loebinger M, et al. The EMBARC European bronchiectasis registry: Protocol for an international observational study. ERS Monogr. 2016;2.

[21] Marques F, Dubost F, Kemner-van de Corput M, Tiddens HA, de Bruijne M. Quantification of lung abnormalities in cystic fibrosis using deep networks: SPIE; 2018.

[22] Brown RH. Mechanisms of limited airway dimension with lung inflation. Pulm Pharmacol Ther. 2007;20:118-25.

[23] Reiff DB, Wells AU, Carr DH, Cole PJ, Hansell DM. CT findings in bronchiectasis: Limited value in distinguishing between idiopathic and specific types. AM J ROENTGENOL. 1995;165:261-7.

[24] Bedi P, Chalmers JD, Goeminne PC, Mai C, Saravanamuthu P, Velu PP, et al. The BRICS (Bronchiectasis Radiologically Indexed CT Score): A Multicenter Study Score for Use in Idiopathic and Postinfective Bronchiectasis. Chest. 2018;153:1177-86.

[25] Martínez-García MA, De Gracia J, Relat MV, Girón RM, Carro LM, De La Rosa Carrillo D, et al. Multidimensional approach to non-cystic fibrosis bronchiectasis: The FACED score. Eur Respir J. 2014;43:1357-67.

[26] Olveira C, Olveira G, Espildora F, Giron RM, Muñoz G, Quittner AL, et al. Validation of a Quality of Life Questionnaire for Bronchiectasis: psychometric analyses of the Spanish QOL-B-V3.0. Qual Life Res. 2014;23:1279-92.

[27] Hill AT, Haworth CS, Aliberti S, Barker A, Blasi F, Boersma W, et al. Pulmonary exacerbation in adults with bronchiectasis: a consensus definition for clinical research. Eur Respir J. 2017;49.

[28] Petersen J, Nielsen M, Lo P, Nordenmark LH, Pedersen JH, Wille MM, et al. Optimal surface segmentation using flow lines to quantify airway abnormalities in chronic obstructive pulmonary disease. Med Image Anal. 2014;18:531-41.

[29] Perez-Rovira A, Kuo W, Petersen J, Tiddens HA, de Bruijne M. Automatic airway-artery analysis on lung CT to quantify airway wall thickening and bronchiectasis. Med Phys. 2016;43:5736.

Supplementary material

Supplement 1. In- and exclusion criteria iBEST study[1]

Key inclusion criteria:

- Written informed consent must be obtained before any assessment is performed.
- Male and female patients of ≥ 18 years of age at screening (Visit 1).
- Proven diagnosis of non-cystic fibrosis bronchiectasis as documented by computed tomography or high-resolution computed tomography.
- At least two or more exacerbations treated with oral antibiotics OR one or more exacerbation requiring intravenous antibiotic treatment within 12 months prior to screening.
- Forced expiratory volume in 1 second ≥ 30% predicted at screening (Visit 1).
- *Pseudomonas aeruginosa* must be documented in a respiratory sample at least one time within 12 months and also present in the expectorated sputum culture at Visit 1.

Key exclusion criteria:

- Patients with a history of cystic fibrosis.
- Patients with a primary diagnosis of bronchial asthma.
- Patients with a primary diagnosis of chronic obstructive pulmonary disease associated with at least a 20 pack year smoking history.
- Any significant medical condition that is either recently diagnosed or was not stable during the last three months, other than pulmonary exacerbations, and that in the opinion of the investigator makes participation in the trial against the patients' best interests.
- Clinically significant (in the opinion of the investigator) hearing loss that interferes with patients' daily activities (such as normal conversations) or chronic tinnitus. Patients with a past history of clinically significant hearing loss in the opinion of the investigator may be eligible only if their hearing threshold at screening audiometry is 25dB or lower at frequencies 0.5-4 kHz. The use of a hearing device is reflective of a clinically significant hearing loss; hence patients using hearing aids at screening are not eligible.
- Patients with active pulmonary tuberculosis.
- Patients currently receiving treatment for nontuberculous mycobacterial pulmonary disease.
- Patients who are regularly receiving inhaled anti-pseudomonal antibiotic (during the study inhaled anti-pseudomonal antibiotics are not allowed other than the study drug).

[1] https://clinicaltrials.gov/ct2/show/study/NCT02712983?cond=NCT02712983&draw=2&rank=1

Supplement 2. Clinical parameters iBEST study

Bronchiectasis severity index

The bronchiectasis severity index (BSI) is a multidimensional clinical prediction tool for morbidity (hospital admissions and exacerbations) and mortality in bronchiectasis patients. A BSI of 0-4 can be considered as mild disease, between 5-8 as moderate disease, and a BSI ≥ 9 as severe disease [19]. The BSI contains the following parameters [10]:

- Body mass index
- Forced expiratory volume in 1 second (FEV_1) percentage predicted
- Previous hospital admission
- Has the patient been hospitalised with a severe exacerbation in the past two years?
- Number of exacerbations in previous year
- Modified Medical Research Council dyspnoea scale
- *Pseudomonas aeruginosa (Pa*) colonisation (chronic colonisation is defined by the isolation of *Pa* in sputum culture on two or more occasions, at least three months apart in a one year period)
- Colonisation with other organisms (chronic colonisation is defined by the isolation of potentially pathogenic bacteria in sputum culture on two or more occasions, at least three months apart in a one year period)
- Radiological severity

Microbiology

Sputum samples from each patient were collected at baseline. *Pa* sputum density expressed in log colony forming units per gram were assessed from these samples.

Quality of Life Questionnaire for Bronchiectasis (QOL-B)

The QOL-B is a patient-reported outcome measure that evaluates the quality of life of bronchiectasis patients. Quality of life is assessed on eight scales: respiratory symptoms; physical, role, emotional, and social functioning; vitality; health perceptions; and treatment burden. No total score is calculated but scores are presented per scale, scores ranging from 0-100. Higher scores indicate a better quality of life [26].

Pulmonary exacerbations

Pulmonary exacerbations are defined in the study protocol as: Events for which it is clinically determined by the site investigator that antibiotic therapy is required AND at least three of the following six symptoms, signs, or findings were present outside of normal variation:

1. Increased sputum volume, or change in viscosity / consistency or purulence for more than 24 hours;
2. Increased shortness of breath at rest or on exercise for more than 24 hours;
3. Increased cough for more than 24 hours;
4. Fever of ≥ 38° Celsius within the last 24 hours;
5. Increased malaise / fatigue / lethargy for more than 24 hours;
6. A reduction in FEV_1 or forced vital capacity of least 10% from screening;

A worsening of symptoms that either did not meet the above symptom definition but was treated by the investigator with antibiotics, or that met the symptom definition but was not treated with antibiotics, was not considered a pulmonary exacerbation for the study.

For the above reported signs and symptoms, additional information was collected to document if the reported signs and symptoms last for more than 48 hours, in line with the recently published consensus definition of pulmonary exacerbations for clinical research [27].

Supplement 3. BEST-CT development

To adapt the grid based scoring system for bronchiectasis, first, computed tomography (CT) scans with relevant structural abnormalities for bronchiectasis (BE) disease were selected from the LungAnalysis database. This database included CT scans of patients with cystic fibrosis (CF), primary ciliary dyskinesia, and granulomatous lymphocytic interstitial lung disease (GLILD). Next, the BronchiEctasis Scoring Technique for CT (BEST-CT) training module was developed by a certified thoracic radiologist and a medical doctor respectively with 10 and 4 years of experience in BE imaging analysis (PC and JM), which includes examples of annotated images of relevant structural CT changes from the LungAnalysis database and explanatory text.

The observers (OD and JM) followed the training module and scored the first test batch of 20 CT scans. This test batch contains a random selection of CT scans of CF patients and of patients with GLILD [7]. GLILD patients were selected from a previous study as they show a wide spectrum of relevant severe structural lung abnormalities that also could occur in BE patients. Annotations of observers were compared, and disagreements were discussed in consensus meetings with the thoracic radiologist. Only minor discrepancies were observed which were used to further improve the

BEST-CT training module by adding extra example images and by changes in the explanatory text. Finally, a second batch of five CT scans of patients with CF and GLILD were scored, and satisfactory agreement was reached.

To determine the minimum number of slices that need to be annotated for BEST-CT the observers scored 20 equally spaced axial slices per CT scan from the first test batch. The grid size was set at 10 by 10 mm. Next, scoring outcomes were computed. Next, for each CT scan every second slice was deleted and scoring outcomes were again computed. BEST-CT outcomes obtained through the analysis of 20 slices were similar to those of 10 slices (ICC values were excellent). For this reason, a sample size of ten slices for BEST-CT was selected.

Supplement 4. Intra-branch tapering

To assess intra-branch tapering in our BE population, airway dimensions were computed automatically on the inspiratory CT scans as follows. As input for the analysis, approximated centrelines of the bronchial tree were manually drawn by trained observers using specialist image analysis software (Myrian version 2.1.2, Intrasense, Montpelier, France). Next, 3D segmentations of the airway lumen and outer walls were automatically computed around these centrelines using a surface graph-cut method [28, 29]. Airway lumen diameter was then measured for each individual branch and every 0.5 mm along the centreline. Finally, luminal intra-branch tapering measurements are presented as the percentage reduction of airway lumen diameter per mm along the centreline, following the procedure in Kuo et al. [9]. The trachea and first four branches of the airway tree were excluded in our analysis as these airways do not typically show bronchiectatic disease.

Supplement 5. Correlation between BEST-CT and Hartmann scores and Quality of Life Questionnaire for Bronchiectasis

		BEST-CT			Hartmann	
QOL-B	**Score**	**r**	**p**	**Score**	**r**	**p**
Treatment burden (n = 50)	%BE	0.26	0.071	HM-BE	0.09	0.531
	%MP	0.06	0.700	HM-MP	0.15	0.312
	%AD	0.19	0.192	HM-AD	0.15	0.293
	%DIS	0.14	0.343	HM-DIS	0.14	0.350
Vitality (n = 54)	%BE	0.03	0.836	HM-BE	0.10	0.488
	%MP	0.13	0.354	HM-MP	0.15	0.291
	%AD	0.08	0.569	HM-AD	0.14	0.327
	%DIS	0.03	0.855	HM-DIS	0.10	0.497
Physical functioning (n = 55)	%BE	-0.13	0.351	HM-BE	-0.11	0.446
	%MP	0.04	0.754	HM-MP	-0.09	0.511
	%AD	-0.08	0.588	HM-AD	-0.11	0.435
	%DIS	-0.24	0.075	HM-DIS	-0.19	0.162
Respiratory symptoms (n = 55)	%BE	-0.09	0.502	HM-BE	0.02	0.899
	%MP	-0.11	0.416	HM-MP	-0.17	0.212
	%AD	-0.14	0.306	HM-AD	-0.06	0.676
	%DIS	-0.23	0.088	HM-DIS	-0.11	0.420
Role functioning (n = 55)	%BE	-0.13	0.337	HM-BE	-0.07	0.595
	%MP	0.12	0.374	HM-MP	-0.10	0.492
	%AD	-0.02	0.907	HM-AD	-0.10	0.477
	%DIS	-0.16	0.258	HM-DIS	-0.12	0.407
Social functioning (n = 55)	%BE	0.05	0.723	HM-BE	0.04	0.797
	%MP	0.08	0.556	HM-MP	-0.12	0.382
	%AD	0.09	0.534	HM-AD	-0.04	0.756
	%DIS	0.12	0.382	HM-DIS	-0.01	0.933
Emotional functioning (n = 55)	%BE	-0.03	0.803	HM-BE	0.08	0.552
	%MP	-0.03	0.804	HM-MP	0.07	0.591
	%AD	-0.50	0.714	HM-AD	0.08	0.579
	%DIS	-0.08	0.557	HM-DIS	0.05	0.738
Health perceptions (n = 54)	%BE	0.05	0.703	HM-BE	0.90	0.502
	%MP	0.09	0.506	HM-MP	0.01	0.967
	%AD	0.07	0.616	HM-AD	0.06	0.645
	%DIS	0.00	0.980	HM-DIS	0.06	0.647

This table shows the Pearson correlation coefficients of BronchiEctasis Scoring Technique for computed tomography (BEST-CT) scores and Hartmann (HM) CT scores and Quality of Life Questionaire for Bronchiectasis (QOL-B) scores.

Supplement 6. Intraclass correlation coefficients of BEST-CT and Hartmann scoring methods

ICCs BEST-CT			ICCs Hartmann		
Scores	**Intra**	**Inter**	**Scores**	**Intra**	**Inter**
%ATCON	0.81	0.41	HM-ATCON	0.69	0.25
%BEMP	0.65	0.68	-	-	-
%BE	0.90	0.78	-	-	-
%AWT	0.39	0.54	HM-AWT	0.10	0.23
%MP	0.88	0.89	-	-	-
%GGO	0.97	0.91	HM-GGO	0.81	0.63
%EMPBUL	0.82	0.23	HM-EMP	< 0	< 0
%HA	0.78	0.28	-	-	-
%HP	0.90	0.87	-	-	-
%TBE[#]	0.87	0.80	HM-BE	0.82	0.47
%TMP[*]	0.90	0.89	HM-MP	0.23	0.45
%AD[^]	0.92	0.86	HM-AD	0.62	0.37
%DIS[&]	0.88	0.85	HM-DIS	0.71	0.40

This table presents intra- and inter-observer agreement for the BronchiEctasis Scoring Technique for Computed Tomography (BEST-CT) and for the Hartmann method expressed in intra-class correlation coefficients (ICC). ATCON = Atelectasis and/or consolidation. BE = Bronchiectasis. MP = Mucus plugging. AWT = airway wall thickening. GGO = Ground-glass opacities. EMP = Emphysema. BUL = Bullae. HA = Healthy airways. HP = Healthy parenchyma. AD = Airway disease. DIS = Total disease. - No comparable subscore Hartmann. <0 : ICC cannot be calculated. [#]BE with MP + BE. *BEMP + MP. ^ BEMP + BE + MP + AWT. &100% - Healthy airways - healthy parenchyma.

SECTION II

Chapter 6

Home videos of cystic fibrosis patients using tobramycin inhalation powder: Relation of flow and cough

Pediatric Pulmonology 2019; 54:1794-1800

Jennifer J. Meerburg, Mehdi Albasri, Els C. van der Wiel, Eleni-Rosalina Andrinopoulou, Menno M. van der Eerden, Christof J. Majoor, Hubertus G.M. Arets, Harry G.M. Heijerman, Harm A.W.M. Tiddens

Abstract

Background Many cystic fibrosis (CF) patients chronically infected with *Pseudomonas aeruginosa* are on maintenance tobramycin inhalation therapy. Cough is reported as a side effect of tobramycin inhalation powder (TIP) in 48% of the patients. Objectives of this study were to investigate the association between the inspiratory flow of TIP and cough and to study the inhalation technique. We hypothesized that cough is related to a fast inhalation.

Materials and Methods In this prospective observational study, CF patients ≥ 6 years old on TIP maintenance therapy from four Dutch CF centers were visited twice at home. Video recordings were obtained and peak inspiratory flow (PIF) was recorded while patients inhaled TIP. Between the two home visits, the patients made three additional videos. CF questionnaire-revised, spirometry data, and computed tomography scan were collected. Two observers scored the videos for PIF, cough, and mistakes in inhalation technique. The associations between PIF and cough were analyzed using a logistic mixed-effects model accounting for FEV_1% predicted and capsule number.

Results Twenty patients were included, median age 22 (18-28) years. No significant associations were found between PIF and cough. The risk of cough was highest after inhalation of the first capsule when compared to the second, third, and fourth capsule ($P \leq .015$). Fourteen patients (70%) coughed at least once during TIP inhalation. A breath-hold of less than 5 seconds after inhalation and no deep expiration before inhalation were the most commonly observed mistakes.

Conclusion PIF is not related to cough in CF patients using TIP.

Introduction

Cystic fibrosis (CF) is a genetic disorder characterized by severe chronic lung disease. The mucus of CF patients is thickened, resulting in impaired clearance of pathogens [1]. Patients with CF suffer from chronic infections and increased inflammatory response in the lungs. This causes irreversible lung damage, resulting in a reduced quality of life, and a shortened life span [1]. *Pseudomonas aeruginosa (Pa)* is the most predominant pathogen that causes progressive lung disease [2]. The overall prevalence of chronic infection with *Pa* in 2016 was around 30% in Europe and the United States of America [3, 4].

Suppressive inhalation antibiotic therapy is a standard treatment for patients with chronic *Pa* infection: The guidelines of the United States of America recommend long-term use of tobramycin inhalation solution (TIS) as the first-line choice, and the more recent European guidelines add that TIS and tobramycin inhalation powder (TIP) is equally effective. Alternatively, options are aztreonam lysine (both guidelines) and colistin (European guidelines) [5-7]. Nebulization therapy comes with some disadvantages: it is time-consuming, nebulizers are in general not easy to carry around, need disinfection after each use, and require periodic technical maintenance [8]. To overcome these disadvantages, TIP was developed. TIP is administered with the T-326 inhaler (Tobi Podhaler™; Novartis Pharma AG, Basel, Switzerland). A full dose of TIP contains four capsules of 50 mg each (28 mg tobramycin + 22 mg excipients). It is advised to inhale each capsule at least twice. Like TIS, TIP is administered twice daily. The administration time of TIP is one-third of that of TIS, the T-326 inhaler is pocket-size, and does not require extensive post-use cleaning or technical maintenance [9, 10]. Importantly, TIP has shown to be noninferior compared to TIS in terms of reducing exacerbations and P. aeruginosa colony-forming units. In addition, higher treatment satisfaction was reported for TIP compared to TIS [9]. However, a disadvantage of TIP is the occurrence of cough immediately after inhalation. In the pivotal noninferiority study comparing TIS and TIP, the cough was reported in 48% of patients using TIP (n = 308) compared to 31% using TIS (n = 209) [9]. The authors did not mention specific instructions given to patients with regard to an inspiratory flow. TIP particles might induce a cough reaction for various reasons: First of all, TIP particles are dry where TIS particles are wet. Second, TIP particles might hit the throat wall with greater impact, due to the relatively faster inhalation of TIP compared to TIS. The T-326 inhaler has a low-to-medium resistance (approximately 0.08 [cm H2O]½/[L/min]), fast inspiratory flows between 40 up to 115 L/min were observed in a laboratory setting when inhaling TIP [11]. On the contrary, TIS is inhaled with tidal volume breathing. Third, tobramycin sputum concentrations were found to be double after inhalation of TIP

compared to that of TIS [9]. This might be a result of higher upper airway deposition. Importantly, according to an in vitro study by Haynes et al [11], the total lung dose of TIP is independent of inspiratory flow.

It is unknown which inspiratory flows are generated by patients for routine use of TIP in the home setting. Furthermore, we do not know what the prevalence of cough is in the home setting, nor whether correct inhalation techniques are being used.

The primary objective of our study was to record TIP inhalations by CF patients on video in the home setting and to study the association between inspiratory flow and cough. We hypothesized that a faster inhalation maneuver by patients would increase the risk of cough. Secondary objectives were (a) to assess the percentage of patients that coughed after inhaling TIP, and (b) to study mistakes in the inhalation technique of TIP inhalations. In a multicenter, prospective observational study, we assessed inhalation maneuvers and the relation with cough for TIP in the home setting.

Materials and methods

Study population

Patients were recruited from four CF centers in the Netherlands: Erasmus Medical Center in Rotterdam, Haga Hospital in The Hague, University Medical Center Utrecht and Academic Medical Center in Amsterdam.

Inclusion criteria:

1. Proven diagnosis with CF.
2. Minimum age of 6 years.
3. Maintenance treatment with TIP for at least 1 month.

Exclusion criteria:

1. Respiratory exacerbation requiring intravenous treatment with antibiotics at the time of inclusion or during the study period.
2. Any medical condition that increases the risk of cough according to the treating physician, not directly related to CF lung disease (ie, otitis media).
3. Unable to understand and execute instructions.

Informed consent was obtained from both parents if the patient was younger than 12 years, from the patient and both parents if the patient's age was between 12 to 18 years, and only from the patient if the patient was 18 years and older. This study was approved by the Institutional Review Board of the Erasmus Medical Center (MEC- 2015-329).

Study design

The study design is shown in Figure 1. The study consisted of five study moments: two home visits by an investigator (JM) and three video recordings by the patient between the home visits.

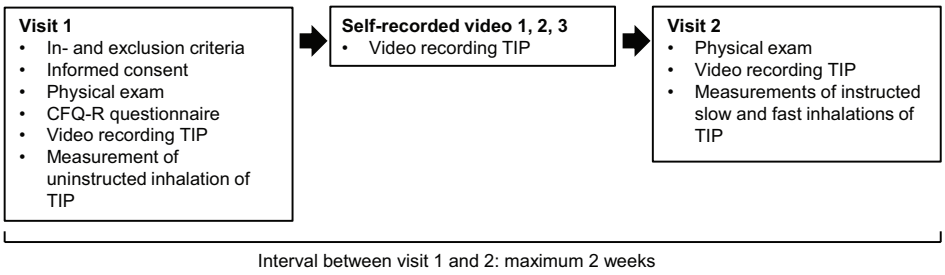

Figure 1. Study design

Patients were visited twice by an investigator. On three separate days in between, the patients were asked to record their inhalations on video. CFQ-R = Cystic fibrosis questionnaire-revised. TIP = Tobramycin inhalation powder.

During the first home visit (visit 1), the patient inhaled a full dose of TIP without any instructions, while being recorded on video by the investigator. Inspiratory flow patterns of the first inhalation of the third capsule were measured with an inspiratory profile recorder (IPR). When inhaling the third capsule, we assumed the patient was used to the situation, and the fourth capsule could be used if measurements failed. Furthermore, the patient received instructions to record himself/herself on video on three separate days while inhaling a full dose of four TIP capsules (self-recorded video 1, 2, and 3). The investigator and patient together looked for a suitable place to record, and a video-camera including a tripod was left behind with the patient.

During the second home visit (visit 2), the patient also inhaled a full dose of TIP while being recorded on video by the investigator. However, the patient was randomized and instructed to either inhale the first capsule slowly and the second capsule fast, or vice versa. The inspiratory flows of the first two capsules were recorded with the IPR, and if the recordings failed, the third and fourth capsule were recorded with the same instructions. Otherwise, the third and fourth capsule were inhaled as usual and not recorded with the IPR. In case the investigator noticed any mistakes in the inhalation technique, this was recorded and discussed with the patient after completion of all study proceedings.

Importantly, except for the instructed fast and slow inhalation of visit 2, the patients were asked to inhale TIP the way they would normally do.

Patient demographics (age, sex, duration of treatment) were collected at visit 1. Chest computed tomography (CT) scans were collected when available and made within 24 months before inclusion. Structural changes on CT scans were analyzed using the PRAGMA-CF scoring method [12]. The highest forced expiratory volume in 1 second (FEV_1) measured within 12 months before inclusion and the forced vital capacity (FVC) were collected. Both values were expressed as a percentage of predicted values [13].

Inhalation measurements

The IPR measured the dynamic pressure drop at the mouthpiece of the inhaler during inhalation and converted the data to inspiratory flow in L/min [11]. The peak inspiratory flow (PIF) was used to analyze the association between inspiratory flow and cough, to which we refer as "recorded PIF." Furthermore, inhaled volume and flow acceleration were extracted from these recorded measurements.

Standardization of video scoring

The estimated PIF was independently assessed by two observers (JM and MA). The observers were trained as follows: First, reference videos were made of a slow (40 L/min or less), medium (40-85 L/min), and fast (85 L/min or higher) inhalation, referring to the PIF. Next, a practice batch of videos was made for which 20 volunteers performed one inhalation with an empty TIP capsule. The volunteers were at random instructed to inhale slow, medium or fast. The two observers, blinded for these instructions, scored the estimated PIF of this practice batch. The agreement between the observers on the estimated PIF of this practice batch was 80%. To standardize the assessment of inhalation technique, both observers scored 10 videos made for a previous study by Bos et al [14], in which patients inhaled using various nebulizers. Although the inhalation maneuvers of nebulizers and TIP differ, some of the technique items "lips sealed around the mouthpiece," "upright position during inhalation", and "a horizontal position of the inhaler" could be practiced.

All videos were renamed and randomized, and scored by both observers. Because the T-326 inhaler has a distinctive rattle depending on inspiratory flow, scoring was performed using a high-quality active noise-canceling headset. Nonmatching scores for estimated PIFs and cough were discussed during a consensus meeting to come upon a final score.

Nonmatching scores for inhalation technique were not discussed during the consensus meeting since these were no main outcome parameters. For these latter scores, the mean of both observers was calculated.

Checklist video recordings

Every inhalation was scored using a checklist that contained the following items:

1. Estimated PIFs: slow, medium, or fast.
2. Occurrence and moment of cough (during inhalation, breath-hold, exhalation or afterward).
3. Inhalation technique. These items were derived from the manufacturers' instructions: deep exhalation before inhalation, exhalation outside of the inhaler, lips sealed around the mouthpiece, upright position during inhalation, a horizontal position of the inhaler, and breath-hold ≥ 5 seconds after inhalation.

Statistical analysis

Descriptive data are expressed as median with interquartile ranges (IQR), as numbers and as percentages (%).

To analyze the association between cough and PIF, a McNemar test was planned to compute the difference between the risk of cough after a slow inhalation (assuming p_{cough} = lowest reported cough rate, 0.10) [15] and a fast inhalation (assuming p_{cough} = highest reported cough rate, 0.48) [9] resulting in a sample size of 30 patients. However, in total only 20 patients were included and the performed instructed inhalations (slow and fast) did not meet the study definitions (slow PIF < 35 L/min, fast PIF > 85 L/min) for which reasons the McNemar was not appropriate. Instead, two analyses were performed using logistic mixed-effects models, to correct for other variables while investigating the association of PIF and cough, accounting for multiple measurements per patient: analysis 1 was performed to study the association between all recorded PIFs and cough, and analysis 2 to study the association between the all estimated PIFs and cough. For this latter analysis, estimated PIFs were collected of visit 1, and self-recorded videos 1, 2, and 3. The estimated PIFs of visit 2 were excluded, because they included instructed inhalations which could bias results.

For both analyses, only the first inhalation of each capsule was included, as some capsules (25%) were only inhaled once. We accounted for FEV_1% predicted as we assumed that lung function would be a confounding factor. In analysis 2, we added the capsule number to our model, as this showed to be a confounder.

Additionally, with mixed-effects model analyses the relation between inhaled volume (accounting for FEV_1% predicted and height) and cough, and between flow acceleration (accounting for FEV_1% predicted) and cough were assessed.

To determine the prevalence of cough after the inhalation of TIP, we assumed each capsule of TIP would be empty after two inhalations [16]. Therefore, only data of the first, and if present, the second inhalation per capsule are presented. Also for this analysis, visit 2 videos were excluded as they contained instructed inhalations which could bias the results.

Mistakes made in the inhalation technique are presented as mean percentages of both observers. All inhalations were included and overall technique scores were calculated as follows: for each checklist item on inhalation technique, one point was assigned per item when executed correctly, and scores of both observers were added. The mean technique score was expressed as a percentage of the maximum score. The differences in inhalation technique between the videos with and without the presence of the investigator were calculated with the Wilcoxon signed-rank test.

To assess the inter-observer and intra-observer agreement of the checklist items Cohen's kappa was calculated. The inter-observer agreement was calculated for all inhalations. The intra-observer agreement was calculated after each observer rescored 20 randomly selected videos. We interpret Cohen's kappa values as follows: poor (< 0), slight (0-0.20), fair (0.21-0.40), moderate (0.41-0.60), substantial (0.61-0.80), and almost perfect (> 0.80) [17].

Statistical analyses were performed using SPSS version 24.0 and R version 3.4.3. The significance level was defined as $P < .05$.

Results

Study population

We approached 55 eligible patients, of whom 20 patients were included. Characteristics of the study patients are summarized in Table 1. Sixteen adults (80%) and four children (20%) were included, of whom 13 (65%) were male. Seventeen patients (85%) used TIP month-on month-off, three patients (15%) used TIP continuously, and the median duration of treatment at the time of participation was 19 months. Details of the PRAGMA-CF [12] scores and Cystic Fibrosis Questionnaire - Revised [18] scores are presented in Tables S1 and S2 (Supplementary material).

Table 1. Patient characteristics

Characteristic	Values	Outcome
Age in years	median [IQR]	22 [18-28]
Male gender	n (%)	13 (65)
Use of TIP in months	median [IQR]	19 [11-53]
PRAGMA-CF CT analyses		
Total disease score (n=12)	median [IQR]	9 [7-17][1]
Trapped air score (n=11)	median [IQR]	17 [1-30][1]
Spirometry		
FEV_1 % predicted	median [IQR]	82 [62-100]
FVC % predicted	median [IQR]	98 [83-106]

CT = Computed tomography; FEV_1 = Forced expiratory volume in 1 second; FVC = Forced vital capacity; IQR = Interquartile range; TIP = Tobramycin inhalation powder. [1]Expressed as a percentage of the total lung volume. In total 20 patients were included.

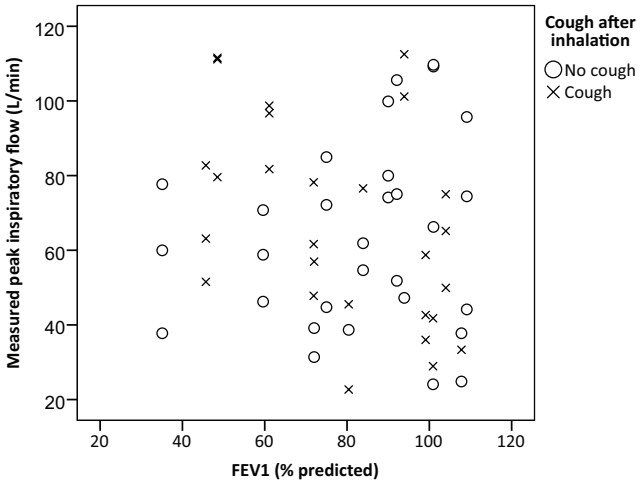

Figure 2. Scatter plot of recorded peak inspiratory flows

This scatter plot shows the recorded peak inspiratory flows (PIF) in relation to cough and the forced expiratory volume in one second (FEV_1) % predicted. The x-axis shows the FEV_1% predicted and the y-axis shows the PIF in liter per minute. The circles represent the inhalations without cough and the crosses represent the inhalations with cough. Three inhalations per patient were obtained, of 19 patients (data missing of one patient); resulting in 57 measurements.

Association between recorded PIF and cough

Recorded PIFs of an uninstructed, instructed fast, and instructed slow inhalation were obtained from 19 patients, resulting in 57 measurements. Data of one patient were lost in the data transfer process. Figure 2 shows a scatter plot of the recorded PIFs in L/min

in relation to the outcome cough and to FEV_1% predicted, in which no association could be detected. In line with the interpretation of the scatter plot, the mixed-effects model analysis showed no association between the recorded PIF and cough (P = .182) (Table 2). The additional analyses showed that inhaled volume and flow acceleration were also not associated with cough (P = .506 and .138) (Table S3, Supplementary material).

Table 2. Output mixed model analyses for association between cough and recorded and estimated peak inspiratory flow

	Effect (log odds)	Standard error (log odds)	P-value
Recorded PIF (n = 57)			
Baseline	-0.38	5.20	
PIF (L/min)	0.02	0.04	0.182
FEV_1 (% predicted)	-0.01	0.06	0.616
Estimated PIF (n = 319)			
Baseline[1]	2.24	3.08	
PIF			
Medium	-0.96	1.15	0.080
Fast	-1.12	1.39	0.094
FEV_1 (% predicted)	-0.02	0.04	0.149
Capsule number			
2nd Capsule	-0.88	0.53	< 0.001*
3rd Capsule	-0.56	0.50	0.015*
4th Capsule	-1.17	0.58	< 0.001*

This table shows the output of the mixed model analysis to study the association between cough and recorded and estimated peak inspiratory flow (PIF). Forced expiratory volume in one second (FEV_1) % predicted was added to both models as possible confounder. In the analysis of the estimated PIF, the capsule number was also added as this was a significant confounder. [1]A slow inhalation of the first capsule and FEV_1 % predicted of 0 is baseline. *P < 0.05

Association between estimated PIF and cough

We obtained 319 estimated PIFs. For one patient the inhalation of one capsule was missing on one of the self-recorded videos. Initially, the mixed-effects model analysis was performed without accounting for capsule number, and then it seemed that a fast PIF significantly reduced the risk of cough (P = .039). However, we identified capsule number as a significant confounder and therefore added this to our model. We found no significant association between the estimated PIF and cough (P medium

inhalation = .080 and P fast inhalation = .094) (Table 2). However, the risk of cough is significantly lower for the second, third, and fourth capsule compared to the first capsule (P < .001, P = .015, and P < .001, respectively).

Prevalence of cough

A total of 319-first and 240-second inhalations of the capsules were analyzed on the visit 1 and self-recorded videos. The prevalence of cough per estimated PIF of the first inhalation was 22% (slow), 28% (medium), and 29% (fast). The first inhalation of the first capsule resulted in cough in 42% of the inhalations, compared to 22%, 26%, and 16% for the second, third, and fourth capsule. Forty-eight % of the inhalations were performed with a medium PIF, 28% with a slow PIF, and 25% with a fast PIF. Fourteen patients (70%) coughed at least once. The patients coughed during inhalation in 27% of the cases, during breath-hold in 17%, during exhalation in 32%, and after exhalation in 24% of the cases.

Of 319 inhaled capsules, 25% of the capsules were inhaled only once, 54% were inhaled twice, 13% were inhaled three times, and 9% of the capsules were inhaled four up to seven times.

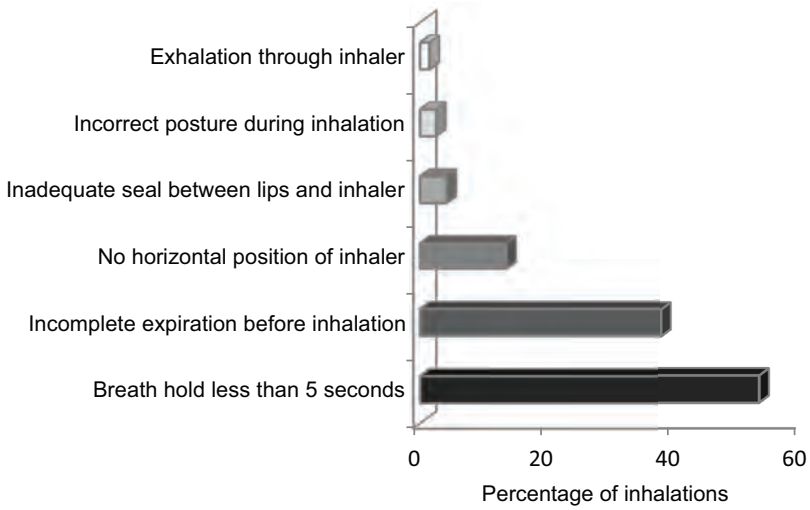

Figure 3. Bar chart of mistakes of inhalation technique

This bar chart presents the mean prevalence of the two observers of mistakes made in the inhalation technique while inhaling tobramycin inhalation powder. All inhalations captured on video were used for this analysis (n = 828).

Inhalation technique

The inhalation technique varied widely among patients. The median (IQR) total score for all patients on the inhalation technique was 75 (71-92). Table S4 (Supplementary material) shows the median [IQR] scores on inhalation technique per patient. One patient was excluded from this analysis because of the low quality of the self-recorded videos.

The mean prevalence of both observers for each mistake in the inhalation technique of all 828 inhalations is shown in Figure 3. Most commonly made mistakes were a breath-hold after inhalation less than 5 seconds (54% and 52% of the inhalations according to observer 1 and 2, respectively), followed by an inhalation that was not preceded by a complete exhalation (54% and 22%). The presence of an investigator was not of influence on the inhalation technique (P = .133).

Inter-observer and intra-observer agreement

Table S5 (Supplementary material) shows Cohen's kappa for the inter-observer and intra-observer agreement. The inter-observer agreement was fair (0.29-0.36) for the items deep exhalation, exhalation outside the inhaler, upright position of the patient, and horizontal position of the inhaler. The inter-observer score on estimated PIF was moderate (0.48), however, disagreement on PIF was solved during consensus meetings. One observer scored systematically more mistakes than the other observer. The intra-observer was for moderate for three items of one observer, while the remaining scores were substantial or almost perfect.

Discussion

With this multicenter observational study, we assessed whether cough after inhalation of TIP is associated with the inspiratory flow. The inspiratory flow was assessed using objective measurements of the PIF and was estimated using video registrations.

We did not find a significant relation between recorded nor estimated PIF and cough, even though cough occurred frequently. Our estimated PIF analysis initially showed that a fast inhalation reduced the risk of cough. However, the order of capsules was a significant confounder, and when accounting for the order of the capsules, the correlation between estimated PIF and cough disappeared. The first capsule resulted in more cough than the second, third, and fourth (P ≤ .015). It is well possible that patients inhale the first capsule more slowly than the consecutive capsules in their

attempt to reduce cough. Then, once they have managed the first inhalations, they are more confident and start inhaling faster, which results in counterintuitive associations of more cough for the slower inhalations.

With a post hoc analysis of the IPR data, we did not find an association between inhaled volume and cough or the acceleration of flow and cough.

Around two-thirds of patients coughed at least once after inhaling TIP. The reported prevalence of cough for TIP in the literature is in general lower and varies between 10% and 48% [9, 15]. An explanation for our higher numbers is that we used video registrations while in the referred studies only adverse event registrations from emergency care visits (which indicates very severe cough), or self-reporting surveys were used. Self-reporting surveys are known to suffer from recall bias. Hence, we think our numbers are likely to be more realistic.

The video recordings of TIP inhalations provided a unique opportunity to assess the inhalation technique of the patients. Two relevant mistakes in inhalation technique were most frequently observed: half of the inhalations showed a breath-hold of fewer than 5 seconds, and two-fifths of patients did not perform a deep exhalation before inhalation. Of note is that when cough occurred, patients were often unable to hold their breath for at least 5 seconds. Both these mistakes are likely to reduce the efficiency of drug deposition in the small airways. Importantly, proper instruction of the patient and repeated (video) evaluation of inhalation technique offers a great opportunity to reduce the prevalence of mistakes empowering patients to get the most out of their inhalation treatment.

A strength of our study is the large number of supervised and unsupervised video registrations in the home setting. We believe to have obtained a realistic impression of the use of TIP that is reflecting daily life practice. Another strength was the thorough observation of all videos by two observers, providing detailed information on both (estimated) inspiratory flow and inhalation technique.

A limitation of the study is the relatively small sample size. The planned statistical test (McNemar) was not performed and instead, we used the more complex mixed-effects model. An important advantage of this analysis is the chance to correct for multiple measurements within patients and to add confounders. Due to a large number of observations and the lack of association in both the raw data plot and both mixed-effects models we believe that the lack of association between inspiratory flow and cough in our study population indicates that the occurrence of cough might be explained by other factors than inspiratory flow. A possible explanation that was

not studied, is adherence to treatment. A hypothesis is that the patient who is more compliant gets used to TIP, and as a result, suffers less from cough. Another factor that might be related to cough is respiratory effort during inhalation, which has been measured in CF patients using electromyogram [19].

Another limitation of the study is that observer 1 was somewhat stricter in scoring inhalation technique than observer 2. However, the intra-observer agreement was good for most scored items which is an important condition for a robust statistical analysis. For future similar studies, the inter-observer variability can be further improved by using training material specifically developed for dry powder inhalers.

Instead of estimating the PIF, the flow analysis could have been optimized by using the IPR in all observations. Alternatively, automated sound analysis has been described in other studies to successfully perform flow analysis [20]. However, the primary aim of this current study was to observe inhalation in a real-life situation, even without the presence of an investigator. The methods described above would have interfered with this aim. Therefore, although we realize that it is at the expense of precision, we choose not to add more advantaged analysis methods.

The final remark on the technique scores is that all steps were weighted equally. Consequently, inhalations of patients with similar overall technique scores might not be equally effective.

Conclusion

In summary, cough immediately after inhalation of the first capsule is a common side effect of TIP. Less cough occurs after inhalation of the consecutive capsules. Cough was not related to inspiratory flow. Furthermore, we found that inhalation techniques are often suboptimal, and therefore periodical counseling is highly recommended to optimize the treatment effect of TIP.

Acknowledgments

We would like to thank the patients and their families for participating in this study, HM Janssens for input in concept of study, BG Bannink for technical support, and the CF research staff of participating centers: AL Geel, M Geerdink, I Heeres, NE Kok, P Mau Assam, S Michels, RDB Meijer, W Olde, M Smink.

References

[1] Elborn JS. Cystic fibrosis. Lancet. 2016;388:2519-31.

[2] Emerson J, Rosenfeld M, McNamara S, Ramsey B, Gibson RL. Pseudomonas aeruginosa and other predictors of mortality and morbidity in young children with cystic fibrosis. Pediatr Pulmonol. 2002;34:91-100.

[3] European Cystic Fibrosis Society Patient Registry At-A-Glance Report 2016. 2018.

[4] Cystic Fibrosis Foundation Annual Data Report 2016. 2017.

[5] Mogayzel PJ, Jr., Naureckas ET, Robinson KA, Mueller G, Hadjiliadis D, Hoag JB, et al. Cystic fibrosis pulmonary guidelines. Chronic medications for maintenance of lung health. American journal of respiratory and critical care medicine. 2013;187:680-9.

[6] Castellani C, Duff AJA, Bell SC, Heijerman HGM, Munck A, Ratjen F, et al. ECFS best practice guidelines: the 2018 revision. J Cyst Fibros. 2018;17:153-78.

[7] Langton Hewer SC, Smyth AR. Antibiotic strategies for eradicating Pseudomonas aeruginosa in people with cystic fibrosis. Cochrane Database Syst Rev. 2017;4:CD004197.

[8] Tiddens HA, Bos AC, Mouton JW, Devadason S, Janssens HM. Inhaled antibiotics: dry or wet? Eur Respir J. 2014;44:1308-18.

[9] Konstan MW, Flume PA, Kappler M, Chiron R, Higgins M, Brockhaus F, et al. Safety, efficacy and convenience of tobramycin inhalation powder in cystic fibrosis patients: The EAGER trial. J Cyst Fibros. 2011;10:54-61.

[10] McKeage K. Tobramycin inhalation powder: a review of its use in the treatment of chronic Pseudomonas aeruginosa infection in patients with cystic fibrosis. Drugs. 2013;73:1815-27.

[11] Haynes A, Geller D, Weers J, Ament B, Pavkov R, Malcolmson R, et al. Inhalation of tobramycin using simulated cystic fibrosis patient profiles. Pediatr Pulmonol. 2016;51:1159-67.

[12] Rosenow T, Oudraad MC, Murray CP, Turkovic L, Kuo W, de Bruijne M, et al. PRAGMA-CF. A Quantitative Structural Lung Disease Computed Tomography Outcome in Young Children with Cystic Fibrosis. American journal of respiratory and critical care medicine. 2015;191:1158-65.

[13] Quanjer PH, Stanojevic S, Cole TJ, Baur X, Hall GL, Culver BH, et al. Multi-ethnic reference values for spirometry for the 3-95-yr age range: the global lung function 2012 equations. Eur Respir J. 2012;40:1324-43.

[14] Bos AC, van Holsbeke C, de Backer JW, van Westreenen M, Janssens HM, Vos WG, et al. Patient-specific modeling of regional antibiotic concentration levels in airways of patients with cystic fibrosis: are we dosing high enough? PLoS One. 2015;10:e0118454.

[15] Konstan MW, Flume PA, Galeva I, Wan R, Debonnett LM, Maykut RJ, et al. One-year safety and efficacy of tobramycin powder for inhalation in patients with cystic fibrosis. Pediatr Pulmonol. 2016;51:372-8.

[16] Standaert TAS, R.J.; Rao N.; Ung K.; Tep, V.; Lin, T.; Rourke, A.M.; Challoner, P. Young cystic fibrosis patients can effectively use a novel high-payload capsule-based dry powder inhaler with tobramycin powder for inhalation (TPI). Pediatr Pulmonol. 2004;38:284.

[17] Landis JR, Koch GG. The measurement of observer agreement for categorical data. Biometrics. 1977;33:159-74.

[18] Quittner AL, Buu A, Messer MA, Modi AC, Watrous M. Development and validation of The Cystic Fibrosis Questionnaire in the United States: a health-related quality-of-life measure for cystic fibrosis. Chest. 2005;128:2347-54.

[19] Reilly CC, Ward K, Jolley CJ, Lunt AC, Steier J, Elston C, et al. Neural respiratory drive, pulmonary mechanics and breathlessness in patients with cystic fibrosis. Thorax. 2011;66:240-6.

[20] Taylor TE, Lacalle Muls H, Costello RW, Reilly RB. Estimation of inhalation flow profile using audio-based methods to assess inhaler medication adherence. PLoS One. 2018;13:e0191330.

Supplementary material

Table S1. Computed tomography (CT) scores

PRAGMA-CF item	Median score [IQR]
Inspiratory (n = 12)	
Healthy lung	90.6 [83.4-93.1]
Bronchiectasis[1]	3.2 [1.0-8.7]
Mucus plugging[1]	1.5 [0.6-2.8]
Bronchial wall thickening[1]	2.9 [1.8-3.2]
Atelectasis[1]	0.3 [0.2-0.7]
Total disease[2]	9.4 [6.9-16.6]
Expiratory (n = 11)	
Healthy lung	83.5 [70.1-98.9]
Trapped air	16.6 [1.1-29.9]

In this table the disease severity assessed by CT scan, for which the Perth Rotterdam Annotated Grid Method Analysis for cystic fibrosis (PRAGMA-CF) was used, is presented [12]. The scores are expressed as percentage of the total lung volume. [1] PRAGMA-CF scores the items bronchiectasis, mucus plugging, bronchial wall thickening and atelectasis in a hierarchical order, meaning that if, for example, bronchiectasis is scored, no other abnormality will be scored in that grid cell. [2] Total disease is the sum of bronchiectasis, mucus plugging, bronchial wall thickening and atelectasis.

Table S2. Health related quality of life scores

CFQ-R dimension	Age 6-13 years (n = 4) median [IQR]	Parents of children age 6-13 years (n = 4) median [IQR]	Age ≥14 years (n = 16) median [IQR]
Physical functioning	100 [67-100][1]	96 [70-100]	81 [71-96]
Emotional functioning	92 [84-99]	97 [78-100]	83 [75-93]
Social functioning	86 [86-89]	-	75 [67-89]
Body image	94 [81-100]	89 [78-100]	89 [89-100]
Eating	100 [100-100]	92 [58-100]	100 [89-100]
Treatment burden	94 [81-100]	67 [47-94]	67 [56-75]
Respiratory symptoms	79 [75-90]	86 [71-93]	83 [64-88]
Digestive symptoms	83 [67-100]	67 [67-75]	78 [67-89]
Health perception	-	61 [56-92]	56 [36-75]
Role functioning	-	-	83 [75-92][1]
Weight	-	100 [75-100]	100 [75-100]
Vitality	-	73 [57-95]	67 [58-67]
School functioning	-	75 [69-81]	-

This table presents the scores of the Cystic Fibrosis Questionnaire-Revised (CFQ-R) scores per dimension [18]. A higher score reflects a greater health related quality of life. Median scores are presented [interquartile range (IQR)]. - Item not covered in CFQ-R for this group. [1]One patient was excluded from this dimension because of a missing value.

Table S3. Output mixed model analyses for association between cough and acceleration and flow volume

	Log odds	Standard error	P-value
Acceleration (n = 57)			
Baseline	0.402	4.215	
Flow acceleration (L/s^2)	0.136	0.544	0.506
FEV_1 (% predicted)	-0.009	0.048	0.603
Inhaled volume (n = 57)			
Baseline	2.254	4.255	
Inhaled volume (L)	-0.643	1.047	0.138
FEV_1 (% predicted)	-0.014	0.046	0.475
Height (cm)	-0.474	0.999	0.255

This table shows the output of the mixed model analysis to study the association between cough and flow acceleration and cough and inhaled volume. Forced expiratory volume in the one second (FEV_1) % predicted was added to both models as possible confounder, and patient height in the model with inhaled volume. $P < 0.05$ is considered significant. No significant associations were found.

Table S4. Median scores of inhalation technique of tobramycin inhalation powder (TIP) per patient

Patient	Median inhalation technique score [IQR]
1	67 [58 - 67]
2	67 [63 - 71]
3	67 [67 - 71]
4	71 [61 - 79]
5	71 [67 - 75]
6	71 [67 - 75]
7	71 [67 - 79]
8	75 [67 - 79]
9	75 [67 - 85]
10	75 [75 - 79]
11	75 [75 - 83]
12	83 [75 - 88]
13	83 [75 - 88]
14	83 [79 - 83]
15	92 [83 - 92]
16	92 [83 - 92]
17	92 [88 - 92]
18	92 [89 - 92]
19	92 [92 - 92]

Table showing the median scores and interquartile ranges (IQR) of the inhalation technique of TIP expressed as percentage of the maximal score for each patient. One patient was excluded because checklist items were not scored in most of his/her inhalations due to low video quality. The scores were calculated as follows: One point was given for every checklist item on technique (six in total), that was performed well. The scores of both observers were used to calculate the total score for each inhalation, expressed as a percentage of the maximum score of 12 points. A higher score means a better performance, with a score of 100% meaning that all six technique items were well performed according to both observers.

Table S5. Inter- and intra-observer agreement of tobramycin inhalation powder (TIP) videos

Checklist item TIP	Inter-observer agreement (n = 828)	Intra-observer, observer 1 (n = 146)	Intra-observer, observer 2 (n = 146)
Deep exhalation before inhalation	0.30	0.84	0.83
Exhalation outside of inhaler	0.29	1.00	0.66
Lips sealed around the mouthpiece	0.75	0.87	0.53
Upright position during inhalation	0.39	0.74	-[1]
Horizontal position of the inhaler	0.36	0.77	0.60
Peak inspiratory flow	0.48	0.70	0.68
Breath hold	0.63	0.77	0.79
Cough	0.89	0.94	0.96
Moment of cough	0.86	0.91	0.88

Table showing the inter and the intra-observer agreement expressed as Cohen's kappa. All inhalations were used to assess the inter-observer agreement between the two observers. For the intra-observer agreement, each observer rescored 20 video recordings containing 146 inhalations.

[1] The value could not be calculated because the dataset showed too little diversity.

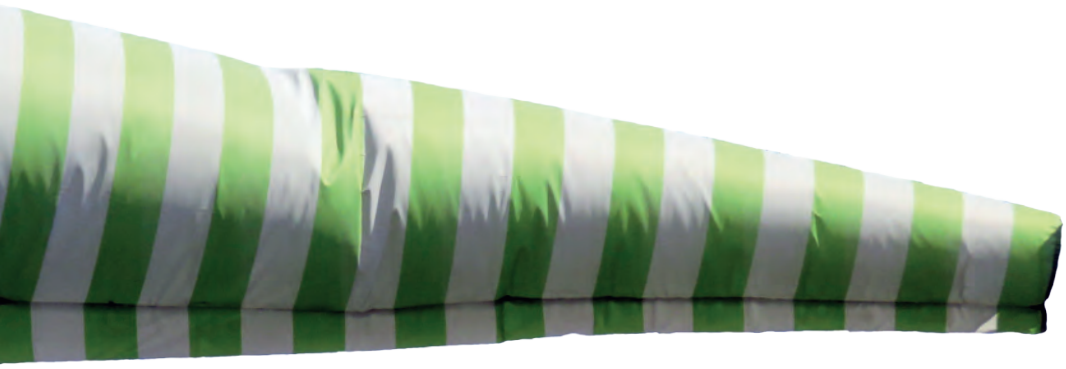

Chapter 7

Effect of inspiratory maneuvers on lung deposition of tobramycin inhalation powder: a modeling study

Journal of Aerosol Medicine and Pulmonary Drug Delivery; 2020: 33(2):61-72

Jennifer J. Meerburg, Eleni-Rosalina Andrinopoulou, Aukje C. Bos, Hwain Shin, Marcel van Straten, Kamal Hamed, Paul Mastoridis, and Harm A.W.M. Tiddens

Abstract

Background Tobramycin inhalation powder (TIP) and tobramycin inhalation solution (TIS) are considered equally effective for the treatment of chronic pulmonary *Pseudomonas aeruginosa* infection in cystic fibrosis (CF) patients. The impact of TIP inhalation maneuvers on distribution of tobramycin is unknown. We hypothesized that (1) fast TIP inhalations result in greater extrathoracic and reduced small airway concentrations compared with slow or uninstructed TIP inhalations; (2) slow TIP inhalations result in greater small airway concentrations than TIS inhalations. The aim of the study was to assess TIP and TIS deposition with computational fluid dynamics (CFD).

Methods Uninstructed, instructed fast, and instructed slow TIP inhalations of CF patients on maintenance TIP therapy, and inhalations during nebulization of saline with PARI LC Plus® were recorded at home. Drug deposition was determined using TIP and TIS aerosol characteristics together with CFD simulations based on airway geometries from chest computed tomography scans. The drug concentration was assessed in extrathoracic, central, large, and small airways.

Results Twelve patients aged 12-45 years were included, and 144 CFD simulations were performed. In all individual analyses, the tobramycin concentrations were well above the threshold for effective dose of 10 times minimal inhibitory concentration throughout the bronchial tree. Extrathoracic concentrations were comparable between fast and uninstructed TIP inhalations, while slow inhalations resulted in reduced extrathoracic concentrations compared with uninstructed TIP inhalations ($p = 0.024$). Small airway concentrations were comparable between fast and uninstructed TIP inhalations, while slow TIP inhalations resulted in greater small airway concentrations than uninstructed TIP inhalations ($p < 0.001$). Small airway concentrations of TIS were comparable with those of slow TIP inhalations ($p = 0.065$), but greater than those of fast and uninstructed TIP inhalations ($p < 0.001$).

Conclusion All TIS and TIP inhalation maneuvers resulted in high enough concentrations, however, inhaling TIS or inhaling TIP slowly results in the greatest small airway deposition.

Introduction

Cystic fibrosis (CF) is a serious hereditary disease. The airways of patients with CF are covered by a layer of viscous mucus, resulting in impaired mucociliary clearance of pathogens. CF patients are particularly prone to chronic pulmonary infection by *Pseudomonas aeruginosa* (*Pa*), which induces chronic inflammation leading to progressive structural damage of the lung. Damaged lungs are a good environment for *Pa* to survive, and when not eradicated *Pa* can transform to a mucoid form, which is more resistant to treatment [1]. With increasing age, more patients become chronically infected with *Pa*. According to annual registries from 2016, 31% of patients with CF in Europe and 29% of patients in the United States are chronically infected with *Pa* [2, 3]. Fortunately, these chronic infections can be suppressed effectively with maintenance inhaled antibiotic therapy. Long-term inhaled antibiotic therapy is recommended in this case by both the European and United States CF guidelines [4, 5].

For chronic *Pa* infections, nebulization therapy with tobramycin inhalation solution (TIS) has been widely studied [6-8]. However, this therapy is relatively time-consuming, nebulizers require thorough cleaning after use, and technical maintenance. Therefore, tobramycin inhalation powder (TIP), a formulation using spray-dried porous particles (PulmoSphere™) administered with a T-326 inhaler (Podhaler™), was developed as a more patient-friendly therapy. The T-326 inhaler is pocket-size, requires minimal cleaning, is disposable after 1 week of use, and administration takes only 5 minutes [9].

Noninferiority studies showed similar efficacy (forced expiratory volume in 1 second and *Pa* colony forming units in the sputum) and pharmacokinetic characteristics of TIP compared with TIS [9, 10]. However, in the phase III EAGER trial (n = 553), sputum concentrations of TIP were almost twice as high as those of TIS [10]. This could possibly be explained by high deposition of tobramycin in the extrathoracic and large airways. Whether this results in a difference in tobramycin concentration in the small airways between TIP and TIS is unknown.

It is important to get the antibiotic to the area where *Pa* is located. *Pa* is ubiquitous in the lungs, and found in both large and small airways, and even in the alveoli [11]. Due to major morphological changes in CF patients starting early in life, efficient targeting of the small airways is important [12, 13]. The concentrations of inhaled antibiotics in the small airways need to be well above the minimal inhibitory concentration (MIC) for effective killing of *Pa* [1]. Consequently, it is believed that treatment efficacy of inhaled antibiotics might be improved by maximizing deposition of the antibiotic in the small airways.

To date, it is not known whether the concentrations of tobramycin in the small airways after inhalation of TIP and TIS are above the MIC, as this is extremely hard to measure in vivo. To estimate concentrations of inhaled antibiotics throughout the bronchial tree, computational fluid dynamic (CFD) models have been developed [14]. These in silico models allow us to improve our insight on the relationship between aerosol particle characteristics, inhalation maneuvers, disease severity, and small airway antibiotic concentrations. Using these CFD models, it was shown that for aztreonam lysine for inhalation, high inspiratory flows during nebulization resulted in a suboptimal treatment compared with low inspiratory flows [15]. To our knowledge, small airway concentrations of TIP and TIS have not been studied using CFD models. There are reasons to expect differences in deposition patterns in the small airways between both formulations. The particle characteristics of the TIP and TIS formulations are different, and the inhalation of TIP versus TIS requires different inhalation maneuvers. TIS is inhaled with the use of a PARI LC Plus® (PARI Medical Holding GmbH, Starnberg, Germany) nebulizer and Porta-Neb® compressor (Philips Respironics, Chichester, United Kingdom) while the patient is breathing quietly in and out with low flow rates until the complete dose is nebulized, which can take up to 20 minutes [16]. On the contrary, TIP is inhaled through specific breathing maneuvers consisting of a full expiration followed by deep inspiration. It takes one or two of these maneuvers to empty one capsule of TIP, and one dose comprises four capsules. As patients are instructed to inhale at least twice per capsule, up to eight inhalations are needed to inhale one dose of TIP. Of note, the T-326 inhaler for TIP has a low to medium airflow resistance (0.08 square root of a centimeter H2O * L/min) [17]. As a result, patients inhaling TIP show a wide variation of inspiratory flow rates between 40 and 120 L/min [18]. In vitro experiments showed that the total lung dose of TIP is relatively unaffected by differences in flow rate [18]. However, the deposition pattern of this dose in the large and small airways is unknown.

Based on the above, we formulated the following research questions:

(1) Is tobramycin deposition for TIP in the large and small airways influenced by inspiratory flow rate?
(2) Are deposition patterns of TIP different from that of TIS, and do they both result in concentrations of tobramycin that are high enough throughout the lungs?

The aim of our study was to assess the deposition patterns of TIP and TIS using CFD simulations based on three-dimensional (3D) airway models of computed tomography (CT) scans of patients with CF, for various patient-specific flow rates.

We hypothesized that high inspiratory flow rates of TIP would result in greater extrathoracic and reduced small airway tobramycin concentrations compared with low flow rates. In addition, we hypothesized that for TIP inhaled with low inspiratory flow rates, small airway concentrations would be higher relative to TIS inhalations with tidal volume breathing.

Materials and Methods

Study design

This study is an in silico study based on CFD simulations with use of flow profiles from an observational study.

Patient selection

For the computational investigation, we used the recorded inspiratory flows of the first 12 patients who were enrolled in a larger observational study of TIP and TIS (NTR5212). Inclusion criteria for the observational study were a diagnosis of CF, age six years and older, and maintenance treatment with TIP for at least one month. Exclusion criteria were pulmonary exacerbation defined as the need for intravenous antibiotics at the time of the inspiratory flow registrations, and inability to follow instructions. Both adolescents and adults from four Dutch CF centers were included: Amsterdam University Medical Center, Erasmus Medical Center (Rotterdam), Haga Teaching Hospital (The Hague), and University Medical Center Utrecht.

Flow recordings

The inspiratory flows were recorded during two study visits that took place at the patient's home using an inhalation profile recorder (The Technology Partnership, Cambridge, United Kingdom) as described before by Haynes et al [18]. In short, the inhalation profile recorder was adjusted to the T-326 inhaler or the PARI LC plus nebulizer with an extra mouthpiece that fitted closely. This mouthpiece was connected with a tube to a pressure gauge, which was connected to a transducer and a laptop. With this system, the pressure drop over the mouthpiece during inhalation was measured and plotted as flow/time curve (area under the curve representing the inhaled volume). The flow was calculated by dividing the square root of pressure drop by resistance. For the T-326 inhaler, the inhaler resistance was 0.088 square root of a centimeter H2O * L/min. For the PARI LC Plus, the inhaler resistance was 0.030 square root of a centimeter H2O * L/min.

For TIP simulations, the inspiratory flows during inhalation of tobramycin with the T-326 inhaler were recorded. Three inhalation maneuvers for each patient were measured during two study visits: an uninstructed, an instructed fast, and an instructed slow inhalation. At the first study visit, the uninstructed inhalation was measured after patients were asked to inhale TIP in the way they would normally do. At the second study visit, the instructed fast and slow inhalation were measured as follows: patients were asked (in random order) to inhale one TIP capsule as fast as possible, and to inhale another TIP capsule as slow as possible, but with a flow that was high enough to let the capsule rattle in the T-326 inhaler.

For the TIS simulations, inspiratory flows were recorded while inhaling 0.9% saline with a Porta-neb compressor and PARI LC Plus nebulizer during the second home visit. The inspiratory flows during nebulization were measured in four recordings, of 15 seconds each. From these four recordings, a mean inhalation curve was computed. Expiratory flows were not recorded, but computed, using the recorded inhaled volume and total time between inhalations.

CFD modeling of aerosol deposition

CFD modeling was used to simulate aerosol deposition in 3D computer lung models. This method has been extensively described elsewhere [14, 19]. In short, the flow dynamics within lung models are determined to predict the course and velocity of the particles after they are virtually injected into the model. To assess the internal flow distribution, the differences between lobar volumes on expiratory and on inspiratory CT scans were used. With this technique, local airway deposition of inhalation medication can be computed in patient-specific models. The CFD model has been validated against single-photon emission computed tomography (SPECT-CT) [19], and has been used in CF [15] and non-CF (asthma/chronic obstructive pulmonary disease) studies [14, 20-22]. CFD model simulations were performed in Fluent 14.0 (Ansys, Inc., Canonsburg, PA).

3D model reconstruction

To execute CFD modeling, nine 3D lung models were reconstructed using chest CT scans from patients with CF. An image of a reconstructed 3D model showing a coupled mouthpiece, the extrathoracic, central, and large airways is shown in Supplement 1. The process is extensively described elsewhere [15]. Briefly, the following five steps were carried out:

First, we selected nine CT scans of a data set from Sophia Children's Hospital (n = 187 patients) of routinely acquired biennial chest CT scans of patients with CF. The selection criteria of the CT scans are described in the next paragraph.

Second, the central and large airways were reconstructed from the chest CT scans. The central airways are defined as the area from the trachea up to the lobar bronchi. The large airways, often referred to in the literature as the distal airways, are defined as the airways from the first segmental bronchi to airways with a diameter of ± 1-2 mm that are still visible on chest CT scan.

Third, the extrathoracic airways, defined as the mouth and throat, including the larynx, until the trachea, were reconstructed. These airways were not imaged on the chest CT scans of the patients. The minimal cross-sectional diameter is decisive for extrathoracic airway deposition [23]. Therefore, an adult extrathoracic airway model with a median minimal cross-sectional diameter was selected from a database (n = 105) of FLUIDDA NV (Kontich, Belgium). The model was then scaled down such that both the anteroposterior and lateral dimension of the scaled model's trachea at the location of the sternum matched the lung model.

Fourth, computer-aided design models of the T-326 inhaler or PARI LC plus mouthpiece were connected to the mouth of the model.

Fifth, the small airways were defined for each lung lobe. Small airways, also referred to in literature as peripheral airways, are airways with a diameter smaller than ± 1-2 mm. These airways are not visible on chest CT images and therefore cannot be reconstructed from a CT scan. Instead, their surfaces were determined using Phalen's description of the airway tree in infants, children, and adolescents, based on the patient's height [24].

Chest CT selection

The selected CT scans had to meet the following technical requirements: volumetric, spirometer-controlled; availability of both inspiratory and expiratory scans; and a maximum slice thickness of 1 mm or smaller. Furthermore, CT scans had to match the TIP-TIS study population as closely as possible based on age, height, and gender. For this purpose, we divided our study patients into three subpopulations: adolescents and female and male adults. We calculated the average height of each subpopulation. The height of the patients for whom we used CT scans differed by a maximum of 5% from the average height of the corresponding subpopulation.

The CT scans from the Sophia database were obtained from patients younger than 18 years. For the female adult and male adult subpopulations, CT scans from adolescents after they were fully grown were selected, as determined by a flattened individual growth curve.

In addition to age, CT scans of patients with different disease severities were selected. Therefore, three lung models were reconstructed per subpopulation, each with a different lung disease severity category: mild, moderate, and severe.

To assess the severity of CF lung disease on CT scan, we used the validated Perth-Rotterdam Annotated Grid Morphometric Analysis for cystic fibrosis (PRAGMA-CF) scoring method [25], which is a morphometric method using a grid to score CT images for percentage of lung disease. Using this score, the extent of bronchiectasis, mucus plugging, and airway wall thickening was computed. The differentiation between mild, moderate, and severe disease was based on the combination of these subscores. To select CT scans within each severity category, we first divided the scans in the Sophia database according to our three subpopulations (adolescents and female and male adults). Next, all CT scans were ranked according to the outcomes of the PRAGMA-CF scores for percentage disease. We defined the lowest tertile as mild, the middle tertile as moderate, and the upper tertile as severe disease. Finally, one CT scan within each tertile was selected for each subpopulation, resulting in the selection of nine CT scans. In addition, the selected CT scans were reviewed unblinded by a pediatric pulmonologist (HT) to evaluate whether in his opinion, the disease severity corresponded to the selected severity group. This evaluation confirmed that the selection represented a good spread of disease severity for each of the three subpopulations.

An overview showing how the flow profiles from the three subpopulations were applied on the CT models is presented in Figure 1.

Aerosol characteristics

For TIP, particle characteristics are dependent on flow rate. In general, when the flow rate through the T-326 inhaler increases, the mass median aerodynamic diameter (MMAD) of the generated particles decreases. With a next-generation impactor (NGI), particle characteristics, including the MMAD, geometric standard deviation, fine particle fraction, and delivered dose, were derived for three different inspiratory flows (40, 60, 85 L/min) (Table 1).

The mean flow rate of each simulated inhalation was calculated, and the particle characteristics (aerodynamic particle size distribution) of the flow that was closest to this mean flow were selected. A single inhalation maneuver was simulated and the deposited mass scaled to the total of four capsule inhalations. We assumed that the complete capsule dose of TIP would be released after an inhaled volume of 1.2 L (data on file). Although it is required to inhale TIP twice, it was shown that most patients are able to empty the capsule in a single inhalation [26]. To strengthen our

statistical models (all patients having the same amount of inhalations), only the first inhalation was simulated. We did not check after each inhalation whether the capsule was emptied but instead relied on the inhaled volume. If a patient was not able to inhale with a volume of 1.2 L, the dose of TIP injected into the model was adjusted relatively to the inhaled fraction of 1.2 L. In the TIP simulations, we did not account for exhalations as the patient instructions list a breath holding of 5 seconds, during which the medication is assumed to be deposited [27].

Table 1. Particle characteristics assessed with next-generation impactor

Treatment	Flow (L/min)	MMAD (µm)	GSD (µm)	FPF (%)	DD (%)
TIP	40	3.8	1.7	57	95
TIP	60	3.3	1.7	59	102
TIP	85	3.0	1.8	61	103
TIS	15	4.2	2.4	58	35

Particle characteristics of TIP and TIS derived from tests with next-generation impactor. The impactor was not cooled. These data were used as starting point for fluid dynamic modeling simulations. DD = Delivered dose. FPF = Fine particle fraction. GSD = Geometric standard deviation. MMAD = Mass median aerodynamic diameter. TIP = Tobramycin inhalation powder. TIS = Tobramycin inhalation solution.

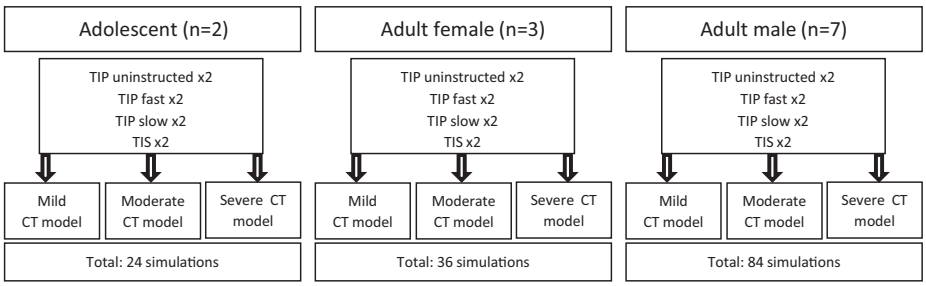

Figure 1. Overview of simulations

An overview of how the flows of the three groups (adolescent, adult female, and adult male) were applied on the CT models is presented in this figure. For every patient, we collected an uninstructed, instructed fast, and instructed slow inhalation of TIP, and we calculated a mean inhalation of TIS from 60 seconds of recording. Every flow was used as input on three different CT models. This resulted in a total of 144 simulations with computational fluid dynamics modeling. CT = Computed tomography. TIP = Tobramycin inhalation powder. TIS = Tobramycin inhalation solution.

For TIS, we considered the characteristics of nebulized droplets to be flow independent. We used aerosol characteristics (MMAD, geometric standard deviation, fine particle fraction, and delivered dose) that were measured with an NGI at a flow rate of 15 L/min for all CFD computations (Table 1). In each individual TIS simulation, TIS was continuously released until a full dose of 5 mL (300 mg of tobramycin) would have been nebulized: the injected dose was calculated by doubling the deposited dose from the NGI, as the NGI based on a 1:1 inhalation-exhalation cycle and no particles can enter the system during exhalation. Next, the patient's specific inhalation-exhalation cycle was stimulated. Exhaled drug (drug that left the model during expiration phase) and drug released by the nebulizer during expiration were considered lost to the environment. Thus, the exhalation time of an individual patient had a large impact on the total amount of lost drug.

For both TIP and TIS, we accounted for dead volume by using the delivered doses of the NGI as the starting point for injected dose, as the dead volume is not measured with the NGI and thus excluded by default.

Tobramycin concentration

To compute tobramycin concentrations throughout the bronchial tree, the surface area of each reconstructed airway and of all the combined small airways was calculated. We only accounted for deposition in the 3D models, as we assumed that tobramycin would not be deposited in the alveoli. Concentrations of tobramycin in µg/mL were computed for the extrathoracic and central airways and for each lung lobe, with distinction between the large and small airways. To assess the deposition with CFD, we made the following assumptions. First, we assumed that particles were deposited once they touched the airway walls. Second, we assumed that particles delivered beyond the reconstructed airway model were distributed evenly over the small airway surface area (determined by the Phalen model as described above). Third, we assumed the thickness of the airway surface liquid to be constant to compute concentrations. The ratio of deposited drug mass and airway surface liquid volume of each lung region is defined as its averaged drug concentration. These concentrations were computed for three different scenarios: a moderate thin (3 µm) [28], in between (5 µm), and a thick layer (7 µm) of airway surface liquid [29]. For the concentrations of deposited drug presented in this article, the airway surface liquid thickness was 7 µm (worst-case scenario). Concentrations for the other lining fluid layer scenarios can easily be calculated by dividing the outcomes by 7 µm and multiplying them by 3 or 5 µm.

Effective tobramycin concentration

To set the tobramycin concentration for effective inhibition of *Pa* growth, we selected as starting point an MIC of 4 µg/mL, as described by the European Committee on Antimicrobial Susceptibility Testing (EUCAST) (www.eucast.org/clinical_breakpoints/). However, we defined an effective conservative tobramycin concentration as 10 times MIC, that is, 40 µg/mL, as there are many factors such as mucus binding and mucociliary clearance that may negatively affect the activity of tobramycin [1].

Statistical analysis

Patient characteristics are tabulated using descriptive statistics, categorical data being presented as counts (n) and proportions (%). Continuous data are presented as median and interquartile ranges (IQRs). The outcomes of the assessment are shown in box-and-whisker plots. To investigate differences in concentrations between different TIP inhalation maneuvers and differences in concentration between TIP and TIS, generalized estimating equation models for correlated data were used. These models account for multiple measurements within each patient. The reference conditions for the models were uninstructed TIP inhalations to assess differences within TIP, and TIS inhalations to assess differences between TIP and TIS. CT scan model and lung region were considered possible confounders. To check whether our results were biased by patients who did not receive a full dose of TIP because not all their inhaled volumes reached the needed 1.2 L to empty a capsule, sensitivity analyses were done without those patients. Results of testing are considered significant if the p-value is below 0.05. SPSS/PC statistics (SPSS, Inc. Chicago, IL) and statistical software package R, version 3.4.3 (free download from www.rproject.org) were used for the statistical calculations.

Ethics

Written informed consent for the use of deidentified data was obtained from the patients and/or their parents or guardians depending on their age. Approval for both the observational study and the Sophia database was obtained by the Institutional Review Board of Erasmus Medical Center, Rotterdam, the Netherlands (MEC-2015-329 and MEC-2013-078, respectively).

Results

Patient selection

The patient population selected from the clinical study consisted of 4 females (33%) and 8 males (66%). Patients were divided into the three subpopulations as follows: adolescent (n = 2), adult female (n = 3), and adult male (n = 7). Patient demographics and lung function data are presented in Table 2.

Table 2. Patient characteristics

Patient	Sex	Age (years)	FEV_1 % predicted*
1	M	12	104
2	F	13	94
3	M	18	92
4	M	20	63
5	M	22	72
6	M	25	106
7	M	25	110
8	M	25	49
9	F	29	35
10	M	35	60
11	F	41	80
12	F	45	95

*Best forced expiratory volume in 1 second (FEV_1) % predicted of the year before inclusion, using global lung initiative 2012 references. Patients were divided into three groups based on sex and age: adolescents (patients 1 and 2), adult females (patients 9, 11, and 12), and adult males (patients 3, 4, 5, 6, 7, 8, and 10). F = Female. M = Male.

Flow recordings

The patients inhaled TIP with a wide range of flows. Figure 2a-c shows the inspiratory flow curves of the uninstructed, instructed fast, and instructed slow TIP inhalations. All patients performed an instructed fast inhalation that was faster than the uninstructed inhalation. Similarly, the instructed slow inhalation for all patients was slower than the uninstructed inhalation. Except for two situations, all patients were able to inhale more than the minimum volume of 1.2 L needed to inhale the full content of the capsule. One patient inhaled only 0.5 L through the T-326 inhaler with the instructed fast inhalation, and another patient inhaled only 0.7 L with the uninstructed inhalation. For the modeling of this maneuver, the inhaled dose of TIP was adjusted to 42% and 58%, respectively.

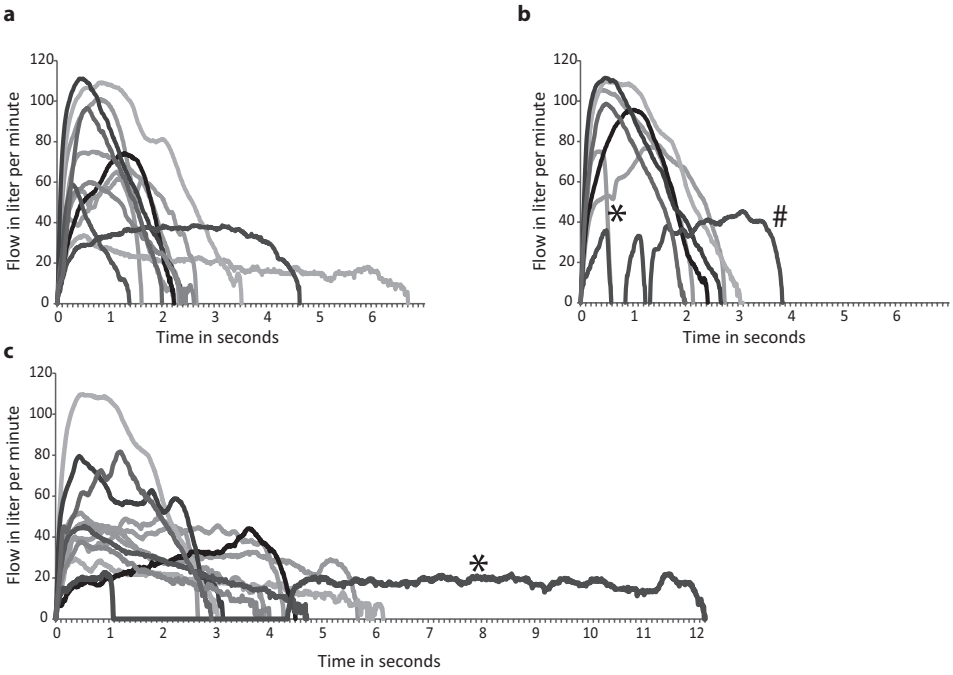

Figure 2. Inspiratory flow curves of TIP

The inspiratory flow curves of TIP inhalations are shown for each patient. (a-c) Show the flow curves of the uninstructed, instructed fast, and instructed slow inhalations, respectively. The x-axis represents the time in seconds, and the y-axis represents the inspiratory flow in L/min. Each color represents a single patient. All study patients reached a higher peak inspiratory flow (PIF) in the fast inhalation compared with the uninstructed inhalation, and lower PIFs in the slow inhalations compared with the uninstructed inhalations. (a) Inspiratory flow curves of uninstructed inhalations. (b) Inspiratory flow curves of instructed fast inhalations. *Patient coughed during inhalation. #Irregular inhalation. (c) Inspiratory flow curves of instructed slow inhalations. *Patient coughed during inhalation.

For TIS, mean inspiratory flow curves from the same population that were calculated for each individual ranged from 0.2 to 2.4 L.

Tobramycin concentration

Figure 3 illustrates the computed tobramycin concentrations throughout the bronchial tree for uninstructed, instructed fast, and instructed slow inhalations of TIP and the TIS inhalations for three single-study subjects and for three of the nine CT models.

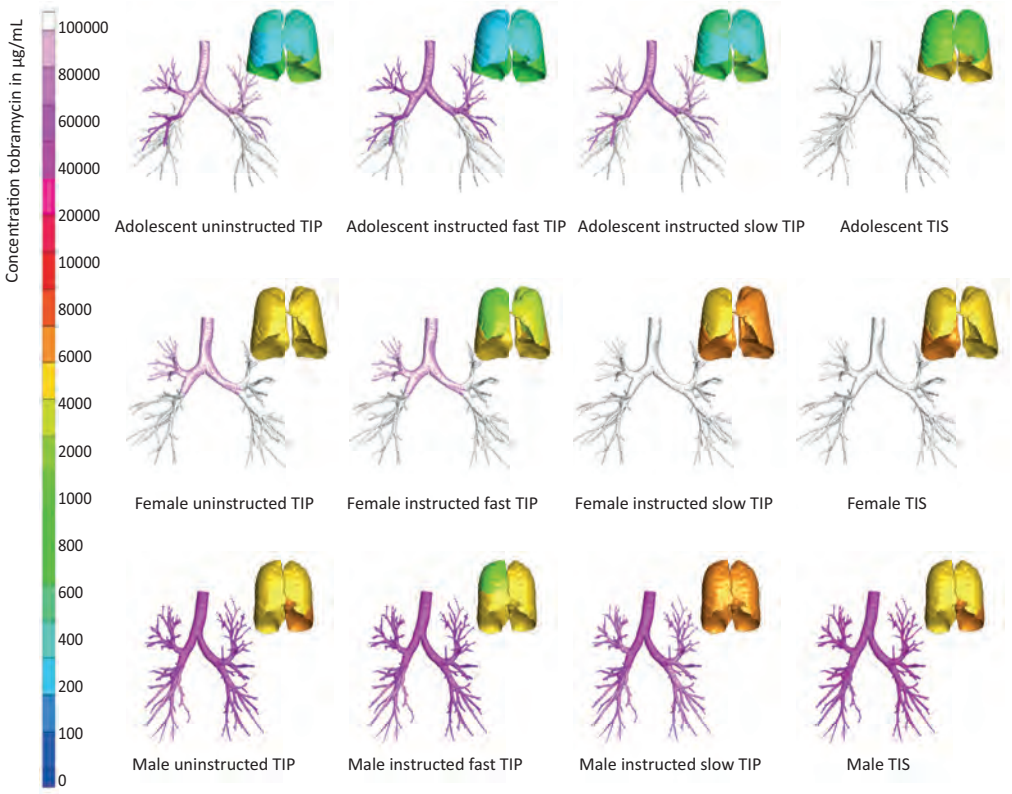

Figure 3. Concentration of tobramycin in µg/mL for all flow types in three single-study subjects

This figure shows 3D airway models constructed from CT scans of an adolescent (upper row), adult female (middle row), and adult male (lower row). The concentration is presented for each flow type: uninstructed, instructed fast, and instructed slow inhalation of TIP and the inhalations with TIS. The colors in the figures represent the tobramycin concentrations in µg/mL. The concentration in the central and large airways is shown in the image of the bronchial tree on the left, and the concentration in the small airways is indicated with the colored lung images in the right corners. White is the highest possible concentration, whereas dark blue represents the lowest concentration. Note the variability in deposition pattern between different flows within patients, and the very high concentrations in central and large airways. Furthermore, for these three patients, the minimal concentrations in the small airways were all above 200 µg/mL, which is well above the threshold for effective concentrations of 40 µg/mL.

In Figure 4, the box-and-whisker plots summarized the computed tobramycin concentrations in the large and small airways of all simulations for each flow type and device. Large airway concentrations were up to 100-fold greater compared with

small airway concentrations, which is a result of the much smaller airway surface in the large airways compared with the small airways. Median (IQR) concentration in the large airways was 73,597 (41,587-126,353) µg/mL, which is 1839 times larger than the threshold value. Median (IQR) concentration in the small airways was 1038 (719-1500) µg/mL, which is 26 times larger than the threshold. Especially for TIP, the box plot shows that differences in deposition are relatively small.

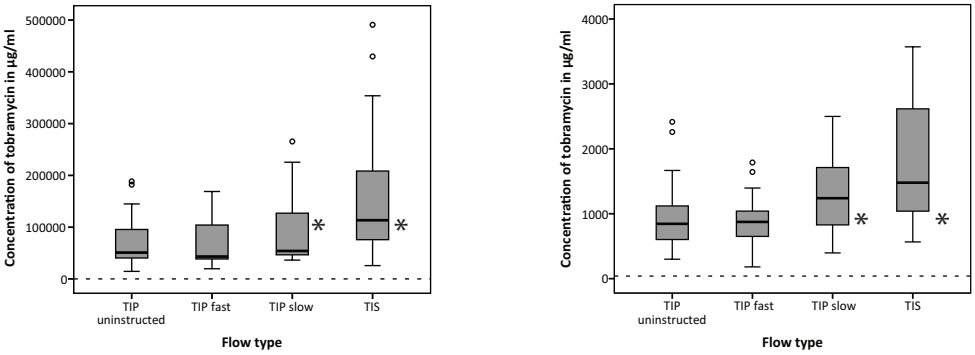

Figure 4. Concentration of tobramycin in large and small airways, per flow type

Box-and-whisker plots of the concentration of tobramycin in µg/mL in the large airways (left) and in the small airways (right). On the x-axis, the four different flow types are shown: uninstructed, instructed fast, and instructed slow inhalations with TIP and the inhalations with TIS. Note the difference in scale between the two graphs. The bolt line in each box represents the median; the bottom and top lines of the box represent the 25th and 75th percentile. The whiskers represent either 1.5 times the 25th or 75th percentile value or the minimum and maximum values. The circles outside of the T-bars are outliers. The dotted line in both graphs represents the threshold value for effective dose of 10 times MIC, that is, 40 µg/mL. Concentrations that were significantly different from the concentrations of the uninstructed flow of TIP ($p < 0.05$) using generalized estimating equation models are marked with an asterisk. Left: Tobramycin concentration in the large airways. The instructed slow inhalations with TIP ($p = 0.006$) and the inhalations with TIS ($p < 0.001$) resulted in significantly greater concentrations of tobramycin, when compared with the uninstructed inhalation of TIP. Right: Tobramycin concentration in the small airways. The instructed slow inhalations with TIP and the inhalations with TIS resulted in significantly greater concentrations of tobramycin ($p < 0.001$ in both cases), when compared with the uninstructed inhalation of TIP.

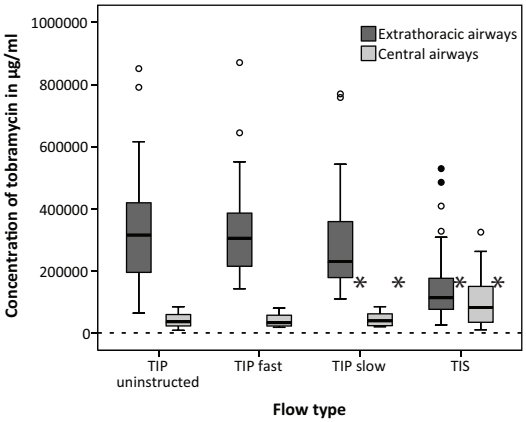

Figure 5. Concentration of tobramycin in the extrathoracic and central airways, per flow type
Box-and-whisker plots of the concentration of tobramycin in µg/mL in the extrathoracic and central airways (dark versus light box). On the x-axis, the four different flow types are shown: uninstructed, instructed fast, and instructed slow inhalations with TIP and the inhalations with TIS. The bolt line in each box represents the median; the bottom and top lines of the box represent the 25th and 75th percentile. The whiskers represent either 1.5 times the 25th or 75th percentile value or the minimum and maximum values. The circles outside of the T-bars are outliers. The dotted line in both graphs represents the threshold value for effective dose of 10 times minimal inhibitory concentration, that is, 40 µg/mL. Concentrations that were significantly different from the concentrations of the uninstructed flow of TIP ($p < 0.05$), using generalized estimating equation models, are marked with an asterisk. In the extrathoracic airways, the concentration of TIP was reduced after instructed slow TIP inhalations or inhalations with TIS ($p < 0.001$), compared with the uninstructed inhalation of TIP. Conversely, in the central airways, the instructed slow TIP ($p = 0.047$) and TIS ($p < 0.001$) inhalations resulted in greater tobramycin concentrations than the uninstructed inhalations of TIP.

In Figure 5, the concentrations of tobramycin in the extrathoracic and central airways are shown. Median (IQR) tobramycin concentration in the extrathoracic airways was 226,721 (159,044-368,656) µg/mL, which is 5668 times larger than the threshold value. Median concentration in the central airways was 44,378 (23,142-65,819) µg/mL, which is 1109 times larger than the threshold value.

Figures 4 and 5 show that compared with TIP, TIS particles were deposited deeper in the respiratory system, with less deposition in the extrathoracic region, and more deposition in the central, large, and small airways. The complete results of the generalized estimating equation models are presented in Supplement 2. First, we assessed whether tobramycin concentrations differed between instructed inhalations of TIP or TIS inhalations and uninstructed TIP inhalations (Table A in Supplement 2),

with the latter being the reference in the generalized estimating equation model. Both instructed slow TIP inhalations and TIS inhalations resulted in significantly reduced extrathoracic airway concentrations ($p = 0.024$ and $p < 0.001$), and greater central ($p = 0.047$ and $p < 0.001$), large ($p = 0.006$ and $p < 0.001$), and small (both $p < 0.001$) airway concentrations when compared with uninstructed TIP inhalations. Instructed fast inhalations did not result in significantly different concentrations when compared with uninstructed inhalations for any airway region.

Second, we assessed whether tobramycin concentrations of all TIP inhalations different significantly from that of TIS inhalations (Table B in Supplement 2), with TIS being the reference in the generalized estimating equation model. TIS inhalations resulted in significantly reduced concentrations in the extrathoracic airways and in significantly greater central, large, and small airway concentrations when compared with all TIP inhalations (all $p < 0.001$), except for instructed slow TIP inhalations, which resulted in similar small airway concentrations as TIS.

When redoing the analysis excluding the two patients who did not reach a volume of 1.2 L in all their inhalations, the outcomes of the generalized estimating equation models did not show different significant results.

Effective tobramycin concentration

In Supplement 3, the deposition of tobramycin per lung lobe in the large and small airways is presented for both TIP and TIS. The tobramycin concentrations in both the large and small airways in all lung lobes were all well above the cutoff value for effective inhibition of 40 µg/mL, assuming an airway surface liquid layer of 7 µm. For this airway surface liquid layer, of the patients who received a complete dose of TIP, the lowest local concentration of tobramycin in our simulations was found in the small airways in the left upper lobe of an adult female after an uninstructed inhalation of TIP. The tobramycin concentration was 128 µg/mL, which is still more than triple the amount of the effective threshold concentration of 40 µg/mL. The highest local concentration of tobramycin in the small airways was found in the left lower lobe of an adult male, after inhalation of TIS. The tobramycin concentration was 5656 µg/mL, which is 141-fold greater than the effective threshold concentration.

Discussion

We studied the effect of inhalation maneuvers and different formulations of tobramycin on the deposition throughout the lung with CFD, in a study population of CF patients of 12 years and older. Instructed slow inhalations of TIP result in greater

tobramycin concentrations in the large and small airways compared with inhalations of TIP without instruction. Furthermore, inhalations with TIS results in greater large and small airway concentrations when compared with all TIP inhalations, except for the instructed slow TIP inhalations. For the slow TIP inhalations, the small airway concentrations were similar to those of TIS. Importantly, all inhalations led to a concentration of tobramycin that was at least triple the amount of the effective clinical cutoff value of 40 µg/mL. Furthermore, we conclude that it is feasible to instruct patients to perform specific inhalation maneuvers.

According to our results, the drug deposition of TIP is dependent on inspiratory flow rates. This finding contradicts the results of an earlier study that concluded that the T-326 inhaler is flow-rate independent, when experimentally measuring total lung doses at the level of the trachea with in vitro mouth throat deposition models [18]. However, there were a few differences between the two studies. First, different throat models were used (no comparative studies between these models were performed). Furthermore, we assessed lung deposition for a larger number of flows: 36 compared with 10 flows that were selected from 152 flows of 38 patients in the earlier study. In addition, our flows showed a wider variation: we measured peak inspiratory flows of 30-113 L/min compared with 49-88 L/min in the study of Haynes et al. Hence, our results are likely to be representative of a more heterogeneous patient population. A flow-dependency investigation for the TIS formulation was not part of the investigation, and so, the influence of individual flow patterns on the delivery of a nebulized solution remains unknown.

Results reported here show greater tobramycin deposition in large and small airways by TIS, when compared with TIP inhalations.

This finding contradicts results of a gamma scintigraphy study in healthy volunteers, more drug was delivered into the lungs with TIP than with TIS [17, 27, 30]. There are several differences between the two studies. First, the gamma scintigraphy study was carried out with healthy volunteers, whereas the current study was carried out with CF patients. Second, the inspiratory flows for the TIS simulations were based on mean inhalation recordings of 15 seconds and assumed consistent, periodic inhalation cycles during the use of nebulizer for the complete treatment. When comparing the mass balances of tobramycin delivery with the PARI LC Plus nebulizer observed by Newhouse et al. [27] with those from Lenney et al. [31], the important relevance of the exhaled mass fraction on the much smaller lung deposition fraction can be detected. Even though device and extrathoracic losses are very similar in both publications, differences in patients or in their instruction can lead to different amounts of exhaled drug. As the computational modeling in this study did not account for exhalation

once a drug particle reached the small airways, the amount deposited in these small airways and therefore the drug concentration might be overestimated for TIS. This modeling bias may explain the inconsistency with the results from scintigraphy studies and motivate further investigation on the sensitivity of nebulized therapies on variability of inhalation maneuver and its influence on deposited and exhaled fraction.

Uninstructed inhalations with TIP resulted in greater extrathoracic airway concentrations of tobramycin compared with TIS. This finding could be explained by the fact that the flows through the relatively small mouthpiece cross section of the T-326 inhaler are much higher than when inhaling quietly through the relatively wide PARI LC Plus nebulizer. This jet effect in combination with the higher inhalation rate results in greater velocity of the aerosol particles for TIP compared with TIS. The consequence is higher inertial forces and increased deposition of the inhaled aerosol particles in the oral cavity, which was already observed in the clinical deposition studies using scintigraphy [27]. Greater extrathoracic deposition might also explain the observations reported by Konstan et al., who found greater sputum concentrations of tobramycin with use of TIP compared with TIS [16]. Sputum concentrations are probably more representative for the extrathoracic deposition than for the deposition deeper in the respiratory system. High concentrations in the upper airways might be disadvantageous as increased numbers of fungal organisms (Candida albicans and Aspergillus species) are found in patients who nebulized TIS [32]. Greater extrathoracic airway concentrations of tobramycin might further increase this effect.

On the contrary, greater concentrations in the lower airways might lead to increased serum concentrations of tobramycin, and overdosing of tobramycin can lead to nephrotoxicity and ototoxicity. However, in the pivotal studies of both TIP and TIS, it was described that trough and peak levels stay well below the potentially toxic levels [10, 33]. In our models, the differences in small airway concentrations are relatively small, and with these results it is highly unlikely that in patients in vivo the slow inhalations result in increased risk of toxicity relative to uninstructed inhalations. Uninstructed inhalations were also used in the pivotal studies.

However, in silico studies require many assumptions, which are potential confounders of our results. We will discuss the most important limitations of this study:

First, due to the fact that TIP is inhaled by single-breath inhalation and TIS is inhaled with continuous inhalations, different assumptions were made to perform the simulations for TIP and TIS. More specifically, for TIP we did not account for exhaled

particles. TIS is inhaled with continuous breathing, and particles that were not deposited before exhalation phase were more likely to be exhaled. Furthermore, particles that were injected in the model during the exhalation phase were not inhaled at all. Besides, we did not account for differences in particle release between inspiratory and expiratory phases. Due to these different assumptions, the comparison between TIP and TIS might be less valid, since we do not know the effect of these assumptions.

Another limitation is the fact that CFD analyses are validated with SPECT-CT scan studies with asthma patients using nebulized aerosol particles at lower flow rates (30 L/min) that might behave differently than TIP PulmoSphere particles [19]. Due to the porous formulation of TIP, the particles have a low contact surface area, reducing cohesive forces among particles, which prevents agglomeration [17, 18]. Therefore, our models might have led to an underestimation of the true deposition of TIP. We did not perform a SPECT-CT versus CFD validation study with CF patients using TIP PulmoSphere particles. That said, physical characteristics such as MMAD and its geometric standard deviation are the most decisive factors to predict aerosol behavior. By taking these characteristics of TIP into account, we fitted our simulations as closely as possible to the real situation.

Another limitation is the fact that the same throat model was used for all models instead of using the throats of patients. The geometry of the mouth and throat plays an important role in deposition of medication, and by standardizing the throat, this is not accounted for. Furthermore, we scaled the throat in such a way that it fitted our trachea, while there are more nuances in throat geometry between female and male adolescents, adult females, and adult males than the diameter at the trachea. However, the aim of our study was to assess the relationship between flow and lung deposition, and by limiting variation in other parameters, we could study this relationship with more precision.

We concluded that tobramycin concentrations are sufficiently high throughout the bronchial tree, using a clinical effective cutoff value of 10 times MIC. We decided to relate our results to the data provided by EUCAST (www.eucast.org/clinical_breakpoints/), that is, an MIC of tobramycin for *Pa* of 4 µg/mL. Conservatively, we set our clinical cutoff value at 10 times MIC or 40 µg/mL. Nevertheless, our clinical cutoff value at 10 times MIC does not necessarily mean that concentrations are high enough to be effective. Bos et al. described in a review that the effectiveness of inhaled antibiotics is influenced by multiple factors. The binding of thick CF mucus

to tobramycin molecules actuates various mechanisms that can lead to a decreased number and/or inactivation of these molecules [1]. Therefore, our in silico situation might be more positive that the in vivo situation.

Furthermore, we assumed that particles were distributed evenly over the small airway surface area. In reality this distribution is uneven [34], as some airways may be partially or totally occluded by mucus, resulting in no or less tobramycin deposition to the periphery of those airways, while other airways are open enabling inhaled particles to pass. Hence, our models of the small airways ignore the fact that some areas may not receive any tobramycin at all.

Patients are required to inhale TIP at least twice per capsule. However, of the 36 recorded inhalations with TIP, 34 were of a volume above the required 1.2 L to empty the content of a capsule (94%). In our simulations, only one inhalation was simulated per occasion. Hence, we underestimated the delivered dose in the simulations because of the two patients who did not empty their capsule in one inhalation. However, when we performed a sensitivity analysis excluding these patients, the results were similar.

The 3D lung models were constructed with CT scans that were from other CF patients than the flow patients. In the Sophia Children's Hospital, CT scans are made of CF patients on routine basis biannually. This is not a national policy for CF health care in the Netherlands, and we did not have CT scans of all patients of other CF centers included in this study. Therefore, CT scans were selected from the database of Sophia Children's hospital, and matched for height.

Finally, in this study, the tobramycin deposition was assessed using CFD. We did not investigate whether the significantly higher small airway depositions after slow TIP inhalation or inhalations with TIS would result in better treatment effects.

In conclusion, in CF patients, 12 years and older, instructed slow inhalation of TIP resulted in greater concentrations of tobramycin in both the large and small airways of our models compared with uninstructed inhalation as well as instructed fast inhalations. When patients are instructed to inhale TIP slowly, the deposition in the small airways of our models is comparable with that of TIS. Importantly, all simulated inhalation maneuvers with both TIP and TIS resulted in concentrations well above a concentration of 10 times MIC for *Pa*, even in the small airways. Careful and repeated instructions of patients regarding appropriate inhalation are important to target the small airways with an antibiotic deposition as high as possible.

Acknowledgments

We acknowledge the patients and their families who participated in the studies; C. Holsbeke and W. Vos of FLUIDDA NV for performing the CFS simulations; the local principal investigators of participating centers H.G.M. Arets, M.E. van der Eerden, C.J. Majoor, H.G.M. Heijerman; Novartis Pharma AG for technical input; and P. Robberts of Cresco Pharma for providing nebulizers.

References

[1] Bos AC, Passe KM, Mouton JW, Janssens HM, Tiddens HA. The fate of inhaled antibiotics after deposition in cystic fibrosis: How to get drug to the bug? J Cyst Fibros. 2017;16:13-23.

[2] Cystic Fibrosis Foundation Annual Data Report 2016. 2017.

[3] European Cystic Fibrosis Society Patient Registry At-A-Glance Report 2016. 2018.

[4] Castellani C, Duff AJA, Bell SC, Heijerman HGM, Munck A, Ratjen F, et al. ECFS best practice guidelines: the 2018 revision. J Cyst Fibros. 2018;17:153-78.

[5] Mogayzel PJ, Jr., Naureckas ET, Robinson KA, Mueller G, Hadjiliadis D, Hoag JB, et al. Cystic fibrosis pulmonary guidelines. Chronic medications for maintenance of lung health. American journal of respiratory and critical care medicine. 2013;187:680-9.

[6] Ratjen F, Munck A, Kho P, Angyalosi G, Group ES. Treatment of early Pseudomonas aeruginosa infection in patients with cystic fibrosis: the ELITE trial. Thorax. 2010;65:286-91.

[7] Ramsey BW, Pepe MS, Quan JM, Otto KL, Montgomery AB, Williams-Warren J, et al. Intermittent administration of inhaled tobramycin in patients with cystic fibrosis. Cystic Fibrosis Inhaled Tobramycin Study Group. N Engl J Med. 1999;340:23-30.

[8] Smith WD, Bardin E, Cameron L, Edmondson CL, Farrant KV, Martin I, et al. Current and future therapies for Pseudomonas aeruginosa infection in patients with cystic fibrosis. FEMS Microbiol Lett. 2017;364.

[9] Geller DE, Konstan MW, Smith J, Noonberg SB, Conrad C. Novel tobramycin inhalation powder in cystic fibrosis subjects: pharmacokinetics and safety. Pediatr Pulmonol. 2007;42:307-13.

[10] Konstan MW, Geller DE, Minic P, Brockhaus F, Zhang J, Angyalosi G. Tobramycin inhalation powder for P. aeruginosa infection in cystic fibrosis: the EVOLVE trial. Pediatr Pulmonol. 2011;46:230-8.

[11] Moore JE, Mastoridis P. Clinical implications of Pseudomonas aeruginosa location in the lungs of patients with cystic fibrosis. J Clin Pharm Ther. 2017;42:259-67.

[12] de Jong PA, Nakano Y, Lequin MH, Mayo JR, Woods R, Pare PD, et al. Progressive damage on high resolution computed tomography despite stable lung function in cystic fibrosis. Eur Respir J. 2004;23:93-7.

[13] Mott LS, Park J, Murray CP, Gangell CL, de Klerk NH, Robinson PJ, et al. Progression of early structural lung disease in young children with cystic fibrosis assessed using CT. Thorax. 2012;67:509-16.

[14] De Backer JW, Vos WG, Devolder A, Verhulst SL, Germonpre P, Wuyts FL, et al. Computational fluid dynamics can detect changes in airway resistance in asthmatics after acute bronchodilation. J Biomech. 2008;41:106-13.

[15] Bos AC, van Holsbeke C, de Backer JW, van Westreenen M, Janssens HM, Vos WG, et al. Patient-specific modeling of regional antibiotic concentration levels in airways of patients with cystic fibrosis: are we dosing high enough? PLoS One. 2015;10:e0118454.

[16] Konstan MW, Flume PA, Kappler M, Chiron R, Higgins M, Brockhaus F, et al. Safety, efficacy and convenience of tobramycin inhalation powder in cystic fibrosis patients: The EAGER trial. J Cyst Fibros. 2011;10:54-61.

[17] Geller DE, Weers J, Heuerding S. Development of an inhaled dry-powder formulation of tobramycin using PulmoSphere technology. J Aerosol Med Pulm Drug Deliv. 2011;24:175-82.

[18] Haynes A, Geller D, Weers J, Ament B, Pavkov R, Malcolmson R, et al. Inhalation of tobramycin using simulated cystic fibrosis patient profiles. Pediatr Pulmonol. 2016;51:1159-67.

[19] De Backer JW, Vos WG, Vinchurkar SC, Claes R, Drollmann A, Wulfrank D, et al. Validation of computational fluid dynamics in CT-based airway models with SPECT/CT. Radiology. 2010;257:854-62.

[20] Vinchurkar S, Backer LD, Vos W, Holsbeke CV, Backer JD, Backer WD. A case series on lung deposition analysis of inhaled medication using functional imaging based computational fluid dynamics in asthmatic patients: effect of upper airway morphology and comparison with in vivo data. Inhal Toxicol. 2012;24:81-8.

[21] De Backer LA, Vos WG, Salgado R, De Backer JW, Devolder A, Verhulst SL, et al. Functional imaging using computer methods to compare the effect of salbutamol and ipratropium bromide in patient-specific airway models of COPD. Int J Chron Obstruct Pulmon Dis. 2011;6:637-46.

[22] Vos W, De Backer J, Poli G, De Volder A, Ghys L, Van Holsbeke C, et al. Novel functional imaging of changes in small airways of patients treated with extrafine beclomethasone/formoterol. Respiration. 2013;86:393-401.

[23] Vos W, Backer Jd, Schroeder J, Sommerville M, Dwivedi S, K. , Backer Wd. In-Silico Assessment of Airway Deposition Using Functional Respiratory Imaging for Mono, Dual and Triple Combination Co-Suspension Metered Dose Inhaler Formulations. C69 Here's looking at you: Imaging studies in copd. p. A5811-A.

[24] Phalen RF OM, Kleinman MT, Crocker TT. Tracheobronchial deposition predictions for infants, childern and adolescents. Ann occup Hyg. 1988;32:11-21.

[25] Rosenow T, Oudraad MC, Murray CP, Turkovic L, Kuo W, de Bruijne M, et al. PRAGMA-CF. A Quantitative Structural Lung Disease Computed Tomography Outcome in Young Children with Cystic Fibrosis. American journal of respiratory and critical care medicine. 2015;191:1158-65.

[26] Standaert TAS, R.J.; Rao N.; Ung K.; Tep, V.; Lin, T.; Rourke, A.M.; Challoner, P. Young cystic fibrosis patients can effectively use a novel high-payload capsule-based dry powder inhaler with tobramycin powder for inhalation (TPI). Pediatr Pulmonol. 2004;38:284.

[27] Newhouse MT, Hirst PH, Duddu SP, Walter YH, Tarara TE, Clark AR, et al. Inhalation of a dry powder tobramycin PulmoSphere formulation in healthy volunteers. Chest. 2003;124:360-6.

[28] Tarran R, Button B, Picher M, Paradiso AM, Ribeiro CM, Lazarowski ER, et al. Normal and cystic fibrosis airway surface liquid homeostasis. The effects of phasic shear stress and viral infections. J Biol Chem. 2005;280:35751-9.

[29] Tarran R, Button B, Boucher RC. Regulation of normal and cystic fibrosis airway surface liquid volume by phasic shear stress. Annu Rev Physiol. 2006;68:543-61.

[30] Challoner PB FM, Hirst PH, Klimowicz MA, Newman SP, Schaeffler BA, Speirs RJ, Wallis SJ. Gamma scintigraphy lung deposition comparison of TOBI in the Pari LC Plus nebulizer and the Aerodose inhaler. American journal of respiratory and critical care medicine. 2001;163.

[31] Lenney W, Edenborough F, Kho P, Kovarik JM. Lung deposition of inhaled tobramycin with eFlow rapid/LC Plus jet nebuliser in healthy and cystic fibrosis subjects. J Cyst Fibros. 2011;10:9-14.

[32] Cheer SM, Waugh J, Noble S. Inhaled tobramycin (TOBI): a review of its use in the management of Pseudomonas aeruginosa infections in patients with cystic fibrosis. Drugs. 2003;63:2501-20.

[33] Geller DE, Pitlick WH, Nardella PA, Tracewell WG, Ramsey BW. Pharmacokinetics and bioavailability of aerosolized tobramycin in cystic fibrosis. Chest. 2002;122:219-26.

[34] Kleinstreuer C, Zhang Z, Donohue JF. Targeted drug-aerosol delivery in the human respiratory system. Annu Rev Biomed Eng. 2008;10:195-220.

Supplementary materials

Supplement 1. Coupled 3D model of the mouthpiece and extrathoracic, central and large airways

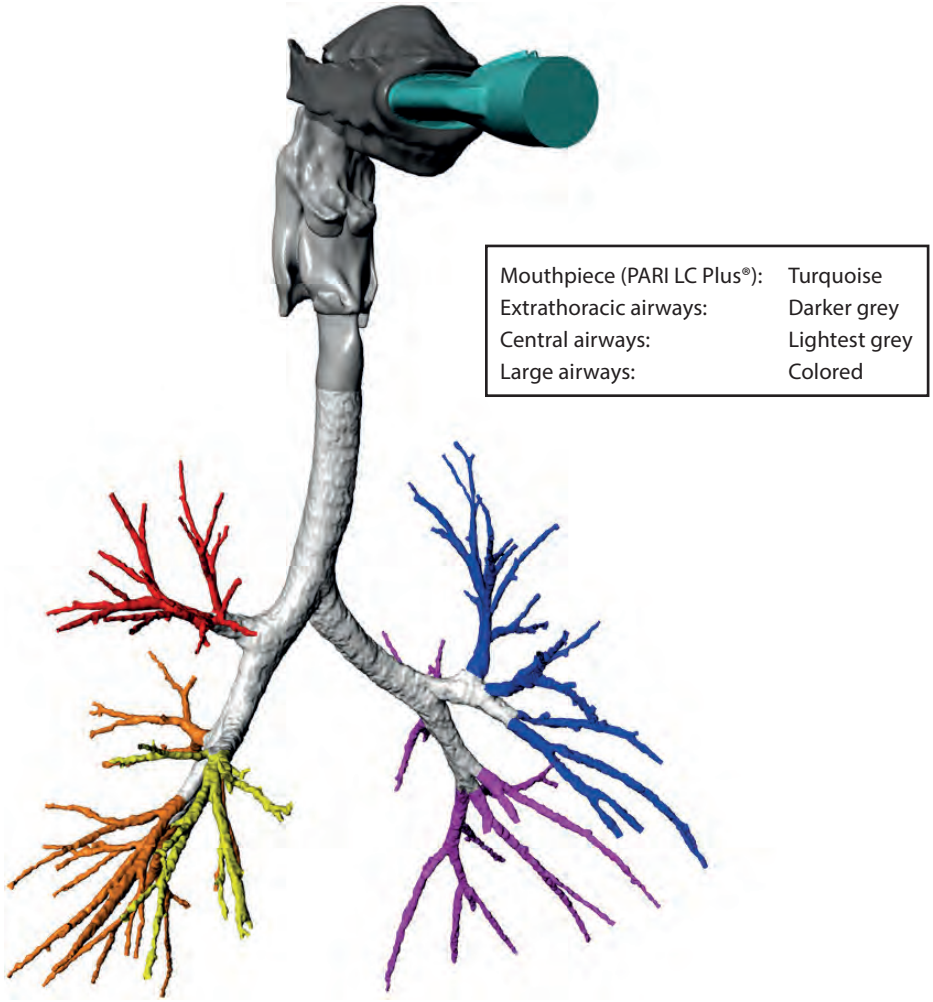

Coupled mouthpiece and extrathoracic, central and large airways model. For the extrathoracic airways, a generic upper airway model was scaled down so it would fit the trachea of the patient. The central airways and large airways are segmented from computed tomography (CT) scans. The small airways are not imaged because these airways could not be segmented from the CT scan. This image originates from the publication by Bos et al and is used with permission of the authors [15].

Supplement 2. Generalized estimating equation (GEE) analysis, association of flow type and tobramycin concentration

We first assessed whether instructed fast or instructed slow inhalations with tobramycin inhalation powder (TIP) and tobramycin inhalation solution (TIS) inhalations resulted in statistically significant differences, when compared to uninstructed inhalations with TIP (uninstructed TIP being the reference in the GEE model) (Table A). In a second analysis, we assessed whether uninstructed, instructed slow and fast inhalations resulted in statistically significant differences when compared to TIS inhalations (TIS being the reference in the GEE model) (Table B). The results of the GEE analysis are presented per lung region, for the extrathoracic, central, large and small airways. Differences were calculated within patients accounting for the CT scan model that was used. Results of testing are considered significant if the p-value is below 0.05.

Table A. Differences in tobramycin concentrations (µg/mL) between TIP instructed and TIS inhalations , and uninstructed inhalation with TIP (reference), using a GEE model

Region	Flow type	Difference with TIP uninstructed	Standard error	P-value
Extrathoracic airways	TIP fast	-6613	33446	0.843
	TIP slow	-34426	15266	0.024*
	TIS	-176713	25905	< 0.001*
Central airways	TIP fast	-1602	3453	0.643
	TIP slow	3448	1738	0.047*
	TIS	57276	12776	< 0.001*
Large airways	TIP fast	-2222	4932	0.652
	TIP slow	14024	5059	0.006*
	TIS	86869	14593	<0.001*
Small airways	TIP fast	-62	81	0.441
	TIP slow	370	94	< 0.001*
	TIS	835	207	< 0.001*

*P-value < 0.05. In the extrathoracic airways, slow TIP inhalations and TIS inhalations resulted in reduced concentrations, compared to uninstructed TIP inhalations. In the central, large and small airways, slow TIP inhalations and TIS inhalation resulted in greater concentrations, compared to uninstructed TIP inhalations.

Table B. Differences in tobramycin concentrations (µg/mL) between TIP and TIS inhalations (reference), using a GEE model

Region	Flow type	Difference with TIS	Standard error	P-value
Extrathoracic airways	TIP uninstructed	176713	259045	< 0.001*
	TIP fast	170100	37198	< 0.001*
	TIP slow	142287	21421	< 0.001*
Central airways	TIP uninstructed	-57276	12776	< 0.001*
	TIP fast	-58877	14560	< 0.001*
	TIP slow	-53828	12727	< 0.001*
Large airways	TIP uninstructed	-86869	14593	< 0.001*
	TIP fast	-89090	14212	< 0.001*
	TIP slow	-72844	13743	< 0.001*
Small airways	TIP uninstructed	-835	208	< 0.001*
	TIP fast	-897	209	< 0.001*
	TIP slow	-465	252	0.065

*P-value < 0.05. In the extrathoracic airways, all TIP inhalations resulted in greater concentrations, compared to TIS inhalations. In the central and large airways, all TIP inhalations resulted in reduced concentrations, compared to TIS inhalations. In the small airways, only uninstructed and fast TIP inhalations resulted in significant reduced concentrations, compared to TIS inhalations.

Supplement 3. Concentration of tobramycin per lung lobe

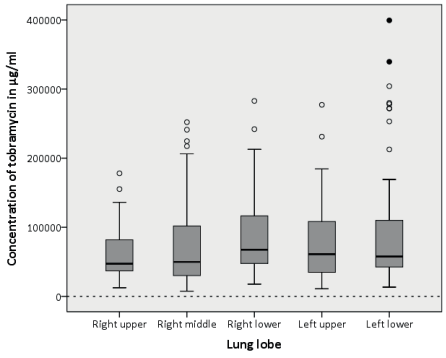

Figure a. TIP in large airways

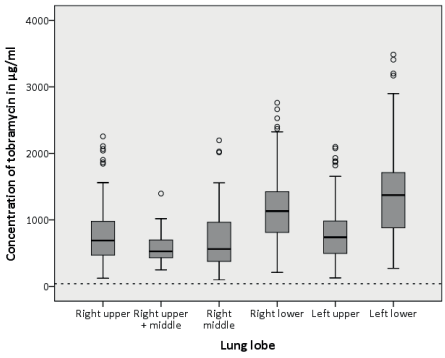

Figure b. TIP in small airways

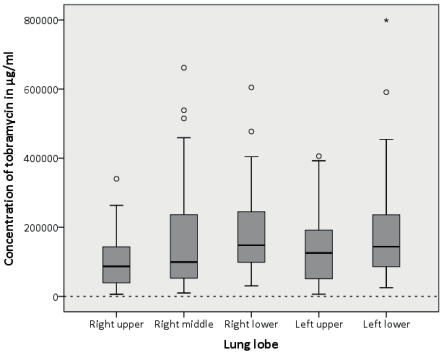

Figure c. TIS in large airways

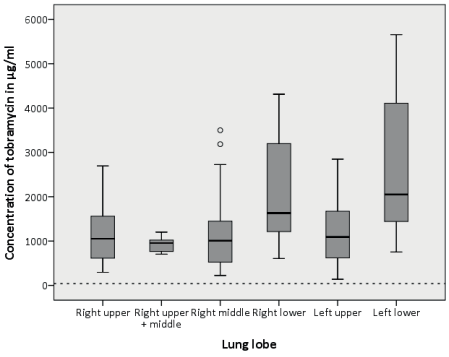

Figure d. TIS in small airways

Box-and-whisker plots of the concentration of tobramycin in µg/mL per lung lobe for tobramycin inhalation powder (TIP), in the large and small airways (Figure a and b) and for tobramycin inhalation solution (TIS), in the large and small airways (Figure c and d). In lung models, due to technical reasons the small airway region of the right upper and right middle lobe was combined. On the x-axis, the different lung lobes are presented. The bolt line in each box represents the median; the bottom and top lines of the box represent the 25th and 75th percentile. The whiskers represent either 1.5 times the 25th or 75th percentile value or the minimum and maximum values. The circles outside of the T-bars are outliers. The dotted line in both graphs represents the threshold value for effective dose of 10 times minimal inhibitory concentration, i.e. 40 µg/mL. Note the difference in scale between the two graphs. In all cases, the concentration of tobramycin was above the threshold value.

SECTION III

Chapter 8

General discussion

This thesis focuses on the definition, quantification and treatment of bronchiectasis using chest computed tomography (CT). This chapter reflects on the implications of our findings. Furthermore, future directions of the role of chest CT scanning in bronchiectasis are being discussed.

Definition of bronchiectasis

Bronchiectasis is mostly a radiological diagnosis. However, universally accepted diagnostic criteria are lacking. We have identified three key challenges to overcome for the diagnosis of bronchiectasis on chest CT scans.

Firstly, age and gender related reference values are needed for airway and artery dimensions. As discussed in chapter 3, there is a positive relation between age and airway-artery ratio [1-3]. Furthermore, females have smaller airway diameters than males, even when adjusted for height [4, 5]. A recommendation would be to develop gender specific cut-off values of airway-artery ratios for preschool children up to the age of six, six to twelve years, twelve to eighteen, and eighteen years and older.

Secondly, while bronchiectasis is often defined as an airway which diameter is larger than that of the adjacent artery, healthy individuals with increased airway-artery ratios can occur [6]. For this reason population-based studies are needed to generate reference values for airway-artery ratios. A challenge for such studies is that healthy individuals would need to be exposed to ionising radiation. However, recent developments in CT technology have reduced radiation dose for a chest CT substantially, making such studies ethically feasible [7]. As an alternative, large numbers of chest CT scans could be collected for various other clinical indications, that were evaluated as being normal by radiologists.

Thirdly, we found that both inner and outer airway diameters are currently being used to diagnose bronchiectasis and there is no conclusive evidence to support either one of these. However, when using the inner diameter, the presence of mucus will result in decreased airway-artery ratios, resulting in underestimation of bronchiectasis (Figure 1). Also, the outer diameter is less dependent on lung volume relative to the inner diameter. Therefore we suggest the use of the outer airway diameter for comparison with the adjacent artery for the diagnosis of bronchiectasis.

Until proper reference values are available, a conservative cut-off value for the diagnosis of bronchiectasis can be used. Aliberti et al performed a Delphi process in an international taskforce to come up with a radiological definition for adults that is likely to be supported by most experts in the field of bronchiectasis {Aliberti, in press Lancet respiratory}. The conclusions of this process were that a conservative

airway-artery ratio of 1.5 should be used, and that this limit accounts for both inner or outer diameters. Whether this conservative cut-off of 1.5 is also adequate for children requires further research. The outcomes of the Delphi process could be used as guideline until more extensive studies have been performed to define a more accurate cut-off value.

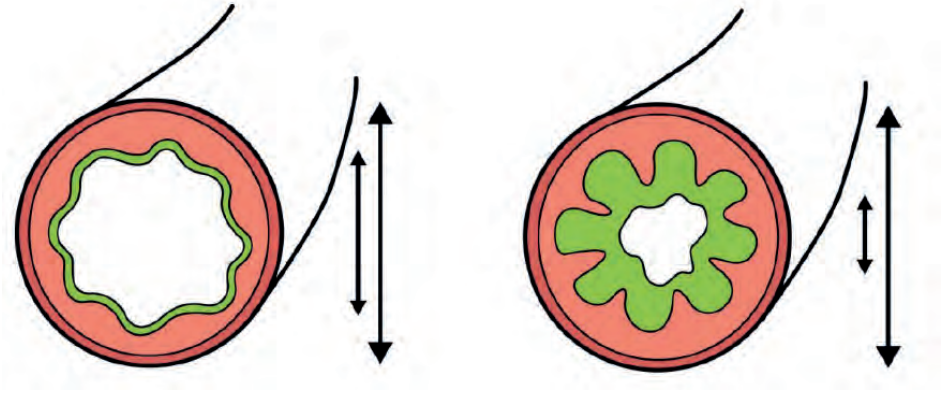

Figure 1. Consequences of using the inner or outer airway diameter for the diagnosis of bronchiectasis.

The figure on the left shows a healthy small airway and on the right an inflamed small airway with a thickened wall due to mucus impaction at full inspiration. On inspiration, the mucosa of the healthy airway is only slightly folded. The inflamed airway has larger folds compared with the normal airway. Mucus fills up the gaps between the mucosal folds. On a chest CT, the folds and mucus will be interpreted as a thickened airway wall. This figure illustrates why the outer diameter is a more robust parameter for diagnosing and quantifying bronchiectasis because in contrast to the inner diameter, it is not influenced by the presence of mucus in the lumen [8]. Image provided by Marloes Meerburg.

Standardisation of CT acquisition

Standardisation of chest CT protocols

There is still a wide variety in chest CT protocols [9] between hospitals. Standardisation of CT protocols for both clinical care and clinical trials is needed to reduce variability between hospitals and within patients, and to optimise the risk benefit ratio in relation to the use of ionising radiation. Furthermore, a higher level of protocol standardisation will allow the use of chest CT related outcome measures for patient registries.

Standardisation of lung volume

Airway dimensions are highly dependent on lung volume [10-12]. As such, to further optimise the diagnostic yield of chest CT scans, lung volume should also be standardised during scanning. Methods to accomplish standardised lung volume per age group are discussed in chapter 3. In the Erasmus MC Sophia Children's Hospital, lung volume standardisation was implemented successfully in the routine workflow for all chest CT scans in 2007, and also for chest magnetic resonance imaging (MRI) scans in 2010 [13]. This volume standardisation has improved the quality of the image acquisition substantially. Standardisation of lung volume during CT scanning is a shared responsibility of radiologists and pulmonologists. Our research group has initiated courses and certification projects, for radiologists and pulmonologists, encouraging implementation of volume standardisation. To boost its implementation worldwide, taskforces and international guidelines by learned societies are needed.

Certification of hospitals

To synchronise CT acquisition between hospitals, clinicians of different hospitals will need to collaborate. An example of a standardisation initiative was the Standardised Chest Imaging Framework for Interventions and Personalised Medicine in CF (SCIFI-CF) project aiming to optimise CT acquisition for cystic fibrosis (CF) centres participating in the European Cystic Fibrosis Society Clinical Trial Network (ECFS-CTN). This was done by visiting research centres, testing CT scanners settings using phantoms and by providing training on lung volume and CT protocol standardisation [9]. More recently, SCIFI-II was started within the ECFS-CTN for the certification of all 58 sites with the aim to prime the network for clinical studies that include chest CT as outcome measure. Similarly, the European Multicentre Bronchiectasis Audit and Research Collaboration (EMBARC) registry has the ambition to include chest CT outcomes as part of the registry, for which a pilot project has been started. To roll out standardisation programs on a larger scale, our image analysis laboratory developed an online application for training and certification in standardised CT scanning.

Standardisation of chest CT analysis

To date, analysis of CT scans is largely expert based. To diagnose clinical patients requires advanced medical knowledge of diseases and their radiological presentations. For this purpose, analysis by appropriately trained radiologists is essential. However, to objectively assess the extent of structural lung abnormalities, for example to monitor disease progression in clinical follow up or to use CT scans as outcome measures in clinical trials, a standardised approach is needed. Standardised CT analysis requires the ability to detect and quantify specific abnormalities in a systematic way. In our studies we used scoring methods to systematically quantify and describe the structural changes on chest CT scans of patients with bronchiectasis. The scoring for

the studies described in chapter 4 and 5 was done by trained and certified observers. In the reviewing process of these papers, some reviewers considered it a significant draw-back that these observers were not radiologists. However, we showed in many studies that scoring of images can be reliably performed by observers with varying medical knowledge, as long as adequate standardised training is given [2, 14-16]. Each step of the scoring process in our studies is documented in standard operating procedures in great detail. In addition, we report inter- and intra-observer variability, which is needed to assess reproducibility. In the systematic review in chapter 2 we came across a large number of studies where scoring was performed by radiologists, but no information is given on training, certification and inter- and intra-observer variability. Thus, the quality of scoring in these studies is difficult to evaluate. To conclude, standardised image analysis, using systematic scoring methods is needed for the analysis of chest CTs of bronchiectasis patients in both clinical practice and clinical studies. This scoring can be executed by trained observers.

Image analysis methods for bronchiectasis

To systematically analyse structural lung disease including bronchiectasis on chest CT images, we used the Baumann and Hartmann scoring method for common variable immunodeficiency disease in chapter 4, and we developed the BronchiEctasis Scoring Technique for CT (BEST-CT) for bronchiectasis patients in chapter 5. The comparison between the Baumann and Hartmann methods showed that the Hartmann method was slightly better in terms of reproducibility and ability to detect longitudinal change of bronchiectasis scores. However, the BEST-CT outperformed the Hartmann method in reproducibility. Further validation of BEST-CT in cohorts is needed to assess its sensitivity to measure changes in lung structural changes in bronchiectasis patients over time. An important advantage of BEST-CT over other currently used scoring methods for bronchiectasis is that the annotated images of the BEST-CT can be used for the development and validation of artificial intelligence (AI) based image analysis algorithms.

Besides the BEST-CT, there are more image analysis methods to quantify bronchiectasis, namely measurements of airway tapering and airway-artery ratios. An advantage of obtaining tapering measurements over airway-artery ratios is that tapering is independent of arterial diameter. To date, these analysis methods are semi-automated, and the manual annotations that are needed are time-consuming [17, 18]. Fortunately, fully automated AI-algorithms are in development. For image analysis of bronchiectasis chest CT scans it is likely that BEST-CT outcomes will be used to capture the pattern of the disease and that both tapering measurements and airway-artery ratios will be used for the sensitive analysis of airway and artery related changes.

Chest CT in bronchiectasis studies

In clinical bronchiectasis studies chest CT scans can play an important role in patient selection, in phenotyping included patients, and in generating outcome measures.

Firstly, CT scans can be used as part of the inclusion criteria for study patients. Clear radiological inclusion criteria will result in a more optimal selection of bronchiectasis patients than inclusions based on clinical symptoms, and a diagnosis of bronchiectasis that was given in an earlier phase by the local radiologist or the treating physician. Furthermore, CT facilitates inclusion of patients based on extent of structural lung disease. This is especially relevant for intervention studies focused on patients with more advanced lung disease. In previous studies, patients were selected based on a minimum number of exacerbations before the year of inclusion. However, this inclusion criterion resulted in studies that did not meet the study endpoints, because exacerbations did not occur as much as expected. This phenomenon can partly be explained by regression to the mean [19]. CT outcomes probably give a more accurate representation of severity of disease than the number of exacerbations.

Secondly, CT scans can be used to phenotype bronchiectasis patients. In chapter 5, 84 bronchiectasis patients who participated in a phase II study were phenotyped using BEST-CT. As expected, substantial heterogeneity in structural lung disease was observed, as bronchiectasis can be the result of a broad spectrum of underlying diseases. This information can contribute to improve our understanding of the response to treatment in subgroups. In chapter 4, we used the Baumann and Hartmann methods to phenotype patients with granulomatous lymphocytic interstitial lung disease (GLILD). A striking finding of our study was that the vast majority of GLILD patients suffered from bronchiectasis. This is a clinical relevant observation, as the presence of bronchiectasis on CT independent of the underlying disease requires special treatment directed to reduce sputum production and cough. To conclude, phenotyping in bronchiectasis studies is important due to the heterogeneous nature of the disease. In the future, treatment strategies could be developed for subgroups of bronchiectasis patients based on their chest CT phenotype, resulting in more personalised treatment options.

Thirdly, chest CT outcomes are likely to play a more important role in intervention studies in the near future. To date, lung studies often use spirometry outcomes (forced expiratory volume in 1 second, FEV_1) and number of exacerbations as study endpoints. However, FEV1 and exacerbations are relative imprecise outcomes and thus large numbers of patients are needed to run such studies. Several studies with bronchiectasis patients that included FEV1 and exacerbations as primary outcomes failed to show significant benefit between treatment groups [19]. New outcome

parameters such as CT outcomes or microbiology related outcomes are more likely to detect changes after intervention. For example, in the iBEST-study *Pseudomonas aeruginosa (Pa)* sputum density showed significant differences between study treatment and placebo-arm [20]. However, the effect of a treatment on this single outcome measure is not sufficient to understand whether the treatment is effective, i.e. whether the treatment improves the patient's health. Multiple outcome measures are needed, using multiple modalities, to understand the effect of an intervention on bronchiectasis disease. CT scans can be included in clinical bronchiectasis studies to obtain information on the effect of an intervention on structural lung disease. The selection of the CT outcomes should be based on the type of drug. For example, when the treatment effect of a mucolytic agent is being studied, the amount of mucus plugging and airway wall thickness could be used as outcome measure. In other pulmonary diseases such as CF, CT outcomes from the CF-CT [16] and Maffesanti [21] scoring methods have recently been used as primary outcomes to study the effect of CF transmembrane conductance regulator modulators and of inhalation therapies such as recombinant human DNAse (clinicaltrials.gov, NCT02730208 and NCT00179998). Furthermore, a phase III study was completed where the efficacy between inhaled hypertonic saline and isotonic saline was compared using CT outcomes (PRAGMA-CF [14] in preschool children with CF. It was concluded that inhaled hypertonic saline for 48 weeks slowed down structural lung disease on chest CT in these children (in writing). Currently, the ASPEN study with bronchiectasis patients is ongoing (ClinicalTrials.gov, NCT04594369) which includes a sub-study investigating the effect of brensocatib on chest CT outcomes.

Chest CT for clinical care

In clinical follow up, CT scans are already an important tool to gain information on disease progression. In this thesis we retrospectively collected CT scans that were made during clinical follow up of GLILD and bronchiectasis patients (chapters 4 & 5). Interestingly, intervals between CT scans varied widely from a few weeks up to sixteen years, as CT scans were acquired probably primarily for diagnosis and in relation to symptoms. Chest CT can play an important role in monitoring disease progression and to guide treatment [22]. To do so it is important to make the chest CT scan at predefined intervals based on the risk profile of the patient. This is common practice for other chronic lung diseases such as cystic fibrosis [23]. Standardised quantitative analysis of these routine chest CT scans will further contribute to the clinical impact of this monitoring strategy. Furthermore, such quantitative CT outcomes can be incorporated in clinical registries such as the EMBARC registry [24].

Aerosol treatment for bronchiectasis patients

Inhaled antibiotics are registered for CF patients with chronic infection of *Pa*, and prescribed off-label to patients with bronchiectasis disease. The success of inhalation therapy is highly dependent on the inhalation technique. Unfortunately, as shown in chapter 6, the majority of patients make mistakes during inhalations. In the instance of a suboptimal inhalation technique, less drugs will be deposited in the small airways, and the effect of treatment will mostly be suboptimal. To maximise the effect of the treatment, inhalation technique should be practiced on a regular basis. In addition, clinicians should actively discuss barriers experienced by patients in respect to their inhalation treatment. Training devices such as metered dose inhalers with whistles or built-in connections to smartphone applications have been developed and significantly decreased mistakes made during inhalations in asthma patients [25]. However, the use of such tools will cost time and energy, increasing the burden of treatment. Whether bronchiectasis patients are willing to use such devices needs to be investigated.

We studied small airway deposition of tobramycin inhalation powder in CF patients. *Pa* is an important pathogen in bronchiectasis patients and chronic infection is associated with increased morbidity and mortality. As this pathogen causes small airway disease, sufficient amount of drugs need to be deposited in small airways to reach drug levels above the minimum inhibitory concentration. As shown in chapter 7, slow inhalations increase small airway deposition of tobramycin inhalation powder in CF patients, and resulted in comparable concentrations of tobramycin as nebulisation. Both formulations have their pros and cons; Dry powder tobramycin is portable but results in cough in many patients, while nebulisation therapy causes less cough but is more time consuming. A new development in this field might be the development of a tobramycin dose-aerosol (TobrAir®) which is portable like the dry powder inhaler but might induce less coughing. Though, this product is not yet available on the market [26].

Future directions

Aetiology studies show a large diversity of associated diseases of the bronchiectasis population [27]. This is a great challenge for therapeutic studies and might be a reason why the one size fits all approach in many therapeutic trials have not resulted in registered new therapies [19]. The availability of objective image analysis systems for chest CT scans allows the addition of quantitative information to registries. Currently, BEST-CT is being used to phenotype 500 CT scans of patients from the EMBARC registry. With these data, it is possible that clinically relevant subgroups, based on CT pattern, can be identified. It is likely that more precise phenotyping of the chest CT will help to direct the diagnostic workup for those cases where the associated

disease-causing bronchiectasis is unknown. For example, a diagnostic workup could be started in cases where the CT pattern fits the pattern as seen in primary ciliary dyskinesia or immune deficiencies. It is likely that phenotyping chest CTs of bronchiectasis patients using state of the art image analysis techniques, will help to further reduce the number of bronchiectasis patients without a clear diagnosis.

An important step forward will be the introduction of automated image analysis systems to phenotype and quantify structural lung disease. The BEST-CT lends itself for automated analysis using machine learning techniques [28]. Such AI-based algorithms should be seamlessly integrated in the workflow of radiologists. Fully automated image analysis methods for bronchiectasis patients, such as the airway-artery and tapering measurements, are coming to market [17, 29, 30].

Ultimately chest magnetic resonance imaging (MRI) could also become important for imaging the lungs of bronchiectasis patients. An important advantage over chest CT is that no ionising radiation is needed. As discussed in chapter 3, the image quality of MRI is not yet comparable to CT in the detection of bronchiectasis, but new sequences with better resolutions have been developed [31, 32]. A great advantage of chest MRI over CT is that with MRI functional data such as ventilation and perfusion is more easily acquired. However, for MRI it is more challenging to standardise acquisition across vendors and centres and the spatial resolution of CT is hard to beat. In the coming years, the detection and quantification of bronchiectasis by chest MRI needs to be further expanded, by developing and testing new sequences for bronchiectasis patients.

Conclusion

In this thesis we studied how to diagnose and quantify bronchiectasis and related lung abnormalities on chest CT scans. Furthermore, we analysed the inhalation of aerosols and calculated drug deposition with CT models in CF patients. CT scans contain a large amount of information on lung structure that is currently unused. To use CT scans, acquisition and analysis need to be standardised, and this is a shared responsibility of pulmonologists and radiologists. International networks such as EMBARC could play a leading role in standardisation of study centres. Chest CT outcomes presented in this thesis can be used for phenotyping and monitoring disease. Longitudinal intervention studies must be performed to further validate the CT outcomes as study endpoints. The use of chest CT outcomes in clinical trials is likely to boost the development of novel treatment for bronchiectasis patients.

References

[1] Matsuoka S, Uchiyama K, Shima H, Ueno N, Oish S, Nojiri Y. Bronchoarterial ratio and bronchial wall thickness on high-resolution CT in asymptomatic subjects: Correlation with age and smoking. Am J Roentgenol. 2003;180:513-8.

[2] Kuo W, Andrinopoulou ER, Perez-Rovira A, Ozturk H, de Bruijne M, Tiddens HAWM. Objective airway artery dimensions compared to CT scoring methods assessing structural cystic fibrosis lung disease. J Cyst Fibrosis. 2017;16:116-23.

[3] Kuo W, Soffers T, Andrinopoulou ER, Rosenow T, Ranganathan S, Turkovic L, et al. Quantitative assessment of airway dimensions in young children with cystic fibrosis lung disease using chest computed tomography. Pediatr Pulmonol. 2017;52:1414-23.

[4] Ripoll JG, Guo W, Andersen KJ, Baker SE, Wiggins CC, Shepherd JRA, et al. Sex differences in paediatric airway anatomy. Exp Physiol. 2020;105:721-31.

[5] Dominelli PB, Ripoll JG, Cross TJ, Baker SE, Wiggins CC, Welch BT, et al. Sex differences in large conducting airway anatomy. J Appl Physiol (1985). 2018;125:960-5.

[6] Diaz AA, Young TP, Maselli DJ, Martinez CH, Maclean ES, Yen A, et al. Bronchoarterial ratio in never-smokers adults: Implications for bronchial dilation definition. Respirology. 2016.

[7] Tækker M, Kristjánsdóttir B, Graumann O, Laursen CB, Pietersen PI. Diagnostic accuracy of low-dose and ultra-low-dose CT in detection of chest pathology: a systematic review. Clin Imaging. 2021;74:139-48.

[8] Tiddens H, Meerburg JJ, van der Eerden MM, Ciet P. The radiological diagnosis of bronchiectasis: what's in a name? Eur Respir Rev. 2020;29.

[9] Kuo W, Kemner-van de Corput MP, Perez-Rovira A, de Bruijne M, Fajac I, Tiddens HA, et al. Multicentre chest computed tomography standardisation in children and adolescents with cystic fibrosis: the way forward. Eur Respir J. 2016;47:1706-17.

[10] Bakker ME, Stolk J, Reiber JH, Stoel BC. Influence of inspiration level on bronchial lumen measurements with computed tomography. Respiratory medicine. 2012;106:677-86.

[11] Matsuoka S, Kurihara Y, Yagihashi K, Hoshino M, Nakajima Y. Airway dimensions at inspiratory and expiratory multisection CT in chronic obstructive pulmonary disease: correlation with airflow limitation. Radiology. 2008;248:1042-9.

[12] Petersen J, Wille MM, Rakêt LL, Feragen A, Pedersen JH, Nielsen M, et al. Effect of inspiration on airway dimensions measured in maximal inspiration CT images of subjects without airflow limitation. Eur Radiol. 2014;24:2319-25.

[13] Salamon E, Lever S, Kuo W, Ciet P, Tiddens HA. Spirometer guided chest imaging in children: It is worth the effort! Pediatr Pulmonol. 2017;52:48-56.

[14] Rosenow T, Oudraad MC, Murray CP, Turkovic L, Kuo W, de Bruijne M, et al. PRAGMA-CF. A Quantitative Structural Lung Disease Computed Tomography Outcome in Young Children with Cystic Fibrosis. American journal of respiratory and critical care medicine. 2015;191:1158-65.

[15] Tiddens H, Andrinopoulou ER, McIntosh J, Elborn JS, Kerem E, Bouma N, et al. Chest computed tomography outcomes in a randomized clinical trial in cystic fibrosis: Lessons learned from the first ataluren phase 3 study. PLoS One. 2020;15:e0240898.

[16] Wainwright CE, Vidmar S, Armstrong DS, Byrnes CA, Carlin JB, Cheney J, et al. Effect of bronchoalveolar lavage-directed therapy on Pseudomonas aeruginosa infection and structural lung injury in children with cystic fibrosis: a randomized trial. Jama. 2011;306:163-71.

[17] Kuo W, Perez-Rovira A, Tiddens H, de Bruijne M, Normal Chest CTsg. Airway tapering: an objective image biomarker for bronchiectasis. Eur Radiol. 2020;30:2703-11.

[18] Ferraro V, Andrinopoulou ER, Sijbring AMM, Haarman EG, Tiddens H, Pijnenburg MWH. Airway-artery quantitative assessment on chest computed tomography in paediatric primary ciliary dyskinesia. ERJ Open Res. 2020;6.

[19] Metersky M, Chalmers J. Bronchiectasis insanity: Doing the same thing over and over again and expecting different results? F1000Res. 2019;8.

[20] Loebinger MR, Polverino E, Chalmers JD, Tiddens H, Goossens H, Tunney M, et al. Efficacy and safety of TOBI Podhaler in Pseudomonas aeruginosa-infected bronchiectasis patients: iBEST study. Eur Respir J. 2021;57.

[21] Maffessanti M, Candusso M, Brizzi F, Piovesana F. Cystic fibrosis in children: HRCT findings and distribution of disease. J Thorac Imaging. 1996;11:27-38.

[22] Bortoluzzi CF, Pontello E, Pintani E, de Winter-de Groot KM, D'Orazio C, Assael BM, et al. The impact of chest computed tomography and chest radiography on clinical management of cystic fibrosis lung disease. J Cyst Fibros. 2020;19:641-6.

[23] Smyth AR, Bell SC, Bojcin S, Bryon M, Duff A, Flume P, et al. European Cystic Fibrosis Society Standards of Care: Best Practice guidelines. J Cyst Fibros. 2014;13 Suppl 1:S23-42.

[24] Chalmers JD, Aliberti S, Polverino E, Vendrell M, Crichton M, Loebinger M, et al. The EMBARC European bronchiectasis registry: Protocol for an international observational study. ERS Monogr. 2016;2.

[25] Tony SM, Abdelrahman MA, Osama H, Abdelrahim MEA. Advanced counselling using training device and smartphone application on inhalation technique from metered-dose inhaler with spacer equipped with different interfaces in asthmatic children. Int J Clin Pract. 2021:e14413.

[26] Beckert MdK, W; Norling, T; . A phase I study investigating the delivery of tobramycin usingthe TobrAir®device compared with (TOBI®) PARI LC®PLUSand PARI TurboBOY®Podhaler™using pharmacokinetic andpharmacoscintigraphic methods. Journal of Cystic Fibrosis. 2016;15:S51-S120.

[27] Chandrasekaran R, Mac Aogain M, Chalmers JD, Elborn SJ, Chotirmall SH. Geographic variation in the aetiology, epidemiology and microbiology of bronchiectasis. BMC Pulm Med. 2018;18:83.

[28] Zou JN, Sun L, Wang BR, Zou Y, Xu S, Ding YJ, et al. The characteristics and evolution of pulmonary fibrosis in COVID-19 patients as assessed by AI-assisted chest HRCT. PLoS One. 2021;16:e0248957.

[29] Perez-Rovira A, Kuo W, Petersen J, Tiddens HA, de Bruijne M. Automatic airway-artery analysis on lung CT to quantify airway wall thickening and bronchiectasis. Med Phys. 2016;43:5736.

[30] Quan K, Tanno R, Shipley RJ, Brown JS, Jacob J, Hurst JR, et al. Reproducibility of an airway tapering measurement in computed tomography with application to bronchiectasis. J Med Imaging (Bellingham). 2019;6:034003.

[31] Tepper LA, Ciet P, Caudri D, Quittner AL, Utens EM, Tiddens HA. Validating chest MRI to detect and monitor cystic fibrosis lung disease in a pediatric cohort. Pediatr Pulmonol. 2016;51:34-41.

[32] Dournes G, Menut F, Macey J, Fayon M, Chateil JF, Salel M, et al. Lung morphology assessment of cystic fibrosis using MRI with ultra-short echo time at submillimeter spatial resolution. Eur Radiol. 2016;26:3811-20.

Chapter 9

Summary / Samenvatting

Summary

This thesis focuses on the diagnosis and treatment of bronchiectasis. Section I describes the radiological diagnosis and image analysis of bronchiectasis. Section II focuses on the use of inhaled antibiotics by bronchiectasis patients, and studies the deposition of antibiotics with computational fluid dynamics, using computed tomography (CT) images of bronchiectasis patients.

Section I

Chapter 2 and 3 focus on the radiological criteria of bronchiectasis. Chapter 4 and 5 present CT analysis methods for bronchiectasis patients.

In chapter 2, we describe the results of our extensive literature review of radiological criteria to diagnose bronchiectasis. From 4182 publications, we selected 122 relevant studies that reported radiological criteria for bronchiectasis. The gold standard to diagnose bronchiectasis is CT. The most frequently reported criterion is an airway-artery ratio ≥ 1. However, we did not find any validation studies that support this number. Furthermore, we found evidence that the airway-artery ratio is also influenced by age, sex and smoking behaviour. Importantly, it is unknown whether the inner (luminal) or outer diameter of the airway should be used for comparison with the adjacent artery. Two other criteria for bronchiectasis that were often reported are tapering of the airways, and visibility of small airways in the periphery of the lungs. We also studied how bronchiectasis was quantified, and found as many as 42 different CT analysis methods to quantify the amount of bronchiectasis. We concluded that there are no validated diagnostic criteria for bronchiectasis, and CT acquisition and analysis is often not standardised.

In chapter 3, we focus on the challenges of the radiologic diagnosis of bronchiectasis. To diagnose bronchiectasis, the following factors are of importance. First, there is a need for clear, validated criteria and cut-off values. Second, lung volume during scanning should be standardised. As the diameter of an airway is dependent on the respiratory phase, it is important that CT scans are acquired at total lung capacity (TLC). Lung volume control can be accomplished by spirometry-guided CT scanning, or if this is not feasible, by lung function technician guided CT scanning. Third, CT protocols have to be synchronised across centres. Preferably, volumetric CT scans are made that allow ≤ 1 mm slice reconstruction. Furthermore, attention should be paid to the choice of reconstruction kernels. Although CT is the gold standard to diagnose bronchiectasis, magnetic resonance imaging (MRI) is emerging. An advantage of MRI over CT is that with MRI, patients are not exposed to ionising radiation. Furthermore, MRI allows studying functional outcomes such as ventilation and perfusion. However,

image quality is not yet comparable to that of CT, standardisation of MRI protocols and image analysis is challenging, and extensive validation of MRI outcomes is needed before MRI can replace CT.

In chapter 4, we performed image analysis of patients with granulomatous lymphocytic interstitial lung disease (GLILD), which is a subgroup of patients with common variable immunodeficiency disorders. GLILD patients show ground-glass opacities, nodules and reticulation on chest CT. We used two CT scoring methods, the Baumann and Hartmann method, to analyse 356 CT scans of 138 GLILD patients. An important outcome of the study is that bronchiectasis was present in 82% of the GLILD patients. Furthermore, we compared the outcomes of both scoring methods and concluded that the reproducibility of the Hartmann method was slightly better than that of the Baumann method, and that the Hartmann method was more sensitive to detect progression of bronchiectasis. Therefore, the Hartmann method is probably more suitable for clinical studies.

In chapter 5, we describe the development of a new CT analysis system for bronchiectasis patients, the BronchiEctasis Scoring Technique for CT (BEST-CT). Furthermore, we present the results of the radiological analysis with this method in 84 bronchiectasis patients with a chronic *Pseudomonas aeruginosa* (*Pa*) infection, and of the cross-validation against other CT and clinical parameters. The BEST-CT is a morphometric scoring system in which an overlaying grid is placed on CT scan slices, after which the grid boxes are annotated by an observer for the presence of abnormalities. The following items are assessed in hierarchical order: atelectasis and/or consolidation, bronchiectasis with mucus plugging, bronchiectasis without mucus plugging, airway wall thickening, ground-glass opacities, emphysema or bullae, healthy airways, and healthy parenchyma. Component scores of the BEST-CT are expressed as a percentage of total lung volume, and composite scores such as the total bronchiectasis score (bronchiectasis with mucus plugging + bronchiectasis without mucus plugging) can be calculated. The outcomes of the analysis with BEST-CT were compared with those of the Hartmann method, intra-branch tapering, forced expiratory volume in one second (FEV_1), bronchiectasis severity index, quality of life, exacerbations, and *Pa* sputum density. An important result was that we observed a considerable heterogeneity of structural lung changes. The total amount of disease varied from 1-42 % of the total lung volume. BEST-CT scores correlated well with corresponding Hartmann scores, and furthermore, significant correlations were found between total amount of bronchiectasis and FEV_1 and intra-branch tapering. We did not find significant correlations between BEST-CT scores and other clinical parameters. BEST-CT scores showed good reproducibility within and between observers. The next step is to validate BEST-CT outcomes in longitudinal studies.

Section II

Many bronchiectasis patients suffer from chronic *Pa* infection, for which inhaled tobramycin is often prescribed. In chapter 6 we describe the inhalation technique of tobramycin inhalation powder in patients with cystic fibrosis (CF), and we studied whether inspiratory flow is related to cough. In chapter 7, we describe the deposition of tobramycin inhalation powder and inhalation solution in the large and small airways using fluid dynamic modelling, for which three-dimensional lung models were made from CT scans of CF patients.

In chapter 6, we studied the relation between inspiratory flow of tobramycin inhalation powder and immediate cough after inhalations. Furthermore, we studied which mistakes were made during inhalation. Twenty patients with CF were visited twice at home. Inhalations were recorded on video, and inspiratory flow was measured. The main result was that we did not find a correlation between cough and inspiratory flow, although the majority of patients (70%) coughed after inhalation. Another important finding was that multiple mistakes were made during inhalations, the most frequent made mistake was a breath-hold of less than five seconds after inhalation. From the results of this study, we conclude that cough occurs regardless of inspiratory flow, and that repetitive training of inhalation technique on the outpatient clinic is essential.

In chapter 7, we describe the deposition of inhaled tobramycin in the large and small airways. This was done with in silico analysis using computational fluid dynamics. We compared tobramycin inhalation powder with tobramycin inhalation solution. Furthermore, we studied whether there is a difference in tobramycin deposition in the large and small airways between slow, fast, and uninstructed inhalations. Three-dimensional lung models were constructed of CT scans of patients with CF. This was done for three patient groups, namely children, and adult women and men, and for each group, a mild, moderate, and severely diseased model was constructed. Inspiratory flows were collected from 12 CF patients during home visits. The patients were instructed to inhale tobramycin inhalation powder slow, fast, or without specific instructions, and furthermore, inhalations with a nebuliser were recorded. In total, 144 computer simulations were performed. We showed that tobramycin concentrations were at least 10 times above the minimal inhibitory concentration, both in the large and small airways. However, slow inhalations with tobramycin inhalation powder resulted in higher concentrations in the small airways when compared with fast or uninstructed inhalations. Finally, tobramycin concentrations in the small airways were similar between slow inhalations with tobramycin inhalation and tobramycin

inhalation solution. Based on these results, tobramycin inhalation powder and inhalation solution are equivalent treatment options, and the choice of treatment could be based on the patients preference.

Samenvatting

Dit proefschrift is gericht op de diagnose en behandeling van zieke abnormaal verwijde luchtwegen, oftewel bronchiëctasieën. Deel I van het proefschrift is gericht op de radiologische diagnose en op de beeldanalyse van bronchiëctasieën. Deel II van het proefschrift is gericht op het optimale gebruik van een inhalatie-antibioticum door patiënten met bronchiëctasieën, waarbij de behandeling met behulp van radiologische beelden is onderzocht.

Deel I

Hoofdstuk 2 en 3 zijn gericht op de radiologische criteria voor bronchiëctasieën. Hoofdstuk 4 en 5 zijn gericht op analysemethoden voor patiënten met bronchiëctasieën.

In hoofdstuk 2 beschrijven we de bevindingen van ons uitgebreide literatuuronderzoek naar criteria voor de radiologische diagnose van bronchiëctasieën. Uit 4182 publicaties werden uiteindelijk 122 relevante studies geselecteerd waarin radiologische criteria voor bronchiëctasieën werden beschreven. De gouden standaard om bronchiëctasieën te diagnosticeren is met een computertomografie (CT) scan. Het meest frequente genoemde criterium voor bronchiëctasieën is een verhouding tussen de dwarsdoorsnedes van een luchtweg en van het naastgelegen bloedvat die gelijk of groter dan 1 is. We konden echter geen studies vinden die dit getal onderbouwen. Bovendien vonden we studies waaruit bleek dat naast ziekte van de luchtwegen ook leeftijd, geslacht en roken van invloed zijn op de luchtweg-bloedvat verhouding. Ook blijkt er geen consensus te zijn of de binnenste of buitenste diameter van de luchtweg moet worden gebruikt voor het berekenen van de luchtweg-bloedvat verhouding. Twee andere veelgenoemde criteria voor bronchiëctasieën zijn het niet smaller worden van vertakkende luchtwegen, en de zichtbaarheid van kleine luchtwegen in het buitenste gedeelte van de longen. We hebben ook onderzocht hoe beelden met bronchiëctasieën worden geanalyseerd in wetenschappelijke studies. Uit ons onderzoek blijkt dat er wel 42 verschillende analyse methoden gebruikt werden. Verder bleek dat er grote verschillen zijn tussen de scanprotocollen voor de CT-scans. Wij concluderen dan ook dat er nog veel winst te behalen is in het standaardiseren van CT-onderzoek.

In hoofdstuk 3 focussen we op de uitdagingen van het radiologisch diagnosticeren van bronchiëctasieën. Voor de radiologische diagnose zijn er een aantal factoren van belang. Ten eerste moeten er duidelijke criteria en afkapwaarden worden afgesproken, bijvoorbeeld voor de luchtweg-bloedvat ratio. Ten tweede is het bij het maken van CT-scans belangrijk dat de hoeveelheid ingeademde lucht op het moment van scannen steeds hetzelfde is; de diameter van de luchtwegen is hier

namelijk afhankelijk van. Dit kan worden bereikt door de hoeveelheid ingeademde lucht tijdens de CT-scan te meten met behulp van spirometrie. Een eenvoudigere maar eveneens effectieve methode is door patiënten tijdens de scan te laten begeleiden door een longfunctie-analist. Deze technieken worden al in meerdere ziekenhuizen toegepast. Ten derde zouden er afspraken moeten worden gemaakt over de instellingen van de CT-scanners, en zouden de beelden op dezelfde manier moeten worden gereconstrueerd. Op dit moment wordt CT het meeste gebruikt om bronchiëctasieën af te beelden, maar beeldvorming met magnetische resonantie (MRI) is in opkomst. Een groot voordeel aan deze methode is dat de patiënt niet wordt blootgesteld aan schadelijke straling. Een nadeel is dat de kwaliteit van de beelden van MRI nog niet zo goed is als CT. Daarom blijft CT vooralsnog het radiologische onderzoek naar keuze bij bronchiëctasieën.

In hoofdstuk 4 is de beeldanalyse beschreven van patiënten met granulomateuze lymfocytische interstitiële longziekte, dit is een zeldzaam ziektebeeld wat voorkomt bij mensen met immuundeficiënties. Op de CT-scan hebben deze patiënten vaak matglas afwijkingen, bolvormige afwijkingen, en netwerkvormende lijnen (reticulaties) in het longweefsel. Met behulp van twee nieuwe scoringsmethoden, de Baumann en de Hartmann methode, zijn 356 CT scans van 138 patiënten geanalyseerd. We zagen dat, naast de reeds beschreven afwijkingen in het longweefsel, bij wel 82% van de patiënten bronchiëctasieën aanwezig waren. De Hartmann en Baumann methode zijn met elkaar vergeleken: de Hartmann methode is uitgebreider maar kost meer tijd dan de Baumann methode, de Hartmann methode bleek beter reproduceerbaar, en bovendien kon alleen met de Hartmann een toename van bronchiëctasieën gemeten worden toen we scans van dezelfde patiënten over een aantal jaren vergeleken. Voor onderzoeksdoeleinden lijkt de Hartmann dus een meer geschikte scoringsmethode om te gebruiken.

In hoofdstuk 5 laten we de ontwikkeling zien van een nieuwe scoringsmethode om longafwijkingen in patiënten met bronchiëctasieën op CT te beschrijven en kwantificeren: de BronchiEctasis Scoring Technique for CT (BEST-CT). De BEST-CT is een methode waarbij er op tien verschillende CT-scan plakjes een raster wordt gelegd, en vervolgens wordt ieder hokje ingekleurd op basis van afwijking die zich daarin bevindt. Dit kunnen de volgende afwijkingen zijn: ontstoken of samengevallen longweefsel, bronchiëctasieën met slijmpluggen, bronchiëctasieën zonder slijmpluggen, luchtwegwand verdikking, slijmpluggen, matglas afwijkingen, en uitgerekte longblaasjes of grotere blazen. Is er geen afwijking, dan wordt gekozen tussen gezonde luchtwegen (indien aanwezig) of gezond longweefsel. Alle uitkomsten worden uitgedrukt als percentage van het totale longvolume. Daarnaast worden samengestelde scores berekend, onder andere de totale hoeveelheid

bronchiëctasieën en de totale hoeveelheid ziekte. Met deze nieuwe methode zijn CT-scans gescoord van 84 patiënten met bronchiëctasieën, die ook een chronische infectie hebben met een bacterie, de *Pseudomonas aeruginosa*. De uitkomsten zijn vergeleken met de scores van de Hartmann methode, de mate waarin luchtwegen versmallen, de longfunctie uitgedrukt in geforceerd expiratoir volume in één seconde (FEV_1), kwaliteit van leven, longaanvallen en de hoeveelheid bacteriën in spuug. Een belangrijke uitkomst van de studie was dat er grote verschillen tussen patiënten werden gezien in de hoeveelheid en soort afwijkingen in de longen. De totale hoeveelheid ziekte varieerde tussen de 1 en 42% van het totale longvolume. De BEST-CT scores kwamen goed overeen met de Hartmann scores, en ook was de BEST-CT totale hoeveelheid bronchiëctasieën gecorreleerd met de mate waarin luchtwegen versmallen en met de FEV_1. Deze verbanden waren statistisch significant. Er werd geen verband gevonden met andere klinische uitkomstmaten. Een andere belangrijke uitkomst van de studie was dat de BEST-CT goed reproduceerbaar is. Een volgende stap is om deze methode te testen in meerjarige studies.

Deel II

Veel patiënten met bronchiëctasieën krijgen een chronische infectie met de bacterie *Pseudomonas aeruginosa*. Om de infectie te stopen of te remmen krijgen deze patiënten vaak inhalatietherapie met een antibioticum, tobramycine. In hoofdstukken 6 en 7 beschrijven we hoe patiënten droog poeder tobramycine inhaleren en hoe we met CT-scans digitale modellen hebben gemaakt om uit te rekenen hoeveel antibiotica er in de luchtwegen terecht komt.

In hoofdstuk 6 is onderzocht wat de relatie is tussen de snelheid waarmee patiënten droog poeder tobramycine inhaleerden en het optreden van hoest door de inhalatie. Ook werd de inhalatietechniek beoordeeld. Twintig patiënten met taaislijmziekte zijn twee keer thuis bezocht en gefilmd terwijl zij inhaleerden met droog poeder tobramycine. Er werden geen significante verbanden gevonden tussen de inhalatiesnelheid en hoesten, ondanks dat het merendeel (70%) van de patiënten ten minste één keer moest hoesten bij inhalatie. De meest voorkomende fouten waren het niet volledig uitademen voor de inhalatie en het niet lang genoeg inhouden van de adem na de inhalatie met tobramycine.

In hoofdstuk 7 beschrijven we hoe geïnhaleerde tobramycine-deeltjes zich over de grote en kleine luchtwegen verdelen. Dit hebben we berekend met computersimulaties. We vergeleken tobramycine in twee verschillende vormen voor inhalatie: droog poeder en vernevelvloeistof. Daarnaast vergeleken we voor droog poeder ook het effect van verschillende inhalatiesnelheden op de verdeling over de luchtwegen. Voor drie groepen patiënten (kinderen en volwassenen mannen

en vrouwen) zijn met CT-scans van taaislijmziekte-patiënten digitale 3D modellen gemaakt. Voor elke groep werd een model met milde, een model met matige en een model met ernstige longafwijkingen gemaakt. Voor de simulaties werden inhalatiecurves gebruikt die thuis zijn opgenomen bij 12 patiënten met taaislijmziekte. De patiënten werden geïnstrueerd om droog poeder tobramycine langzaam, snel, of zonder instructies te inhaleren. Ook hebben zij geïnhaleerd met een vernevelapparaat. In totaal hebben we 144 simulaties gedaan. We hebben laten zien dat er zowel in de grote als in de kleine luchtwegen genoeg tobramycine neersloeg, de concentratie was steeds minstens 10 keer boven de minimum beoogde concentratie. Wel zorgde langzame inhalaties met droog poeder tobramycine voor hogere concentraties in de kleine luchtwegen dan snelle of niet-geïnstrueerde inhalaties. Tot slot bleek dat inhalaties met vernevelvloeistof in even hoge concentraties in de kleine luchtwegen resulteerden als langzame inhalaties met poeder. Dit betekent dat droog poeder en vernevelvloeistof gelijkwaardige alternatieven zijn, en de arts de keuze voor een van beiden het beste bij de patiënt kan laten.

SECTION IV

List of abbreviations

AA ratio	Airway to artery ratio
AD	Airway disease
AI	Artificial intelligence
ATCON	Atelectasis and/or consolidation
B	Bronchial lumen
BE	Bronchiectasis
BEMP	Bronchiectasis with mucus plugging
BEST-CT	Bronchiectasis scoring technique for CT
BEwMP	Bronchiectasis without mucus plugging
BRICS	Bronchiectasis Radiologically Indexed CT Score
BSI	Bronchiectasis severity index
BW	Bronchial wall
BWT	Bronchial wall thickening
CF	Cystic fibrosis
CFD	Computational fluid dynamics
CFQ-R	Cystic Fibrosis Questionnaire - Revised
CFU	Colony forming units
COPD	Chronic obstructive pulmonary disease
CT	Computed tomography
CVID	Common variable immunodeficiency disorders
DIS	Disease
ECFS-CTN	European Cystic Fibrosis Society Clinical Trial Network
E-FACED	FEV_1, age, chronic colonisation, extension and dyspnoea + exacerbations
EMBARC	European Multicentre Bronchiectasis Audit and Research Collaboration
EMPBUL	Emphysema and/or bullae
FACED	FEV_1, age, chronic colonisation, extension and dyspnoea
FEV_1	Forced expiratory volume in one second
FVC	Forced vital capacity
GGO	Ground-glass opacities
GLILD	Granulomatous lymphocytic interstitial lung disease
GSD	Geometric standard deviation
HA	Healthy airways
HM	Hartmann
HP	Healthy parenchyma

ICC	Intraclass correlation coefficient
IPR	Inspiratory profile recorder
IQR	Interquartile range
LAR	Low attenuation regions
MIC	Minimal inhibitory concentration
MMAD	Mass median aerodynamic diameter
MP	Mucus plugging
MRI	Magnetic resonance imaging
NGI	Next-generation impactor
NOD	Nodules
NOR	Normal or high attenuation regions
Pa	*Pseudomonas aeruginosa*
PCD	Primary ciliary dyskinesia
PIF	Peak inspiratory flow
PRAGMA-CF	Perth-Rotterdam Annotated Grid Morphometric Analysis for CF
QOL-B	Quality of Life Questionnaire for Bronchiectasis
RET	Reticulation
STILPAD	Study of Interstitial Lung Disease in Primary Antibody Deficiency
TBE	Total bronchiectasis
TIP	Tobramycin inhalation powder
TIS	Tobramycin inhalation solution
TLC	Total lung capacity
TLC	Total lung capacity
V	Accompanying vessel
VIPS-MRI	Ventilation inflammation perfusion and structure - magnetic resonance imaging

List of publications

This thesis

Meerburg JJ, Andrinopoulou ER, Bos AC, Shin H, van Straten M, Hamed K, et al.
Effect of inspiratory maneuvers on lung deposition of tobramycin Inhalation powder: a modeling study.
Journal of Aerosol Medicine and Pulmonary Drug Delivery. 2020;33:61-72.

Meerburg JJ, Hartmann IJC, Goldacker S, Baumann U, Uhlmann A, Andrinopoulou ER, et al.
Analysis of granulomatous lymphocytic interstitial lung disease using two scoring systems for computed tomography scans - a retrospective cohort study.
Frontiers in Immunology. 2020;11:589148.

Meerburg JJ, Veerman GDM, Aliberti S, Tiddens H.
Diagnosis and quantification of bronchiectasis using computed tomography or magnetic resonance imaging: a systematic review.
Respiratory medicine. 2020;170:105954.

Tiddens H, Meerburg JJ, van der Eerden MM, Ciet P.
The radiological diagnosis of bronchiectasis: What's in a name?
European Respiratory Review. 2020;29.

Meerburg JJ, Albasri M, van der Wiel EC, Andrinopoulou ER, van der Eerden MM, Majoor CJ, et al.
Home videos of cystic fibrosis patients using tobramycin inhalation powder: Relation of flow and cough.
Pediatric Pulmonology. 2019;54:1794-800.

Meerburg JJ, Garcia-Uceda A, Dragt O, Andrinopoulou ER, Kemner van de Corput MPC, Ciet P, Angyalosi G, Elborn JS, Chalmers JD, Tunney M, de Bruijne M, Tiddens HAWM
Quantitative chest computed tomography scoring technique for bronchiectasis (BEST-CT).
Submitted.

Other

Aliberti S, Goeminne PC, O'Donnell AE, Aksamit TR, Al-Jahdali H, Barker AF, Blasi F, Boersma WG, Crichton ML, De Soyza A, Dimakou KE, Elborn SJ, Feldman C, Tiddens HAWM, Haworth CS, Hill AT, Loebinger MR, Martinez-Garcia MA, Meerburg JJ, Menendez R, Morgan LC, Murris MS, Polverino E, Ringshausen FC, Shteinberg M, Sverzellati N, Tino G, Torres A, Vandendriessche T, Vendrell M, Welte T, Wilson R, Wong CA, Chalmers JD.
Criteria and definitions for the radiological and clinical diagnosis of bronchiectasis in adults for use in clinical trials: international consensus recommendations.
Lancet Respiratory Medicine. Accepted for publication.

Affiliations co-authors

Name	Affiliations
Albasri, Mehdi	Department of Paediatric Pulmonology, Leiden University Medical Center, Leiden, the Netherlands
Aliberti, Stefano	Fondazione IRCCS Ca' Granda Ospedale Maggiore Policlinico, Respiratory Unit and Adult Cystic Fibrosis Center, Dept of Pathophysiology and Transplantation, University of Milan, Milan, Italy
Andrinopoulou, Eleni-Rosalina	Department of Biostatistics, and department of Epidemiology, Erasmus Medical Center, Rotterdam, the Netherlands
Angyalosi, Gerhild	Novartis Pharma, AG, Basel, Switzerland
Arets, Hubertus G.M.	Department of Paediatric Pulmonology and Allergology, University Medical Center Utrecht, Utrecht, the Netherlands
Baumann, Ulrich	Department of Paediatric Pulmonology, Allergy and Neonatology, Hannover Medical School, Hannover, Germany
Bos, Aukje C.	Department of Paediatric Pulmonology and Allergology, Sophia Children's Hospital, and department of Radiology and Nuclear Medicine, Erasmus Medical Center, Rotterdam, the Netherlands
Bruijne, Marleen de	Department of Radiology and Nuclear Medicine, Erasmus Medical Center, Rotterdam, the Netherlands Department of Computer Science, University of Copenhagen, Denmark
Chalmers, James D.	Scottish Centre for Respiratory Research, University of Dundee, Ninewells Hospital and Medical School, Dundee, UK
Ciet, Pierluigi	Department of Paediatric Pulmonology and Allergology, Sophia Children's Hospital, and department of Radiology and Nuclear Medicine, Erasmus Medical Center, Rotterdam, the Netherlands
Dragt, Olivier	Department of Paediatric Pulmonology and Allergology, Sophia Children's Hospital, Erasmus Medical Center, Rotterdam, the Netherlands
Eerden, Menno van der	Department of Pulmonology, Erasmus Medical Center, Rotterdam, the Netherlands
Elborn, J. Stuart	Centre for Experimental Medicine, Queen's University Belfast, Belfast, UK
Garcia-Uceda, Antonio	Department of Radiology and Nuclear Medicine, Erasmus Medical Center, Rotterdam, the Netherlands
Goldacker, Sigune	Department of Rheumatology and Clinical Immunology, Faculty of Medicine, University of Freiburg, Medical Center—University of Freiburg, Freiburg, Germany
Hamed, Kamal	Novartis Pharmaceuticals Corporation, East Hanover, New Jersey
Hartmann, Ieneke J.C.	Department of Radiology, Maasstad Hospital, Rotterdam, the Netherlands
Heijerman, Harry G.M.	Department of Pulmonology, University Medical Center Utrecht, Utrecht, the Netherlands
Kemner v/d Corput, Mariette P.C.	Department of Paediatric Pulmonology and Allergology, Sophia Children's Hospital, and department of Radiology and Nuclear Medicine, Erasmus Medical Center, Rotterdam, the Netherlands
Majoor, Christof J.	Department of Pulmonology, Amsterdam University Medical Center, AMC, Amsterdam, the Netherlands

Mastoridis, Paul	Novartis Pharmaceuticals Corporation, East Hanover, New Jersey
Shin, Hwain	Novartis Pharma AG, Basel, Switzerland
Straten, Marcel van	Department of Radiology and Nuclear Medicine, Erasmus Medical Center, Rotterdam, the Netherlands
Tiddens, Harm A.W.M.	Department of Paediatric Pulmonology and Allergology, Sophia Children's Hospital, and department of Radiology and Nuclear Medicine, Erasmus Medical Center, Rotterdam, the Netherlands
Tunney, Michael	School of Pharmacy, Queen's University Belfast, Belfast, UK
Uhlmann, Annette	Institute for Immunodeficiency, Center for Chronic Immunodeficiency (CCI), Medical Center - University of Freiburg, Faculty of Medicine, University of Freiburg, Freiburg, Germany
Veerman, G.D. Marijn	Department of Medical Oncology, Erasmus MC Cancer Institute, Erasmus Medical Center, Rotterdam, the Netherlands
Warnatz, Klaus	Center for Chronic Immunodeficiency (CCI), Faculty of Medicine, University of Freiburg, Medical Center - University of Freiburg, Freiburg, Germany Department of Rheumatology and Clinical Immunology, Faculty of Medicine, University of Freiburg, Medical Center - University of Freiburg, Freiburg, Germany
Wiel, Els C. van der	Department of Paediatric Pulmonology and Allergology, Sophia Children's Hospital, Erasmus Medical Center, Rotterdam, the Netherlands

PhD portfolio

Conferences	Year	Workload
World Bronchiectasis & Non-Tuberculosis Mycobacteria Conference, oral presentation	2020	1
European Respiratory Society International Congress, poster presentation	2018	1
Longdagen, oral presentation	2018	0.3
Sophia Research Day, 2017 and 2018 organising committee	2015, 2016, 2017, 2018	1.5
European Cystic Fibrosis Conference, poster presentation	2016 and 2018	2
North American Cystic Fibrosis Conference, poster presentation	2017	1
European Cystic Fibrosis Young Investigators Meeting, Paris, oral and poster presentation	2017	1
Erasmus MC PhD day	2015, 2016, 2017	0.9
Training Upcoming Leaders in Paediatric Science - Young Investigators day	2015	0.3

Courses	Year	Workload
Erasmus MC - CC02 Biostatistical Methods I: Basis Principles	2017	5.7
European Cooperation in Science and Technology - Inhaled Medicines Emerging Device and Particle Engineering Technologies for Optimal Pulmonary Drug Delivery	2017	0.5
Erasmus MC - CPO-course: Patient Oriented Research	2016	0.3
Erasmus MC - Biomedical English Writing	2016	2.0
Erasmus MC - Basic Introduction Course on SPSS	2016	1.0
Erasmus MC - Open Clinica Course	2015	0.3
Erasmus MC - Basic course Rules and Organisation for Clinical researcher (BROK)	2015	1.5
Erasmus MC - Scientific Integrity	2015	0.3
Erasmus MC - Medical library: Literature retrieval 1, 2, and Endnote	2015	0.5
Erasmus MC - LungAnalysis: PRAGMA-CF CT scoring method	2015	1.4
Erasmus MC - LungAnalysis: CF-CT scoring method	2015	1.4
Stanford University - Statistics in Medicine	2015	1.0

Scientific meetings	Year	Workload
Erasmus MC - Research meeting department of paediatric pulmonology & allergology	2015-2019	4.0
Erasmus MC - Research meeting research group Tiddens	2015-2019	4.0
Erasmus MC - Radiology meeting department of paediatric pulmonology & allergology department	2015-2019	2.5
Medische Aerosol Denktank (MAD)	2015-2019	0.9

Other scientific activities	Year	Workload
Supervising master thesis student	2018	1.5
Peer review of articles for international scientific journals	2016-2019	2.0
Outpatient clinic paediatric pulmonology	2015-2019	2.0
Secretary of Sophia Onderzoekers Vertegenwoordiging	2017	1.5
Standardised Chest Imaging Framework for Interventions and Personalised Medicine in CF - Site visit to provide training in standardised CT scanning	2016	0.5
		Total ECTS
		43.8

About the author

Jennifer Meerburg was born on the 9th of October 1989 in Leiden, and grew up in Hazerswoude. In 2007 she finished her secondary school, 'Stedelijk Gymnasium' in Leiden. After a year delay due to the numerous fixus during which she studied health sciences at the Erasmus University Rotterdam, she was accepted into medical school in 2008 at this same university. During medical studies she had a broad interest in various fields of medicine. Highlights of her study were a summer school in tropical medicine in Yogyakarta, Indonesia, a surgery internship in Willemstad, Curaçao, and an internship at the department of paediatric pulmonology in Sophia Children's Hospital, Erasmus MC, where she met professor Harm Tiddens. Inspired by his innovative research projects on the field of cystic fibrosis, bronchiectasis and computed tomography scanning she started the research projects described in this thesis. Besides doing research she improved her ice-skating skills and participated twice in Skate4air, a fund raising event for cystic fibrosis, for which she is currently a board member. In 2019, she worked as 'ANIOS' at the department of surgery of the Maasstad hospital, Rotterdam. In 2020, she started her training to become a general practitioner at Leiden University Medical Center.

Dankwoord

Onderzoek doe je niet alleen. Dit proefschrift had niet bestaan zonder een hele grote groep mensen die me op verschillende manieren hebben gesteund, en daar wil ik ze heel graag voor bedanken.

Allereerst de patiënten en hun familieleden, die naast de tijd die zij dagelijks kwijt zijn aan behandelingen ook nog tijd vrij wilden maken voor deelname aan wetenschappelijk onderzoek.

Mijn promotor, prof. Harm Tiddens. Lieve Harm, ontzettend bedankt voor je begeleiding in de afgelopen jaren. Je enthousiasme voor onderzoek is aanstekelijk, na het PhD spreekuur liep ik steevast vol goede moed en met allerlei nieuwe plannen je kamer uit. Hoewel het onze samenwerking niet ontbrak aan de nodige dosis humor hield je me altijd bij de les en leerde je me obstakels uit de weg helpen ("if there's a problem – solve it"). Dank voor alles!

Mijn copromotor, dr.ir. Marcel van Straten, beste Marcel, onze samenwerking begon toen ik bij je aanklopte voor een lesje CT-scannen voor het SCIFI project, waarna je als copromotor van een afstandje mee bleef kijken met mijn PhD-traject. Je hielp me tijdens onze voortgangsgesprekken mijn projecten op een rijtje te zetten en kon mijn stukken met een frisse blik voorzien van feedback, dank daarvoor!

De overige leden van de kleine commissie, prof. van Rossum, prof. Aerts en prof. Derom, dank dat u bereid bent geweest mijn proefschrift te beoordelen, een belangrijke laatste stap in dit traject.

Lieve Els, jouw functie zou een aparte titel moeten hebben, want zonder jou was ik nooit op dit punt gekomen. Onwijs bedankt voor onze wekelijkse meetings waarin je me op weg hielp met mijn studies of gewoon met een goed gesprek, altijd onder het genot van een vers gezette cappuccino. Ik heb ontzettend genoten van onze vele avonturen met als hoogtepunt natuurlijk ons reisje naar New York!

Research group Tiddens, bedankt voor de samenwerking! Merlijn, Sergei, Hamed, Pier, Jorien, Badies, Elrozy, Yifan, Qiantin, Yuxin, Olivier, Nynke, Roos, Job, Alain en Mehdi. The Italian colleagues: Greta, Alice, Valentina, Giuseppe Parisi, Giuseppe Cicero, Chiara and Federico, thanks for bringing some temperament and lot's of fun into the office! Marleen en Antonio, bedankt voor jullie waardevolle discussies en hulp ten aanzien van de tapering en AA-ratio analyses. Mariette, onze projecten liepen niet altijd van een leien dakje, maar volgens mij vulden we elkaar goed aan, het was dan

ook erg leuk om met je samen te werken. Aukje en Wieying, dankzij jullie had ik een topstart van mijn PhD-traject, en ook werden congressen en radiologiediners extra leuk! Wytse, klasbak, onze samenwerking was kort maar krachtig, hoog tijd om weer eens samen een rondje te fietsen! Bernadette, mijn paranimf, het was heel tof om met jou het schaatsavontuur aan te gaan, en hoewel ik je niet altíjd aan het lachen kon maken hebben we ongelofelijk veel lol gehad. Superleuk om de promotie met jou aan mijn zijde te kunnen afsluiten!

Dankzij de Sophia PhD-collega's werd het promotietraject ook een beetje een tweede studententijd, wat niet altijd ten goede kwam aan mijn planning maar zeker wel aan het werkplezier. Bedankt daarvoor! Kamer Na1723: Lieve Robin, van kamergenoot tot paranimf, heel leuk dat we er ook met mijn verdediging samen staan. Hoewel onze eerste discussie over de haarkleur van Sophietje wat onfortuinlijk verliep, trokken we daarna gelukkig steeds meer met elkaar op. Ook zonder eetclub geniet ik altijd enorm van onze dinertjes en ik hoop dat we daar lang mee door blijven gaan! Ries & Roos, de drie dagen disco in de bergen waren hilarisch. Manuel, je wist je met je relaxte houding aardig staande te houden tussen al die vrouwen, dus je wordt vast een top kinderarts. Esther, ik heb genoten van jouw nuchtere Friese houding in combinatie met je gevoel voor humor. Tot slot de bestuurs- en commissiegenootjes van de Sophia Onderzoekers Vertegenwoordiging: Bianca, Annelieke, Tanja, Renate, Nienke, Leila, Raisa, Kirsten, Tamara, Ruben, Martine, het was reuzegezellig om met jullie de SOV draaiende te houden!

Collega's van de kinderlong: Allereerst Irma, bedankt voor de vele momenten waarbij je me te hulp bent geschoten. Johan, Mariëlle, Hettie, Liesbeth, Daan, Esmé, Suzanne, Marije, Sanne, en pulmo-PhD's Evelien, Martijn, Rosalie, Esmee, Shelly, Stefanie, het was fijn met jullie te werken, dank voor jullie input tijdens de research meetings. Annelies en Inge, bedankt voor jullie hulp bij de TIPTIS studie en de gezelligheid op congressen en Skate4air. Collega's van de longfunctie, dank voor jullie hulp en alle uitleg op de poli.

Conne Groen, fijn als er uit onverwachte hoek hulp komt bij het printen van je proefschrift.

De 'volwassen' longafdeling: Menno van der Eeden, Marleen Bakker, Rogier Hoek, Ron, Wendy, Annemarie en Bert, dank voor jullie hulp bij de TIPTIS studie!

De local principal investigators van de TIPTIS studie, Christof Majoor, Harry Heijerman en Bert Arets, en de onderzoeksverpleegkundigen Pearl, Marianne, Sabine en Margot, dank voor jullie inzet om patiënten te includeren!

De Nederlandse CF stichting, in het bijzonder Vincent Gulmans, voor het geweldig leuke en leerzame young-investigators weekend in Parijs waar ik mijn werk mocht presenteren.

The team involved in the STILPAD study, especially prof. Warnatz, dr. Goldacker, dr. Uhlman, dr. Hartmann, and prof. Baumann, thank you for your help to improve our work on the CT study.

Marijn, de oliebollen stonden niet in verhouding tot de hoeveelheid werk die het review met zich meebracht. Je bent je zonder enig geklaag blijven inzetten tot het werk af was, heel erg bedankt daarvoor!

I would like to thank the iABC consortium for the pleasant cooperation during the iBEST study, especially Stuart Elborn, Michael Tunney, James Chalmers, Sinead Cahill and Gerhild Angyalosi.

Prof. Aliberti, it was a privilege to work with you on the bronchiectasis review, and to be involved in your paper on the definition manuscript.

The Novartis (former) colleagues involved in the TIPTIS study, specifically Kim Evers, Hwain Shin, Kamal Hamed, and Paul Mastoridis, thank you for your confidence in our research project.

De Vlaamse hulptroepen van FLUIDDA: Cedric Holsbeke, Jan de Backer en Wim Vos, dank voor het meedenken met en het uitvoeren van de modelling simulaties.

De Medische Aerosol Denktank, in het bijzonder Wilbur de Kruijf, bedankt voor de inspirerende bijeenkomsten en de mogelijkheid mijn werk in jullie expertpanel te bediscussiëren.

De Maasstadmeisjes: Merel, Priscilla en Nadine, het jaar met jullie bij de chi was er een van rennen en vliegen en veel komische momenten, terwijl ondertussen de publicaties binnendruppelden. Merel, bedankt dat je mijn werk- ski- borrel- en fietsmaatje bent! Pris en Nadien, nu op naar jullie verdediging!

Christina Garden, many thanks for helping me with the discussion of this thesis!

Fiona Cook, bedankt voor het bijbrengen van het nodige zelfinzicht en vertrouwen, je bent naast een fijne dispuutsgenoot ook een hele fijne coach.

Mijn huisartsopleider, Berno Gerts, bedankt voor de ruimte die je me hebt gegeven om het proefschrift af te maken, zodat ik ook nog de tijd had om op de fiets te stappen.

JC F'elle, bedankt voor de nodige afleiding en gezelligheid, geweldig dat we nog steeds met 12 vrouw sterk van de partij zijn!

Sun, Farah en Bianca, met jullie never a dull moment, als studenten begonnen op de Karel Doorman, en inmiddels toch aardig volwassen geworden. Dat er nog maar vele mooie momenten mogen volgen!

Tot slot wil ik mijn familie bedanken voor jullie interesse in het reilen en zeilen van mijn promotietraject. Lodewijk bedankt voor het spelen van de hoofdrol in onze CT-instructiefilm. Oom Appie, je hebt me zowel overtuigd om huisarts te worden als gestimuleerd om eerst een promotietraject te doen, dank daarvoor.

Lieve Erik & Jeanette, bedankt voor jullie warmte en gastvrijheid, het is heerlijk om af en toe weer bij jullie op te kunnen laden.

Lieve Martine en Marloes, we draaien alle drie ons eigen programma, maar als we dan weer samen zijn is het altijd zo gezellig, het is fijn om zulke lieve zussen te hebben! En Loes, superleuk dat je terug te vinden bent in mijn proefschrift.

Lieve pap en mam, er is veel om jullie dankbaar voor te zijn. Tijdens het schrijven van dit proefschrift stonden jullie altijd paraat om me te helpen, om me aan te moedigen en om naar mijn verhalen te luisteren. Bedankt voor alles, ik hou van jullie.

Lieve Niels, bedankt dat je er altijd voor me bent, ik hou heel veel van je. Ook deze berg hebben we samen beklommen, ik kijk uit naar de volgende!

Financial support for the printing of this thesis was kindly provided by

SBOH
voor artsen in opleiding

Erasmus University Rotterdam

and the department of Radiology and Nuclear Medicines, Erasmus MC